Optical biosensor for on-line monitoring of organophosphate pesticides in water

Maria Isabel Gaviria Arroyave

Tesis doctoral presentada para optar al título de Doctor en Ingeniería Ambiental

Director
Gustavo Antonio Peñuela Mesa, Doctor (PhD) en Química ambiental

Codirector
Juan Bernardo Cano, Doctor (PhD) en Ingeniería

Universidad de Antioquia
Facultad de Ingeniería

Doctorado en Ingenieria Ambiental

Medellín, Antioquia, Colombia

2023

Cita	(Gaviria, M.I. 2023)
Referencia **Estilo APA 7 (2020)**	Gaviria, M.I. (2023). Optical biosensor for on-line monitoring of organophosphate pesticides in water. [Tesis doctoral]. Universidad de Antioquia, Medellín, Colombia.

Doctorado en Ingenieria Ambiental, Cohorte XI.

Grupo de Investigación Diagnóstico y Control de la Contaminación.

Centro de Investigación Ambientales y de Ingeniería (CIA).

Financiado por: Minciencias

UNIVERSIDAD DE ANTIOQUIA
Vicerrectoría de Docencia

Sistema de Bibliotecas

Centro de Documentación de Ingeniería (CENDOI)

Repositorio Institucional: http://bibliotecadigital.udea.edu.co

Universidad de Antioquia - www.udea.edu.co

ABSTRACT

Water sources in rural areas are exposed to Chlorpyrifos (CPF) and other harmful organophosphate pesticides (OPs) that should be detected before human consumption, and biosensors have emerged as promising alternatives. The application of nanomaterials, including carbon quantum dots (CD), can significantly improve the performance of optical biosensors. In this work, naturally fluorescent and non-toxic CD were synthesized from African oil palm biochar, in cooperation with the GIBEC research group from Universidad EIA. The CD were integrated and evaluated with two biomolecules and the systems were modulated with Graphene Oxide (GO) producing two fluorescent probes. The first system was developed based on Acetylcholinesterase enzyme (AChE); this biosensor was assessed under pure chlorpyrifos (CPF), but also under a commercial formulation called Lorsban® obtaining a limit of detection (LOD) as low as 0.13 µg L^{-1} and 2.05 µg L^{-1} for CPF and Lorsban® respectively. The second system employed a DNA aptamer to detect CPF and, showed a LOD as low as 0.01 µg L^{-1} with great selectivity. To advance in the field application of fluorescent probes, a portable device was designed, constructed, and evaluated in cooperation with the GIMEL research group from Universidad de Antioquia. Finally, the AChE system was selected for the evaluation of 9 superficial water samples from different rural locations of Antioquia, Colombia, using the portable prototype. The results showed that some physicochemical parameters of natural water sources have an influence on the performance of the system. However, the prototype could detect CPF in real samples from 1 µg L^{-1} and using only 150 µL of the sample. The advantages of the developed nanostructured fluorescent probes using along with a portable device tailored-made for the application, open the way for future commercial applications. To the best of our knowledge, this is one of the few works reporting the integration of nanomaterials with different biomolecules in optical systems for the detection of pesticide formulations in real prototypes, with promising results.

KEYWORDS

Carbon dots, Nanomaterial, Fluorescent biosensor, Pesticide, Chlorpyrifos, Acetylcholinesterase, aptamer, prototype, superficial water.

RESUMEN

Las fuentes de agua en zonas rurales están expuestas a clorpirifos (CPF) y otros pesticidas organofosforados (OP) nocivos que deben detectarse antes del consumo humano, y los biosensores han surgido como alternativas prometedoras. La aplicación de nanomateriales, incluidos los puntos cuánticos de carbono (CD), pueden mejorar significativamente el rendimiento de los biosensores ópticos. En este trabajo, se sintetizaron CD, los cuales son naturalmente fluorescentes y no tóxicos a partir de biochar de Palma Africana de aceite, en cooperación con el grupo de investigación GIBEC de la Universidad EIA. Los CD fueron integrados y evaluados con dos biomoléculas y los sistemas fueron modulados con Óxido de Grafeno (GO) produciendo dos sondas fluorescentes. El primer sistema fue desarrollado basado en la enzima Acetilcolinesterasa (AChE); este biosensor fue evaluado para detectar CPF puro, pero también bajo una formulación comercial llamada Lorsban® obteniendo un límite de detección (LOD) tan bajo como 0.13 µg L-1 y 2.05 µg L-1 para CPF y Lorsban® respectivamente. El segundo sistema empleó un aptámero de ADN para detectar CPF y mostró un LOD tan bajo como 0.01 µg L-1 con gran selectividad. Para avanzar en la aplicación de campo de las sondas fluorescentes, se diseñó, construyó y evaluó un dispositivo portátil en colaboración con el grupo de investigación GIMEL de la Universidad de Antioquia. Finalmente, se seleccionó el sistema enzimático (AChE) para la evaluación de 9 muestras de agua superficial de diferentes localidades rurales de Antioquia, Colombia, utilizando el prototipo portátil. Los resultados mostraron que algunos parámetros fisicoquímicos de las fuentes naturales de agua tienen influencia en el desempeño del sistema. Sin embargo, el prototipo pudo detectar CPF en muestras reales a partir de 1 µg L-1 y utilizando solo 150 µL de la muestra. Las ventajas de utilizar las sondas fluorescentes nanoestructuradas desarrolladas junto con un dispositivo portátil hecho a medida, abren el camino para futuras aplicaciones comerciales. Hasta donde sabemos, este es uno de los pocos trabajos que reportan la integración de nanomateriales con diferentes biomoléculas en sistemas ópticos para la detección de formulaciones de pesticidas en prototipos reales, con resultados prometedores.

PALABRAS CLAVE

Carbon dots, nanomaterials, biosensor fluorescente, pesticida, clorpirifos, acetilcolinesterasa, aptámero, prototipo, agua superficial.

ACKNOWLEDGEMENTS

This doctoral thesis represented a great opportunity to advance in the path of research, proposing solutions with an environmental focus hand in hand with key people and institutions. First, a special thanks to Professor Gustavo Antonio Peñuela for his unconditional support and creative freedom to propose innovative working routes, as well as the great autonomy he gave me. In the same way, I want to thank my co-advisor, Professor Juan Bernardo Cano, for leading the development of the portable device and risking the idea of using self-synthesized nanomaterials instead of commercial compounds.

To all the GDCON research group members for their great support in several technical activities of the project, which allowed me to go further with higher quality.

To the GIBEC research group and in general to the EIA Universidad for the collaborative work and support to finish my internship. Especially to my super lab team, Kaory Barrientos and Juan Pablo Arango. Similarly, the Crystallography Institute (IC-CNR, Italy) received me for a short but exciting period, on behalf of Covid 19 pandemic.

A very representative thank to the Ministry of Science, Technology, and Innovation - Minciencias, for the doctoral scholarship (Grant number 785 of 2017) that allowed me to make this dream come true.

Lastly, I would like to thank my husband Diego Alejandro for being by my side all these years and sharing the adventures of knowledge with me.

TABLE OF CONTENTS

LIST OF FIGURES

LIST OF TABLES

1. Introduction

1.1. General background

Pesticides are a group of chemicals released in the environment to kill undesirable organisms and preserve the agricultural produce (Rani and Shanker, 2018a). Pesticides include insecticides, herbicides, fungicides, disinfectants, among others (Kumar et al., 2018). According to their chemical structure, pesticides can be classified as organochlorines, organophosphates, carbamates, chlorophenols, and synthetic pyrethroids (Hamza et al., 2016).

Only between 10 and 15% of the total amount of pesticides applied is effective, leading to high environmental pollution (Rani and Shanker, 2018b). By 2020 (last available data), the top 5 countries with the highest annual consumption (data in thousands of tons) were the United States (407), Brazil (377), China (262), Argentina (245), and the Russian Federation (90) (FAO, 2022).

Organophosphate pesticides (OPs) are widely used in agriculture and in controlling vector-borne diseases (Rani and Shanker, 2018a); OPs's toxicity is based on the inhibition of the acetylcholinesterase enzyme (AChE). AChE is essential for the functioning of the central nervous system (CNS) of vertebrates and insects, and OPs blockage will cause an accumulation of the neurotransmitter acetylcholine (ACh), which interferes with the muscular responses and causes respiratory and myocardial defects and even death (Dzudzevic Cancar et al., 2016; Vinotha Alex and Mukherjee, 2021).

OPs have been reported to be responsible for more deaths in developing countries (South Asia and Latin America) than any other class of drug or chemical with an estimated fatality rate of 10% to 20% (Vale, 2015). The clinical effects of intoxication by OPs and carbamates are divided into muscarinic and nicotinic categories. The former presents excessive sweating, salivation, lacrimation, decrease in blood pressure among others (Cervantes et al., 2019). The last one is the most frequent type and includes fasciculations, cramps, weakness, and spasms, among others (Cervantes et al., 2019). Additionally, some studies link exposure to the OPs with possible cases of Parkinson's, with symptoms like tremors, lack of blinking, impaired speech, and swallowing (Chuang et al., 2017); however, long-term studies are needed to establish the confirmation.

OPs contamination of surface waters is mainly caused by dew spillage, runoff water, and drainage water (Hamza et al., 2016). Currently, some water treatment plants use fish as bioindicators to produce an alarm when toxic compounds are present at high-risk levels (Ali et al., 2020). However, this practice does not indicate the type of or amount of the pollutant present in the water. The use of advanced techniques such as gas chromatography (GC) and liquid chromatography are needed for the pollutants characterization (LC) (Marican and Durán-Lara, 2018).

Although GC and LC are excellent for the analysis of pesticides with high sensitivity and reproducibility, even at very low concentrations, many drawbacks, such as the need for sophisticated equipment, long times, tedious sample preparation and purification steps, limit their

on-site application, particularly in cases of emergency and in remote areas (Gaviria et al., 2023). Therefore, great efforts have been made to the research of alternative or complementary strategies to detect pesticides in an easy, fast, precise, and user-friendly way.

The on-site detection of pesticides could be achieved with biosensors, employing biomarker interactions such as enzyme-substrate, antigen-antibody reactions, and recognition of DNA or RNA aptamers (Gaviria et al., 2023). For the transduction and interpretation of the signal, biosensors use electrical properties (current, resistance, impedance); optical properties (colorimetry, refractive index, luminescence, fluorescence), among others. The changes in the transduction variables can be measured through digitalization and data analysis (H. Li et al., 2018; Zhao et al., 2018). In recent years, optical biosensors based on nanomaterials have been developed with lower detection limits and greater stability. The application of nanomaterials, including Carbon Dots (CD), can significantly improve the performance of the systems (Abdul et al., 2019). CDs have gained a lot of attention because they have optoelectronic properties like quantum dots, especially when it comes to fluorescence (M. L. Liu et al., 2019).

Since OPs and their metabolites are toxic and prevalent in the environment, there is a need to develop sensitive and selective systems that allow online detection of those substances in drinking-water treatment plants, thus facilitating rapid decision-making for mitigating or preventing adverse effects. This thesis addressed the following research question: How to achieve field detection and real-time monitoring of organophosphate pesticides in water, with adequate sensitivity and specificity?

Organophosphate pesticides

OPs are the most used insecticides worldwide. These compounds are esters of phosphoric acid linked to a wide variety of alcohols, most of them fat-soluble (Rathnayake and Northrup, 2016). OPs structure exhibits a central phosphorus atom, either with oxygen with a double bond (P = O) or a sulfur atom linked by a double bond (P = S), two radical groups (R1 and R2), are generally simple alkyl or aryl groups and a group X which can be aliphatic, aromatic or heterocyclic groups attached to the phosphorous atom and acts as a branched leaving group (Vinotha Alex and Mukherjee, 2021).

According to the WHO, pesticides and their active ingredients are classified based on dermal and oral toxicity (LD50) in rats (WHO, 2009) (Table 1-1). Colombian resolution 631 of 2015 has regulated the maximum permissible level of pesticides belonging to categories Ia, Ib, and II in wastewater. The established values are 0.001mg/L for Ia, 0.05mg/L for Ib and 0.10mg/L for II (except organochlorines, which continue to be at 0.05mg/L) (Ministerio de medio ambiente y desarrollo sostenible, 2015). On the other hand, resolution 2115 of 2007 has defined the general limit of any pesticide in drinking water at 0.1 µg/L (Ministerio de la protección social, 2007). This value agrees with European regulations (Europeo et al., 2006), challenging the sensitivity of newly developed biosensors.

Table 1-1. Pesticide classification according to the WHO.Modified from (WHO, 2009)

WGO Class		LD_{50} for the rat (mg/kg body weight)	
		Oral	**Dermal**
Ia	Extremely hazardous	<5	<50

Ib	Highly hazardous	5-50	50-200
II	Moderately hazardous	50-2000	200-2000
III	Slightly hazardous	Over 2000	Over 2000
U	Unlike to present acute hazard	5000 or higher	

Some studies in African populations have detected levels of OPs like Diazinon and Malathion in different water sources for human consumption, which are twofold higher than the daily intake dose recommended by the European drinking water guide (Mekonen et al., 2016). Among OPs, Chlorpyrifos (CPF) is the main active principle used in a wide range of crops, and it has a relatively low persistence and low toxicity. However, CPF and CPF-oxon as common bioactive products, block AChE. In Colombia, studies carried out on water samples for rural consumption and milk samples from a livestock area showed the presence of CPF in concentrations up to 100% above that indicated in resolution 2115 of 2007 for toxicological category II products. (moderately toxic) (Rodriguez et al., 2013).

OPs cause mainly neurotoxic effects in humans: cholinergic syndrome, intermediate syndrome, organophosphate-induced delayed polyneuropathy, and organophosphate-induced chronic neuropsychiatric disorder (Jokanović, 2018). OPs exhibit neurotoxicity because they can block the acetylcholinesterase enzyme (AChE) irreversibly (Vinotha Alex and Mukherjee, 2021)(Mostafalou and Abdollahi, 2018). AChE acts as a neurotransmitter both, in the CNS and at the skeletal muscle nerve junction. Each AChE molecule breaks down approximately 25,000 ACh molecules per second into choline and acetic acid (Vinotha Alex and Mukherjee, 2021). The choline produced is transported back to the nerve terminals to be reused for new ACh molecules.

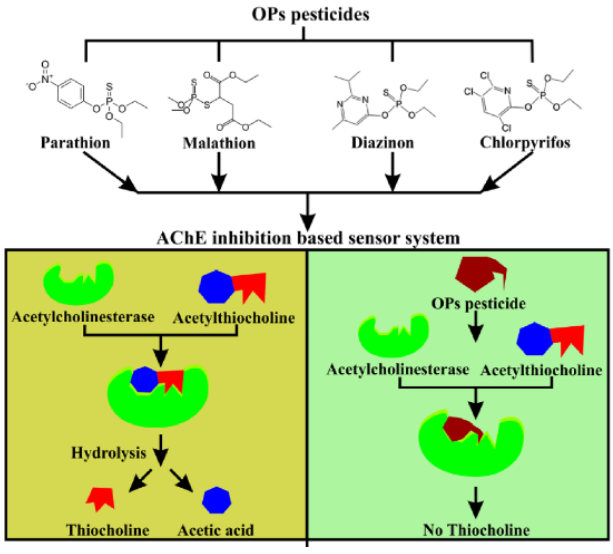

Figure 1-1. Some OPs structures and the mechanism of AChE inhibition. (Vinotha Alex and Mukherjee, 2021)

OPs presence in water sources has increased attention because those compounds are highly hydrophilic, increasing the probability of human consumption. Additionally, the degradation products could be more toxic than the original OPs, such as oxons, diesters, and dieldrin (King and Aaron, 2015). OPs toxicity is not due to a single molecular event or interaction but to a cascade of

events beginning with exposure and culminating in the expression of one or more toxic endpoints. This cascade includes adsorption, distribution, metabolism (detoxification and activation), metabolite distribution, interaction with cellular macromolecules (such as RNA, DNA, and protein), repair, and excretion. The processes involved may be reversible and could be modified by chemical and physiological interactions (Hodgson, 2012).

In this thesis, two widely used OPs were selected as model compounds: chlorpyrifos (CPF) and profenofos (PF). Both pesticides belonging to the toxicological category number II (moderately hazardous) and their structures are presented in Figure 1-2.

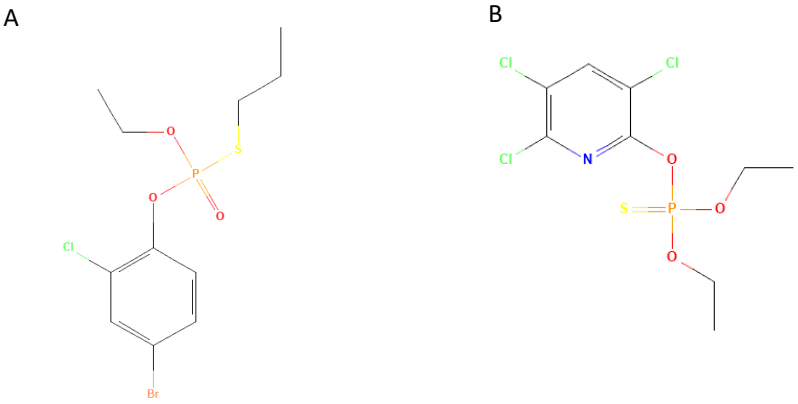

Figure 1-2. Chemical structures of A) Profenofos (National Center for Biotechnology Information, 2022) *and B) Chlorpyrifos* (National Center for Biotechnology Information., 2022) *as model compounds of the thesis.*

References

Abdul, S., Nor, R., Zobir, M., 2019. Synthesis, Technology and Applications of Carbon Nanomaterials. Elsevier, Oxford.

Ali, D., Almarzoug, M.H.A., al Ali, H., Samdani, M.S., Hussain, S.A., Alarifi, S., 2020. Fish as bio indicators to determine the effects of pollution in river by using the micronucleus and alkaline single cell gel electrophoresis assay. J King Saud Univ Sci 32, 2880–2885. https://doi.org/10.1016/j.jksus.2020.07.012

Arvand, M., Mirroshandel, A.A., 2017. Highly-sensitive aptasensor based on fluorescence resonance energy transfer between L-cysteine capped ZnS quantum dots and graphene oxide sheets for the determination of edifenphos fungicide. Biosens Bioelectron 96, 324–331. https://doi.org/10.1016/j.bios.2017.05.028

Cervantes, S., Estefanía, I., Valverde, M., Monge, D., del Pilar, M., 2019. Intoxicación por organofosforados 36.

Chuang, C.S., Su, H.L., Lin, C.L., Kao, C.H., 2017. Risk of Parkinson disease after organophosphate or carbamate poisoning. Acta Neurol Scand 136, 129–137. https://doi.org/10.1111/ane.12707

Dzudzevic Cancar, H., Soylemez, S., Akpinar, Y., Kesik, M., Göker, S., Gunbas, G., Volkan, M., Toppare, L., 2016. A Novel Acetylcholinesterase Biosensor: Core-Shell Magnetic Nanoparticles Incorporating a Conjugated Polymer for the Detection of Organophosphorus Pesticides. ACS Appl Mater Interfaces 8, 8058–8067. https://doi.org/10.1021/acsami.5b12383

Europeo, E.L.P., Consejo, E.L., Uni, D.E.L.A., Europeo, P., 2006. Directiva 2006/118 Aguas Subterraneas 2006.

FAO, 2022. Pesticides Use [WWW Document]. FAOSTAT.

Gaviria, M.I., Arango, J.P., Barrientos, K., Jaramillo, M., 2023. Optical Biosensors for Environmental Analysis, in: Encyclopedia of Sensors and Biosensors. Elsevier, pp. 528–548. https://doi.org/10.1016/b978-0-12-822548-6.00156-4

Hamza, R.A., Iorhemen, O.T., Tay, J.H., 2016. Occurrence, impacts and removal of emerging substances of concern from wastewater. Environ Technol Innov. https://doi.org/10.1016/j.eti.2016.02.003

Hodgson, E., 2012. Pesticide biotransformation and disposition, 3rd ed. Elsevier, London.

Jokanović, M., 2018. Neurotoxic effects of organophosphorus pesticides and possible association with neurodegenerative diseases in man: A review. Toxicology 410, 125–131. https://doi.org/10.1016/j.tox.2018.09.009

King, A.M., Aaron, C.K., 2015. Organophosphate and Carbamate Poisoning. Emerg Med Clin North Am 33, 133–151. https://doi.org/10.1016/j.emc.2014.09.010

Kołątaj, K., Krajczewski, J., Kudelski, A., 2020. Plasmonic nanoparticles for environmental analysis. Environ Chem Lett 18, 529–542. https://doi.org/10.1007/s10311-019-00962-1

Kumar, S., Kaushik, G., Dar, M.A., Nimesh, S., López-Chuken, U.J., Villareal-Chiu, J.F., 2018. Microbial Degradation of Organophosphate Pesticides: A Review. Pedosphere 28, 190–208. https://doi.org/10.1016/S1002-0160(18)60017-7

Li, C., Zhang, G., Wu, S., Zhang, Q., 2018. Aptamer-based microcantilever-array biosensor for profenofos detection. Anal Chim Acta 1020, 116–122. https://doi.org/10.1016/j.aca.2018.02.072

Li, H., Huang, X., Huang, J., Bai, M., Hu, M., Guo, Y., Sun, X., 2022. Fluorescence Assay for Detecting Four Organophosphorus Pesticides Using Fluorescently Labeled Aptamer. Sensors (Basel) 22. https://doi.org/10.3390/s22155712

Li, H., Yan, X., Lu, G., Su, X., 2018. Carbon dot-based bioplatform for dual colorimetric and fluorometric sensing of organophosphate pesticides. Sens Actuators B Chem 260, 563–570. https://doi.org/10.1016/j.snb.2017.12.170

Liu, M.L., Chen, B. Bin, Li, C.M., Huang, C.Z., 2019. Carbon dots: Synthesis, formation mechanism, fluorescence origin and sensing applications. Green Chemistry 21, 449–471. https://doi.org/10.1039/c8gc02736f

Liu, Q., Wang, H., Han, P., Feng, X., 2019. Fluorescent aptasensing of chlorpyrifos based on the assembly of cationic conjugated polymer-aggregated gold nanoparticles and luminescent metal–organic frameworks. Analyst 144, 6025–6032. https://doi.org/10.1039/c9an00943d

Marican, A., Durán-Lara, E.F., 2018. A review on pesticide removal through different processes. Environmental Science and Pollution Research 25, 2051–2064. https://doi.org/10.1007/s11356-017-0796-2

Mekonen, S., Argaw, R., Simanesew, A., Houbraken, M., Senaeve, D., Ambelu, A., Spanoghe, P., 2016. Pesticide residues in drinking water and associated risk to consumers in Ethiopia. Chemosphere 162, 252–260. https://doi.org/10.1016/j.chemosphere.2016.07.096

Ministerio de la protección social, 2007. Resolución 2115/2007. Gaceta Oficial 23. https://doi.org/10.1017/CBO9781107415324.004

Ministerio de medio ambiente y desarrollo sostenible, 2015. Resolución 631 de 2015. Colombia.

Mostafalou, S., Abdollahi, M., 2018. The link of organophosphorus pesticides with neurodegenerative and neurodevelopmental diseases based on evidence and mechanisms. Toxicology 409, 44–52. https://doi.org/10.1016/j.tox.2018.07.014

National Center for Biotechnology Information, 2022. PubChem Compound Summary for CID 2730, Chlorpyrifos. [WWW Document].

National Center for Biotechnology Information., 2022. PubChem Compound Summary for CID 38779, Profenofos. [WWW Document].

Rani, M., Shanker, U., 2018a. Degradation of traditional and new emerging pesticides in water by nanomaterials: recent trends and future recommendations. International Journal of Environmental Science and Technology 15, 1347–1380. https://doi.org/10.1007/s13762-017-1512-y

Rani, M., Shanker, U., 2018b. Degradation of traditional and new emerging pesticides in water by nanomaterials: recent trends and future recommendations. International Journal of Environmental Science and Technology 15, 1347–1380. https://doi.org/10.1007/s13762-017-1512-y

Rathnayake, L.K., Northrup, S.H., 2016. Structure and mode of action of organophosphate pesticides: A computational study. Comput Theor Chem 1088, 9–23. https://doi.org/10.1016/j.comptc.2016.04.024

Rodriguez, D.C., Carvajal, S., Peñuela, G., 2013. Effect of chlorpyrifos on the inhibitio of the enzyme acetylcholinesterase by cross-linking in water suppky samples and milk from dairy cattle. Talanta 1–7.

Shen, Z., Xu, D., Wang, Guangxian, Geng, L., Xu, R., Wang, Guanjie, Guo, Y., Sun, X., 2022. Novel colorimetric aptasensor based on MOF-derived materials and its applications for organophosphorus pesticides determination. J Hazard Mater 440. https://doi.org/10.1016/j.jhazmat.2022.129707

Singh, P., Kumar, S., Verma, S.K., 2023. Development of fluorescent aptasensor for detection of acephate by utilizing graphene oxide platform. Talanta 252. https://doi.org/10.1016/j.talanta.2022.123843

Vale, A., 2015. Organophosphorus insecticide poisoning.

Vinotha Alex, A., Mukherjee, A., 2021. Review of recent developments (2018–2020) on acetylcholinesterase inhibition based biosensors for organophosphorus pesticides detection. Microchemical Journal 161. https://doi.org/10.1016/j.microc.2020.105779

Wang, G., Dong, H., Han, J., Zhang, M., Huang, J., Sun, J., Guan, F., Shen, Z., Xu, D., Sun, X., Guo, Y., Zhao, S., 2022. Interference-resistant aptasensor with tetrahedral DNA nanostructure for profenofos detection based on the composites of graphene oxide and polyaniline. Bioelectrochemistry 148. https://doi.org/10.1016/j.bioelechem.2022.108227

WHO, 2009. The who reccomended calssification of pesticides by hazard.

Zhao, F., Wu, J., Ying, Y., She, Y., Wang, J., Ping, J., 2018. Carbon nanomaterial-enabled pesticide biosensors: Design strategy, biosensing mechanism, and practical application. https://doi.org/10.1016/j.trac.2018.06.017

Zhu, C., Liu, X., Li, Y., Yu, D., Gao, Q., Chen, L., 2023. Dual-ratiometric electrochemical aptasensor based on carbon nanohorns/anthraquinone-2-carboxylic acid/Au nanoparticles for simultaneous detection of malathion and omethoate. Talanta 253, 123966. https://doi.org/10.1016/j.talanta.2022.123966

1.2. Research aim

This research is focused on the development of an optical biosensor for the detection of organophosphate pesticides in water sources. This doctoral thesis is part of the Project "Redes de biosensores aplicados a la detección de contaminantes tóxicos en fuentes naturales que abastecen a las plantas de potabilización" funded by Minciencias (code 111571451059, contract number FP44842-147-2016). To achieve this aim, three specific objectives were established 1) define the biomediator- transductor more appropiate for the detection of model pesticides, according to actual law; 2) evaluate appropriate strategies for the detection and signal conditioning of the bioremediator-transductor couple selected; and, 3) establish the biosensor performance through real water sources evaluation. Additionally, carbon quantum dots (CD) used as a fluorescent transductor were synthesized in cooperation with Universidad EIA before the experimental development of the biosensors (Appendix I: Synthesis, Characterization and Ecotoxicity Evaluation of Biochar-Derived Carbon Dots from Spruce Tree, Purple Moor-Grass and African Oil Palm.). For the first objective, acetylcholinesterase enzyme (AChE) which has been widely reported for pesticide detection, was used as a model system to evaluate the appropriate protocols and performance of CD to detect chlorpyrifos (CPF) and profenofos (PF) in an innovative system. In the same objective and based on the previous results, a newly technology based on aptamers was tested. For that, a DNA aptamer was identified and used to detect CPF and PF, using a molecular approach. Considering the AChE and aptamer systems, the second objective was carried out simultaneously with the first one, and the results were used to cooperate with GIMEL research group in the development of the portable prototype. Finally, despite the good sensitivity of the aptameric system, the stability and wider linear range of the AChE system showed better potential for real implementation. Considering that for objective 3) only the AChE system was used and 9 rural sites in Antioquia were selected to obtain superficial water samples and evaluate CPF recovery.

The above shows the potential of developing functional biosensors with remarkable competitive advantages as the use of value-add nanomaterials as CD, obtained in a revalorization process of biochar under a circular bioeconomy approach. Also, the biological platform based con CD and AChE could be adapted to detect other pollutants in different matrices and the aptameric system could be optimized for more sophisticated applications. Moreover, the developed prototype enhanced the properties of CD for biosensing applications and paves the way for the implementation of portable systems based on nanotechnology for the detection of environmental pollutants.

1.3. Thesis scope

The Ph.D. thesis is arranged in five chapters, each self-contained as a journal paper (some already published, under review or in the process of being published). The chapters are connected in sequence as described below:

Chapter 1: this chapter is a state of the art of the different types of *Optical biosensing techniques* not just for OPs detection but for different environmental targets. This chapter shows that optical biosensors are both sensitive and straightforward. In this review, a discussion was made about how to detect high-risk compounds including metal ions, pesticides, toxins, and so-called emerging contaminants. Simple strategies, such as direct detection of these pollutants that cause colorimetric changes, are described, as well as more complex methods, such as those relying on "turning on" fluorescence and bioluminescence principles. The chapter concludes that nanomaterials and synthetic biology have emerged as viable options for improving performance, so the advance to further incorporate CD and aptamers is well justified.

Chapter 2: considering the novelty of nanomaterials for biosensing applications, this chapter is also part of the state of the art and talks about *Nanomaterial-based fluorescent biosensors,* focusing on pesticides and integrating a critical position about the advantages and drawbacks of those systems. In this chapter, the advanced optoelectronic properties of nanomaterials show that those systems are quite sensitive and simple. The use of nanomaterials like carbon dots (CD), quantum dots (QD), gold nanoparticles, nanoclusters, graphene (G), graphene oxide (GO), transition metal dialcogens (TMDC) and organometallic frameworks (MOF), for biosensing applications are reviewed. This review conducts a critical analysis of the operating principle of different nanomaterial-based fluorescent biosensors. This chapter allowed us to extract valuable information and protocols to apply in the development of enzymatic (AChE) and aptameric systems, based on the integration of CD and GO.

Chapter 3: This chapter is an original paper and shows the results of the *enzymatic (AChE) system development* and preliminary evaluation under close-to-real conditions for the detection of pure CPF, PF and a commercial formula called Lorsban®. In this work, naturally fluorescent and non-toxic CD were conjugated with acetylcholinesterase (AChE) as a bioreceptor, to produce a fluorescent biosensor. The results show a high sensibility, with a very low limit of detection for CPF and Lorsban®. PF did not show any recovery signal. The system is one of the few works reporting the detection of commercial pesticide formulations.

Chapter 4: Based on the results of chapter 3, this chapter is an original paper that shows the results of the *Aptameric system development,* integrating the evaluation of real samples and the explanation about detection based on the molecular theory of docking energy, not commonly found in reported biosensors works. In this chapter, a good sensibility for CPF detection is found, but the reproducibility and stability of the system should be improved. This paper gives valuable information

for the academic community about the implementation of aptamers for environmental biosensing applications.

Chapter 5: In this final chapter, the process of the *Portable prototype development and its implementation for the evaluation of real samples* is showed. This original paper described the electronic and hardware development of the prototype, and the optimization of the key control parameters. This paper also shows the process of the real evaluation protocol, focusing on the sample evaluation under three different methods: i) UPLC chromatography as standard gold; ii) AChE system with a Fluorimeter analyzer; and iii) AChE system with the portable analyzer. This triple comparison allows extraction recovery and reproducibility parameters for future optimization and field implementation.

2. Optical Biosensors for Environmental Analysis

Abstract

The need for quick detection of pollutants in various matrices has led to the development of optical biosensors in the environmental field. These systems are both sensitive and straightforward. We talk about how to detect high-risk compounds including metal ions, pesticides, toxins, and so-called emerging contaminants. Simple strategies, such as direct detection of these pollutants that cause colorimetric changes, are described, as well as more complex methods, such as those relying on "turning on "fluorescence and bioluminescence principles. Nanomaterials and synthetic biology have emerged as viable options for improving performance. In this scenario, optical biosensors use bioreceptors such as antibodies, enzymes, or aptamers to achieve specific pollutant detection in real samples. The operating principle of colorimetric, surface plasmon resonance, fluorescence, and bioluminescence-based biosensors for environmental applications is critically examined in this chapter. The methods 'benefits and drawbacks are discussed, as well as suggestions for future approaches and the possibility of massification of these systems.

Published in:
Encyclopedia of Sensors and Biosensors. Elsevier
Date: 2023
Cite as:
Gaviria, M. I., Arango, J. P., Barrientos, K., & Jaramillo, M. (2023). Optical Biosensors for Environmental Analysis. In *Encyclopedia of Sensors and Biosensors* (pp. 528–548). Elsevier. https://doi.org/10.1016/b978-0-12-822548-6.00156-4

2.1. Introduction

Environmental degradation and its consequences, such as climate change, are major global concerns present in countries' political and economic agendas (United States environmental protection agency, 2016; Sousa et al., 2018). According to estimates, 30% more water, 40% more food, and 50% more energy will be needed by 2030 (Ellen MacArthur Foundation, 2015). Obtaining enough water, food, and energy implies the use of chemical compounds, thus leading to big pollution problems in soils, water, and the atmosphere (Stahel, 2016).

Compounds used to boost agricultural productivity, heavy metals resulting from mining-industrial activities, and so-called emerging pollutants of various and primarily urban origin, pose a threat to basic sanitation. Acute exposure to several compounds, grouped for several years under the term emerging pollutant, can produce endocrine consequences. Personal hygiene goods, household cleaning products, cosmetic additives, sunscreens, plastics industry supplies, and drug residues are all included in this category (Mirzaei et al., 2016). On the other hand, pesticide exposure is related to diseases such as lymphoma (Hodgkin's) (Luo et al., 2016), Parkinson's (Brouwer et al., 2017), and cancer (Paul et al., 2018). Heavy metals are found in water sources, particularly in impoverished or developing countries with a big extractive economy. Heavy metals can generate soluble complexes that are transported and dispersed across ecosystems until they are absorbed into the food chain (Londoño Franco et al., 2016). All the pollutants have bioaccumulation potential due to low concentrations, making them difficult to detect for current analytical systems. The most widely used methods for the detection of environmental pollutants are those based on electrochemical measurements, liquid chromatography-tandem mass spectrometry (LC-MS), and enzyme-linked immunosorbent assay (ELISA) (Timofeyenkoet al., 2006;Trojanowicz et al., 2011;Liu et al., 2016). Apart from the pretreatment of the samples, the specialized instruments for the detection of the signal, and the long times for obtaining results using these techniques; many of them do not carry out the requirements to be used outside the laboratory. Biosensors have been developed rapidly as a complement to standard analytical methods for the detection of contaminants of concern in water sources and soils, due to advantages such as simplicity of handling, the low-cost potential of their components, and the possibility of real-time quantification (Gaviria-Arroyave et al., 2020). Biosensors are analytical devices that have a biomediator element (which is responsible for analyte recognition) in contact with a transducer element (in charge of converting the interaction into a measurable signal). Biomediators and transducers come in different shapes and sizes, with optical and electrochemical biosensors having the most potential for detecting contaminants with sufficient sensitivity and specificity (Gaviria-Arroyave et al., 2020). Based on changes in signals like fluorescence, absorbance, or luminescence, an optical sensor could provide a fast, and low-cost approach for pollutants detection in different environmental matrices (Yan et al., 2018b). Recognition components such as enzymes, antibodies, molecularly imprinted polymers, aptamers, and host-guest recognizers attract growing interest from scientists looking to improve sensor analytical performance. In this chapter, we will discuss the detection of environmental pollutants

with optical biosensors belonging to the following categories: (i) colorimetric, (ii) surface plasmon resonance (SPR), (iii) fluorescence, and (iv) bioluminescence. Basic strategies will be compared with advanced mechanisms to give a comprehensive view of the use of optical systems in environmental monitoring.

2.2. Colorimetric-based biosensors

Colorimetric sensors (CL) transduce the biological recognition event into a color change, and its use date back even long before the beginning of chemistry (Kong et al., 2014;Li et al., 2019). The integration of analytical science with nanotechnology and biotechnology has allowed the synthesis of CL based on nanoparticles (NPs) (Cheng et al., 2016;Li et al., 2021b;Qiang et al., 2020;Kimet al., 2021), quantum dots (Hwang et al., 2021), nanotubes/nanofibers (CNTs/CNFs) (De Almeida et al., 2015), among other two-dimensional materials; and biomimetic systems such as nano enzymes (Wang et al., 2016b;Kong et al., 2017) showing great potential for the fabrication of increasingly robust devices (Zhu et al., 2021). Depending on the nanomaterial or optical probe used for the development of the CL, different transduction mechanisms are used, such as Surface Plasmon Resonance (Patel et al., 2015;Donget al., 2016;Bhattacharjee et al., 2018;Kim et al., 2021), mimic enzymatic catalyzation (Wang et al., 2016b;Kong et al., 2017), fluorescence modulation (Cheng et al., 2016), ligand-receptor binding (Duyen et al., 2017), and based on photonic structures (Wang and Zhang, 2013). The development of CL has attracted attention due to the high sensitivity, the speed of their response, color changes that can be detected by the naked eye, not requiring specialized instrumentation, it is ease to manufacture and can be easily applied with real samples (Reddy et al., 2017;Liu et al., 2020). Therefore, they have the potential to be used in the development of analytical detection techniques of biomarkers that represent biological risks and dangers to human health.

Emerging pollutants

Emerging pollutants (EP) are a diverse group of chemical and biological agents whose effects are causing growing concern because of the inability of the traditional wastewater plants systems to remove them (Hamza et al., 2016), and the great diversity of chemical structures. Pharmaceutical, personal care products, surfactants, and disinfection by-products, among others, are now considered EP. The effects of EP on human health are related to geno and cytotoxicity, causing obesity, diabetes, and cardiovascular and reproductive disorders (Bilal et al., 2019), the latter related to estrogenic activity. Some of the systems developed to detect emerging pollutants use nanomaterials to mimic the behavior of enzymes since these nanomaterials are more stable under extreme reaction conditions and are more cost-effective candidates (Gao et al., 2008). Wang et al. (Wang et al., 2016b) and Kong et al. (Konget al., 2017) developed a system based on Fe_3O_4 and $ZnFe_2O_4$ magnetic nanoparticles (MNPs), respectively. These MNPS can catalyze the colorimetric reaction between $H_2O_2$and 3,30,5,50-tetramethylbenzidine (TMB) in a blue product. Kong et al. used the affinity of the Tetracyclines (TC) (oxytetracycline (OTC), tetracycline (TC), and doxycycline (DOX)) with MNPs to markedly improve the colorimetric reaction; while Kong et al. used a microfluidic paper-based analytical device (mPADs) with the molecularly imprinted polymer (MIP) technique on membranes to detect bisphenol-A. This technique could be used for the detection of other analytes

since MIP leaves reactive groups with the ability to bind to a specific molecule, this affinity is due to the polymerization in the presence of the target (Vasapollo et al., 2011). Another developed method is the one reported by My Duyen et al. (Duyen et al.,2017), this system uses an In vitro transcription/translation (IVVT) system from *Escherichia coli (E. coli*), DNA template (LacZ), and the colorimetric substrate CPGR; which are embedded into paper disks and then freeze-dried. The disks are rehydrated with real water samples, and in the absence of antibiotics, the DNA template is transcribed to mRNA, and the protein-GAL is synthesized. This protein hydrolyzes the colorimetric substrate, giving a color change from yellow to purple. This device showed limits of detection (LODs) of 0.5, 2.1, 0.8, and 6.1 mg mL^{-1} for paromomycin, tetracycline, chloramphenicol, and erythromycin, respectively.

Metal ions and pesticides

Metal ions and organic compounds are the most common environmental pollutants with a wide impact on public health and food safety. Their toxicities are usually divided into acute and chronic toxicity based on the exposure time, making early detection and analysis of these pollutants are indispensable. For cyanide detection in drinking and industrial wastewater, the use of biosensors with a wide detection range is a must. Cheng et al. (Cheng et al., 2016) developed a dual fluorescence and colorimetry system for small and wide-range detection, respectively. The turn-on fluorescent system uses the Fluorescein isothiocyanate (FITC) probe, which, in the presence of low concentrations of cyanide [0–7mM] is removed from the surface of the AuNPs, restoring their respective fluorescence. While the colorimetric system uses polysorbate 20 (PS20) as a stabilizer for AuNPs against high ionic strength. But at high concentrations of cyanide [150–300 mM], the system loses stability, generating the aggregation of the AuNPs, and therefore, a color change. Although the sensor showed a response when evaluated with real samples and selectivity for the analyte with various metal ions; the fluorescence system cross-reacts with Pb^{2+} and Hg^{2+}. The methodology that uses interactions with different molecules to induce the aggregation of NPs, and produce a color change, has been widely used for the detection of toxins and bacteria, as well as some pesticides and heavy metals. Efforts on portable devices have been made. For instance, Castañeda et al. (Castañeda-Loaiza et al., 2019) developed a disposable and miniaturized optical sensor for the detection of aluminum, which proposes to immobilize the colorimetric reagent pyridoxalsalicyloylhydrazone (PSH) on poly(styrene-divinylbenzene) (SDB) membrane disks for the construction of a colorimetric solid-phase extraction (C-SPE) system. This technique allows selectively concentrating the analyte using PSH molecules that form complexes with various heavy metals and enables its quantification by diffuse reflectance spectroscopy. Although the device detected aluminum ions in real samples, such as aluminum leachates from cookware, antacid drugs, and a spray deodorant; it was found to have significant interference by some ions and salts. On the other hand, pesticides are compounds that are widely used for the prevention and control of pests, mainly in agriculture and forestry. The effects on the environment caused by the excess of pesticides in the soils include acidification, fertility and microbial biodiversity decrease, damage to fauna, and water pollution (Gaviria-Arroyave et al., 2020). Regarding human exposure, pesticides are related to nervous diseases like Alzheimer's and Parkinson's. For the colorimetric detection of heavy metals and pesticides, plasmonic nanomaterials, like, gold, silver, and copper nanoparticles are widely

used. AuNPs are preferred due to their easy functionalization and ability to display different colors depending on their shape, size, and aggregation state (Aldewachi et al., 2017;Liuet al., 2018b). AgNPs, compared to AuNPs, have a higher extinction coefficient and are more cost-effective, however, at defined concentrations, they can be toxic and are usually less reported in the literature for the development of CL (Vilela et al., 2012;Zhenget al., 2018). The use of CuNPs for biosensors is even more scarce, even though this material is widely used in many fields, the advantages of CuNPs are low cost and more availability compared to precious metals Au and Ag. However, they are susceptible to oxidation when exposed to air and have poor colloidal stability (Ayaz Ahmed et al., 2016;Gawande et al., 2016;Ojha et al.,2017). Roto et al. (2019) and Bhattacharjee et al. (Bhattacharjee et al., 2018) developed a CL based on AgNPs for the detection of Pb^{2+} and Hg (II), respectively. These metal ions are among the top five heavy metals present in water, and their elevated level in the blood can cause severe health problems (Kim and Lee, 2017). The aggregation of AgNPs was given by the adding Pb^{2+}. This is due to the presence of dithizone since this ligand forms a complex with Pb^{2+} ions more selectively than with other ions, and the sulfide group formed allows the generation of a covalent bond with the NPs. For the detection of Hg (II), the AgNPs were functionalized with mercapto benzo heterocyclic compounds (mercaptobenzooxazole (MBO), mercaptobenzoimidazole (MBI), and mercaptobenzothiazole (MBT)); patches of the silver surface were left exposed in the presence of the analyte, which leads to Age Hg nano alloys and therefore a color change. Although all the functionalization allowed to obtain LOD lower than the base value suggested by the WHO (2 ppb) (WHO, 2008), the functionalization with MBO was the one that produced the lower LOD (1.8 ppt). On the other hand, Dong et al. (Dong et al., 2016) developed a system based on AuNPs modified with gallic acid for the simultaneous detection of Cr (III) and Cr (IV) (Sun et al., 2015;DesMarias and Costa, 2019). For simultaneous detection, they used masking agents: citrate, thiosulfate, and ethylenediaminetetraacetic acid disodium salt (EDTA); the first two mask Cr (IV), allowing the aggregation and therefore the color change to occur exclusively due to the presence of Cr (III), while the function of EDTA is to mask Cr(III), allowing the detection to Cr (IV). Fahimi-Kasani et al. (Fahimi-Kashani and Hormozi-Nezhad, 2016) developed a CL based on AuNPs to discriminate organophosphate pesticides (Sidhu et al., 2019; Che Sulaiman et al., 2020). This device uses Hierarchical cluster analysis (HCA), linear discriminant analysis (LDA), and leave-one-out cross-validation methods to obtain classification patterns, quantitatively differentiate response profiles, and find the fingerprint of the analyzed pesticides. These patterns are obtained by aggregating the AuNPs at different pHs and ionic strengths in the presence of the analytes. Zheng et al. and Petel et al. (Patel et al., 2015; Zheng et al., 2018) developed systems based on AgNPs to detect 6-benzyl amino purine (6-BAP) and carbendazim, respectively. 6-BAP is the first generation of phytohormones (Sun and Zhang, 2006), and carbendazim is widely used to control fungal diseases in fruit crops (Singh et al., 2016). For these systems, the AgNPs were conjugated with Thioglycolic Acid (TA) and 4-aminobenzenethiol (ABT), improving the interaction between the analyte and the NPs. Finally, Ameen et al. (Ghoto et al., 2019) developed a CL based onCuNPs for the detection of dithiocarbamates (Ziram, Zineb, and Maneb) which are some of the most widely used sulfur-containing pesticides (Wang et al., 2020). For the colloidal stability of these NPs, CTAB (capping agent) was used due to its amphi-philic nature since the hydrophilic part creates a positive charge on the surface of the CuNPs, while the hydrophobic creates an obstacle for their agglomeration and

oxidation. The interaction of these NPs with pesticides occurs due to the small distance between their sulfur atoms, which makes them vulnerable to attraction with metallic elements, and due to the electrostatic interaction between the hydrophilic part of CTAB and the sulfides of the analytes. Other authors, such as Almeida et al. (De Almeida et al., 2015), developed the first generation of nanofiber-based CL strip to detect glyphosate in water (Gillezeau et al., 2019). This method uses nanofibers synthesized from poly (vinyl) alcohol (PVA) by electrospinning and doped with copper, forming a yellow complex when interacting with the intermediate molecule dithiocarbamicacid formed from the reaction that occurs between the amine group of glyphosate with carbon disulfide.

Toxins and pathogens

Most of the CLs for detecting toxins and bacteria are based on the aggregation of NPs and use aptamers as bioreceptor molecules. Aptamers are short oligonucleotide chains that can recognize and bind to a different target (Pehlivan et al., 2019). Kim et al. (Kimet al., 2021), Li et al. (X.Li et al., 2016b), and Qiang et al. (Qiang et al., 2020) developed CL aptasensors for the detection of *Bacillus carboniphilus,* microcystin-LR, and saxitoxin, respectively. These biosensors use the aptamers to protect the AuNPs from salt-induced aggregation, due to the negative charges that the aptamer contributes through its phosphate groups, however, in the presence of the target, the aptamer binds specifically to it, thus reducing its interaction with the AuNPs, leaving them exposed to salt-induced aggregation and therefore, a color change occurs (Yang et al., 2011; Li et al., 2016b). Other authors, such as Gupta et al. (Gupta et al.,2021), used AuNPs coated with graphene oxide (GO) to increase the surface area of the NPs and therefore increase the active and available sites to interact with the aptamers covalently immobilized by the carbodiimide method; the presence of the *E. coli* bacteria(target) promotes the agglomeration of GO coated AuNPs and therefore their color change (Figure 2-1).

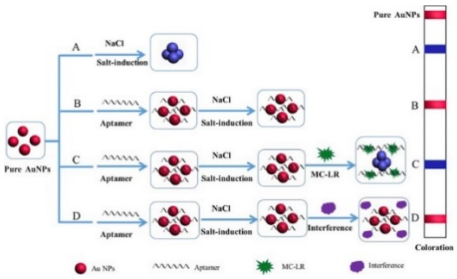

Figure 2-1. Schematic illustration for de CL and the mechanism for salt-induced aggregation of NPs. Reprinted from Ref. (X. Li et al., 2016) with permission from Elsevier.

2.3. Surface plasmon resonance - SPR biosensors

SPR biosensors are devices capable of detecting interactions between a biological recognition element immobilized on a gold film (functionalized surface) and the analyte in solution. An SPR sensor with suitable surface functionalization as a biorecognition element transforms into an SPR biosensor. Biological analytes, represented in Figure 2-2 as green dots, are shown to interact with the biorecognition elements, represented as brown Y. The large blue arrow indicates the flow of the

solution to be analyzed; practically, this flow is generated by a microfluidic system (Wijaya et al., 2011).

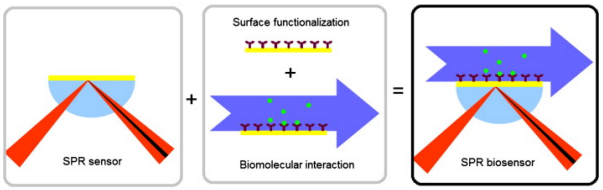

Figure 2-2. General scheme of an SPR biosensor. Reprinted from Ref. (Wijaya et al., 2011) with permission from Elsevier.

Figure 2-3 shows how in SPR systems, the incident polarized light is coupled by a glass prism on the biosensor chip coated with a thin layer of gold and integrated with a flow channel for continuous flow of buffer. At a defined incidence angle, the SPR phenomenon is seen as a dip in the intensity of the reflected light, characteristic of the specific angle of reflection. The shift of the angle of reflection from position 1 to position 2 reveals a change in the composition of the medium near the gold film because of the binding between the ligand and the analyte. The angular variations are recorded in resonance units (RU) and plotted versus time in a sensorgram (Brogioni and Berti, 2014; Ong et al., 2021).

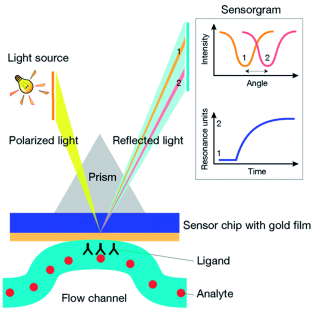

Figure 2-3. Schematic configuration of an SPR detector and sensorgram. Reprinted with permission from Ref. (Brogioni and Berti, 2014). Royal society of chemistry.

SPR measurements can be performed in real-time, allowing the user to collect kinetic data, as well as thermodynamic data. SPR is a versatile technique capable of detecting analytes over a wide range of molecular weights and binding affinities (McDonnell, 2001). SPR has been used for real-time monitoring of dynamic processes such as adsorption or degradation of specific components of interest without the need for labeling. Various substances, from small molecules to proteins and even living cells have been verified as detectable by these biosensors (Wang et al., 2013). Some research on SPR biosensor systems for the detection of environmental pollutants, including pesticides, pathogens, and heavy metals, is presented below.

Pesticides

The detection of atrazine (ATZ) using SPR biosensors is difficult since these types of analytes are small molecules present at the trace level (Xi Huang et al., 2009). To overcome this, the SPR

biosensor coupled with AuNPs as an amplification reagent has attracted attention for the detection of small molecules (M. et al., 2009). AuNPs are used not only as labels by antigen (antibody) conjugates but also as sensor elements by immobilization on the chip surface to amplify SPR signals (Sungho et al., 2009). Liu et al. used AuNPs to amplify the applied SPR signal in an in situ direct detection assay of ATZ. The best sensitivity was obtained for AuNPs with a diameter of 30.35 nm, and the minimum detectable concentration of atrazine was 1.0 ng mL-1 (Liu et al., 2015). In another work, Yilmaz et al. proposed the detection of atrazine by affinity nanosensor prepared by the attachment of atrazine imprinted poly (HEMA-MAAsp) nanoparticles onto the gold surface of SPR chips. The results showed that the imprinted nanosensor has high selectivity and sensitivity for ATZ with a LOD of 0.7134 ng mL^{-1} (Yılmaz et al., 2017). Overall, the pesticide imprinted SPR sensors are highly selective and sensitive.

Some works report the use of AuNPs for the detection of other types of pesticides. For instance, Dong et al. exploited a novel SPR detection system based on the analyte induced network architecture of supermolecules modified AuNPs on the chip Surface and Sulfonatocalix (pSC4) was used as a recognition molecule for paraquat (PQ), one of the widely used herbicides in the world [4]. PQ can mediate the aggregation of pSC4 capped AuNPs (pSC4-AuNPs) through the host-guest recognition, which can be used as signal amplification for PQ assay. The LOD for PQ was found to be 2.2 pM (Dong et al., 2018). Simultaneous detection of multiple pesticides has been researched. Saylan et al. fabricated molecularly imprinted nanofilms and integrated them with SPR sensors for sensitive, selective, rapid, real-time detection of SNZ, SMZ, and ATZ (Saylan et al., 2017). LODs of 0.095, 0.031, and 0.091 nM were found for Cyanazine (SNZ), Simazine (SMZ), and ATZ, respectively. These SPR sensors also hold great potential to be used as an alternative method for the existing pesticide monitoring approaches due to their reusability, fast response, and easy-to-use properties. Organophosphorus pesticides detection has been reported with recent SPR systems. Tan et al. developed an ultrasensitive and highly selective detection method using SPR combined with molecularly imprinted films (MIF) for the detection of methyl parathion (Tan, Ahmad and Wei, 2015). In this work, the minimum detectable concentration was 10-13 mol L^{-1}. The detection of another type of organophosphate such as triazophos was proposed by Guo et al. They described a non-competitive immunoassay for trace detection of triazophos using a direct SPR biosensor (Guo et al., 2018). The biosensor assay showed high specificity and a low LOD of 0.096 ng mL^{-1}. The results showed that the developed immunosensor could be used as a fast, convenient, and reliable tool to regularly monitor triazophos in water sources.

Pathogens

Waterborne disease-related bacteria is the world's most significant health predicament. (P.S. et al., 1999). A specific example is Legionellosis a severe form of pneumonia caused by the opportunistic pathogen known as Legionella, bacteria commonly found in poor drinking water. The use of SPR for whole-cell bacterial detection suffers from inherent drawbacks such as the limited range of the evanescent electromagnetic field wave produced by the instrument, the similarity of the refractive index (RI) of the bacterial cytoplasm and the aqueous medium; and, the diffusion-limited mass transport of the bacteria to the metal-dielectric Surface (Galvan et al., 2018),(Torun et al., 2012).

However, in a recent investigation, it was proposed a Surface Plasmon Resonance Imaging (SPRi) based on titration assay for whole Legionella pneumophila cell detection (Saad et al., 2022). This work shows for the first time that aptamers can be adapted in this format for SPRi-based detection of bacteria providing enhanced specificity and simplicity. Aptamers were used to detect L. pneumophila down to a LOD of 104.3 cells mL^{-1}. The use of aptamers improves this method by minimizing complex handling steps as well as costs since antibodies are less stable and more expensive to produce (Saad et al., 2022).

Endocrine-disrupting chemicals (EDCs)

Bisphenol A (BPA) belongs to the group of xenoestrogen compounds called EDCs (Xiang-li et al., 2007). BPA could bind to estrogen receptors in wildlife and mimic the actions of endogenous estrogen, causing reproductive disorders. The endocrine-disrupting properties of these compounds can lead to feminization and carcinogenesis in numerous organisms (Grzeskowiak et al., 2009).
The use of SPR immunosensors for the detection of trace levels of BPA has been reported (Bakar et al., 2013), but these sensors have not been found to have high sensitivity for the detection of small molecules (Wu et al., 2015). MIF technique is playing an important role in the production of sensitive SPR sensors (Sener et al., 2011), (Osman et al., 2013). Shaikh et al. proposed a sensitive SPR sensing protocol based on MIF for the detection of BPA (Shaikh et al., 2015). The poly (EGDMA-MAPA-VI) based thin nanofilm highly selective for BPA was prepared on the SPR sensor via radical polymerization under UV light. A water-compatible MIF has been developed for rapid, sensitive, and label-free detection of BPA in aqueous solutions prepared in Milli Q water, tap water, and synthetic wastewater. The real-time response allows the detection of BPA with concentrations ranging from 0.08 to 10 µg L^{-1} with LOD and LOQ values of 0.02 and 0.08 µg L^{-1} in Milli Q water, 0.06 and 0.2 µg L^{-1} in tap water, and 0.08 and 0.3 µg L^{-1} in synthetic wastewater, respectively. Those results suggest that the imprinted SPR sensing method can be used as a promising alternative for the detection of BPA.

Metal ions

The presence of mercury and other so-called heavy metal ions in the environment is a threat for human health (C. Liu et al., 2018). In the last several years, some 2D material flake (such as MoS_2, GeSe, $Bi2Se_3$) modified SPR sensors have been used for the detection of heavy metal ions (Hg2+, Pb^{2+}, among others) (Xue, Qi and Hu, 2019; Zhao et al., 2020). Graphene, transition metal dichalcogenides (TMDs), and metal oxide nanosheets, all these two-dimensional (2D) materials are the main candidate materials for next-generation sensors advisable to future electronics due to their unique properties such as high surface-to-volume ratio, numerous active edge sites, flexibility, high sensitivity, and transparency at room temperature. Sensitivity enhanced SPR sensor was fabricated to detect Hg^{2+} through Au-film adjusted by overlayered 2D Material NbS_2 nanosheets, which have unique photoelectric characteristics, high refractive index, and large specific surface area. The NbS_2 modified sensor film exhibits a LOD of 1.0 pM (Jia et al., 2021).

For the effectiveness improvement of SPR analysis, strategies like depositing a sensing material's thin film on the metal film have been studied. The presence of this sensing material's thin film can contribute to the change of the refractive index of the medium adjacent to the metal film. Ramdzan et al. proposed the use of nanocrystalline cellulose (NCC) for mercury detection (Ramdzan et al., 2021). The conducting polymer, poly (3,4-ethylenedioxythiophene) (PEDOT) is combined with NCC to improve the performance of the sensing layer. The results displayed the potential sensing of NCC/PEDOT-based sensor for mercury ion detection with a LOD of 2 ppb.

Polycyclic aromatic hydrocarbons (PAHs)

Polycyclic aromatic hydrocarbons (PAHs), a group of organic compounds composed of two or more blended aromatic rings, are an important class of environmental pollutants (Barron et al., 1999). A significant amount of PAHs is produced by processing coal via the burning of petroleum fuel and organic substances such as oil, coal and, gas (Simon et al., 2008). These compounds are ubiquitous environmental contaminants and are widespread in the atmosphere, soil, and water. They have low biodegradability, high lipophilicity, and are potentially highly carcinogenic, genotoxic, and mutagenic (Wong and Wang, 2001).
To overcome the disadvantages of low sensitivity in the detection of small molecules presented by SPR biosensor, Wang et al. proposed nanoporous gold (NPG) films as an alternative technique for trace detection of Benzo[a]pyrene, one of the most toxic members of the PAH family. Application of the NPG film in SPR sensor not only enhanced sensitivity because of supporting surface plasmon wave and analyte enrichment but also maintained the simple structure of SPR sensors. Consequently, the interaction depth for the SPR based NPG-film is much more sensitive than conventional SPR with a naked gold sensor. The LOD of the SPR sensor with the functionalized NPG film with antibody was 5 pmol L^{-1}, which is about 20 times larger than other conventional SPR sensors with the dense gold film (Wang et al., 2017).

2.4. Fluorescence-based biosensors

The fluorescence phenomenon (FL) consists of the emission of photons in a determined wavelength after the absorption of photons at a shorter wavelength (Dertinger et al., 2012). Fluorescence-based methods are the most used techniques in the field of optical biosensors because they combine the high selectivity provided by specific bioreceptors (antibodies, enzymes, aptamers) and the high sensitivity of the fluorescence detection (Tjandra et al., 2019). Moreover, thanks to the advances in the development of analytical platforms (microplate readers, flow cytometry, imaging techniques) combined with the increase in the available fluorescent molecules, like metal nanoparticles and quantum dots, have allowed the development of a range of sensors for biomolecule detection (Thompson, 2005).

FL-based biosensors have been widely used in medical (H. Wang et al., 2016; Xiao et al., 2018; Liu, Wang and Bao, 2019) and environmental applications (Das et al., 2019; Liang et al., 2019; Liu et al.,

2019) because they present a lesser time of response when compared with other detection techniques (Girigoswami and Akhtar, 2019). The wide variety of possible methodologies for FL biosensors has made them the most used type of biosensors (Staiano et al., 2005; Borisov and Wolfbeis, 2008). The common methods for fluorescence-based biosensors are based on fluorescence intensity (FI), the Forster resonance energy transfer (FRET), fluorescence polarization (FP), and fluorescence correlation spectroscopy (FCS).

FI or steady-state – biosensors are based on the direct measurement of the FL intensity after the excitation of the molecule using a specific light source (Camarca et al., 2021). FRET-based biosensors usually consist in having two fluorescent molecules (called donor and acceptor) where, under optimal conditions, after the excitation of the donor probe. energy is transferred to the acceptor resulting in different fluorescent intensities (Otten et al., 2019). FP – based biosensors work by recording the FL produced by the irradiation of fluorophore-labeled molecules with a plane-polarized light and then determining the degree of FP with several defined equations, like the Perrin equation (Hendrickson et al., 2020). FCS – based biosensors consist of the measurement of the intensity fluctuations generated by the molecules after being excited with a focused laser beam (Strianese et al., 2012). Figure 2-4 shows a schematic illustration of a fluorescent biosensor based on the intrinsic fluorescence of a nanomaterial.

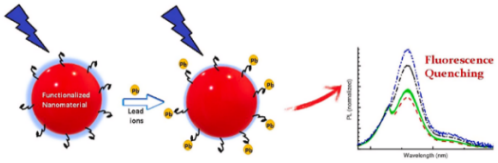

Figure 2-4.Schematic illustration of a nanomaterial fluorescent biosensor. Reprinted from Ref. (Singh et al., 2021) with permission from Elsevier.

The newer advances in nanotechnology have led to an increase in the number of nanomaterials (nanoparticles, quantum dots, nano bars, among others) fabricated in recent years, and the discovery of their novel properties has made their application in biosensors also advance (Zhang, Guo and Cui, 2009). Nanomaterials-based biosensors, which combine biotechnology with chemistry and material science, have further improved the sensibility and functioning of the biosensors, and present a great potential for pathogen detection and environmental monitoring (Pandit et al., 2016; Plácido et al., 2019; Luo et al., 2020). Table 2-1 present a compilation of the most used nanomaterials in fluorescence-based biosensors and their application.

Table 2-1. Most used nanomaterials in fluorescence-based biosensors

Nanomaterial name	Application	Reference
Carbon Dots	Antibiotic, bacteria, ion detection	(Yan et al., 2018; Chu et al., 2020; Tafreshi et al., 2020)
Gold nanoparticles	Ion detection	(B. Li et al., 2016; Zhu et al., 2018; Wang et al., 2019)
Nanosheets	Organic pollutants	(Chen et al., 2015; Liang et al., 2016; Yin and Ji, 2017)

Nanoclusters	Ion detection	(Bain et al., 2018; Burratti et al., 2021; Wong et al., 2021)
Hydrogel	Ion detection	(Xu et al., 2020; Cheng et al., 2021; Zheng et al., 2021)

Pathogens

Is in the nanomaterials FL-based biosensors, that investigations on the environmental field like the one performed by Hu et al (Hu et al., 2019), have made great advances. They developed a rapid and sensitive foodborne pathogen detection assay for the detection of a waterborne disease agent *Salmonella typhimurium* (*S. Typhi*), employing colorimetric- fluorescent-magnetic nanospheres (CFMNs), obtaining a quantitation range of 1.88 x 10^4 to 1.88 x 10^7 CFU mL^{-1} by measuring the fluorescence intensity of the probe in a complex matrix (e.g., Tap water). Furthermore, they developed a lateral flow immunoassay, which indicated its potential application for the rapid and sensitive detection of the parasite in real samples.

Water control is traditionally made by collecting water samples and then taking them to the laboratory to analyze them with time-consuming methods that are not usually accurate because of the point of water sample collecting or short time contamination (Köster et al., 2003). Notably, continuous, and real-time detection of pathogens could play an important part, and investigations like the ones carried out by Simões and Dong (Simões and Dong, 2018) are making promising advances. They developed a low-cost optofluidic sensor for detecting *E. coli* and *Legionella sp* based on the intrinsic fluorescence of the Tryptophan contained in the pathogenic bacteria obtaining a LOD of 1.4 x 10^3 CFU mL^{-1} in real-time drinking water measurements. Recently, there has been a great amount of effort in the rapid detection of *E. coli* in water since it can cause health problems when consumed. An investigation like the one performed by Aisiyah et al (Aisyiyah Jenie et al., 2021), Yao et al (Yao et al., 2021), and Hesari et al (Hesari et al., 2016) have made promising advances in this area where the first two based their methods in metallic NPs and the latter in the fluorescence intensity produced by the enzymatic reaction of 4-methylumbelliferyl- β-d-glucuronide (MUG) with the bacteria.

Emerging pollutants

It is known that when monitoring water sources, there is more than one contaminant that needs to be evaluated (Rodriguez-Mozaz et al., 2004). The development of multianalyte biosensors is an interesting approach for environmental monitoring because it reduces the amount of sample and time needed for the essay and provides an "easier" way of monitoring. After all, they allow an in-situ analysis without the need for complex training or equipment (Antonacci et al., 2021; Hashem et al., 2021). In this sense, Liu et al. (L. Liu et al., 2018) developed a multianalyte FL assay for several environmental pollutants such as ATZ, BPA, and microcystin-LR in a single water sample, obtaining LOD of 0.2, 0.06, and 0.22 μg mL^{-1}, respectively. Moreover, they evaluated the recovery of the proposed probe for simultaneous detection of the analytes and found average recovery methods between 84% to 120%, indicating the potential of the assay in the simultaneous detection of water

contaminants in real samples. This device is based on the affinity between Cy5.5-labeled antibodies with their respective analyte.

Hurtado-Sánchez et al (Hurtado-Sánchez et al., 2015) developed a strategy for the simultaneous detection and quantification of anticonvulsant carbamazepine (CBZ), fluoroquinolone ofloxacin (OFL), and anti-inflammatory piroxicam (PX) frequently found in water samples. They based the essay on the photoinduced fluorescence of the pollutants after they were irradiated with UV light. Finally, the probe developed by Hua et al. (Hua et al., 2005) developed a multianalyte sensor for the detection of estrone in water samples, obtaining a LOD of 1 ng mL^{-1} and because the hormone is a byproduct of several pharmaceuticals, it enables the possible detection of up to 32 pollutants.

Metal ions and pesticides

One of the most used bioreceptors in the field of FL-based biosensors are enzymes because they have great binding properties and present catalytic activity (Gaviria-Arroyave, Cano and Peñuela, 2020). There are a couple of ways that enzymes can be used in biosensors for environmental monitoring. The first one is by taking advantage of their catalytic activity and detecting several analytes depending on their application, for example, hydrolases are used when detecting analytes related to hydrolysis reaction, Oxidoreductases are used for oxidation-reduction reactions, Ligases for the joining of two molecules, Isomerases for isomerization and transferases for group transfer (Jennings, 1970).

The other way of using enzymes in biosensors is with their FL properties. The most common enzymes that present fluorescent properties are the ones that contain flavin or heme groups (Kłos-Witkowska, 2015). The optical properties of the flavin groups are dependent on the rate of oxidation and its bounding to a protein or a solution (Ortega et al., 2016), and the changes in these properties can be properly assigned to the analytes observed (FAD, FAD.H_2) (Galbán et al., 2012). Heme groups show molecular absorption and fluorescence during the enzymatic reaction when the central iron atom is replaced in the oxidation state (Postnikova and Yumakova, 1991). These properties have made enzymatic biosensors the go-to a biosensor for the detection of metal ions and pesticides. Some of the most used enzymes in fluorescence-based biosensors are presented in Table 2-2.

Table 2-2. Enzyme fluorescence-based biosensors for environmental pollutants detection

Enzyme	Application	Sample	Reference
Acetylcholinesterase	Organophosphorus pesticides	Water samples	(Meng et al., 2013; Li et al., 2020)
Urease	Mercury detection	Tap water	(L. Li et al., 2021)
Laccase	Phenol detection	Wastewater	(Esen et al., 2018)
Methyl parathion hydrolase	Parathion-methyl detection	River water and soil	(Song et al., 2017)
Hydrolase	Paraoxon detection	Tap water	(Karami et al., 2016)

Quo et al. (Luo et al., 2018), developed a fluorescent biosensor for the detection of organophosphate pesticides based on the fluorescence from Rhodamine modified silver/gold nanoparticles, obtaining an ultrasensitive LOD of 0.0018 ng mL^{-1} in water samples. They also proved

the anti-interference ability of the sensor exposing it to a sequence of interfering ions. Gaviria et al. (Gaviria et al., 1AD), developed a highly sensitive biosensor for the detection of Chlorpyrifos (CPF) and Lorsban®, with LODs of 0.14 and 2.05 ppb respectively. They proved the sensor´s selectivity in the presence of organic substances like glucose or proteins like BSA that are usually present in drinking water presenting promising results for the detection of commercial pesticides.

Finally, in the last years, there has been an increasing interest in the use of unicellular microorganisms for water pollutant detection, like for example, fluorescent algae or yeast (Norlinf, Wood-Black and Masciangioli, 2004). This type of biosensors is interesting because they are based on the autochthonous FL of the microorganisms and the changes in intensity and absorbance produced in the presence of water pollutants (Durrieu and Tran-Minh, 2002; Wong et al., 2018; Moscovici et al., 2020). Investigations like the one performed by Sun and Wang (Sun and Wang, 2021), where they developed a novel biosensor based on the autofluorescence intensity of an adenine deficient yeast for the detection of Labile Zn (II) in sea water solutions have demonstrated the broad application of these biosensors in real samples.

2.5. Bioluminiscence-based biosensors

Bioluminescence (BL) is the natural phenomenon by which living organisms, especially marine organisms, bacteria, fungi, and insects, emit light-independent from external stimuli (Syed and Anderson, 2021). BL could be generated through two main types of systems: luciferase enzymes and photoproteins (Syed and Anderson, 2021). When BL is generated by luciferase systems, various chemical reactions are catalyzed by luciferase enzyme who oxidizes luciferin (substrate) in the presence of oxygen, leading to a photons emission and highly luminescent products, the oxyluciferins. In bacteria, firefly, Renilla, and Gaussia, luciferase reaction is the main bioluminescent mechanism to form a product in the excited state (Y. Li et al., 2021). Regarding photoproteins, usually, they are a stable complex of enzymes, where substrates when triggered by Ca^{2+} ions emit a flash of light. Examples of this category are the Aequorin from jellyfish and Obelin from the hydrozoa Obelia longissimi (Y. Li et al., 2021).

The most abundant BL bioreceptors are bacteria and the application for pollutants detection in biosensors systems is mostly based on luciferase assays using whole cell as biomediators. BL bacteria are divided into three categories: *Vibrio*, *Photobacterium*, and *Xenorhabdus*, based on their luciferases, lux genes, and luminescent systems (Y. Li et al., 2021). Like other classes of optical biosensors previously mentioned, BL systems could work in “light-off” or “light-on”. The former is known for being less-specifical and is used for quantifying general toxicity in a sample (i.e *Vibrio fisheri* Microtox® assay), while the last one is based on the regulatory, promoter, and reporter genes that are activated in stress or pollution situations leading to a BL recovery (Figure 2-5). Currently, most of the microorganism strains used for BL systems are genetically engineered.

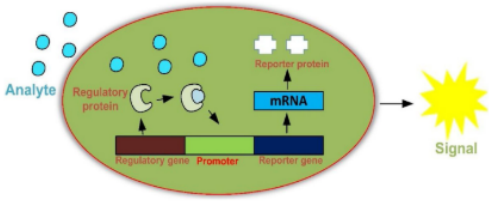

Figure 2-5. Schematic illustration of whole-cell "light-on" BL biosensor. Reprinted from Ref. (Bilal and Iqbal, 2019) with permission from Elsevier.

Some advantages of BL systems are high sensitivity, easy operation, and independence from an external stimulus (Y. Li et al., 2021). However, whole-cell systems could require long-incubation times with the analyte because diffusional barriers and sometimes big molecules could not be detected at all; other drawbacks for BL sensors are flash-type kinetics of wild luciferase systems, poor stability, high variability, overestimated signals in complex matrixes, and low selectivity. However, with the raising of synthetic biology, most of these drawbacks are overcome (Lopreside, Calabretta, et al., 2021). Due to the advantages of luciferase enzymes and photoproteins, these molecules and other related systems have been used frequently as in vitro reporters of environmental pollutants and biologically relevant molecules, as discussed below (Syed and Anderson, 2021).

Metal ions

Genetically engineered bacteria have become the most common systems for selective metal ions detection. For example, Soltani et al. developed a system to detect arsenic in groundwater in a turning-on mode (Soltani et al., 2021). Arsenic, like other toxic metal ions, causes human diseases such as skin necrosis, cardiovascular problems, or difficulties related to the gastrointestinal tract and respiratory system. The biosensor is based on a genetically engineered E. coli strain (pJAMA-arsR) and reports a LOD as low as 10 ppb (10-90 ppb linear range). When in the absence of arsenic, the ArsR repressor binds to its operator/promotor site preventing further expression. When the cell is exposed to arsenic, the ArsR repressor interacts with the pollutant, and the ARsR protein suffers a conformational change and is released from the operator. In this way, lux AB gene coding for luciferase is activated and light emitted corresponding to arsenic concentration.

Other works have been made exploiting the versatility of E. coli-based platforms to whole-cell developments. Lopreside et al. used E. coli TOP10 J23109- merR-PmerT-NanoLuc bacterial to detect mercury (II) (Lopreside, Montali, et al., 2021). The innovation of the system is the combination of an E. coli reporter with a purified β-GAL enzyme for visual detection on a smartphone-paper sensor and Aliivibrio fischeri (A. fisheri) naturally bioluminescent strain which is used to quantitatively assess sample toxicity and correct the analytical signal. The ultra-low LOD was set at 0.58 ppb for Hg2+ in tap water. In this work, the BL detection mechanism is analogous to the previous arsenic detection.

It can be seen how whole-cell naturally bioluminescent bacteria systems are used to complement or correct the main signal. Also, recent efforts have been made to research different gene promoters to respond to different pollutants; however, there is still a lack of promoter libraries to cover the

current wide range of environmental pollutants. Su et al. developed a multiple lux reporter array for a sensitive determination of multiple metal ions (Cu^{2+} Al^{3+} Zn^{2+} Fe^{2+} Ce^{3+} Li^{+} Zr^{4+} Pb^{2+}) in tap water (Su et al., 2020). In this work, a lux gene cassette without any specific promoter transforms three different bacterial hosts: *E. coli, Agrobacterium tumefaciens*, and *Bacillus subtilis*. They combined those genetically engineered hosts with naturally bioluminescent *Vibrio fisheri*. The system reports different ultra-low LOD, and the detection is based on the theory that significant differences in morphology, cell wall composition, and metabolic pathways existing among the different bacterial hosts could lead to a differential bioluminescent behavior. In this way, a simple system has been developed, without needing specific promoters.

Finally, less common systems based on naked luciferase enzymes to detect pollutants in a complex matrix are reported. Esimbekova et al. developed a BL sensor for the detection of different heavy metal ions (Pb^{2+}, Zn^{2+}, Cu^{2+}, Hg^{2+}, Al^{3+}, Cr^{3+}) and pesticides, based on luciferase EC 1.14.14.3 from the recombinant strain of *E. coli* and NAD(P)H: FMN-oxidoreductase EC 1.5.1.29 from *Vibrio fischeri* (Esimbekova et al., 2021). The system could detect some of the pollutants below the permissible levels in a complex matrix like fruit and vegetables. The authors recommended strategies like using mutant forms and nanomaterials for improving enzyme performance. Belleti et al. report the synthesis of a gold nanoparticle–luciferase hybrid composite to take advantage of the specificity of the enzyme and the Opto-electronic properties of the nanomaterial (Belleti et al., 2021). The authors found an increase in the enzyme operational stability with the free enzyme at least for 7 hours after substrate addition. When using non-porous nanomaterials, the immobilization of enzymes acts as a stabilization strategy with minimal diffusional drawbacks, thus improving the practical applications of cell-free systems.

Emerging pollutants

The identification and quantification of emerging pollutants in different environmental matrices (i.e, drinking water, soil, and food) is an urgent necessity, however, there is a lack of portable systems to detect those pollutants easily and accurately in the real world. Some authors like Ceveni et al., report the development of a cell-based mobile platform to detect total estrogenic activity, in tap water, with a LOD of 0.08 nM for 17β-estradiol as a quantification model (Cevenini et al., 2018). They used Saccharomyces cerevisiae cells (nanoYES) that were genetically engineered with a yeast codon-optimized variant of NanoLuc luciferase (yNLucP). The ready-to-use system was based on 3D cartridges with nanoYES immobilized on alginate beds that respond to the analyte thanks to a hERα human estrogen receptor, giving a “light-on” BL signal. The authors achieve 20% more BL emission signal using furimazine (NanoLuc substrate) in the culture media. Since luciferase systems emit light when a respective substrate (luciferin) is oxidized, the election of the right substrate is crucial for the system's performance. In this way, NanoLuc systems, despite their superior BL emission, have been limited because of the low solubility and bioavailability of the furimazine (Gaspar et al., 2021). In contrast, lux systems use fatty aldehyde as a substrate, making them easier and cheaper to use.

Usually, estrogenic activity has been monitored by mammalian cells in high-tech labs, making it impossible the real-time quantification in a complex matrix. However, the development of novel NanoLuc-based systems, like nanoYES, allow the development of high-accurate portable systems.

Like the previous work, Lopreside et al. report the use of nanoYES for the detection of estrogenic activity with a LOD of 0.38 nM for 17β-estradiol (Lopreside et al., 2019). The system uses the hERβ human estrogen receptor and the signal output is corrected with a second reporter strain with a chimeric luciferase of *Photinus pyralis* (PLG2). This system also uses 3D cartridges and a mobile camera for better portability.

Other emerging compounds that have been quantified through BL systems are antibiotic residues. Lu et al. follow the trend of developing systems based on smartphones (Lu et al., 2019). They report a 16 individual bioluminescent wells-based biosensor called LumiSense to quantify ciprofloxacin in milk at LOD of 7.2 ng mL^{-1}. The bioreporter in this study is a genetically engineered *E. coli* with recA promoter: luxCDABE plasmid-borne fusion. The main advantage of this system is that the genetic mechanism responds to the analyte by activation of the SOS DNA repair system (Clarke, Ha and Edwards, 2021), allowing the detection of other antibiotic residues (especially from the fluoroquinolone group). This advantage also implies that the bioreporter does not respond to proteins, lipids, and other biomolecules in milk, so steps of sample extraction and purification could be avoided. In LumiSense as well as previous works (Cevenini et al., 2018; Lopreside et al., 2019), the hardware allows the bioreceptor to be interchangeable, with promising commercial applications.

Finally, a recent study uses machine learning algorithms to train a model for the identification of different antibiotics compounds and seven modes of action classes (Huang et al., 2022). A similar bioreporter, genetically engineered *E. coli* with luxCDABE, allows the detection of residues between 125 ppb to 1000 ppb. The model showed 65% and 90% accuracy for compound and class classification, respectively. Furthermore, with great results, the model was applied to other antibiotics not used in the training phase. Technological advances in terms of hardware and software, along with bioreporter improvement, are the key to successful biosensor applications.

Mycotoxins

Mycotoxins are fungal secondary metabolites that have toxic effects on humans. Contrary to other types of toxins, like bacterial ones, mycotoxins are not made of proteins, so detection by immune systems is not possible (Goud et al., 2018). Mycotoxins can be found in different agro-industrial products such as grains, spices, nuts, dried beans, and fruits. The probability of mycotoxins contamination in food arises with the temperature and humidity (Nabok et al., 2019). Considering the dangerous effects of these pollutants (i.e dermal toxicity, immunotoxicity, liver and kidney disease, among others), the interest in quick and accurate detection systems is a must. To improve the sensibility and the speed of mycotoxins detection, Senko et al. report an easy system based on naturally bioluminescent bacteria *Photobacterium phosphoreum* immobilized onto PVA cryogel (Senko et al., 2019). The system showed shorter detection times (10 minutes) compared to the state of the art, thanks to the stabilization of *P. phosphoreum* in the porous matrix and the operation of the dispositive in a flow-rate mode. With this technique, they achieve LOD as low as 0.017 ppm for ochratoxin A and 0.009 ppm for zearalenone (ZEA). The porous structure of the PVA allows the system to work in higher flow rates without the “washing-out” phenomena of the bacterial cells

and, consistently, ensuring effective contact of the cells with most mycotoxins molecules present in the analyzed sample.

Recently, Alsulami et al. uses a homogeneous competitive inmunosensor to detect fumonisin B1 (FB1). The system is based on a new BL technology called NanoLuc Binary Technology (NanoBiT) (Kozielewicz and Schulte, 2021). NanoBit is composed of a large subunit (LgBiT 18 kDa) and a small subunit (SmBiT 11 amino acid peptides) that have low affinity by themselves but, when are conjugated with a pair antibody-antigen, both subunits are brought close, and the BL is addressed. The authors conjugated anti-fumonisin antibody with LgBiT (FLgBiT) and used it in a competitive assay with FB1-SmBiT in a turning-off system, obtaining a LOD of 0.079 ppm. When in the absence of FB1 in the sample, FLgBiT and FB1-SmBiT are close, and the BL reaches its maximum. However, when FB1 toxin is present in the sample the competitive assay makes the BL signal decrease proportional to FB1 concentration. The system showed a great selectivity against other mycotoxins (aflatoxin, deoxynivalenol, ochratoxin, and zearalenone); however, the manipulation of the FB1 to make the conjugates is a major drawback.

The use of antibodies for the detection of different analytes is well known, however, the detection of small size molecules like mycotoxins in competitive assays requires conjugation of the target molecule with carriers or labels, as we previously mentioned. Mimotopes are developed to target the same antibody paratope as the target toxin and elicit an antibody response like that of the analyte (Peltomaa, Benito-Peña and Moreno-Bondi, 2018). A more sophisticated system was developed by Peltomaa et al., also looking for ZEA detection (Peltomaa et al., 2020). The authors used a newly reported technology called peptide mimetics or mimotopes, coupled with a GLuc luciferase, for the development of a competitive assay and detection of ZEA in cereals. In this work, they used anti-ZEA, and when a sample is analyzed, the mimotope-GLuc conjugates compete with ZEA molecules. For the analyses, the antibodies are recovered using protein-G (interacts with antibodies) in magnetic beads. After the addition of GLuc substrate, a BL signal could be established and correlated with ZEA concentration. With this system, a LOD of 4.2 ppm was achieved, which is below the commercial ELISA kits for ZEA.

Other pollutants

BL systems for pesticides detection are not the most common, but some reports are interesting. For instance, Bergua et al. developed a system based on *A. fisheri* quorum-sensing mechanism, this is the trigger of *A. fischeri* bioluminescent luciferase according to the cellular density that could be affected in the presence of Tributyltin (TBT) and pentachlorophenol (Bergua et al., 2021). The authors found an increase in bacterial population when growing in solid media instead of broth. However, since handling a liquid culture is easier, they investigated how nanomaterials like GO increase bacterial growth. As we previously said, nanomaterials are a promising approach to improve BL performance, and, in this work, they found that *A. fisheri* cultures with GO at 100 ppm doubled the population. This work reported EC50 for TBT in the range of ppb (17 and 70 $\mu g\ L^{-1}$) and pentachlorophenol in the range of ppm (0.16 and 21.06 $mg\ L^{-1}$). It is worth mentioning that GO was also used in the detection experiment, but the synergistic effect was not clear.

Along with water safety, soil pollution is a serious problem, not just for the soil damage for crops, but the cross-contamination with air and water. A group of oily pollutants called BTEX (volatile benzene, toluene, ethylbenzene, and xylene) are related to brain damage and cancer in humans (LAparicio et al., 2022). For toluene detection, Bae et al. proposed a system based on 3 different strains of *E.coli* modified with protomor: luxCDABE genes (Bae et al., 2020). The authors immobilized those strains on alginate beads and covered them with poly-dopamine (PD) for the construction of a "mini bioreactor" for soil analysis, taking care of not releasing the genetically engineered bacteria to the field. They achieved detection of the minimal concentration of toluene (1%). Contrary to other luciferase systems (i.e NanoLuc) that require the addition of external substrate, the expression of luxCDABE can generate luciferase enzyme encoded and the aliphatic aldehyde that serves as its substrate. The use of PD showed great improvement of the alginate-beads stability, promoting field applications.

Dioxin-like compounds (DLCs) are another class of pollutants with a major interest in soil and water. They are a group of structurally related halogenated aromatic hydrocarbons including polychlorinated dibenzo-p-dioxins (PCDDs), polychlorinated dibenzofurans (PCDFs), and some polychlorinated biphenyls (PCBs) (Xu et al., 2018). DLCs are related to endocrine and reproductive damage, neurotoxicity, and metabolic alterations. A bioluminescent *Saccharomyces cerevisiae* BLYAhS bioreporter was reported by Xu et al. for a model 2,3,7,8-tetrachlorodibenzo-p-dioxin (TCDD) detection (Xu et al., 2018). They used the previously mentioned advantages of the luxCDABE system to detect the pollutant in a "turning on" mode, with an aryl hydrocarbon receptor (AhR) agonist and a dioxin-responsive promoter reaching a LOD of 500 pM. The study showed some advantages like high throughput, ease of use, and the independence of external reagents. However, the sensibility must be increased with other types of receptor-promoter pairs.

2.6. Conclusions and perspectives

Concerns about environmental pollution and the need for real-time monitoring have promoted the advance in the biosensor field. Optical biosensor provides a facile, rapid, and low-cost approach for sensitive detection of different pollutants such as antibiotic and pharma residues, pesticides, toxins, and metal ions. These last are the most detected pollutants, with simple and sophisticated techniques applied with CL, SPR, FL, and BL transductors. Table 2-3 shows some optical biosensors with ultra-low detection limits. Several investigations with promising results in the detection of some pollutants such as pesticides, polycyclic aromatic hydrocarbons (PAH), heavy metals (HM), endocrine-disrupting chemicals (EDC), and pathogens are reported.

CL-based biosensors have advantages such as portability, flexibility, sensitivity, reproducibility, and in some cases, specificity. However, to be used with real samples, it is necessary to improve some aspects, since, despite the good results achieved under controlled laboratory conditions, the interference of unknown molecules in complex biological samples can cross-react with the device, leading to obtaining false-positive results. For instance, NPs-based CL systems are affected by the pH variations in real samples because of the presence of other molecules. In addition, it is recommended not only to select low LOD methodologies but also to explore the possibility of

developing systems with wider detection ranges in industrial samples. In the case of SPR-based biosensors, label-free detection with real-time response that reach high sensitivities could be addressed. Considering the small size of some environmental pollutants (i.e mycotoxins and EDCs), adequate modifications to the surface are required to obtain the proper sensitivities.

FL-based and BL-based biosensors are the most used type of optical biosensors for environmental applications due to their properties and the different types of methodologies of detection that allow them to be designed with many biomolecules (enzymes, antibodies, aptamers). However, one of the biggest challenges in FL biosensors is the reproducibility of the results since there are several factors involved in the principle of fluorescence that needs to be controlled. Nonetheless, they are an excellent complementary method for environmental molecules detection, and further research is continuing to be explored thanks to the potential of the technique. Regarding BL biosensors, currently, the general rule is the use of whole-cell genetically engineered biorecognition elements. They are often cheaper, more resistant to pH and temperature changes, self-renewable, and do not require extraction and purification steps. However, cell-free biosensors generally provide higher sensitivity, lower LOD, safer procedures, and shorter detection time because of the lack of diffusional barriers.

Based on the information presented above, the following are some ways that the stability, accuracy, sensitivity, and selectivity of an optical biosensor can be improved: (1) the use of synthetic biology to create detection units with less reactivity to interaction substances. (2) the application of new nanomaterials as signal reporters, substrates, or catalysts. Nonetheless, the conjugation of recognition elements with functionalized nanomaterials will inevitably raise the complexity, cost, and time of an optical biosensor. Nanomaterials-based analytical systems are in the early stages of development in terms of nanomaterials.

Even though optical biosensors have a bright future for detecting environmental contaminants, there are long-term obstacles to overcome in the field. Most optical sensors still have proof-of-concept testing and verification at the laboratory level, which has not been used in actual applications. However, we presented several works focusing on mobile devices working with the aid of 3D printing technologies, the combination of field-deployable equipment with sensing devices performs promising on-site applications. These developments boost the sensor's reproducibility and stability. The recognition event of the pollutant can be translated into a measured digital signal by hand-held devices, such as a smartphone, and then the detection findings can be delivered to the servers, thanks to tiny devices and wire-free networking. As a result, lightweight detecting platforms can be used outside of the laboratory with little user interaction, clearing the way for a new generation of real-time detection analytical instruments.

Table 2-3. Comparison of optical biosensors with ultra-low detection limits for environmental applications

Detection method	Bioreceptor/ transducter	Analyte	Matrix	LOD	Linear range	Ref

CL	N/A	Pesticides: AM, CP, FP, PM, and PS	Rice and paddy water	AM: 75, CP: 118, FP: 75, PM: 30, and PS: 37 ng mL^{-1}	AM: 80-400, CP: 120-280 and 320-800, FP: 80-400, PM: 40-800, and PS: 40-320 ng mL^{-1}	(Fahimi-Kashani and Hormozi-Nezhad, 2016)
CL	Aptamer	Microcystin-LR	Tap water and pond water	0.37 nM	0.5 nM – 7.5 μM	(X. Li et al., 2016)
SPR	Molecularly imprinted nanoparticles (plastic antibodies)	Pesticide: paraquat	Water	2.2 pM	10 pM to 100 nM	(Dong et al., 2018)
SPR	N/A	Heavy metals: mercury ion (Hg^{2+})	Water	2 ppb	2–100 ppb	(Ramdzan et al., 2021)
SPR	N/A	Endocrine disruptors: BPA	Water	5 pmol L^{-1}	Not reported	(Wang et al., 2017)
FL	1-(4-carboxylbenzene) -1,2,2-triphenyl (CTPY)- peptide conjugate	Toxins: Bacterial endotoxcin	Water	6.97 nM.	0.1-1 µM	(Tang et al., 2020)
FL	Aptamer	Antibiotic	Tap and pond water	0.1 ng mL^{-1}	0.1 ng mL^{-1} - 10 µg mL^{-1}	(Zhang et al., 2018)
BL	pRLucMer19 plasmid-containing *E. coli*	Heavy metals: mercury ion (Hg^{2+})	Water	1 ppb (Hg)	1 – 104 ppb	(Gupta et al., 2019)
BL	*E. coli* TOP10 J23109 merR-PmerT-NanoLuc and Naturally BL bacteria *A. fischeri*.	Heavy metals: mercury (II)	Water	0.58 ppb	Not reported	(Lopreside, Montali, et al., 2021)
BL	nanoYES: *Saccharomyces cerevisiae* with NanoLuc luciferase	Endocrine disruptors:17β-estradiol	Tap water	0.08 nM	0.05 to 10 nM	(Cevenini et al., 2018)
BL	NanoBit system conjugated with antibody.	Mycotoxins: fumonisin B1	Maize	0.079 ppm	0.533–6.81 ppm	(Alsulami et al., 2021)

*****Azinphos-methyl (AM), chlorpyrifos (CP), fenamiphos (FP), pirimiphos-methyl (PM), and phosalone (PS)

2.7. Abbreviations

Abbreviation	Definition	Abbreviation	Definition
2D	Two-dimensional	M	Molar
3D	Three-dimensional	MBI	Mercaptobenzoimidazole
6-BAP	6-benzyl amino purine	MBO	Mercaptobenzooxazole
ABT	4-aminobenzenethiol	MBT	Mercaptobenzothiazole

AgNPs	Silver nanoparticles	MIF	Molecularly imprinted films
AhR	Aryl hydrocarbon receptor	MIP	Molecularly imprinted polymer
AM	Azinphos-methyl	MNPs	Magnetic nanoparticles
ATZ	Atrazine	mRNA	Messenger ribonucleic acid
AuNPs	Gold nanoparticles	MUG	4-methylumbelliferyl- β-d-glucuronide
BL	Bioluminescence	NanoBiT	NanoLuc Binary Technology
BPA	Bisphenol A	nanoYES	Yeast-estrogen screen biosensor
BSA	Bovine Serum Albumin	NCC	Nanocrystalline cellulose
C-SPE	Colorimetric solid-phase extraction	NLucP	NanoLuc luciferase
CBZ	Carbamazepine	NPG	Nanoporous gold
CL	Colorimetric sensors	NPs	Nanoparticles
CNFs	Carbon nanofibers	OFL	Fluoroquinolone ofloxacin
CNTs	Carbon nanotubes	OTC	Oxytetracycline
CPF	Chlorpyrifos	PAH	Polycyclic aromatic hydrocarbon
CPGR	Chlorophenol red-β-D-galactopyranoside	Pb	Lead
Cr	Chromium	PCB	Polychlorinated biphenyls
CTAB	Cetyltrimethyl ammonium bromide	PCDD	Polychlorinated dibenzo-p-dioxins
CuNPs	Copper nanoparticles	PCDF	Polychlorinated dibenzofurans
Cy	Cyanine	PD	Poly-dopamine
DLC	Dioxin-like compounds	PEDOT	Poly(3,4-ethylenedioxythiophene)
DNA	Deoxyribonucleic acid	PM	Pirimiphos-methyl
DOX	Doxycycline	ppb	Parts per billion
EDC	Endocrine-disrupting chemical	ppm	Parts per million
EDTA	Ethylenediaminetetraacetic acid disodium	PQ	Paraquat
ELISA	Enzyme-linked immunosorbent assay	PS	Phosalone
EP	Emerging pollutants	PSH	Pyridoxal salicyloylhydrazone
et. al	And others	PVA	Poly (vinyl) alcohol
FAD	Flavin adenine dinucleotide	PX	Piroxicam
FB1	Fumonisin B1	Ref	Reference
FCS	Fluorescence correlation spectroscopy	RI	Refractive index
FI	Fluorescence intensity	RU	Resonance units
FITC	Fluorescein isothiocyanate	SDB	Poly(styrene-divinylbenzene)
FL	Fluorescence	SmBiT	Small subunit
FP	Fluorescence polarization	SMZ	Simazine
FP	Fenamiphos	SNZ	Cyanazine
FRET	Forster resonance energy transfer	SPR	Surface plasmon resonance
g	Gram	SPRi	Surface Plasmon Resonance imaging

GO	Graphene oxide	TA	Thioglycolic Acid
HCA	Hierarchical cluster analysis	TBT	Tributyltin
Hg	Mercury	TC	Tetracyclines
HM	Heavy metals	TCDD	2,3,7,8-tetrachlorodibenzo-p-dioxin
i.e	That is	TMB	3,3',5,5'-tetramethylbenzidine
IVVT	In vitro transcription/translation	TMD	Transition metal dichalcogenide
L	Liter	WHO	World Health Organization
LC-MS	Liquid Chromatography-tandem Mass Spectrometry	ZEA	Zearalenone
LDA	Linear discriminant analysis	Zn	Zinc
LgBiT	Large subunit	β-GAL	β-galactosidase
LOD	Limit of detection	µPADs	Microfluidic paper-based analytical device

2.8. References

Aisyiyah Jenie, S. N. et al. (2021) 'Rapid fluorescence quenching detection of Escherichia coli using natural silica-based nanoparticles', Sensors (Switzerland), 21(3), pp. 1–13. doi: 10.3390/s21030881.

Aldewachi, H. et al. (2017) 'Gold nanoparticle-based colorimetric biosensors', Nanoscale, 10(1), pp. 18–33. doi: 10.1039/C7NR06367A.

De Almeida, L. K. S. et al. (2015) 'A novel colorimetric sensor strip for the detection of glyphosate in water', Sensors and Actuators, B: Chemical, 206, pp. 357–363. doi: 10.1016/j.snb.2014.09.039.

Alsulami, T. et al. (2021) 'Development of a novel homogeneous immunoassay using the engineered luminescent enzyme NanoLuc for the quantification of the mycotoxin fumonisin B1', Biosensors and Bioelectronics, 177(December 2020), p. 112939. doi: 10.1016/j.bios.2020.112939.

Antonacci, A. et al. (2021) 'Photosynthesis-based biosensors for environmental analysis of herbicides', Case Studies in Chemical and Environmental Engineering, 4, p. 100157. doi: 10.1016/j.cscee.2021.100157.

Ayaz Ahmed, K. B. et al. (2016) 'Highly selective colorimetric cysteine sensor based on the formation of cysteine layer on copper nanoparticles', Sensors and Actuators B: Chemical, 233, pp. 431–437. doi: 10.1016/J.SNB.2016.04.125.

Bae, J. W. et al. (2020) 'An optical detection module-based biosensor using fortified bacterial beads for soil toxicity assessment', Analytical and Bioanalytical Chemistry, 412(14), pp. 3373–3381. doi: 10.1007/s00216-020-02469-z.

Bain, D. et al. (2018) 'Core-Size Dependent Fluorescent Gold Nanoclusters and Ultrasensitive Detection of Pb2+ Ion', ACS Sustainable Chemistry and Engineering, 6(2), pp. 2334–2343. doi: 10.1021/acssuschemeng.7b03794.

Bakar, N. A. et al. (2013) 'Localized Surface Plasmon Resonance Sensor Using Gold Nanoparticles for Detection of Bisphenol A.', in In Key Engineering Materials. Trans Tech Publications, Ltd., pp. 342–345. doi: doi.org/10.4028/www.scientific.net/kem.543.342.

Barron, M. G. et al. (1999) 'Are aromatic hydrocarbons the primary determinant of petroleum toxicity to aquatic organisms?', Aquatic Toxicology, 46(3–4), pp. 253–268. doi: doi.org/10.1016/S0166-445X(98)00127-1.

Belleti, E. et al. (2021) 'Synthesis of bioluminescent gold nanoparticle–luciferase hybrid systems for technological applications', Photochemical and Photobiological Sciences, 20(11), pp. 1439–1453. doi: 10.1007/s43630-021-00111-0.

Bergua, J. F. et al. (2021) 'Improved Aliivibrio fischeri based-toxicity assay: Graphene-oxide as a sensitivity booster with a mobile-phone application', Journal of Hazardous Materials, 406, p. 124434. doi: 10.1016/j.jhazmat.2020.124434.

Bhattacharjee, Y., Chatterjee, D. and Chakraborty, A. (2018) 'Mercaptobenzoheterocyclic compounds functionalized silver nanoparticle, an ultrasensitive colorimetric probe for Hg(II) detection in water with picomolar precision: A correlation between sensitivity and binding affinity', Sensors and Actuators, B: Chemical, 255, pp. 210–216. doi: 10.1016/j.snb.2017.08.066.
Bilal, M. et al. (2019) 'Emerging contaminants of high concern and their enzyme-assisted biodegradation – A review', Environment International. Elsevier Ltd, pp. 336–353. doi: 10.1016/j.envint.2019.01.011.
Bilal, M. and Iqbal, H. M. N. (2019) 'Microbial-derived biosensors for monitoring environmental contaminants: Recent advances and future outlook', Process Safety and Environmental Protection, 124, pp. 8–17. doi: 10.1016/j.psep.2019.01.032.
Borisov, S. M. and Wolfbeis, O. S. (2008) 'Optical biosensors', chem. Rev., 108(941), pp. 423–461. doi: 10.1021/cr068105t.
Brogioni, B. and Berti, F. (2014) 'Surface plasmon resonance for the characterization of bacterial polysaccharide antigens: a review', MedChemComm, 5, pp. 1058–1066. doi: 10.1039/c4md00088a.
Brouwer, M. et al. (2017) 'Environmental exposure to pesticides and the risk of Parkinson's disease in the Netherlands', Environment International, 107, pp. 100–110. doi: 10.1016/j.envint.2017.07.001.
Burratti, L. et al. (2021) 'Fluorescent silver nanoclusters embedded in hydrogel matrix and its potential use in environmental monitoring', Applied Sciences (Switzerland), 11(8). doi: 10.3390/app11083470.
Camarca, A. et al. (2021) 'Emergent biosensing technologies based on fluorescence spectroscopy and surface plasmon resonance', Sensors (Switzerland), 21(3), pp. 1–35. doi: 10.3390/s21030906.
Castañeda-Loaiza, V. et al. (2019) 'Disposable optical sensor for Al(III) ions determination by coupled colorimetric solid-phase extraction-reflectance spectroscopy in leachates from cookware, antacids and hygienic care products', Talanta, 205(June), p. 120102. doi: 10.1016/j.talanta.2019.06.102.
Cevenini, L. et al. (2018) 'A novel bioluminescent NanoLuc yeast-estrogen screen biosensor (nanoYES) with a compact wireless camera for effect-based detection of endocrine-disrupting chemicals', Analytical and Bioanalytical Chemistry, 410(4), pp. 1237–1246. doi: 10.1007/s00216-017-0661-7.
Che Sulaiman, I. S. et al. (2020) 'A review on colorimetric methods for determination of organophosphate pesticides using gold and silver nanoparticles', Microchimica Acta, 187(2), pp. 1–22. doi: 10.1007/S00604-019-3893-8/FIGURES/1.
Chen, H. Y. et al. (2015) 'Trace detection of nitro aromatic explosives by highly fluorescent g-C3N4 nanosheets', Analyst, 140(2), pp. 637–643. doi: 10.1039/c4an01693a.
Cheng, C. et al. (2016) 'A highly sensitive and selective cyanide detection using a gold nanoparticle-based dual fluorescence-colorimetric sensor with a wide concentration range', Sensors and Actuators, B: Chemical, 227, pp. 283–290. doi: 10.1016/j.snb.2015.12.057.
Cheng, F. et al. (2021) 'Hydrothermal synthesis of nanocellulose-based fluorescent hydrogel for mercury ion detection', Colloids and Surfaces A: Physicochemical and Engineering Aspects, 636(October 2021), p. 128149. doi: 10.1016/j.colsurfa.2021.128149.
Chu, H. W. et al. (2020) 'Carbon quantum dots for the detection of antibiotics and pesticides', Journal of Food and Drug Analysis, 28(4), pp. 539–557. doi: 10.38212/2224-6614.1269.
Clarke, R. S., Ha, K. P. and Edwards, A. M. (2021) 'RexAB promotes the survival of staphylococcus aureus exposed to multiple classes of antibiotics', Antimicrobial Agents and Chemotherapy, 65(10). doi: 10.1128/AAC.00594-21.
Das, T. et al. (2019) 'Biology Blue-fluorescent and biocompatible carbon dots derived from abundant low-quality coals', Journal of Photochemistry & Photobiology, B: Biology, 195(April), pp. 1–11. doi: 10.1016/j.jphotobiol.2019.04.004.
Dertinger, T. et al. (2012) 'Nano-Biotechnology for Biomedical and Diagnostic Research', 733, pp. 17–21. doi: 10.1007/978-94-007-2555-3.
DesMarias, T. L. and Costa, M. (2019) 'Mechanisms of chromium-induced toxicity', Current Opinion in Toxicology, 14, pp. 1–7. doi: 10.1016/J.COTOX.2019.05.003.
Dong, C. et al. (2016) 'Selective colorimetric detection of Cr(III) and Cr(VI) using gallic acid capped gold nanoparticles', Dalton Transactions, 45(20), pp. 8347–8354. doi: 10.1039/c5dt04099j.
Dong, H. et al. (2018) 'Analyte induced AuNPs aggregation enhanced surface plasmon resonance for sensitive detection of paraquat', Biosensors and Bioelectronics, 117, pp. 605–612. doi: 10.1016/j.bios.2018.06.057.

Durrieu, C. and Tran-Minh, C. (2002) 'Optical algal biosensor using alkaline phosphatase for determination of heavy metals', Ecotoxicology and Environmental Safety, 51(3), pp. 206–209. doi: 10.1006/eesa.2001.2140.
Duyen, T. T. M. et al. (2017) 'Paper-based colorimetric biosensor for antibiotics inhibiting bacterial protein synthesis', Journal of Bioscience and Bioengineering, 123(1), pp. 96–100. doi: 10.1016/j.jbiosc.2016.07.015.
Ellen MacArthur Foundation. (2015) Economía circular.
Esen, E. et al. (2018) 'Laccase assay based on electrochemistry and fluorescence detection via anthracene sequestered poly(amic acid) films', Reactive and Functional Polymers, 131(July), pp. 36–43. doi: 10.1016/j.reactfunctpolym.2018.07.001.
Esimbekova, E. N. et al. (2021) 'Design of bioluminescent biosensors for assessing contamination of complex matrices', Talanta, 233(February), p. 122509. doi: 10.1016/j.talanta.2021.122509.
Fahimi-Kashani, N. and Hormozi-Nezhad, M. R. (2016) 'Gold-nanoparticle-based colorimetric sensor array for discrimination of organophosphate pesticides', Analytical Chemistry, 88(16), pp. 8099–8106. doi: 10.1021/acs.analchem.6b01616.
Galbán, J. et al. (2012) 'Reagentless fluorescent biosensors based on proteins for continuous monitoring systems', Analytical and Bioanalytical Chemistry, 402(10), pp. 3039–3054. doi: 10.1007/s00216-012-5715-2.
Galvan, D. et al. (2018) 'Sensitive bacterial detection via dielectrophoretic-enhanced mass transport using surface-plasmon-resonance biosensors', Anal. Chem., 90, pp. 14635–14642.
Gao, L. et al. (2008) 'Magnetite Nanoparticle-Linked Immunosorbent Assay', Journal of Physical Chemistry C, 112(44), pp. 17357–17361. doi: 10.1021/JP805994H.
Gaspar, N. et al. (2021) 'Evaluation of NanoLuc substrates for bioluminescence imaging of transferred cells in mice', Journal of Photochemistry and Photobiology B: Biology, 216(December 2020), p. 112128. doi: 10.1016/j.jphotobiol.2021.112128.
Gaviria-Arroyave, M. I., Cano, J. B. and Peñuela, G. A. (2020) 'Nanomaterial-based fluorescent biosensors for monitoring environmental pollutants: A critical review', Talanta Open, 2(June), p. 100006. doi: 10.1016/j.talo.2020.100006.
Gaviria, M. I. et al. (2022) 'Highly Sensitive Fluorescent Biosensor Based on Acetylcholinesterase and Carbon Dots–Graphene Oxide Quenching Test for Analytical and Commercial Organophosphate Pesticide Detection', Frontiers in Environmental Science, 0, p. 91. doi: 10.3389/FENVS.2022.825112.
Gawande, M. B. et al. (2016) 'Cu and Cu-Based Nanoparticles: Synthesis and Applications in Catalysis', Chemical reviews, 116(6), pp. 3722–3811. doi: 10.1021/ACS.CHEMREV.5B00482.
Ghoto, S. A. et al. (2019) 'Applications of copper nanoparticles for colorimetric detection of dithiocarbamate pesticides', Journal of Nanostructure in Chemistry, 9(2), pp. 77–93. doi: 10.1007/s40097-019-0299-4.
Gillezeau, C. et al. (2019) 'The evidence of human exposure to glyphosate: A review', Environmental Health: A Global Access Science Source, 18(1), pp. 1–14. doi: 10.1186/S12940-018-0435-5/FIGURES/3.
Girigoswami, K. and Akhtar, N. (2019) 'Nanobiosensors and fluorescence based biosensors: An overview', International Journal of Nano Dimension, 10(1), pp. 1–17.
Goud, K. Y. et al. (2018) 'Progress on nanostructured electrochemical sensors and their recognition elements for detection of mycotoxins: A review', Biosensors and Bioelectronics, 121(June), pp. 205–222. doi: 10.1016/j.bios.2018.08.029.
Grzeskowiak, A. Z. et al. (2009) 'Determination of nonylphenol and short-chained nonylphenol ethoxylates in drain water from an agricultural área Chemosphere', Chemosphere, 75, pp. 513–518.
Guo, Y. et al. (2018) 'A non-competitive surface plasmon resonance immunosensor for rapid detection of triazophos residue in environmental and agricultural samples', Science of The Total Environment, 613–614, pp. 783–791. doi: 10.1016/J.SCITOTENV.2017.09.157.
Gupta, R. et al. (2021) 'Naked eye colorimetric detection of Escherichia coli using aptamer conjugated graphene oxide enclosed Gold nanoparticles', Sensors and Actuators, B: Chemical, 329(June 2020), p. 129100. doi: 10.1016/j.snb.2020.129100.
Gupta, S. et al. (2019) 'Development of a Cell-Free Optical Biosensor for Detection of a Broad Range of Mercury Contaminants in Water: A Plasmid DNA-Based Approach', ACS Omega, 4(5), pp. 9480–9487. doi: 10.1021/acsomega.9b00205.
Hamza, R. A., Iorhemen, O. T. and Tay, J. H. (2016) 'Occurrence, impacts and removal of emerging substances of concern from wastewater', Environmental Technology and Innovation. Elsevier B.V., pp. 161–175. doi: 10.1016/j.eti.2016.02.003.

Hashem, A. et al. (2021) 'Nanomaterials based electrochemical nucleic acid biosensors for environmental monitoring: A review', Applied Surface Science Advances, 4(January), p. 100064. doi: 10.1016/j.apsadv.2021.100064.
Hendrickson, O. D. et al. (2020) Fluorescence polarization-based bioassays: new horizons.
Hesari, N. et al. (2016) 'A biosensor platform for rapid detection of E. coli in drinking water', Enzyme and Microbial Technology, 83, pp. 22–28. doi: 10.1016/j.enzmictec.2015.11.007.
Hu, J. et al. (2019) 'Colorimetric-Fluorescent-Magnetic Nanosphere-Based Multimodal Assay Platform for Salmonella Detection', Analytical Chemistry, 91(1), pp. 1178–1184. doi: 10.1021/acs.analchem.8b05154.
Hua, P. et al. (2005) 'Integrated optical fluorescence multisensor for water pollution', Optics Express, 13(4), p. 1124. doi: 10.1364/opex.13.001124.
Huang, W.-C. et al. (2022) 'Machine-learning assisted antibiotic detection and categorization using a bacterial sensor array', Sensors and Actuators B: Chemical, 355. doi: https://doi.org/10.1016/j.snb.2021.131257.
Hurtado-Sánchez, M. D. C. et al. (2015) 'Green analytical determination of emerging pollutants in environmental waters using excitation-emission photoinduced fluorescence data and multivariate calibration', Talanta, 134, pp. 215–223. doi: 10.1016/j.talanta.2014.11.022.
Hwang, J. et al. (2021) 'Green synthesis of reduced-graphene oxide quantum dots and application for colorimetric biosensor', Sensors and Actuators A: Physical, 318, p. 112495. doi: 10.1016/J.SNA.2020.112495.
Jennings, I. . (1970) 'Enzymes', in Vitamins in Endocrine metabolism, pp. 11–24. doi: https://doi.org/10.1016/B978-0-433-17320-5.50006-5.
Jia, Y. et al. (2021) 'Niobium disulfide nanosheets modified surface plasmon resonance sensors for ultrasensitive detection of mercury ion', J. Alloys Compd., 869, p. 159328.
Karami, R. et al. (2016) 'A novel nanobiosensor for the detection of paraoxon using chitosan-embedded organophosphorus hydrolase immobilized on Au nanoparticles', Preparative Biochemistry and Biotechnology, 46(6), pp. 559–566. doi: 10.1080/10826068.2015.1084930.
Kim, H. K. et al. (2021) 'Colorimetric aptasensor for detecting bacillus carboniphilus using aptamer isolated with a non-selex-based method', Chemosensors, 9(6). doi: 10.3390/chemosensors9060121.
Kim, H. T. and Lee, T. G. (2017) 'A simultaneous stabilization and solidification of the top five most toxic heavy metals (Hg, Pb, As, Cr, and Cd)', Chemosphere, 178, pp. 479–485. doi: 10.1016/J.CHEMOSPHERE.2017.03.092.
Kłos-Witkowska, A. (2015) 'Enzyme-based fluorescent biosensors and their environmental, clinical and industrial applications', Polish Journal of Environmental Studies, 24(1), pp. 19–25. doi: 10.15244/pjoes/28352.
Kong, H. et al. (2014) 'Hydrogen sulfide detection based on reflection: From a poison test approach of ancient China to single-cell accurate localization', Analytical Chemistry, 86(15), pp. 7734–7739. doi: 10.1021/AC5016672/SUPPL_FILE/AC5016672_SI_001.PDF.
Kong, Q. et al. (2017) 'A novel microfluidic paper-based colorimetric sensor based on molecularly imprinted polymer membranes for highly selective and sensitive detection of bisphenol A', Sensors and Actuators, B: Chemical, 243, pp. 130–136. doi: 10.1016/j.snb.2016.11.146.
Köster, W. et al. (2003) 'Analytical methods for microbiological water quality testing', in Assessing Microbial Safety of Drinking Water: Improving Approaches and Methods, pp. 237–292. doi: 10.1787/9789264099470-en.
Kozielewicz, P. and Schulte, G. (2021) 'NNanoBRET and NanoBiT/BRET-Based Ligand Binding Assays Permit Quantitative Assessment of Small Molecule Ligand Binding to Smoothened', in Methods in Molecular Biology.
LAparicio, J. D. et al. (2022) 'The current approach to soil remediation: A review of physicochemical and biological technologies, and the potential of their strategic combination', Journal of Environmental Chemical Engineering, 10(2).
Li, B. et al. (2016) 'Aggregation-induced emission from gold nanoclusters for use as a luminescence-enhanced nanosensor to detect trace amounts of silver ions', Journal of Colloid and Interface Science, 467, pp. 90–96. doi: 10.1016/j.jcis.2016.01.002.
Li, H. et al. (2020) 'Rapid detection of organophosphorus in tea using NaY/GdF4:Yb, Er-based fluorescence sensor', Microchemical Journal, 159(June). doi: 10.1016/j.microc.2020.105462.
Li, L. et al. (2021) 'Visual and ultrasensitive detection of mercury ions based on urease catalysis and responsive photonic crystals', Dyes and Pigments, 195(August), pp. 1–5. doi: 10.1016/j.dyepig.2021.109676.

Li, X. et al. (2016) 'A simple highly sensitive and selective aptamer-based colorimetric sensor for environmental toxins microcystin-LR in water samples', Journal of Hazardous Materials, 304, pp. 474–480. doi: 10.1016/j.jhazmat.2015.11.016.
Li, Y. et al. (2021) 'Bacterial bioluminescence assay for bioanalysis and bioimaging'.
Li, Z., Askim, J. R. and Suslick, K. S. (2019) 'The Optoelectronic Nose: Colorimetric and Fluorometric Sensor Arrays', Chemical Reviews, 119(1), pp. 231–292. doi: 10.1021/acs.chemrev.8b00226.
Liang, G. et al. (2016) 'Bioinspired Fluorescent Nanosheets for Rapid and Sensitive Detection of Organic Pollutants in Water', ACS Sensors, 1(10), pp. 1272–1278. doi: 10.1021/acssensors.6b00530.
Liang, Y. et al. (2019) 'Hydrothermal growth of nitrogen-rich carbon dots as a precise multifunctional probe for both Fe3+ detection and cellular bio-imaging', Optical Materials, 89(November 2018), pp. 92–99. doi: 10.1016/j.optmat.2019.01.008.
Liu, B., Zhuang, J. and Wei, G. (2020) 'Recent advances in the design of colorimetric sensors for environmental monitoring', Environmental Science: Nano, 7(8), pp. 2195–2213. doi: 10.1039/d0en00449a.
Liu, C. et al. (2018) 'Black phosphorus integrated tilted fiber grating for ultrasensitive heavy metal sensing', Sensors and Actuators B: Chemical, 257, pp. 1093–1098. doi: doi.org/10.1016/j.snb.2017.11.022.
Liu, G. et al. (2016) 'In-situ hydrothermal synthesis of molecularly imprinted polymers coated carbon dots for fluorescent detection of bisphenol A', Sensors and Actuators B: Chemical, 228, pp. 302–307. doi: 10.1016/J.SNB.2016.01.010.
Liu, G. et al. (2018) 'Application of Gold-Nanoparticle Colorimetric Sensing to Rapid Food Safety Screening', Sensors 2018, Vol. 18, Page 4166, 18(12), p. 4166. doi: 10.3390/S18124166.
Liu, J., Wang, L. and Bao, H. (2019) 'A novel fluorescent probe for ascorbic acid based on seed-mediated growth of silver nanoparticles quenching of carbon dots fluorescence', Analytical and Bioanalytical Chemistry, 411(4), pp. 877–883. doi: 10.1007/s00216-018-1505-9.
Liu, L. et al. (2018) 'TriPleXTM waveguide-based fluorescence biosensor for multichannel environmental contaminants detection', Biosensors and Bioelectronics, 106(December 2017), pp. 117–121. doi: 10.1016/j.bios.2018.01.066.
Liu, M. L. et al. (2019) 'Anthrax biomarker: An ultrasensitive fluorescent ratiometry of dipicolinic acid by using terbium(III)-modified carbon dots', Talanta, 191(Iii), pp. 443–448. doi: 10.1016/j.talanta.2018.08.071.
Liu, Xia et al. (2015) 'SPR quantitative analysis of direct detection of atrazine traces on Au-nanoparticles: Nanoparticles size effect', Sensors and Actuators B: Chemical, 218, pp. 1–7. doi: 10.1016/J.SNB.2015.04.099.
Londoño Franco, L. F., Londoño Muñoz, P. T. and Muñoz Garcia, F. G. (2016) 'Los Riesgos De Los Metales Pesados En La Salud Humana Y Animal', Biotecnoloía en el Sector Agropecuario y Agroindustrial, 14(2), p. 145. doi: 10.18684/BSAA(14)145-153.
Lopreside, A. et al. (2019) 'Prêt-à-porter nanoYESA and nanoYESB bioluminescent cell biosensors for ultrarapid and sensitive screening of endocrine-disrupting chemicals', Analytical and Bioanalytical Chemistry, 411(19), pp. 4937–4949. doi: 10.1007/s00216-019-01805-2.
Lopreside, A., Calabretta, M. M., et al. (2021) 'Bioluminescence goes portable: recent advances in whole-cell and cell-free bioluminescence biosensors', Luminescence, 36(2), pp. 278–293. doi: 10.1002/bio.3948.
Lopreside, A., Montali, L., et al. (2021) 'Orthogonal paper biosensor for mercury(II) combining bioluminescence and colorimetric smartphone detection', Biosensors and Bioelectronics, 194(June), p. 113569. doi: 10.1016/j.bios.2021.113569.
Lu, M. Y. et al. (2019) 'A smartphone-based whole-cell array sensor for detection of antibiotics in milk', Sensors (Switzerland), 19(18). doi: 10.3390/s19183882.
Luo, D. et al. (2016) 'Exposure to organochlorine pesticides and non-Hodgkin lymphoma: A meta-analysis of observational studies', Scientific Reports, 6(1), pp. 1–11. doi: 10.1038/srep25768.
Luo, Q. et al. (2018) 'An ultrasensitive fluorescent sensor for organophosphorus pesticides detection based on RB-Ag/Au bimetallic nanoparticles', Sensors and Actuators, B: Chemical, 263, pp. 517–523. doi: 10.1016/j.snb.2018.02.101.
Luo, X. et al. (2020) 'Carbon dots derived fluorescent nanosensors as versatile tools for food quality and safety assessment: A review', Trends in Food Science and Technology. Elsevier Ltd, pp. 149–161. doi: 10.1016/j.tifs.2019.11.017.

M., R. et al. (2009) 'Ultrasensitive surface plasmon resonance detection of trinitrotoluene by a bis-aniline-cross-linked Au nanoparticles composite', Journal of the American Chemical Society, 131(21), pp. 7368–73783. doi: 10.1021/ja9001212.
McDonnell, J. M. (2001) 'Surface plasmon resonance: towards an understanding of the mechanisms of biological molecular recognition', Current Opinion in Chemical Biology, 5(5), pp. 572–577. doi: 10.1016/S1367-5931(00)00251-9.
Meng, X. et al. (2013) 'A simple and sensitive fluorescence biosensor for detection of organophosphorus pesticides using H2O2-sensitive quantum dots/bi-enzyme', Biosensors and Bioelectronics, 47, pp. 402–407. doi: 10.1016/j.bios.2013.03.053.
Mirzaei, A. et al. (2016) 'Removal of pharmaceuticals and endocrine disrupting compounds from water by zinc oxide-based photocatalytic degradation: A review', Sustainable Cities and Society, 27, pp. 407–418. doi: 10.1016/j.scs.2016.08.004.
Moscovici, L. et al. (2020) 'Yeast-Based Fluorescent Sensors for the Simultaneous Detection of Estrogenic and Androgenic Compounds, Coupled with High-Performance Thin Layer Chromatography', Biosensors, 10(11). doi: 10.3390/bios10110169.
Nabok, A. et al. (2019) '[INVITED] Novel optical biosensing technologies for detection of mycotoxins', Optics and Laser Technology, 109(April 2018), pp. 212–221. doi: 10.1016/j.optlastec.2018.07.076.
Norlinf, P., Wood-Black, F. and Masciangioli, T. (2004) Water and Sustainable Development: Opportunities for the Chemical Sciences - A Workshop Report to the Chemical Sciences Roundtable, Water and Sustainable Development: Opportunities for the Chemical Sciences: A Workshop Report to the Chemical Sciences Roundtable. National Academy of Sciences.
Ojha, N. K. et al. (2017) 'Copper nanoparticles as inexpensive and efficient catalyst: A valuable contribution in organic synthesis', Coordination Chemistry Reviews, 353, pp. 1–57. doi: 10.1016/J.CCR.2017.10.004.
Ong, J. J. et al. (2021) 'Optical biosensors - Illuminating the path to personalized drug dosing', Biosensors and Bioelectronics, 188, p. 113331. doi: 10.1016/J.BIOS.2021.113331.
Ortega, E. et al. (2016) 'Fluorescence of the Flavin group in choline oxidase. Insights and analytical applications for the determination of choline and betaine aldehyde', Talanta, 147, pp. 253–260. doi: 10.1016/j.talanta.2015.09.060.
Osman, B. et al. (2013) 'Microcontact imprinted surface plasmon resonance sensor for myoglobin detection', Materials Science and Engineering: C, 33(7), pp. 3609–3614. doi: doi.org/10.1016/j.msec.2013.04.041.
Otten, J. et al. (2019) 'A FRET-based biosensor for the quantification of glucose in culture supernatants of mL scale microbial cultivations', Microbial Cell Factories, 18(1), pp. 1–10. doi: 10.1186/s12934-019-1193-y.
P.S., M. et al. (1999) 'Food-related illness and death in the United States.', Emerging Infectious Disease, 5(5), pp. 607–625. doi: 10.3201/eid0505.990502.
Pandit, S. et al. (2016) 'Nanotechnology based biosensors and its application', The Pharma Innovation Journal, 18(6), pp. 18–25.
Patel, G. M. et al. (2015) 'Recognition of carbendazim fungicide in environmental samples by using 4-aminobenzenethiol functionalized silver nanoparticles as a colorimetric sensor', Sensors and Actuators, B: Chemical, 206, pp. 684–691. doi: 10.1016/j.snb.2014.09.095.
Paul, K. C. et al. (2018) 'Organophosphate pesticide exposure and differential genome-wide DNA methylation', Science of the Total Environment, 645, pp. 1135–1143. doi: 10.1016/j.scitotenv.2018.07.143.
Pehlivan, Z. S. et al. (2019) 'Aptamer and nanomaterial based FRET biosensors: a review on recent advances (2014–2019)', Microchimica Acta 2019 186:8, 186(8), pp. 1–22. doi: 10.1007/S00604-019-3659-3.
Peltomaa, R. et al. (2020) 'Bioluminescent detection of zearalenone using recombinant peptidomimetic Gaussia luciferase fusion protein', Microchimica Acta, 187(10). doi: 10.1007/s00604-020-04538-7.
Peltomaa, R., Benito-Peña, E. and Moreno-Bondi, M. C. (2018) 'Bioinspired recognition elements for mycotoxin sensors', Analytical and Bioanalytical Chemistry, 410(3), pp. 747–771. doi: 10.1007/s00216-017-0701-3.
Plácido, J. et al. (2019) 'Microalgae biochar-derived carbon dots and their application in heavy metal sensing in aqueous systems', Science of the Total Environment, 656, pp. 531–539. doi: 10.1016/j.scitotenv.2018.11.393.
Postnikova, G. B. and Yumakova, E. M. (1991) 'Fluorescence study of the conformational properties of myoglobin structure', European journal of biochemistry, 198(1), pp. 241–246.

Qiang, L. et al. (2020) 'A rapid and ultrasensitive colorimetric biosensor based on aptamer functionalized Au nanoparticles for detection of saxitoxin', RSC Advances, 10(26), pp. 15293–15298. doi: 10.1039/d0ra01231a.
Ramdzan, N. S. M. et al. (2021) 'Detection of mercury ion using surface plasmon resonance spectroscopy based on nanocrystalline cellulose/poly(3,4-ethylenedioxythiophene) thin film', Measurement, 182, p. 109728. doi: 10.1016/J.MEASUREMENT.2021.109728.
Reddy, P. M. et al. (2017) 'Detection of cyanide ions in aqueous solutions using cost effective colorimetric sensor', Journal of Hazardous Materials, 334, pp. 93–103. doi: 10.1016/j.jhazmat.2017.04.001.
Rodriguez-Mozaz, S. et al. (2004) 'Biosensors for environmental applications: Future development trends', Pure and Applied Chemistry, 76(4), pp. 723–752. doi: 10.1351/pac200476040723.
Roto, R. et al. (2019) 'Colorimetric sensing of Pb2+ ion by using ag nanoparticles in the presence of dithizone', Chemosensors, 7(3). doi: 10.3390/CHEMOSENSORS7030028.
Saad, M. et al. (2022) 'Introducing an SPRi-based titration assay using aptamers for the detection of Legionella pneumophila', Sensors and Actuators B: Chemical, 351, p. 130933. doi: 10.1016/J.SNB.2021.130933.
Saylan, Y. et al. (2017) 'Development of surface plasmon resonance sensors based on molecularly imprinted nanofilms for sensitive and selective detection of pesticides', Sensors and Actuators, B: Chemical, 241, pp. 446–454. doi: 10.1016/j.snb.2016.10.017.
Sener, G. et al. (2011) 'Use of molecular imprinted nanoparticles as biorecognition element on surface plasmon resonance sensor', Sensors and Actuators B: Chemical, 160(1), pp. 791–799. doi: doi.org/10.1016/j.snb.2011.08.064.
Senko, O. et al. (2019) 'Immobilized luminescent bacteria for the detection of mycotoxins under discrete and flow-through conditions', Biosensors, 9(2). doi: 10.3390/bios9020063.
Shaikh, H. et al. (2015) 'Molecularly imprinted surface plasmon resonance (SPR) based sensing of bisphenol a for its selective detection in aqueous systems', Anal. Methods-UK, 7, pp. 4661–4670.
Sidhu, G. K. et al. (2019) 'Toxicity, monitoring and biodegradation of organophosphate pesticides: A review', https://doi.org/10.1080/10643389.2019.1565554, 49(13), pp. 1135–1187. doi: 10.1080/10643389.2019.1565554.
Simões, J. and Dong, T. (2018) 'Continuous and real-time detection of drinking-water pathogens with a low-cost fluorescent optofluidic sensor', Sensors (Switzerland), 18(7). doi: 10.3390/s18072210.
Simon, R. et al. (2008) 'Results of a European inter-laboratory comparison study on the determination of EU priority polycyclic aromatic hydrocarbons (PAHs) in edible vegetable oils.', Anal Bioanal Chem, 391, pp. 1397–1408. doi: doi.org/10.1007/s00216-007-1771-4.
Singh, H. et al. (2021) 'Nanomaterial-based fluorescent sensors for the detection of lead ions', Journal of Hazardous Materials, 407(November 2020), p. 124379. doi: 10.1016/j.jhazmat.2020.124379.
Singh, S. et al. (2016) 'Toxicity, monitoring and biodegradation of the fungicide carbendazim', Environmental Chemistry Letters, 14(3), pp. 317–329. doi: 10.1007/S10311-016-0566-2/TABLES/1.
Soltani, T. G. et al. (2021) 'Modeling and characterization of an engineered microbial biosensor for high-throughput screening of arsenic in rural water', Process Safety and Environmental Protection, 153, pp. 215–224. doi: 10.1016/j.psep.2021.07.019.
Song, W. et al. (2017) 'A new fluorescence probing strategy for the detection of parathion-methyl based on N-doped carbon dots and methyl parathion hydrolase', Chinese Chemical Letters, 28(8), pp. 1675–1680. doi: 10.1016/j.cclet.2017.05.001.
Sousa, J. C. G. et al. (2018) 'A review on environmental monitoring of water organic pollutants identified by EU guidelines', Journal of Hazardous Materials, 344, pp. 146–162. doi: 10.1016/j.jhazmat.2017.09.058.
Stahel, W. R. (2016) 'The circular economy', Nature. Nature Publishing Group, pp. 435–438. doi: 10.1038/531435a.
Staiano, M. et al. (2005) 'Glucose biosensors as models for the development of advanced protein-based biosensors', Molecular BioSystems, 1(5–6), pp. 354–362. doi: 10.1039/b513385h.
Strianese, M. et al. (2012) 'Fluorescence-Based Biosensors', Methods in Molecular Biology, 875(2), pp. 482–483. doi: 10.1163/ej.9789004196186.i-584.127.
Su, Y. et al. (2020) 'Different bacterial host-based lux reporter array for fast identification and toxicity indication of multiple metal ions', Analytical and Bioanalytical Chemistry, 412(29), pp. 8127–8134. doi: 10.1007/s00216-020-02943-8.

Sun, A. and Wang, W. X. (2021) 'Adenine deficient yeast: A fluorescent biosensor for the detection of Labile Zn(II) in aqueous solution', Biosensors and Bioelectronics, 179(January), p. 113075. doi: 10.1016/j.bios.2021.113075.
Sun, D. and Zhang, H. (2006) 'Voltammetric determination of 6-benzylaminopurine (6-BAP) using an acetylene black-dihexadecyl hydrogen phosphate composite film coated glassy carbon electrode', Analytica Chimica Acta, 557(1–2), pp. 64–69. doi: 10.1016/J.ACA.2005.10.002.
Sun, H., Brocato, J. and Costa, M. (2015) 'Oral Chromium Exposure and Toxicity', Current environmental health reports, 2(3), pp. 295–303. doi: 10.1007/S40572-015-0054-Z/TABLES/1.
Sungho, K. et al. (2009) 'Directed self-assembly of gold binding polypeptide-protein A fusion proteins for development of gold nanoparticle-based SPR immunosensors', Biosensors and Bioelectronics , 24(8), pp. 2592–2597.
Syed, A. J. and Anderson, J. C. (2021) 'Applications of bioluminescence in biotechnology and beyond', Chemical Society Reviews, 50(9), pp. 5668–5705. doi: 10.1039/d0cs01492c.
Tafreshi, F. A. et al. (2020) 'Ultrasensitive fluorescent detection of pesticides in real sample by using green carbon dots', PLoS ONE, 15(3), pp. 1–17. doi: 10.1371/journal.pone.0230646.
Tan, Y., Ahmad, I. and Wei, T. X. (2015) 'Detection of parathion methyl using a surface plasmon resonance sensor combined with molecularly imprinted films', Chinese Chem. Lett., 26(6), pp. 797–800.
Tang, Ying Ying et al. (2020) 'A robust OFF-ON fluorescent biosensor for detection and clearance of bacterial endotoxin by specific peptide based aggregation induced emission', Sensors and Actuators, B: Chemical, 304. doi: 10.1016/j.snb.2019.127300.
Thompson, R. (2005) 'Fluorescence sensors and biosensors', in Fluorescence sensors and biosensors. Taylor & F. Florida, p. 377. Available at: https://books.google.com/books?hl=es&lr=&id=2-_KBQAAQBAJ&pgis=1 (Accessed: 21 February 2015).
Timofeyenko, Y. G., Rosentreter, J. J. and Mayo, S. (2006) 'Piezoelectric Quartz Crystal Microbalance Sensor for Trace Aqueous Cyanide Ion Determination', Analytical Chemistry, 79(1), pp. 251–255. doi: 10.1021/AC060890M.
Tjandra, A. D. et al. (2019) 'Optical sensors', in Bioengineering Innovative Solutions for Cancer. Elsevier Ltd., pp. 23–45. doi: 10.1016/B978-0-12-813886-1.00003-6.
Torun, Ö. et al. (2012) 'Comparison of sensing strategies in SPR biosensor for rapid and sensitive enumeration of bacteria', Biosensors and Bioelectronics, 37(1), pp. 53–60. doi: 10.1016/J.BIOS.2012.04.034.
Trojanowicz, M., Kowalski, D. and Poboy, E. (2011) 'Flow-injection preconcentration of chloramphenicol using molecularly imprinted polymer for HPLC determination in environmental samples', Journal of Automated Methods and Management in Chemistry, 2011. doi: 10.1155/2011/143416.
United States environmental protection agency (2016) Toxic Substances Control Act. USA.
Vasapollo, G. et al. (2011) 'Molecularly Imprinted Polymers: Present and Future Prospective', International Journal of Molecular Sciences 2011, Vol. 12, Pages 5908-5945, 12(9), pp. 5908–5945. doi: 10.3390/IJMS12095908.
Vilela, D., González, M. C. and Escarpa, A. (2012) 'Sensing colorimetric approaches based on gold and silver nanoparticles aggregation: Chemical creativity behind the assay. A review', Analytica Chimica Acta, 751, pp. 24–43. doi: 10.1016/J.ACA.2012.08.043.
Wang, H. et al. (2016) 'High fluorescence S, N co-doped carbon dots as an ultra-sensitive fluorescent probe for the determination of uric acid', Talanta, 155, pp. 62–69. doi: 10.1016/j.talanta.2016.04.020.
Wang, H. and Zhang, K. Q. (2013) 'Photonic Crystal Structures with Tunable Structure Color as Colorimetric Sensors', Sensors 2013, Vol. 13, Pages 4192-4213, 13(4), pp. 4192–4213. doi: 10.3390/S130404192.
Wang, L. et al. (2017) 'Nanoporous Gold Films Prepared by a Combination of Sputtering and Dealloying for Trace Detection of Benzo[a]pyrene Based on Surface Plasmon Resonance Spectroscopy', Sensors, 17(6), p. 1255. doi: doi.org/10.3390/s17061255.
Wang, N. et al. (2019) 'Synthesis of fluorescent copper nanoparticles and ultrasensitive free label detection of Ag+', Journal of Nanomaterials, 2019. doi: 10.1155/2019/4089731.
Wang, X. et al. (2013) 'Advances and applications of surface plasmon resonance biosensing instrumentation', Instrumentation Science & Technology, 41(6), pp. 574–607. doi: 10.1080/10739149.2013.807822.

Wang, Y. et al. (2016) 'A colorimetric biosensor using Fe3O4 nanoparticles for highly sensitive and selective detection of tetracyclines', Sensors and Actuators, B: Chemical, 236, pp. 621–626. doi: 10.1016/j.snb.2016.06.029.
Wang, Z. et al. (2020) 'Multicolor visual screening of total dithiocarbamate pesticides in foods based on sulfydryl-mediated growth of gold nanobipyramids', Analytica Chimica Acta, 1139, pp. 59–67. doi: 10.1016/J.ACA.2020.09.032.
WHO (2008) Guidelines for Drinking-water Quality. Geneva.
Wijaya, E. et al. (2011) 'Surface plasmon resonance-based biosensors: From the development of different SPR structures to novel surface functionalization strategies', Current Opinion in Solid State and Materials Science, 15(5), pp. 208–224. doi: 10.1016/J.COSSMS.2011.05.001.
Wong, L. S. et al. (2018) 'Bioluminescent Microalgae-Based Biosensor for Metal Detection in Water', IEEE Sensors Journal, 18(5), pp. 2091–2096. doi: 10.1109/JSEN.2017.2787786.
Wong, P. K. and Wang, J. (2001) 'The accumulation of polycyclic aromatic hydrocarbons in lubricating oil over time Ð a comparison of supercritical ¯uid and liquid±liquid extraction methods', Environmental Pollution, 112(3), pp. 407–415. doi: 10.1016/s0269-7491(00)00142-1.
Wong, X. Y. et al. (2021) 'Fluorescence "turn-off/turn-on" biosensing of metal ions by gold nanoclusters, folic acid and reduced graphene oxide', Analytica Chimica Acta, 1175. doi: 10.1016/j.aca.2021.338745.
Wu, X. et al. (2015) 'Molecularly imprinted polymers-coated gold nanoclusters for fluorescent detection of bisphenol A', Sensors and Actuators B: Chemical, 211, pp. 507–514. doi: doi.org/10.1016/j.snb.2015.01.115.
Xi Huang et al. (2009) 'A gold nanoparticle labeling strategy for the sensitive kinetic assay of the carbamate–acetylcholinesterase interaction by surface plasmon resonance', Talanta , 78(3), pp. 1036–1042. doi: doi.org/10.1016/j.talanta.2009.01.018.
Xiang-li, L. et al. (2007) 'Distribution patterns of octylphenol and nonylphenol in the aquatic system Mai Po Marshes nature reserve, a subtropical estuarine wetland in Hong Kong', Environmental Sciences, 19, pp. 657–662.
Xiao, N. et al. (2018) 'B,N-carbon dots-based ratiometric fluorescent and colorimetric dual-readout sensor for H2O2 and H2O2-involved metabolites detection using ZnFe2O4 magnetic microspheres as peroxidase mimics', Sensors and Actuators, B: Chemical, 273(July), pp. 1735–1743. doi: 10.1016/j.snb.2018.07.097.
Xu, S. et al. (2020) 'A boronic acid-based fluorescent hydrogel for monosaccharide detection', Frontiers of Chemical Science and Engineering, 14(1), pp. 112–116. doi: 10.1007/s11705-019-1812-5.
Xu, T. et al. (2018) 'A rapid and reagent-free bioassay for the detection of dioxin-like compounds and other aryl hydrocarbon receptor (AhR) agonists using autobioluminescent yeast', Analytical and Bioanalytical Chemistry, 410(4), pp. 1247–1256. doi: 10.1007/s00216-017-0780-1.
Xue, T., Qi, K. and Hu, C. (2019) 'Novel SPR sensing platform based on superstructure MoS2 nanosheets for ultrasensitive detection of mercury ion', Sensors and Actuators B: Chemical, 284, pp. 589–594. doi: 10.1016/J.SNB.2019.01.004.
Yan, X. et al. (2018) 'MnO2 Nanosheet-Carbon Dots Sensing Platform for Sensitive Detection of Organophosphorus Pesticides', Analytical Chemistry, 90(4), pp. 2618–2624. doi: 10.1021/acs.analchem.7b04193.
Yan, X., Li, H. and Su, X. (2018) 'Review of optical sensors for pesticides', TrAC Trends in Analytical Chemistry, 103, pp. 1–20. doi: 10.1016/J.TRAC.2018.03.004.
Yang, C. et al. (2011) 'Aptamer-based colorimetric biosensing of Ochratoxin A using unmodified gold nanoparticles indicator', Biosensors and Bioelectronics, 26(5), pp. 2724–2727. doi: 10.1016/J.BIOS.2010.09.032.
Yao, Y. et al. (2021) 'Fast detection of E. coli with a novel fluorescent biosensor based on a FRET system between UCNPs and GO@Fe3O4in urine specimens', Analytical Methods, 13(19), pp. 2209–2214. doi: 10.1039/d1ay00320h.
Yin, M. and Ji, C. (2017) 'Nanoscaled Fluorescent Films and Layers for Detection of Environmental Pollutants', Nanoscaled Films and Layers. doi: 10.5772/67869.
Yılmaz, E. et al. (2017) 'Plastic antibody based surface plasmon resonance nanosensors for selective atrazine detection', Materials Science and Engineering: C, 73, pp. 603–610. doi: 10.1016/J.MSEC.2016.12.090.

Zhang, G. et al. (2018) 'A simple FRET-based turn-on fluorescent aptasensor for 17B-estradiol determination in environmental water, urine and milk samples', Sensors and Actuators, B: Chemical, 273(July), pp. 1648–1653. doi: 10.1016/j.snb.2018.07.066.
Zhang, X., Guo, Q. and Cui, D. (2009) 'Recent advances in nanotechnology applied to biosensors', Sensors, 9(2), pp. 1033–1053. doi: 10.3390/s90201033.
Zhao, Y. et al. (2020) 'GeSe nanosheets modified surface plasmon resonance sensors for enhancing sensitivity', Nanophotonics, 9(2), pp. 327–336. doi: 10.1515/nanoph-2019-0170.
Zheng, M. et al. (2018) 'Colorimetric recognition of 6-benzylaminopurine in environmental samples by using thioglycolic acid functionalized silver nanoparticles', Spectrochimica Acta - Part A: Molecular and Biomolecular Spectroscopy, 192, pp. 27–33. doi: 10.1016/j.saa.2017.10.073.
Zheng, Y. et al. (2021) 'Enhanced turn-on fluorescence detection of aqueous lead ions with size-shrinkable hydrogels', ACS Omega, 6(18), pp. 11897–11901. doi: 10.1021/acsomega.1c00150.
Zhu, B. et al. (2018) 'Fluorescent silicon nanoparticles for sensing Hg2+ and Ag+ as well visualization of latent fingerprints', Dyes and Pigments, 149(November 2017), pp. 686–695. doi: 10.1016/j.dyepig.2017.11.041.
Zhu, D., Liu, B. and Wei, G. (2021) 'Two-dimensional material-based colorimetric biosensors: A review', Biosensors, 11(8). doi: 10.3390/bios11080259.

3. Nanomaterial-based fluorescent biosensors for monitoring environmental pollutants: A critical review

Abstract

The growing interest in nanomaterials with advanced optoelectronic properties has promoted the advancement of biosensors with various applications. In the environmental field, the need for rapid detection of pollutants in water sources has opened the door to fluorescent biosensors. These systems are quite sensitive and simple. Nanomaterials such as carbon dots (CD), quantum dots (QD), gold nanoparticles, nanoclusters, graphene (G), graphene oxide (GO), transition metal dialcogens (TMDC) and organometallic frameworks (MOF), have been used in the development of fluorescent detection systems. They are usually based on the Förster resonance energy transfer (FRET) quenching principle. Nanomaterials can be bioconjugated with molecules such as antibodies, enzymes, or aptamers, to achieve specific detection of the target pollutant, even in real samples. This review conducts a critical analysis of the operating principle of different nanomaterial-based fluorescent biosensors. We discuss the detection of substances of high concern like heavy metals, pesticides, and so-called emerging contaminants. The advantages and disadvantages of the methods are discussed, as well as recommendations for future approaches and a possible massification of these systems.

Keywords: Nanostructures, FRET, heavy metals, pesticides, emerging pollutants, bioconjugation

Highlights:

- Nanostructures for environmental pollutants detection have been reviewed.
- Nanomaterial-based fluorescent biosensors with high detection limits are tabulated.
- Fluorescence quenching and other detection mechanism are discussed.
- Biomediators types and bioconjugation techniques have been explored.

Published in:
Talanta Open. Elsevier
Date: june 18, 2020
Cite as:
Gaviria-Arroyave, M. I., Cano, J. B., & Peñuela, G. A. (2020). Nanomaterial-based fluorescent biosensors for monitoring environmental pollutants: A critical review. *Talanta Open*, *2*(June), 100006. https://doi.org/10.1016/j.talo.2020.100006.

3.1. Introduction

The need to obtain enough water, food and energy has become a pressing challenge. It is estimated that by 2030, 30% more water, 40% more food, and 50% more energy will be required (Ellen MacArthur Foundation., 2015). To obtain large amounts of resources, linear production methods based on the extraction, use and disposal process have been implemented; methods that generate major problems of pollution in soils, water, and atmosphere (Stahel, 2016). Environmental pollution and its derived effects, such as climate change, are a major international concern, and are key points on the political and economic agendas of countries (European environment agency, 2013; Sousa et al., 2018; United States environmental protection agency, 2016). The United Nations (UN), within its Sustainable Development Goals (SDGs), has established guidelines to achieve positive changes regarding sustainable development, attention to climate change, and sustainable energy production, as well as water and sanitation (UN, n.d.).

Basic sanitation is threatened by the contamination of water sources by pesticides used to improve agricultural productivity; heavy metals resulting from mining-industrial activities; and the so-called emerging pollutants of varied and mainly urban origin. Exposure to different types of pesticides has been linked to diseases including lymphomas (Hodgkin) (Luo et al., 2016), Parkinson's (Brouwer et al., 2017), cancer (Paul et al., 2018), reproductive disorders (Mazur et al., 2015) and endocrine disorders (Machado and Martins, 2018). Endocrine effects can also be caused by acute exposure to different substances, grouped for some years under the term emerging pollutants. This category includes personal hygiene products, household cleaning products, cosmetic additives, sunscreens, supplies from the plastics industry, and drug residues, among others (Mirzaei et al., 2016). These compounds are especially difficult to detect since they are in very low concentrations, which represents a challenge for current analytical systems. Meanwhile, heavy metals are distributed in water sources, especially in poor or underdeveloped countries that are highly extractivist. Heavy metals cannot be degraded or destroyed, but they can be dissolved or precipitated by physicochemical agents or the environmental conditions of the medium, such as pH or temperature. Some of them form soluble complexes and are transported and distributed to ecosystems until they are incorporated into the food chain (Londoño Franco et al., 2016). In addition to the acute effects of some substances, all the pollutants pose a risk to human health and ecosystems, due to their potential for bioaccumulation that causes chronic effects (Hamza et al., 2016; Patel et al., 2020)

For the detection of pollutants of interest in waters, biosensors have been rapidly developed as a complement to traditional analytical methods, as they have advantages such as ease of handling, the low cost potential of their components and the possibility of real-time quantification (Buonasera et al., 2015). Biosensors are analytical devices with a biomediator element (responsible for the recognition of the analyte) that is in contact with a transducer element (responsible for converting the interaction into a measurable signal). There are various types of biomediators and transducers (Figure 3-1), with optical and electrochemical biosensors being those with the greatest potential for application in the detection of pollutants with adequate sensitivity and specificity (Buonasera et al., 2015). Developments in fluorescent biosensors aim to work without labeling, using the natural

fluorescence property of nanomaterials, some metal cations, and certain biological events (Khansili et al., 2018).

Nanomaterials have introduced an interesting approach to the development of low-cost, portable fluorescent devices [32]. The application of nanomaterials including metallic nanoparticles (NP), multi-walled carbon nanotubes (MWCNT), graphene (G), graphene oxide (GO) quantum dots (QD), carbon dots (CD), nanosheets and metal-organic frames (MOFs) can significantly improve the performance of biosensors. This is due to advantages such as a higher surface area-volume ratio and excellent physicochemical properties [50]. Nanomaterials possess unique optoelectronic properties that are expected to allow the development of sophisticated systems for the detection of multiple analytes simultaneously and at a moderate cost (Zhang et al., 2014).

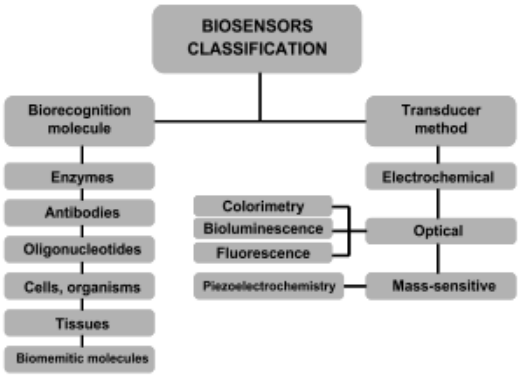

Figure 3-1. Classification of biosensors according to biomediator molecules and the transduction technique (Buonasera et al., 2015)

Nanomaterials are generally defined as "natural, incidental or manufactured materials that contain particles in the aggregate or non-aggregate state where at least 50% of these particles have dimensions between 1 nm and 100 nm"(Bleeker et al., 2013). Nanomaterials have driven the development of new forms of extraction, concentration, and analysis of pollutants, as well as new devices. These is currently significant research on the development of fluorescent biosensors involving nanomaterials, due to their wide impact not only in the environmental field but also in materials science and biomedicine (Pelle and Compagnone, 2018). One of the most important nanomaterials in biosensor field is Graphene (G). G is a two-dimensional (2D) allotrope of carbon, consisting basically of a flat sheet of carbon atoms one atom thick, which are linked by sp2 hybridization. Thanks to this configuration, graphene has high conductivity and electron mobility at room temperature, which gives it superior electrical, optical, thermal, and electrochemical performance (Pelle and Compagnone, 2018). The investigations carried out on graphene have allowed the synthesis of derivatives from this material, with interesting uses especially in the field of optics and sensors. When the carbon source is graphite, graphene oxide (GO) or reduced graphene oxide (rGO) can be obtained. On-GO or rGO are photoluminescent materials, but can be induced by chemical modifications that generate an adequate band gap (Singh et al., 2011). GO and rGO can also be used as starting materials for the synthesis of fluorescent materials such as quantum carbon dots or nanofibers.

As well as Graphene, Metallic nanoparticles (MNPs) has been used as quenching agents. MNPs are nanometric structures made up of pure metals such as gold, silver, platinum, or zinc. These nanomaterials have interesting properties such as large surface area, biocompatibility, easy functionalization, and surface plasmonic resonance (SPR) phenomena (Kumari et al., 2019). Additionally, they report good conductivity and non-linear spectral properties that are exploited in the manufacture of colorimetric, optical, electronic, and biomolecular systems. Also, and as detailed later in this review, MNPs are considered excellent quencher agents in fluorescent systems, due to their broad absorption spectrum, making them good acceptors for FRET processes (Zhan et al., 2019).

Other highly explored nanomaterial are Quantum dots (QDs). QDs can be defined as zero-dimensional semiconductor crystals, with fluorescent properties that depend on their size and composition (Ko et al., 2020). This material has been shown to be superior to traditional fluorescent compounds, as it has a wide excitation spectrum, a narrow emission bandwidth and a strong fluorescence emission. The use of QDs for the development of optical biosensors is based on their photoluminescence as well as their surface properties. When the interaction with the analyte occurs, usually mediated by a bioreceptor, an increase (turn on) or decay (turn off) of the emission is generated. However, QDs are still toxic in some systems because most of them are made of heavy metal like cadmium, leading in vitro toxicity that could limit their practical applications (Chen et al., 2012). Recently, some research in silver-, indium-, carbon- and silicon-containing QDs have shown superior biocompatibility (Liu and Tang, 2020)

To overcome these problems, Carbon dots (CDs) have emerged. CDs are zero-dimension quasi-spherical nanoparticles, composed primarily of carbon and oxygen, usually with sizes below 10 nm (Abdul et al., 2019; Campuzano et al., 2019; Plácido et al., 2019a, 2019b). They were first observed in a single wall carbon nanotube (SWCNTs) purification process in 2004 (Xu et al., 2004) and since then have gained a lot of attention because they have opto-electronic properties like quantum dots, especially when it comes to fluorescence. CDs, unlike QDs, have excellent biocompatibility. This is due to their low toxicity, since they do not involve the use of metallic elements and their synthesis is easier.

In recent years, a new group of nanomaterials have attracted the attention of researchers in various fields. These are 2D nanostructures, usually known as nanosheets or thin films (Tao et al., 2020). These nano blades have thickness of atomic dimension compared to relatively large lateral dimensions (Safarpour et al., 2020). 2D nanomaterials have a high surface-volume ratio when compared to 3D materials, and their optoelectronic characteristics are intrinsically dependent on size, shape, and number of layers (Oh et al., 2018). There are several inorganic solid materials that can be subjected to exfoliation processes to obtain nano blades: transition metal dialcogens (TMDC), metal oxides (TOM), metal hydroxides, metal carbides, MXenes, layered zeolites, hexagonal boron nitrides and organo-metallic frameworks (MOF) among others (Mei et al., 2017). The atoms of the thin layer in the 2D plane are covalently bonded, while the adjacent layers are bonded through weak interactions; this configuration provides high flexibility (Azadmanjiri et al., 2020).

Finally, Organ-metal frameworks (MOFs), also known as porous coordination polymers, are a class of nanomaterial consisting of a network of metal ions or oxides (called nodes) connected by organic molecules (Rodenas, 2019). MOFs can be presented in 2D or 3D structures and have received attention in the last 10 years due to their large surface area, high porosity, and thermal stability (Amini et al., 2020). Recently, MOFs have been used for the detection and quantification of degradation products of environmental interest. There is a versatile material that can be synthesized from the combination of different nodes and organic molecules, giving different properties. Among the successfully detected analytes are heavy metal ions, gases, and low molecular weight organic substances (Amini et al., 2020)

This review presents a critical analysis of the latest developments in fluorescent nanosensors for the detection of pesticides, heavy metals, and some emerging contaminants. It focuses on the types of nanomaterials as well as the detection techniques used by various researchers. The review also shows the great diversity of biomolecules, substrates and processes that can be used to improve the sensitivity and specificity of these devices.

3.2. Fluorescense and quenching mechanisms

Fluorescence can be defined as the phenomenon of light emission from a substance when it absorbs light with an appropriate wavelength. Specifically, it is a low wavelength absorption (more energetic) that results in excitation of electrons; when these electrons relax and return to their basal state, light emission with a greater wavelength is produced (less energy) (Berezin and Achilefu, 2010). Generally, the fluorescence of a substance is illustrated by the Jablonski diagram (Figure 3-2), which shows the absorption and emission of that substance (Berezin and Achilefu, 2010). It is known that in the excitation process of the electrons, they first gain energy by placing themselves in a high vibrational state and then in a relaxed vibrational state known as internal conversion; subsequently, these electrons return to the basal state, in which they emit light of greater wavelength compared to the absorbed light (Kaushal et al., 2020).

Fluorescence is a cyclical process since the same molecule can be repeatedly excited and detected. Additionally, fluorophores emit hundreds of photons, making the sensitivity of this phenomenon high (Lakowicz, 2006). However, the fluorescence of traditional organic molecules can be diminished by photobleaching, a less common phenomenon in emitting nanostructures (M. L. Liu et al., 2019).

The most important characteristics of a fluorescence-emitting molecule are the quantum yield (QY), and the life of the fluorescence (τ). QY is defined as the ratio between the number of photons emitted and the number of photons absorbed; this value is close to unity for molecules with higher emissions (Blagoi, 2004). Few fluorescent molecules have high QY, but even these, when conjugated with biomolecules, undergo a reduction of their efficiency. Several authors focus their efforts on synthesizing nanostructures with high QY (Pandey and Bodas, 2020).

Instead, τ is defined as the time that an excited molecule can interact with its nearby environment. In general, these times are between 10 ns and 10 µs (Lakowicz, 2006).

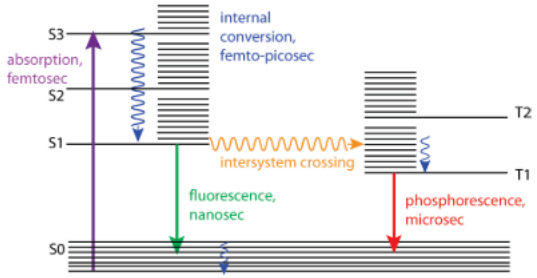

Figure 3-2. Jablonski diagram to show the fluorescence of an organic molecule and the difference with phosphorescence. Reprinted with permission from ref (Berezin and Achilefu, 2010). Copyright 2010.American Chemical Society

Fluorescence-based sensors use changes in intensity, absorption, or emission wavelength (differences in the spectrum), anisotropic, or emission lifetime alterations. Sensors based on changes in fluorescence intensity are the most widely used, as they are usually quite sensitive, easy to use, and adaptable to various analytes and systems (Blagoi, 2004). The main detection technique based on intensity changes is the so-called "quenching" of fluorescence. Quenching is a process in which the fluorescence intensity of an emitting molecule is reduced without affecting its spectrum. This phenomenon is proportional to the concentration of the extinguishing agent or "quencher". Various molecules that interact with the emitter can be used as quencher agents, with different types of extinction: collisional or dynamic, auto quenching, and static (Figure 3-3). The static mechanism is not always considered as quenching, due to the change in the spectra with respect to pure substances (Blagoi, 2004).

In dynamic mechanisms, the excited state of the emitting molecule decays without emission of normal fluorescence; in this case, a decline in both the intensity and the life of the emission is observed. Auto-quenching mechanisms are highly dependent on the concentration of the emitter, where the molecule itself acts as a quencher, either through photon reabsorption or the formation of excimers. In static quenching, basal state complexes are formed between two emitting molecules. These complexes are not emissive and generate a general quenching of the system but modify the spectra because the properties of the complex differ from the starting molecules. (Lakowicz, 2006). It should be noted that, when using a fluorescence test to detect the analyte, quenching can be generated on the emitting molecule, as a result not only of the presence of the substance of interest but also of other substances in the medium that become interferences (matrix effect).

Most fluorescent biosensors involving nanostructures, either as emitters or as acceptors, are based on generating quenching or preventing it, in the presence of the analyte of interest. The categories of quenching already described include the mechanisms of fluorescence resonance energy transfer-FRET, inner filter effect-IFE, photoinduced electron transfer-PET, and Dexter electron transfer -DET (Molaei, 2020) as shown in Figure 3-3. FRET, IFE and PET are the most common in the design of biosensors. These sensors can be of the “Turn off” type, whereby quenching is generated as a result

of the presence of the analyte; or “Turn on”, whereby the system is initially quenched, and the fluorescence is selectively recovered in the presence of the analyte (Neema et al., 2020).

FRET is a specific case of "Resonance energy transfer" -RET, a phenomenon based on dipole-dipole interactions. Depending on the nature of the emitting molecule, RET is divided into CRET (chemiluminescence), BRET (bioluminescence) and FRET (fluorescence) (Molaei, 2020). FRET, also known as "Förster resonance energy transfer", was first described in 1950, since when it has become one of the preferred optical sensor techniques, thanks to its sensitivity and fast response (Pehlivan et al., 2019). FRET is a non-radiative energy transfer process, which normally occurs between two fluorophores at distances around 10 nm (Förster distance), where an emitter is in proximity with an acceptor, transferring its energy from an excited state through dipole-dipole interactions (Neema et al., 2020). In addition to fulfilling the proximity condition, the dipole moments of both molecules must have a favorable orientation for interaction. In the FRET processes, an overlap between the donor emission and the acceptor absorption spectra is also evident, and it has been seen that the donor's emission life must be long enough for the phenomenon to be present (Nsibande and Forbes, 2016). FRET is usually only mentioned when these conditions are met between two fluorophores, but the mechanism is also usually used to explain quenching, fulfilling the previous conditions, in the presence of any type of acceptor (Lakowicz, 2006).

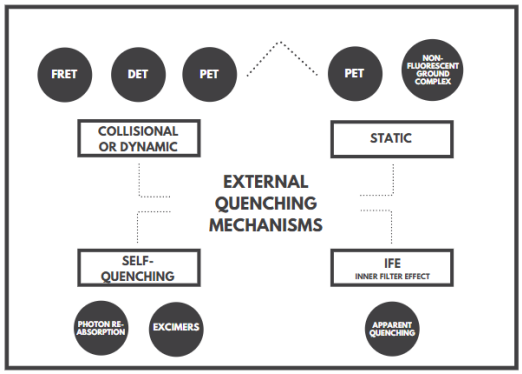

Figure 3-3. Scheme showing the general classification of quenching extinction mechanisms: collisional or dynamic, self-quenching, static, and apparent (IFE). The circles refer to the specific types of quenching related to each mechanism where FRET (Förster resonance energy transfer), DET (Dexter electron transfer), PET (photoinduced electron transfer) and IFE (Inner filter effect) are the most used for biosensors development.

DET is a less common phenomenon, occurring at distances less than the Förster distance, whereby an overlap is generated between the electronic orbitals of the two molecules involved, which produces quenching.

In PET-based processes, an electron transfer (charge) is generated at distances of less than 10 nm, usually through Van der Waals-type interactions between the molecules. As a result, dynamic interaction (from excited states without complex formation) or static interaction (through the formation of non-fluorescent complexes at baseline) can occur; in this mechanism, a partial distribution of loads is generated (Doose et al., 2009).

Finally, the IFE mechanism is based on the absorption of excitation or emission light from the donor by an acceptor of any chemical nature. In this case, the interaction occurs at distances greater than 10 nm and is considered more a shield than a true quenching, so is not classified as static or dynamic (Wang et al., 2018). In IFE there is also an overlap of spectra between both molecules and, when used in detection systems, the donor emission is sought to be independent of the concentration of the analyte, which in this case will be detected by the quencher. We refer to primary IFE when the acceptor absorbs the excitation energy and, secondary IFE when it absorbs the emitted light (Blagoi, 2004).

The use of nanomaterials in detection systems based on FRET implies the control of the interaction distances, so that they are close and strong enough to generate quenching, but also sensitive or weak enough to dissociate in the presence of the analyte (for example on "Turn on" sensors). To ensure that the quenching signal is proportional to the desired analyte, the emitting molecule must usually be linked to the biomolecule (enzyme, antibody, aptamer, etc) that performs the recognition of the substance of interest, a process called bioconjugation (Cardoso Dos Santos et al., 2020).

Bioconjugation involves the union between two or more molecules, through covalent or non-covalent bonds, or weak interactions. At least one of these molecules has a biological origin or is a fragment or derivative (Hermanson, 2008). The shape and functionalities of the final bioconjugate depend not only on the molecules used but also on the binding methods used. Usually, the properties of said conjugate differ with respect to the initial molecules, suppressing, or enhancing characteristics.

3.3. Detection of environmental pollutants

Organophosphorus Pesticides

Pesticides are compounds that are widely used for the prevention and control of pests, mainly in agriculture and forestry. They are also applied in home gardening, care of public spaces, and industrial disinfection. The word pesticide groups a wide variety of chemicals used as insecticide, herbicide, bactericide, fungicide, miticide, molluscicide, nematicide, rodenticide, and wood preservative purposes (Marican and Durán-Lara, 2018).

According to FAO (FAO, 2018), in 2017 (latest available data) the average pesticide use worldwide was 2.63 kg/ha of cultivation, but countries like Saint Lucia, China, and Ecuador used 19.6, 16.5 and 13.9 kg/ha respectively. Additionally, it is estimated that only 10 to 15% of the total amount of pesticide applied is effective, which causes the amount of residual contamination in the environment to increase (Rani and Shanker, 2018). The high mobility of these compounds in the environment means that pesticide contamination of surface waters is mainly caused by dew spillage, runoff water, and drainage water. Organophosphates (OP) are a group of pesticides in which more than 200 chemicals are included and are currently the most widely used in agriculture

and vector control due to their relatively low persistence. These compounds are phosphoric acid esters bound to a wide variety of alcohols, most of which are fat-soluble (Kaur and Prabhakar, 2017).

The effects on the environment caused by the excess of pesticides in the soils include acidification, fertility and microbial biodiversity decrease, damage to fauna, and water pollution. For vertebrates, including humans, OP toxicity is based on the inhibition of cholinesterase enzymes, mainly acetylcholinesterase type (AChE). This enzyme is essential for the functioning of the central nervous system (CNS). AChE disruption results in the accumulation of the neurotransmitter acetylcholine (ACh), which interferes with muscle responses and causes respiratory and myocardial defects, and even death (Dzudzevic Cancar et al., 2016; Pundir and Chauhan, 2012). In developing countries, these pesticides are reported to be responsible for more deaths than any other class of chemical compounds, with an estimated fatality rate of 10-20% (Chaparro-Narváez and Castañeda-Orjuela, 2015). Additionally, some studies link OP exposure with possible Parkinson's cases, with symptoms including tremors at rest, lack of blinking, and impaired speech and swallowing (Chuang et al., 2017). Other studies have linked OPs with oxidative stress and possible genotoxicity (Paul et al., 2018), however, long-term studies are required to confirm this. In the European union, pesticides in drinking water are currently regulated by the Drinking Water Directive using a maximum allowable concentration of 0.1µg/l (Dolan et al., 2013).

Biosensors for the detection of pesticides are varied and may involve immune-chemical properties such as enzyme-substrate, antigen-antibody reactions, recognition of DNA, or RNA aptamers (Kaur and Prabhakar, 2017). Changes in electrical and optical properties can be processed using a transduction system, signal conditioning, digitization, and data analysis (H. Li et al., 2018; Zhao et al., 2018). Optical biosensors, especially fluorescent ones, represent an excellent option to improve detection limits (Rodriguez et al., 2013; Yan et al., 2018). Acetylcholinesterase (AChE) has been widely exploited for enzymatic detection of pesticides. In AChE-based platforms, acetylthiocholine (ATCh) can be catalytically hydrolyzed to produce thiocholine containing the thiol group that is chemically reactive with metal cations, fluorophores, and nanomaterials (Yan et al., 2018). This allows a quantifiable colorimetric or fluorescent signal to be obtained. In the next section, a state-of-the-art is presented, differentiating between enzymatic and aptameric type biosensors.

Enzymatic biosensors

.AChE has high activity and it is estimated that each molecule degrades 25,000 acetylcholine (ACh) molecules per second, resulting in choline and acetic acid (Manetsch et al., 2004). However, in the presence of an inhibitor such as OPs, the serine hydroxyl group at the active site covalently binds to the phosphorous atom of the OP, blocking the active site. For this reason, OP detection methods are mainly based on this inhibition phenomenon (Pundir and Chauhan, 2012).

Biosensors based on AChE and other cholinesterases have been on the rise since 1980, mainly due to the evolution of transduction devices, the appearance of new techniques, and the use of nanomaterials (Pundir and Chauhan, 2012).

The incorporation of nanomaterials such as carbon dots (CDs) allows the development of systems considered label-free. For example, OP recognition platforms based on a dual scheme of colorimetry

and fluorescence without the use of fluorophores have been reported (2018), as shown in Figure 3-5 A. Thiocholine (a product of AChE) breaks down 5,5-dithiobis (2-nitrobenzoic acid) (DTNB) to form yellow 5-thio-2-nitrobenzoic acid (TNBA). This positively charged TNBA quenches the fluorescence of the CDs. With the presence of OPs, the enzymatic activity of AChE is blocked, recovering the fluorescence signal, and decreasing the intensity of absorbance with color variation. Very low detection limits (0.4 ng/L) were achieved with this novel system using paraoxon as an analytical model (Hassani et al., 2017; H. Li et al., 2018).

The use of CDs for the development of fluorescence-based enzyme biosensors has increased in recent years, whether in combination with chromophores (H. Li et al., 2018), nanoparticles (Chun et al., 2016), or emerging materials (X. Wu et al., 2019) (Hu et al., 2019)(X. Y. Xu et al., 2018). Furthermore, CDs have high solubility in water, stability, potential for chemical functionalization and high quantum yields. Compared to organic fluorescent substances, CDs can be obtained by low-cost processes and by green chemistry, for example using agro-industrial waste (Wang et al., 2018). Like QDs, CDs possess fluorescence characteristics depending on the size (Figure 3-4) and, in this case, on the functional groups present on the surface (M. L. Liu et al., 2019). CDs have also been found to be even more resistant to photobleaching than QDs (M. L. Liu et al., 2019).

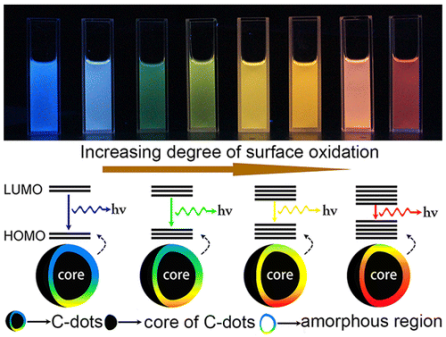

Figure 3-4. Fluorescence mechanism of CDs based on the degree of surface oxidation. Reprinted with permission from ref (Ding et al., 2016). Copyright 2016. American Chemical Society.

Chung et al (Chun et al., 2016) developed a specific system for the detection of paraoxon using AChE. They used CDs doped with nitrogen, a process commonly used to improve the quantum performance of these nanostructures and generate a greater diversity of surface chemical groups (M. L. Liu et al., 2019). The synthesized CDs have superficial -NH groups that interact with the gold nanoparticles (AuNPs) generating a shell-like structure, in which the proximity of both nanostructures generates a quenching effect on the fluorescence of the CDs due to the FRET effect. In the absence of paraoxon, AChE hydrolyzes ACTh in thiocholine, which has an SH-group that can replace the Au-NH interaction of CDs and AuNPs, causing the latter to aggregate and release CDs that regain their fluorescence. -SH groups can form stronger bonds with gold than -NH. In the presence of paraoxon, the amount of thiocholine generated will not be sufficient for the complete recovery of fluorescence from the CDs, establishing a relationship between the concentration of paraoxon and the recovery of fluorescence. The detection limit is 1 ng/L. The authors found that, apart from the FRET effect, the aggregation of nanoparticles in the presence of thiocholine directly influences the detection of the pesticide, especially when it is at high concentrations.

AChE has also been combined with quantum dots (QDs) for pesticide detection. Zhan et al (Zhan et al., 2019) used boron nitride quantum dots (BNQD) with high quantum yields (QY). The AChE enzyme interacts by charges with the negative surface of the BNQDs, condensing there. Additionally, they incorporated AuNP precursor chloroauric acid ($HAuCL_4$) into the mixture. In the presence of its natural substrate (ATCh), thiocholine is produced, whose SH- group reduces $HAuCL_4$ in AuNPs which, in turn, bind to the SH- group present in BNQDs, quenching the fluorescence by a typical FRET process. In the presence of paraoxon, quenching is weak, so the recovery of fluorescence is proportional to the concentration of the contaminant. A detection limit of 33.3 ng / L was achieved. The FRET principle is frequently used in the development of biosensors involving nanostructures such as CDs or QDs, due to its simplicity and the possibility of using "Turn on" or "Turn off" strategies depending on the type of analyte to be detected. In the case of pesticides, it has been seen that "Turn on" approaches usually generate lower detection limits (Yan et al., 2018).

The number of studies involving QDs for the development of optical biosensors has grown in recent years, mainly due to the very high quantum yield (QY), the possibility of surface functionalization and strong resistance to photobleaching, a common phenomenon in organic compounds. In addition, some fluorophores may have high QY, but when conjugated with biomolecules, this property decays. (Pandey and Bodas, 2020).

To improve the sensitivity of AChE-based biosensors, various strategies have been used to take better advantage of the properties of QDs. Additionally, these strategies allow the generations of solid-state detection systems. Hu et al (Hu et al., 2019) generated a novel microchip that combines microfluidics with in situ generation of a CdTe QDs aerogel with AChE, stabilized with L-Glutathione (GSH). The working principle of the developed sensor is quite simple. It is based on the quenching of the fluorescence exerted by the thiocholine that acts as an electron donor, filling the empty valences of the QDs and turning off their fluorescence through a mechanism like PET. In the presence of pesticides, this hydrolysis is inhibited, because of which the system maintains its fluorescence. The aerogel configuration provides a better spatial distribution of AChE, and the inclusion of GSH stabilizes the microenvironment around the enzyme. Detection limits of 1.2 pM, 0.94 pM, 11.7 pM, and 0.38 pM were achieved for paraoxon, parathion, dichlorvos, and deltamethrin respectively. Data were analyzed using image processing software.

The technology of Hu et al appears as an alternative to optical detection systems based on enzymatic conjugation through covalent bonds, non-covalent bonds, or weak interactions. In this case, the action of thiocholine on QDs is intrinsically related to their fluorescence mechanism, which is due to quantum confinement (M. L. Liu et al., 2019).. Another advantage of the system is its ability to detect different pesticides simultaneously, which is difficult to find in other AChE-based systems since the targeting and blocking effect of active sites due to conjugation makes it impossible.

Besides CDs, QDs, and nanoparticles, less conventional nanostructures have been used in combination with AChE. Wu et al (X. Wu et al., 2019) developed a biosensor based on a new fluorescence technology, which uses so-called aggregation-induced emission fluorogens (AIEgens), which emit fluorescence only when in a solid state. In this case, 1,2-bis [4- (3- sulfonatopropoxyl) phenyl] -1,2-diphenylethene (BSPOTPE) was synthesized and deposited on SiO nanoparticles, so that

BSPOTPE became its derivative TPE, also becoming emissive. When conjugating this conglomerate with MnO2 nanosheets, the latter exert a quenching phenomenon on the compound using the well-known FRET process. In the presence of a pesticide, ACTh cannot hydrolyze to thiocholine and fluorescence remains inhibited. However, in the absence of a pesticide, the hydrolysis of ACTh causes the MnO_2 nano blades to hydrolyze from the conjugate, terminating the quenching and recovering fluorescence, as shown in Figure 3-5B. BSPOTPE (+) binds to SiO_2 NPs (-) through charge interaction.

MnO_2 nano blades have been widely used due to their easy synthesis and high biocompatibility (M. Wu et al., 2019). MnO_2 nanoblades have a strong and intense absorption band at 374 nm, working well as a quencher agent in combination with various donors. This is a result of the d-d transitions of the maganese ions in proximity to the donor particle. Their use as a quencher agent is mainly due to two characteristics: the absorption band that can overlap with emissions in FRET phenomena, and the reduction of the structure of MnO2 in Mn2+ ions by catalytic activity (M. Wu et al., 2019).

Even though the system is quite sophisticated and novel, the detection limit of 1 µg/L with a linear range of 1–100 µg / L is higher than in other simpler systems. However, the authors highlight as advantages the low consumption of AChE reagents (0.6 U / mL) and ACTh substrate (0.7mM) and their superiority over tests such as Elisa and electrochemical or colorimetric biosensors. The biggest advantage of using AIEgens is in the manufacture of solid-state sensors. In this work, the manufacture of a test strip was also evaluated, taking advantage of the fact that most fluorophores have little or no ability to fluoresce in the solid-state. The strips were constructed by depositing the conjugate on traditional filter paper and checking that they did not emit fluorescence at the beginning of the test. Then a solution of AChE, ACTh, and paraoxon was added at different concentrations, obtaining by simple visual inspection a possible semi-quantitative result.

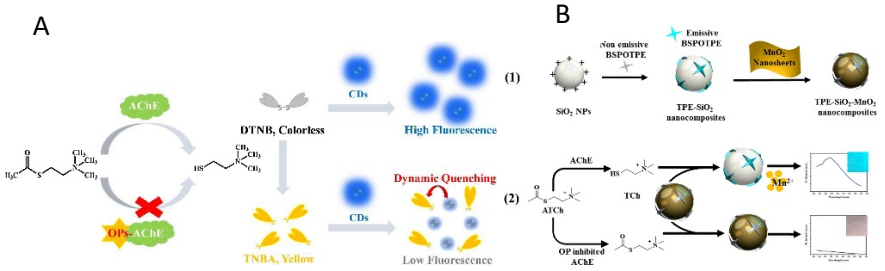

Figure 3-5. A) Operating principle of biosensors for detection of paraoxon based on CD / AChE / DTNB. Reprinted from ref (2018), Copyright 2018, with permission from Elsevier. B) Operating scheme of the biosensor based on BSPOTPE/SiO_2

Aptameric biosensors

Although the detection limits reached by the fluorescent enzyme biosensors are quite satisfactory, their specificity is still low. AChE can be inhibited by any type of organophosphate pesticides, by carbamates, metals, and other compounds normally present in the analysis matrix. For this reason, since 2015 the development of fluorescent aptameric biosensors combined with nanomaterials has been promoted. Aptamers are single-chain oligonucleotides (DNA or RNA), developed using the systematic method of ligand evolution by exponential enrichment – SELEX. These aptamers can bind

to their target molecules with high affinity and selectivity (M. Liu et al., 2019). Aptamers are much more selective than enzymes and have certain advantages over antibodies. Their synthesis does not require in vivo techniques, they are usually more selective, have a lower molecular weight, and allow modifications in a simple way (Odeh et al., 2020). Aptamers can be used in various configurations and combinations, giving greater flexibility for detection.

Dou et al (Dou et al., 2015) developed a biosensor based on a nanobeacon (gold nanoparticles functionalized with DNA aptamers and FAM as fluorophore), achieving isocarbophos detection limits of 10 µg/L. Initially, the proximity of FAM to the nanoparticle inhibits its fluorescence, which recovers with the binding of the aptamer and isocarbophos. Once the pesticide is detected, a portion of the aptamer will bind to it while another part will bind to the nanoparticle, resulting in a decrease of the initial fluorescence. The detection method, therefore, corresponds to "turn off". In this case, the nanoparticles function as an anchor for the beacon system as well as a quenching agent.

Two alternatives have been explored for many authors to improve the performance of fluorescent biosensors: increasing sensitivity by using high QY emitting molecules or decreasing non-specific fluorescence signals (noise) (Swierczewska et al., 2011). The use of AuNPs has been explored particularly in the second strategy, since their performance as quenching agents exceeds 99% [77,78]. For the reduction of noise signals, activatable systems also known as “molecular beacons” are used (Lee et al., 2008). In these systems, the donor molecule, and the acceptor AuNP are in close proximity, blocking the emission of non-specific fluorescence; once the analyte has been detected, the efficiency of the signal with respect to noise is superior and, for this reason, “turn on” systems seem to be more sensitive. In the design of molecular beacons, it has been found that NPs below 40 nm have the highest fluorescence quenching efficiency, which also increases when working with proximities of less than 2 nm between NP and donor (Swierczewska et al., 2011).

Other aptamer-based systems have been developed, obtaining better detection limits and working on immobilized lateral flow type systems. Cheng et al (Cheng et al., 2018a) developed a fluorescent biosensor combining QDs, AuNPs, and complimentary chain type aptamers. They managed to lower the detection limit to 0.73 µg/L using chlorpyrifos as one of the model molecules but simultaneously testing with diazinon and malathion. The operation of the sensor considers the fact that for the detection of smaller molecules with high sensitivity, it is better to use "turn on" strategies than the traditional "turn off". In this sense, when faced with negative samples, the mixture that contains the problem sample, together with the AuNps-Aptamer conjugates, rises by capillarity towards the test zone, where the QDs and the complementary biotinylated sequences of the aptamers are found. The mixtures will be able to hybridize so that the fluorescence of the QDs will be inhibited by the FRET phenomenon with the AuNps, facilitated by the proximity of the aptamers and the electrostatic interactions (Figure 3-6). Additionally, when hybridization occurs the AuNps precipitate, giving a dark line as a result. Otherwise, when faced with a positive sample, the AuNps-Aptamer conjugates of the incubated sample will be inhibited to hybridize in the test area, therefore they will continue to advance by capillary action so that the fluorescence of the QDs will not be inhibited and a positive fluorescence signal will be obtained.

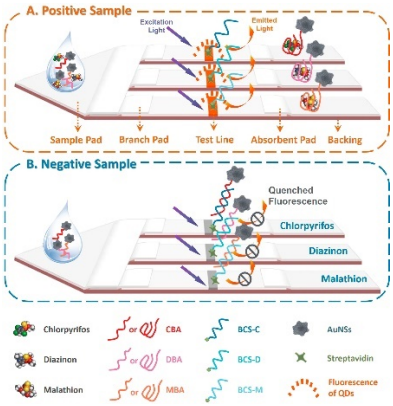

Figure 3-6. Working Principle of Lateral Flow Aptameric Fluorescent Biosensor. The figure represents a "turn on" type biosensor made to simultaneously detect 3 different organophosphate pesticides. Reprinted from ref (Cheng et al., 2018a), Copyright 2018.

Since metallic nanoparticles have a wide absorption spectrum, they are frequently used as an acceptor in FRET phenomena, with different donors. For this reason, the AuNPs-CDs or AuNPs-QDs pair is considered the ideal system for fluorescence-mediated detection. The properties of MNPs are different from metal due to the SPR phenomenon (Figure 3-7). This phenomenon is defined as an oscillation of electrons near the surface of the particles, when the particles have a diameter greater than 2 nm (Ong et al., 2020). When light of the appropriate wavelength strikes the metal nanoparticle, the electrons on the surface gain energy and begin to oscillate, but the electrons in the nucleus do not, causing a restorative force on the surface (Swierczewska et al., 2011). This collective movement is restricted to a range of 300 nm from the surface and is responsible for inducing a certain electric field. As the electric field of the surface is equalized with the electric field of the incident light, the resonance phenomenon becomes concrete (Kaushal et al., 2020). The SPR is influenced by parameters such as the distance between particles, the solvent in which they are dispersed, and the size and shape of the MNPs. The manipulation of these parameters and their effects, such as colorimetric changes, have been used in the development of various diagnostic methods (Bala et al., 2018a).

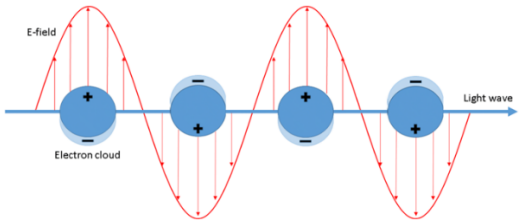

Figure 3-7. SPR representation in a spheric nanoparticle. Reprinted by permission from Springer Nature: Environ. Chem. Lett. Ref (Kołątaj et al., 2020)*. Copyright 2020.*

Another development based on AuNPs is that of Wang et al (Wang et al., 2018) who designed a fluorescent sensor for the detection of acetamiprid, achieving a LOD of 1.08 µg/L. The system is based on the synthesis of CDs from citric acid by the hydrothermal method. The fluorescence of these CDs decreases in the presence of AuNPs and the aptamer due to a combined phenomenon of FRET and IFE. The aptamers interact by charges with the AuNPs, making them more negative and

therefore more stable in high concentrations of salt (Tris buffer), which is why they are available to quench CDs in solution. However, in the presence of acetamiprid, the aptamer binds to this, leaving the AuNPs unstable, aggregated, and unable to quench, allowing CDs to regain their fluorescence (Figure 3-8 A). The selectivity of the biosensor against other pesticides such as dimethoate, chlorpyrifos, and dichlorvos was studied with good results. The recovery in real samples of tomato, cucumber, and cabbage was over 90%.

The quenching effect can also be obtained by combining other types of nanostructures. Li et al (X. Li et al., 2018) focused on the detection of isocarbophos. They developed a system combining multiple walled carbon nanotubes (MWCNTs), N-methyl mesoporphyrin IX (NMM) as a fluorophore, and functionalized complementary aptamers with long guanine-rich sequences (G-Cuadraplex). They achieved an excellent detection limit of 10 nM. The strategy used is known as a sandwich (Figure 3-8 B). This is because the aptamers trap the pesticide when in its presence and, when they meet the MWCNT and the NMM at the same time, the ends of the G-quadruplex that bind to the fluorophore are slightly unfolded by the effect of the MWCNT, so the fluorescence becomes evident. In the absence of the pesticide, the aggregate of aptamers unfolds completely around the MWCNTs, also entangling the fluorophore and exerting a quencher effect. It is quite a complex strategy and difficult to reproduce in the field, although it has good selectivity against other pesticides such as methidathion, chlorpyrifos, acetamiprid, and atrazine.

Lin et al (Lin et al., 2016) also took advantage of the combined properties of MWCNT, ZnS: Mn QDs and aptamers, to develop a detection system for one of the most widely used OPs: acetamiprid. The sensor is based on the turn-on strategy, where the fluorescence of the aptamer functionalized QDs suffers quenching due to the FRET phenomenon between them and the MWCNTs. Once subjected to different concentrations of acetamiprid, the QDs regain fluorescence as the affinity constant between the aptamer-pesticide pair is higher than aptamer-MWCNT. This development incorporates QDs doped with heteroatoms like Mn. The method for conjugation was the well-known carbodiimide chemistry, employing (1-ethyl-3- (3-dimethylamino) propyl carbodiimide, hydrochloride (EDC) in the presence of N-hydroxysuccinimide (NHS), to form a highly stable covalent bond between the amino group of the aptamer and the carboxylates in the QDs. In this type of sensors, based on covalent conjugation instead of weak interactions, it is important to use characterization techniques to demonstrate the formation of the expected bond. In this case, Fourier transform infrared spectroscopy (FTIR) was used, verifying that the bands at 1570 cm-1 and 1627 cm-1 correspond to the amide bands, and showing that the conjugation between the amino group of the aptamer and the carboxylates of ZnS: Mn QDs was successful.

Although MWCNTs are not the preferred nanostructures for design approaches under the FRET phenomenon, it has been speculated that their high quenching efficiency in combination with aptamers may be due to a larger surface area that allows greater π-π-type interaction with DNA. In this type of design, the pH plays a fundamental role in showing better performance near neutrality.

Graphene oxide has been used mainly in electrochemical biosensors, due to its excellent conductive properties. However, some studies have evaluated its potential for the development of other types of systems, including as a quencher agent (M. Xu et al., 2018). Arvand and Mirroshandel (Arvand

and Mirroshandel, 2017) developed a biosensor for the detection of edifenphos, a substance used as a fungicide in crops. To achieve the detection limit of 1.3 ng / L, they used the following strategy: QDs were synthesized from L-cysteine which were doped with Zn to improve fluorescence. Then the FRET effect was used between QDs and graphene oxide (GO) sheets. Under this principle, aptamers were conjugated for the recognition of the pesticide edifenphos through the carbodiimide chemistry previously mentioned. The FRET effect occurs due to the interactions between the aromatic skeletons of the nitrogenous bases of the aptamer and the groups with sp2 hybridization of the GO, bringing the second of these closer to the QDs so that quenching is possible. In the presence of edifenphos, the aptamer-QDs conjugate detaches from GO (weak interactions), recovering fluorescence.

QDs Stabilizers used in aqueous processes include thioglycolic acid (TGA), L-Cysteine, and 3-mercaptopropionic acid, among others. (Huang et al., 2011). The most frequently used QDs for sensors include those synthesized from CdTe and functionalized with thiolated groups. To obtain these, H_2Te gas is introduced in the presence of the Cd precursor, to then grow the crystals by means of a continuous reflux (Gaponik et al., 2002). The aqueous method has been used to obtain not only these types of QDs, but also Mn: ZnS, Mn: CdTe, CdSeTe, CdTe / CdS; in some cases, with increases in QY and stability (Huang et al., 2011).

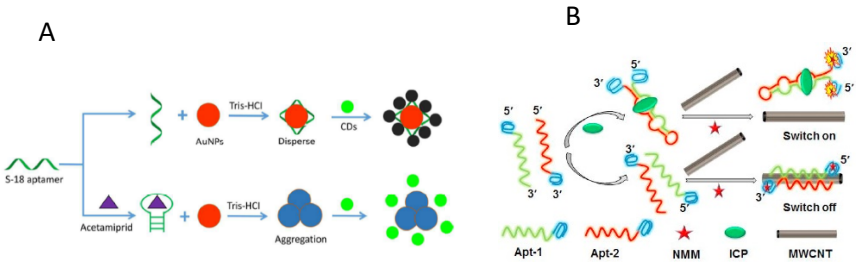

Figure 3-8. Strategies that combine various nanostructures for the detection of pesticides.A) Pair-based biosensor scheme of CD/AuNPs for acetamiprid detection. Reprinted with permission from ref (Wang et al., 2018). Copyright 2019. Royal Society of Chemistry. B) Detection principle of isocarbophos based on G-quadruplex functionalized aptamers. Reprinted from ref (X. Li et al., 2018), Copyright 2018, with permission from Elsevier

The characterization process of the QDs and conjugates yielded interesting data, confirming the fact that aptamers, unlike some proteins, do not interfere with the fluorescence of QDs, which maintain their excitation and emission peak at 265 nm and 359 nm respectively. When evaluating the influence of pH on the fluorescence of the conjugates, it was found that they are more stable at neutral pH, rapidly losing fluorescence at acidic or alkaline pH, probably due to the instability of chemical groups on the surface.

Another important consideration when working with aptamers is ionic strength as a binding determining factor. At low values, hybridization between DNA strands is unlikely, whereas if the ionic strength is too high, this interaction occurs but in a very weak way. In this study, various ionic strength values were analyzed, using increasing concentrations of NaCl, and 150 mM was found to be the optimal value for system performance.

In a recent study, the same authors used GO synthesized from graphite as a quencher agent in an aptasensor for the detection of diazinon, with a LOD of 0.13 nM (Arvand and Mirroshandel, 2019). The sensor is of the "turn on" type, as it is based on an initial quenching state between the QD-Aptamer-GO bioconjugate. In the presence of diazinon, the aptamer will have a greater affinity for the pesticide than for the conjugate, freeing itself from the GO by which it is bound only by weak interactions, whereby the QD regains fluorescence (Figure 3-9). In this case, it was identified by TEM that the QD was "absorbed" by the GO sheets. The conjugates are stable at neutral pH, since deprotonation of carboxylic groups in GO at high pH values affects the surface charge density of GO by repelling the QD-Aptamer pair.

GO is quite efficient for building turn-on sensors. The FRET phenomenon, in this case, is caused by π-π interactions between the aromatic groups of GO and the bases of the ssDNA. Additionally, hydrogen bonds occur between the hydroxyl or carboxyl groups of GO and the amino or hydroxyl groups of the aptamer (Bai et al., 2020).

One of the challenges of working with biosensors is reproducibility. In this case, the authors found a variation of only 2.99%, while, with regard to stability, the system stored at 4 ° C for at least one week-maintained performance values greater than 95%.

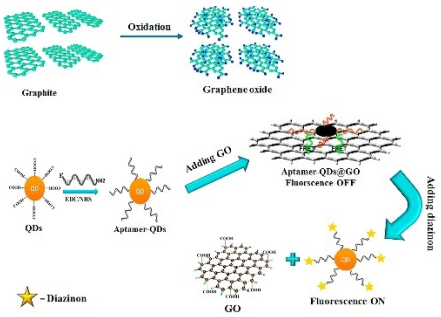

Figure 3-9. Aptasensor based on FRET phenomenon between QD and GO for diazinon detection. The scheme shows how the QD are absorbed by the GO sheets. Reprinted from ref (Arvand and Mirroshandel, 2019), Copyright 2019, with permission from Elsevier.

Finally, Bala et al (Bala et al., 2018b) developed one of the systems with the lowest detection limit. They achieved 4 pM for malathion using a combination of CdTe @ CdS, the polymer poly (N- (3-guanidinopropyl) methacrylamide) (PGPMA) and aptamers. The basis of the technology is the stability of the polymer in solution against various pH changes, resulting from the guanidine functional group that remains charged and is capable of interacting with phosphate groups through hydrogen bonds. This interaction makes it more related to nucleic acids such as the aptamer. In the presence of the pesticide, it binds to the aptamer, leaving the polymer free in solution and acting as a quencher for the QDs. In the absence of the pesticide, the free aptamer binds to the polymer and the fluorescence of the QDs remains intact. The interaction between polymer and QDs is given by the positive charge of the first versus the negative of the second. Specificity was tested against other pesticides such as atrazine, chlorsulfuron, chlorpyrifos, diuron, and 2,4-D with good results, as well as a recovery of more than 80% in lake water samples. Parameters such as the concentration of the quencher and the aptamers were optimized in unifactorial tests. It can be seen how aptameric

systems in combination with FRET processes generally have a better detection limit than enzymatic biosensors.

In FRET-type processes, QDs can act as energy donors, combining with metallic nanoparticles, polymers, graphene, and others. They can also act as acceptors in the presence of organic fluorophores, lanthanide compounds, fluorescent polymers, or other QDs. Again, the high fluorescence emission over a long period, wide excitation spectrum and narrow emission make them the ideal molecule for use in FRET processes. QDs have been bioconjugated with numerous biomolecules such as proteins, peptides, nucleic acids, aptamers, and others (Cardoso Dos Santos et al., 2020).

Heavy metals

Heavy metal contamination is normally associated with mining, soil fertilization, chemical manufacturing, metal processing, and other industrial activities. (Ejeian et al., 2018). Improper management and treatment of metal ions can become a serious environmental problem, especially for developing countries.

Some heavy metals are indispensable for biological processes, among them Co, Cu, Fe, Mn, Mo, Ni, Se, and Zn (Ejeian et al., 2018). However, other non-essential metals such as lead (Pb), chromium (Cr), cadmium (Cd), mercury (Hg), arsenic (As) and antimony (Sb) are highly toxic; these have serious effects on the central nervous system and can cause cancer (Huang et al., 2017). Heavy metals are strictly regulated in most countries. For example, the European Union defines the maximum limits for lead and cadmium in vegetables as 0.1 and 0.05 mg/kg wet weight, respectively; and mercury in fish is limited to 0.5 mg/kg wet weight (European environment agency, 2006).

For the detection of heavy metals, methods such as atomic absorption spectroscopy, UV-visible spectroscopy, and ionic chromatography are used (Ejeian et al., 2018). However, as is the case of pesticide detection, the use of these methods has been limited by their high consumption of resources and time, and the need for specialized equipment (Kanellis, 2018). In response to these drawbacks, the already known advantages of biosensors have been applied. In this case, enzymatic detection systems based on the inhibition of metal ions on enzymes such as laccase (Shtenberg et al., 2015) and urease (Prakash et al., 2008) can be used. However, most of the developments addressed in this review are based on the use of DNA oligonucleotides, either to form DNAzymes, aptamers, or taking advantage of the complementary interaction of Hg^{2+} with thymine (Zhang et al., 2011). Recent developments combine the advancement of DNA-based technologies with nanomaterials, to create systems based on the Förster resonance energy transfer phenomenon (FRET) for the detection of multiple metal ions (Yun et al., 2017).

Direct quenching

The use of the quenching phenomenon of fluorescence nanomaterials for the detection of heavy metal ions has been widely reported in the literature, and is one of the simplest detection strategies, especially when based on the FRET phenomenon (Cui et al., 2015; Liu et al., 2015). Pooja et al (D. et al., 2019) developed a simple system based on the fluorescence inhibition of carbon dots (CDs) in

the presence of chromium ions. For this, papaya pulp residues were used to synthesize CDs by pyrolysis in an oven at high temperatures. These highly fluorescent CDs show a dependent emission-excitation behavior in the blue spectrum.

For the selective detection of chromium, Pooja et al (D. et al., 2019) functionalized CDs with Ethylenediaminetetraacetic acid - EDTA, taking advantage of the carboxyl groups (CDs) and amino (EDTA) by means of carbodiimide chemistry. The detection limit confirms the sensitivity of the method used, reaching 0.708 ppb. In a previous report, Wang et al (Wang et al., 2017) also developed a system for the detection of Cr (VI). In this case, CDs synthesized from cellulose were combined with isophorone diisocyanate (IPDI) and β-cyclodextrin (β-CD) as stabilizing components. The researchers found a decrease in fluorescence by exciting the system at 370 nm, in the presence of the analyte. This can be explained by the presence of carbamate groups and some hydrogen bonds, which can act as chelating agents with metal ions. This sensor was developed for ion detection in digested soil, requiring laborious sample processing.

The origin of the fluorescence of CDs does not have a universally accepted explanation, however three theories are proposed as the most probable: 1) emission of the core of the CDs, when they have high crystallinity and quantum confinement; 2) emission dependent on the surface state and functional groups; or 3) molecular fluorescence induced by impurities resulting from the synthesis. Quantum confinement is closely related to the degree of crystallinity and the electronic distribution, resulting in crystal-dependent relaxation energies. Most of the CDs synthesized from biomass present a photoluminescence associated with the surface state and degree of oxidation; in this process, superficial defects are generated in exciton capture dynamics. The presence of different functional groups generates different energy levels in the CDs, which translates into different colors or emission wavelengths (M. L. Liu et al., 2019). To improve the quantum yield of CDs, some authors have doped them with different chemical elements such as N (if not present in the starting material), S, Mn, P, Co, and others is used (Sharma et al., 2018). This doping or subsequent functionalization also allows the direct detection of some substances such as heavy metals that can interact with said heteroatoms.

Divalent mercury (Hg^{2+}) is one of the main heavy metal ions of interest in waters, due to its proven toxic effects. In recent work, Liu et al (G. Liu et al., 2019) continue the trend of synthesis of nanomaterials from natural sources. They used Chinese carp flakes as a starting material to synthesize CDs rich in sulfhydryl groups (from cysteines). In this system, the affinity of Hg^{2+} for sulfur atoms is used as a detection principle. CDs were synthesized by the hydrothermal autoclave method, assisted by microwave. The binding of Hg^{2+} to the sulfhydryl groups of the CDs acts as a quenching of their fluorescence (Figure 3-10).

Hg^{2+} can interfere with the said electronic transfer, generating a decrease in fluorescence. This inhibition is much more evident when there are sulfhydryl groups on CDs that are more related to the analyte. Additionally, sulfur promotes the electronic transfer of the species involved. It is one of the few studies that address cytotoxicity, finding low values of CDs when evaluating them in vitro using BV2 cells. In this work, CDs are mainly amorphous, with some graphite structure. One of their

fluorescence mechanisms is associated with surface defects that can act as traps for excitons and the presence of functional groups that can exchange electrons (M. L. Liu et al., 2019).

To classify CDs, authors such as Cayuela et al (Cayuela et al., 2016) have considered the nature of the particle, its crystal structure, and its degree of quantum confinement. Thus, the quasi-spherical amorphous particles that do not have quantum confinement characteristics are called carbon nanodots, while the spherical particles that do possess such confinement are called carbon quantum dots. Finally, graphene quantum dots can be obtained from single sheets by π interactions. The type of of CD obtained depends on the precursors used, the type of synthesis and the process variables (M. L. Liu et al., 2019). In recent years, graphene quantum dots (GQDs) have gained considerable interest because they are zero-size fluorescent nanoparticles, but with a base or graphene mesh inside. GQDs combine fluorescent properties with thermoelectric properties, reporting even higher QYs. They also have a larger surface area, and the possibility of functionalization and chemical interaction is greater, due to a high presence of sp^2 hybridizations (Henna and Pramod, 2020).

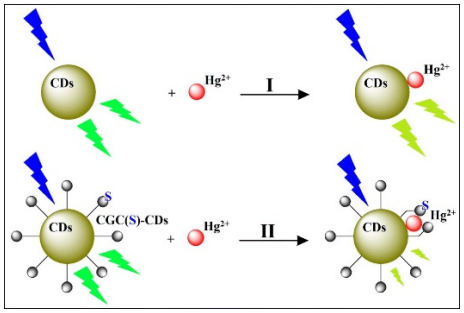

Figure 3-10. Detection mechanism of Hg^{2+} by using the CGCS-CDs as fluorescence probe. The figure shows how the quenching mechanism is enhanced by the sulfur atoms on the CDs. Reprinted from ref (G. Liu et al., 2019), Copyright 2019, with permission from Elsevier

The use of silica nanoparticles has been explored to improve the biocompatibility and performance of QDs nanostructures. In this sense, Jia et al (Jia et al., 2018) developed a system for the detection of Cu^{2+} and Hg^{2+} based on BCNO-QDs that were synthesized using a mesoporous silica matrix called SBA-15 as a template. This system was evaluated in solutions with different concentrations of both metal ions, finding detection limits as low as 10 nM evidenced through the quenching phenomenon. The mechanism for the case of Cu 2+ is related to the formation of chelation complexes between this ion and the N and O atoms in the QDs. In the case of Hg^{2+}, the mechanism is related to the electronic transfer.

There are different combinations of silica and QDs, which allow us to enhance applications and improve not only biocompatibility but stability against environmental conditions. Some alternatives are a) Silica as immobilization support for the QDs; b) Co-encapsulation; c) Covalent bond taking advantage of silane group and d) use of silica for core/shell-type structures (Bagheri et al., 2020).

Other works report more complex systems that integrate metallic nanoparticles with polymeric materials. Wang et al (Wang et al., 2016) developed a system based on a hybrid compound between the thermoplastic polymer Poly (arylene ether nitrile) (PEN) and gold nanoclusters stabilized by bovine serum albumin (BSA). Both compounds show fluorescence compatible with the FRET

phenomenon, where the interaction of the carboxylic groups present in PEN through hydrogen bonds with BSA is essential. The compound PEN-Au NCs shows fluorescence in pink tones, generated by the mixture of the blue fluorescence of PEN and red of the Au NCs. In the presence of Hg^{2+} ions, a quenching of the fluorescence of the Au NCs is generated, showing very good detection of Hg^{2+} up to levels of 10 uM when excited at 365nm (common UV lamp), and detection of up to 10nM when excited at 418nm. The fluorescence quenching only acts on the Au NCs, while the PEN fluorescence remains intact and can serve as a control mechanism, thereby avoiding false positives. The authors do not investigate closely the quenching mechanism of the fluorescence of the AuNCs, only indicating that FRET occurs between PEN and AuNCs. The detection level is quite good (10 nM), but it should be noted that nanoclusters are poorly stable nanomaterials that must be combined with other substances to be used in detection processes. The presence of cysteine, as a good coordination agent; tyrosine, for the reduction of metal ions; and arginine, to stabilize the pH, improves the stability of nanoclusters (Y. Li et al., 2019).

More recently, Maruthupandi et al (Maruthupandi et al., 2020) focused on optimizing the Cu nanocluster synthesis process. The work reports rapid synthesis (1 min) by sonication as the main novelty. For the synthesis, they used copper nitrate, ascorbic acid, and 1-Thio-β-D-glucose in basic medium (NaOH). These nanoclusters are highly fluorescent and can sense Hg^{2+} and S^{2-} ions by means of a fluorescence quenching phenomenon that is directly proportional to the concentration of the analyte, reaching detection limits of 1.7 nM and 1.02 nM for mercury and sulfur respectively. The S^{2-} anion is mainly responsible for environmental contamination and can be related to cirrhosis and Alzheimer's disease (Vasimalai et al., 2018).

Another novelty of the work is the simplicity of the integration with a smartphone. The authors developed a system in a reactive strip (filter paper) in which the nanoclusters are deposited and then placed in contact with the problem sample, as shown in Figure 3-11. The reading is done through a UV LED integrated into a PVC tube and connected to a smartphone. Real samples of well and river water were evaluated, obtaining recoveries between 98.5 to 101.4% for Hg^{2+} and 99 to 101% for S^{2-}.

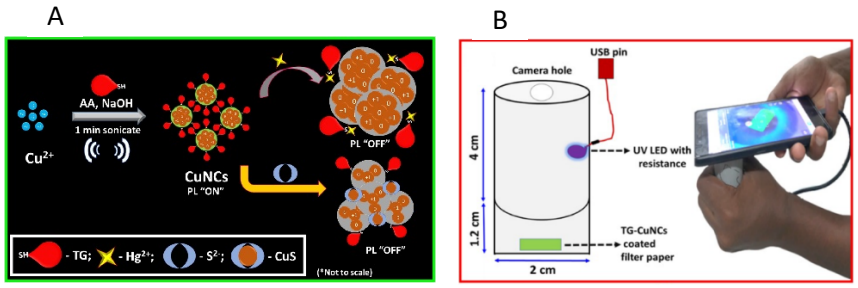

Figure 3-11. Practical approach to detect Hg2+ and S2- ions. A) principle of detection based on fast synthesis Cu NCs. B) Integration of detection system with Smartphone. Reprinted from ref (Maruthupandi et al., 2020), Copyright 2020, with permission from Elsevier

By means of quenching-based systems, it is possible to achieve quite competitive detection limits. Ravikumar et al (Ravikumar et al., 2018) were able to detect As at 18 nM levels using MoS_2

nanosheets. The system proposes a simple quenching mechanism based on FRET. In this case, a specific aptamer was used to detect As (III), which is functionalized with FAM. In the absence of As (III), the fluorescence of the aptamer is strongly reduced by absorption in MoS2 nanosheets. This quenching occurs due to the Van der Waals type interactions between the nitrogenous bases and the basal plane of the nanosheets. Through the addition of As (III), two mechanisms influence the recovery of fluorescence: a) conformational changes in the aptamer due to the guanine-rich sequences (G-quadruplex) that allows the FAM to finish away from MoS_2; b) desorption of the complete ssDNA sequence of the nano blades (Figure 3-12). The analyte concentration is proportional to the recovery of fluorescence. In this case, real samples of river and tap water were analyzed, with recoveries greater than 90%.

2D nano blades of MoS_2, and other compounds, can generate selective fluorescent detection platforms for various analytes of environmental concern (Kalantar-zadeh et al., 2015). Analytes affect not only the fluorescence emission of the 2D nanostructure or its donor, but the emission half-life and anisotropy (Neema et al., 2020). MoS_2 can absorb radiation from a broad spectrum of wavelengths. Additionally, this transition metal dialcogens (TMDC) can interact with various biomolecules, enhancing its efficiency as a fluorescence quenching agent. Multiple studies report the use of MoS_2 nano blades as a receptor agent in FRET models (Geldert et al., 2017; Kenry et al., 2016). MoS_2 nano blades have shown excellent performance in interacting with single-stranded DNA oligonucleotides (ssDNAs) through van der Waals interactions between the nitrogenous bases and the basal plane of the nanostructure, resulting in absorption of the oligonucleotides into the nano blades. As will be presented in several case studies in this review, when using aptamers functionalized with an organic dye or an emitting nanostructure such as quantum / carbon dots, it is possible to use MoS_2 nano blades as quencher agents (Barua et al., 2018). Compared to GO and its derivatives, the use of MoS_2 allows detections with lower limits of detection - LODs (Zhang et al., 2015).

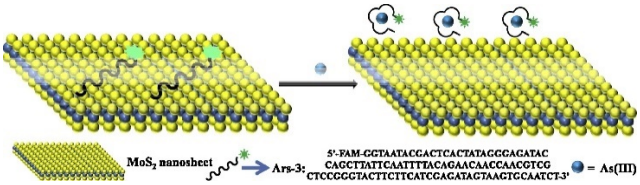

Figure 3-12. As (III) detection principle based on FRET phenomenon between FAM-operated aptamer and MoS_2 nanosheets. Reprinted from ref (Ravikumar et al., 2018)., Copyright 2018, with permission from Elsevier.

Finally, Liu et al (T. Liu et al., 2019) combined the quenching process with fiber optic detection and reading by smartphone, obtaining one of the most sensitive systems reported in the literature (1nM). The Hg^{2+} detection principle is very simple, as it uses CdSe / ZnS QDs, which are highly fluorescent and are immobilized on the fiber optic). The fluorescence of these QDs is affected by the presence of Hg^{2+} ions, through a quenching phenomenon in which it is possible to establish a linear relationship between the analyte concentration and the quenching coefficient. The system has the advantage of being portable, quick to use (3 min per sample) and intuitive; however, the optical fiber cannot be regenerated, so it is for single use only. Nonetheless, manufacturing costs are low and support this single-use system.

DNAzyme

The advancement of technologies associated with nucleic acids has allowed the development of multiple systems based on what are known as functionalized nucleic acids (FNA) (Huang et al., 2017). Within this category, the molecules that have been subject to the most investigation are DNAzymes. These consist of a complex tertiary structure of DNA with two main parts: an enzyme chain (E), whose activity will be dependent on the presence of the ion to be detected; and a substrate chain (S), that will have a fluorophore bond and will be hydrolyzed by the E chain (McGhee et al., 2017) (Figure 13 A). DNAzymes are synthesized in vitro using SELEX technology, also used for the development of aptamers (Figure 3-13A) and are highly active in catalyzing various types of reactions associated with the phosphodiester bond (Yun et al., 2017). The advantages of these types of structures include excellent stability and activity, easy functionalization with various fluorophores or nanomaterials, and low immunogenicity (Huang et al., 2017).

Applying DNAzymes, Li et al (X. Li et al., 2019) developed a simultaneous detection system for Pb^{2+} and Cu^{2+} with LOD of 80 pM and 30 pM respectively. In this case, two S chains were synthesized, functionalized with FAM, and cyanine 5 as fluorophores, and conjugated to gold nanoparticles through the presence of thiol groups in said chains. E chains are synthesized in a clamping form and added to S-functionalized nanoparticles to form a complex tertiary structure (Figure 3-13 B).

In the presence of the metal ions to be detected, the E clamp hydrolyzes the fragments of the S chains. This action gradually releases not only the chromophores, but the clamp structure itself, which becomes available to hybridize with new S chains in subsequent cycles. Fluorescence is recovered.

Different optimization conditions were investigated, such as the stability of the fluorophore and the steric hindrance when conjugating too many S structures on the nanoparticles. A higher system response was also obtained at pH 8.

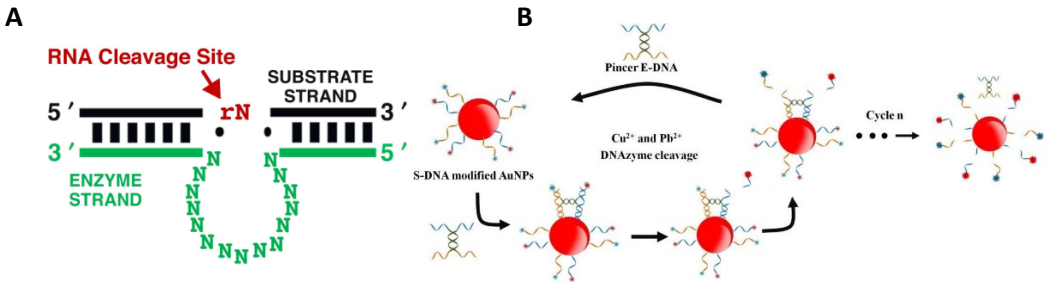

Figure 3-13. A) diagram of the structure of a DNAzyme showing the E and S chains, as well as the active site. Reprinted from ref (McGhee et al., 2017), Copyright 2017, with permission from Elsevier B) DNAzyme clamp type conjugated with Au NPs for the simultaneous detection of Pb2+ and Cu2+. Reprinted from ref (X. Li et al., 2019), Copyright 2019, with permission from Elsevier.

With DNAzymes it is possible to develop complex systems that combine nanomaterials, fluorophores, and catalysts. Li et al (Li et al., 2020) reached a LOD for Pb^{2+} of 0.25nM. For this, they synthesized CDs doped with Au, from glucose and HAuCl4. An aptamer was used for the detection

of Pb^{2+}, through the formation of an Apt-Pb (II) -CD complex which had an excitation peak at 351 nm and an emission peak at 445 nm. The operating principle is based on the synergy between the fluorescence of doped CDs and their catalytic properties that allow an OH radical to be generated from H2O2. This radical oxidizes 3,3 ', 5,5'- Tetramethylbenzidine (TMB) generating a TMBox fluorescent compound, with emission peak at 404nm. Gold atoms in CDs improve electron transfer by promoting the redox reaction. In the absence of the aptamer, CDs can catalyze the reaction, generating higher fluorescence intensity. By adding the aptamer, the CDs are encapsulated, blocking their catalytic capacity, and generating a decrease in fluorescence. Additionally, a system that combines the G-quadruplex formation of the aptamer with hemoglobin can form a DNAzyme system. This system catalyzes the oxidation of TMB to also generate the fluorescent compound TMBox, amplifying the signal. This mechanism occurs due to the accumulation of electrons on the surface of the G-quad. Fluorescence increases linearly with Pb^{2+} concentration. In this way, a synergistic effect is achieved between both systems, enhancing lead detection. The system is quite complex, and the authors do not discuss the repeatability of the method.

"Mismatched" interactions

For some years, it has been reported that the Hg^{2+} ion can interact with the thymine nitrogenous base to form the T-Hg^{2+} -T structure. This structure is much more stable than the natural adenine-thymine bond. In this way, T-rich "mismatched" sequences can be used for the detection of mercury (Huang et al., 2017). Additionally, Ag-ion mediated C-C pairing can be induced so that cytokine-rich sequences can be used for detection of this ion (Figure 3-14).

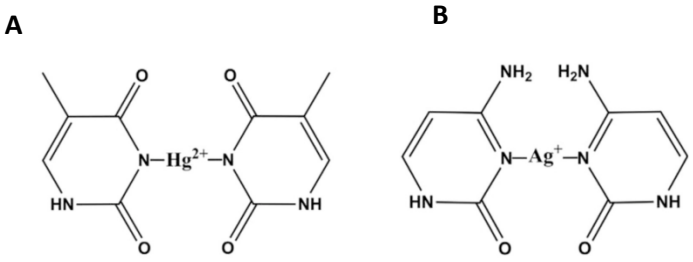

Figure 3-14. Pairing method for A) T-Hg2+-T and B) C-Ag+-C. Reprinted from ref (Huang et al., 2017), Copyright 2017, with permission from Elsevier.

Guo et al (Guo et al., 2019) achieved a LOD of 3.33 nM Hg^{2+}, applying the principle of mismatched bases. They synthesized CdTe QDs with thioglycolic acid. A fraction of these QDs were conjugated to aptamer 1, rich in T sequences capable of interacting and detecting Hg^{2+}. The remaining QDs were conjugated to aptamer 2, also rich in T. The conjugation was performed using the carbodiimide chemistry. The principle of operation of the sensor is based on the fact that, in the absence of Hg^{2+}, both fractions of the aptamer functionalized QDs are free, emitting fluorescence. However, when adding Hg^{2+}, a network of aggregates occurs between both QD-apt fractions, decreasing fluorescence, as shown in. Fluorescence was measured at an excitation wavelength of 370 nm and specificity was evaluated against other ions such as Zn^{2+}, Al^{3+}, Pb^{2+}, Cu^{2+}, Fe^{3+}, Co^{2+}, Ba^{2+}, Mn^{2+}, Cd^{2+}, and Ag^{+}. Before adding Hg^{2+}, the aptamers on the surface of the QDs were in random helical form but were then sandwiched with the analyte. The self-quenching mechanism of QDs when

aggregated was also investigated, exploring theories of electronic coupling and excitation energy transfer. In electronic coupling, there should be an interaction between the orbitals of adjacent QDs, which would be reflected in a change in the absorption spectrum. In this case, the absorption spectrum remains identical, indicating that the second mechanism is more probable. In excitation energy transfer, QDs with absorption at a lower excitation band are likely to transfer energy to those with a higher excitation band, which would also explain the slight shift of the emission peak toward red. Variables such as the concentration of the QD-apta conjugate, incubation time, pH, and Apta-QD ratio in the conjugation were optimized. Li et al (Li and Wei, 2017) also explored the phenomenon of quenching with T-T matings for detection of Hg^{2+} with LOD of 4.5 nM. In this case, silver nanoclusters stabilized with an oligonucleotide were used.

He et al (He et al., 2020) also used a system based on QDs, in this case, CdSe with a core structure and shell with CdS. (Pandey and Bodas, 2020). Despite the advantages of QDs, they are sensitive to deterioration when exposed to different conditions of heat, oxidation, and humidity, since surface defects can be created that alter their fluorescent properties (Bala et al., 2018b). To counteract these drawbacks, the passivation of the QD core with robust inorganic or metallic coatings has been explored, achieving a shell-like structure that can then be functionalized (Cardoso Dos Santos et al., 2020).

In He et al work (He et al., 2020), the response is amplified by a chemiluminescence mechanism, when the QDs encounter an oxidizing agent such as H_2O_2. MoS_2 nanosheets were used, in which the cationic polymer poly (diallyldimethylammonium chloride (PDDA) was deposited and the negatively charged QDs were absorbed by the interaction of charges. The MoS_2-PDDA-QD was deposited on an electrode (GCE), and a DNA strand (DNA 1) was then immobilized using the carbodiimide chemistry. Furthermore, a system based on Au NPs was built, in which a DNA 2 probe and glucose oxidase (GOx) molecules were immobilized. For detection, an Au NPs-ADN2-GO solution mixed with Hg^{2+} and deposited on the MoS_2-PDDA-QD modified electrode was used. The key to detection is in the interaction of Hg^{2+} ions with thymine present in DNA sequences, which forms stable complexes. Thus, in the presence of the pollutant, T-Hg^{2+} -T hybrids are generated, which in turn generate a hybridization between both DNA chains and consequently put the two complexes in contact. GOx, being in proximity, reduces the oxygen present in the environment to form H_2O_2, and this compound amplifies the fluorescent signal of the QD. Therefore, the increase in fluorescence is linear at the Hg^{2+} concentration. The sensor performance is among the best reported (0.1 pM), but the manufacturing process can be complicated, and the authors do not discuss the reproducibility of the process.

Finally, Marieeswaran et al (Marieeswaran and Panneerselvam, 2020) reported the use of a magnetic nanoscale metal-organic framework (MNMOF) to detect mercury at levels as low as 8 nM. The detection system is based on the use of the quencher properties of an MNMOF combined with a FAM-labeled DNA oligonucleotide (Figure 3-15). In the absence of Hg^{2+}, the labeled oligonucleotide is absorbed on the surface of the MNMOF by π-π interactions and hydrogen bonds, causing quenching of 65% of the fluorescence. The researchers hoped that by adding Hg^{2+}, the T-Hg^{2+}-T interactions would cause oligonucleotide desorption and fluorescence recovery, but conversely, the

fluorescence dropped to 52% and the study became a quenching-quenching technique system. In this case, the presence of Hg^{2+} promoted the hybridization of oligonucleotides, generating a dsDNA, and no desorption occurred due to interactions of the carboxyl and phenolic groups in the oligonucleotide with the Fe^{3+} ions on the surface of the MNMOF. Good performance was established for recovery in real samples, as well as for specificity in the detection of Hg^{2+} ions, due to the characteristic interactions of this ion with nitrogen in position 3 of the thymine.

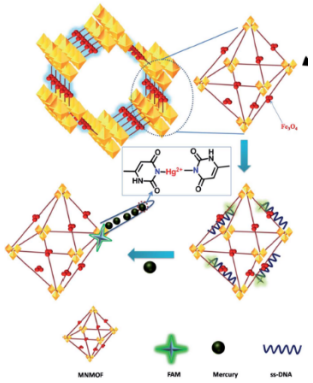

Figure 3-15. Hg2+ detection scheme based on MNMOF and interactions T-Hg2+-T. Reprinted with permission from ref (Marieeswaran and Panneerselvam, 2020). Copyright 2020. Royal Society of Chemistry

The use of 2D MOFs as acceptors in fluorescent sensors has been investigated and enhanced in recent years. The incorporation of various ligands has been evaluated for subsequent modifications, having in this case the advantage of using metallic nodes of more common elements such as copper and iron (non-emitting). DNA, lipids, peptides, and oligonucleotides have been used as attractive ligands (Wu et al., 2020). By using single-stranded DNA functionalized with organic dyes or emitting nanostructures, MOF-DNA hybrids can be obtained. These hybrids are conjugated by covalent bonds or weak interactions, according to the desired detection technique. MOF-DNA hybrids have been widely used for the direct detection of heavy metals such as Hg^{2+} and Ag^{+}, thanks to the pairing between these metals and thymine or cytosine respectively. Regarding optical properties, MOFs, like other nanostructures, can be luminescence emitters or act as acceptor molecules. To act as emitters, lanthanide metals are used or aromatic or fluorescent ligands are involved, so that photoluminescent materials with potential application as sensors can be obtained (Stock and Biswas, 2012).

Emerging contaminants

Population growth has not only lead to interest in detecting and removing contaminants of known toxicity, but has also made evident the presence of a wide variety of chemicals associated with new lifestyles and the growing needs for personal care, food, and health of people. In this context, emerging pollutants (ECs) are defined as chemicals, mostly synthetic, that cannot be easily monitored in situ in the environment, and that have the potential to cause adverse effects to ecology or human health (Patel et al., 2020). These compounds are usually found in very low concentrations, but their presence has been associated with adverse effects on aquatic organisms such as genotoxicity, endocrine disruption, and alterations of the immune system (Bo et al., 2015).

In terrestrial organisms, there has also been a feminization of males, low sperm count, some types of cancer, and thyroid problems (Marcoux et al., 2013; Patel et al., 2020). Studies are still underway to elucidate the effects of ECs on human health. Currently, the most widely accepted effects are related to bacterial resistance caused by residues of antibiotic compounds and endocrine disruption (Garcia-Rodríguez et al., 2014; Ibáñez et al., 2013). ECs mainly originate from pharmaceuticals, personal care and household cleaning products, surfactants, plasticizers, and other substances. Identifying these compounds presents two challenges: a) they are compounds with complex structures present in diverse matrices (wastewater, marine environments); b) their concentrations are generally in parts per billion (ppb) magnitudes, challenging for current analytical methods (Gaudin, 2017; Patel et al., 2020). Additionally, it has been proved that in most wastewater treatment systems worldwide, ECs do not undergo any type of transformation and can still negatively impact bacterial communities responsible for biological treatment (Garcia-Rodríguez et al., 2014; Ibáñez et al., 2013; Mirzaei et al., 2016). Due to the recent nature of ECs, as well as the diversity of associated possibly toxic active substances, the regulation of maximum permissible values in most countries is still incipient. However, the European Union has put some substances on its "watch list" and has defined some maximum limits (Agency, 2015). For example, hormones like 17-Beta-estradiol (E2), Estrone (E1) with 0.4 ng / L, Diclofenac with 10 ng / L, and Macrolide antibiotics with 90 ng / L.

Interest in the use of nanomaterials as amplifiers of the detection signal of ECs has increased, mainly in electrochemical method applications (Ge et al., 2020; Hassanzadeh et al., 2019; Pelle and Compagnone, 2018). In this context, recent studies compiled in this review focus on the use of fluorescent or quenching-capable nanomaterials as key molecules for the development of optical biosensors. These systems allow the detection of phenolic compounds, antibiotic residues, and other ECs in quantities of the nano, pico, and fento molar order.

Phenolic compounds

Phenolic compounds are synthetic substances that are commonly used in the plastic, pharmaceutical, petrochemical, and textile industries. Their presence in the environment is not limited to the waters since they tend to bioaccumulate in aquatic and terrestrial organisms (Jiaqi Wang et al., 2020). Some of the most common phenolic compounds in the environment are 2,4 di-chlorophenol, 2,4,6-trichlorophenol, pentachlorophenol, and bisphenol (Bilal et al., 2019). These types of compounds are characterized by their high toxicity, volatility, and resistance to biodegradation (Tian et al., 2020).

Bisphenol A (BPA) is one of the most representative phenolic compounds, known for its wide use in the plastics industry and for its effects as an endocrine disruptor (Rajabnejad et al., 2020). Even though the market for BPA-free products has grown, its presence still represents a risk to human health and detection systems for it are needed. For BPA detection, Lee et al, (Lee et al., 2018) focused on a dual fluorescent-colorimetric system. With the use of high concentrations of salt (50 mM), the aggregation of gold nanoparticles (AuNPs) is promoted, giving rise to a colorimetric signal that complements the much more sensitive fluorescence signal. The working principle uses an unlabeled aptamer to avoid decreasing the affinity for the analyte; instead, the external fluorescent

agent Syber green (SG) is incorporated, which generates a strong emission of fluorescence only when it is intercalated in the double strand of DNA. Thus, for the measurement of the sample, two sequential readings are done, as shown in Figure 45: 1) in the presence of BPA, the aptamer that is initially interacting with the AuNPs , protecting them from a Na+ ion-induced aggregation effect, changes its conformation by unfolding, so that when SG is added it does not find dsDNA sequences and does not fluoresce; 2) with the addition of high concentrations of salt, since the protective effect of the aptamer is no longer available, AuNPS are added by changing their color from red to dark brown, almost black. In the absence of BPA, fluorescence is emitted in step 1 and no aggregation is generated in step 2. The work presents a very low detection limit, 9 pg/mL, largely due to the careful choice of a 44 bp truncated aptamer.

For the detection of BPA, systems based on quantum dots (QDs) have also been used, using their emissive properties at two wavelengths. Lee et al (Lee et al., 2017) developed a test using QDs-conjugated magnetic nanospheres, a BPA-specific aptamer, and an ssDNA sequence partially complementary to the aptamer also conjugated to QDs. The QDs used had an external ZnS layer. As shown in Figure 3-16, QDs on the surface of the nanospheres fluoresce at 565 nm when excited by UV light at 360nm, while QDs conjugated to the complementary DNA sequence emit at 655 nm. In the absence of BPA, the complementary DNA sequence hybridizes with the aptamer found on the surface of the nanospheres, giving a characteristic QD 655 / QD 565 normalized fluorescence response. In the presence of BPA, this response changes, and a linear relationship can be established with the concentration of the pollutant. A detection limit of 1ng/mL and good selectivity against very close compounds such as bisphenol B and C were reached.

The use of bisphenol S (BPS) has been evaluated as an alternative to BPA. However, this compound has also shown toxicity and its rapid detection has been frustrated due to the lack of appropriate bioreceptors. In this context, Chen et al (Chen et al., 2018) developed a biosensor that combines an excellent selection of the aptamer with the the use of the MoS_2 nanosheets that have been subject to recent interest, to develop a detection system. They used CDs as the emissive nanoparticle. In this case, the aptamers interact through Van der Waals forces with the nanosheets and eventually generate absorption of the oligonucleotide on the surface of the nanomaterial. When the aptamer is functionalized with a fluorophore, the quenching phenomenon can be used to detect the molecule of interest. Additionally, the property of MoS_2 nanosheets to modulate their aggregation in the presence of various concentrations of Na+ (medium salinity) is explored. Conjugation of the fluorophore to the aptamer is known to be a limiting step in the commercial application of aptasensors; therefore, in this case, a system based on three free components is developed: aptamer, CDs in solution and MoS_2 nanosheets for BPS detection. In the absence of BPS and the presence of Na+ ions, the aptamer is absorbed into the MoS_2 nanosheets. This prevents aggregation of the nanosheets, making them available for FRET-based quenching with CDs (Figure 16). In the presence of BPS the aptamer cannot bind to the nanosheets so, in the presence of Na+, they aggregate, and the quenching efficiency on the CDs decreases. MoS_2 nanosheets have optoelectronic characteristics that depend on the thickness and number of layers, like other dialcogenic transition metals (Wang et al., 2012). When the CDs are on the surface of the nano blades, a non-radiative transfer of the delocalized electron pair occurs, consolidating the FRET. Using

high concentrations of Na+ (10mM) decreases the repulsion between negatively charged MoS_2 nanosheets so that aggregation occurs. It was also found that the magnitude of the quenching can reach 97% and is inversely proportional to the aggregation of the nanosheets, since the use of thicker layers decreases the free surface area with which the CDs can interact. Real milk samples with recoveries between 92.0% -104.2% were evaluated. The detection limit was 2nM.

It can be seen how the use of aptamers for the detection of phenolic compounds of environmental interest has gained relevance, especially since these bioreceptors have shown excellent performance for the detection of low molecular weight analytes (Odeh et al., 2020). Additionally, aptamers can be designed to be used in complex matrices with the presence of strong solvents, without losing sensitivity or selectivity, something appreciated in complex samples of environmental interest (Rajabnejad et al., 2020).

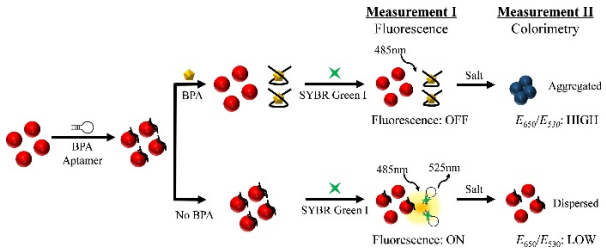

Figure 3-16. Principle of detection of phenolic compounds of environmental interest. Aptamer-based BPA, AuNPs and SG. Reprinted with permission ref (Lee et al., 2017). Copyright 2017. American Chemical Society

More recently and as an alternative to the use of aptamers, Singh et al (Singh et al., 2020) studied the direct detection of nonylphenol in aqueous solution. In the presence of the analyte, there is a quenching phenomenon that is explained by various phenomena such as electron transfer, molecular collisions, and excitation-emission complexes. The decrease in fluorescence is proportional to the concentration of nonylphenol, however, it is a less sensitive method, which is evident in its detection limits (0.1µM). Furthermore, when using direct detection without a bioreceptor, its use in complex matrices can present large interactions that make it impossible. The authors also evaluated the immobilization of the CDs on an agarose gel matrix as support, which was then subjected to the presence of nonylphenol. This matrix was excited by a UV lamp, resulting in a qualitative signal from the analyte.

Antibiotics

Antibiotic compounds are used intensively in humans and animals, not only for their therapeutic effect but as growth promoters in farming animals. This overuse is generating an increasing concentration of antibiotic residues in products for mass consumption and water sources (Majdinasab et al., 2019). These residues can generate what is known as bacterial resistance, which can become a worldwide problem if it is acquired by highly pathogenic and zoonotic strains (Gaudin, 2017). According to the United States Center for Disease Prevention and Control, approximately 23,000 deaths annually are associated with some degree of bacterial resistance (Majdinasab et al., 2019). Some of the most common antibiotics that can be found in food and wastewater belong to

the beta-lactam groups, lincosamides, sulfonamides, cyclins, amphenicol, fluoroquinolones, macrolides, trimethoprim, and glycopeptides (Bilal et al., 2019).

Enrofloxacin (ENR) is an antibiotic from the group of fluoroquinolones that is frequently used for the prevention and treatment of diseases in animals due to its wide spectrum of action. Some authors report effects such as allergies, intestinal bloating, and bacterial resistance (Dolati et al., 2018; Sultan, 2014). For its detection, simple systems have been developed, taking advantage of the native fluorescence of the ENR. It has also been combined with graphene oxide (GO) as a quencher (Dolati et al., 2018). The bioreceptor molecule is a label-free aptamer. In a sample with ENR and without the presence of the aptamer, there will be almost no fluorescence signal due to the absorption of ENR in GO. While in the presence of the aptamer, the ENR will be recognized and the conformational change will prevent the absorption of the aptamer-analyte pair Developmental specificity was evaluated against marbofloxacin, doxorubicin, and epirubicin, with good performances, as well as in milk matrix samples contaminated with ENR. The recovery percentages were higher than 90%, with a detection limit of 3.7 nM.

The use of GO in systems for the detection of antibiotics based on FRET has also been reported in other works. Youn et al (Youn et al., 2019) developed a system for the simultaneous detection of three antibiotic residues in common use in human and veterinary health: sulfadimethoxine, kanamycin, and ampicillin. Conjugated aptamers with 3 different fluorophores were used: Cyanine 3 (Cy3), 6-Carboxyfluorescein (FAM), and

Cyanine 5 (Cy5). The method achieves excellent detection limits by applying a novel system: cyclic enzymatic amplification with DNase I. This non-specific endonuclease acts on ssDNA. GO has been shown to have a protective effect on DNA against the action of DNase1. As shown in Figure 3-17 detection of antibiotics is based on their interaction with the fluorophore-labeled aptamers. In the presence of the analytes, these aptamers cannot interact with GO through weak π-π interactions and remain in solution, emitting fluorescence. Additionally, they are subject to the action of DNase 1, so the cut aptamer residues that still have fluorophore can bind to new antibiotic molecules. Through this process, they amplify the signal and reach detection limits of 1,997, 2,664, and 2,337 ng/mL for sulfadimethoxine, kanamycin, and ampicillin, respectively. Conversely, in the absence of antibiotics in the sample, the labeled aptamers will be absorbed in the GO, resulting in quenching of over 90%.

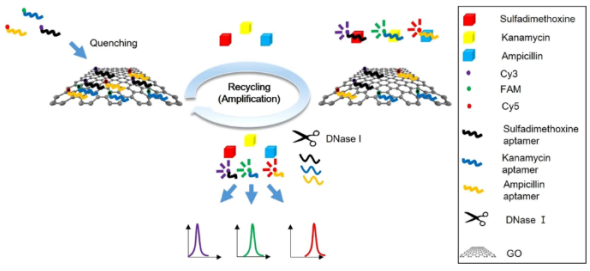

Figure 3-17. Principle of simultaneous detection of sulfadimethoxine, kanamycin, and ampicillin based on aptamers and GO (Youn et al., 2019).

GO is not the only quenching agent. Metallic nanoparticles, especially gold ones, have a wide absorption spectrum, facilitating their application in FRET or IFE phenomena (Chun et al., 2016). For the detection of kanamycin, citrate-coated gold nanoparticles (cc-AuNPs) have been used as quencher agent for CD fluorescence. This strategy has been complemented by the aggregation property of AuNPs in the presence of high salt concentrations (Jinlong Wang et al., 2020). For detection, in the absence of kanamycin, the aptamer interacts with the AuNPs protecting them from the aggregation effect. In this way, CDs can interact with AuNps that quench their fluorescence. Conversely, in the presence of the analyte, the aptamers cannot interact with the AuNps, which aggregate, and as a result, the fluorescence of the CDs remains (Figure 3-18 A). Quenching in this case only reaches 65% and is attributed to IFE, due to the overlapping of absorption-excitation-emission spectra between donor and quencher. The milk matrix system was evaluated with different concentrations of kanamycin, with recoveries between 90 and 98.3% and a detection limit of 18 nM.

Metallo-organic frameworks (MOFs) with interesting optoelectronic properties have also recently emerged, including potential applications as a non-FRET based quencher (Rodenas et al., 2015). Yang et al (Yang et al., 2018) developed a test based on SG fluorescence, as an external fluorophore. This strategy was discussed in a previous example and its advantage is that it avoids the complexity of modifying the bioreceptor used. A hairpin aptamer (HP) was used which has a specific sequence for chloramphenicol recognition and an unused sequence for recognition, which forms a portion of dsDNA. In this case, MOF is synthesized from Cu nanosheets combined with tetrakis (4-carboxyphenyl) porphyrin (TCPP), generating Cu-TCPP. For detection, bst DNA polymerase and its respective primers are used, applying the following principle (Figure 3-18 B): in the presence of chloramphenicol, HP is deployed for detection, leaving the end-sequence that is not involved in recognition free to mate with the primer and undergo polymerization. In the presence of this dsDNA, the SG will emit a high fluorescence and the dsDNA cannot be absorbed into the Cu-TCPP, whereby the fluorescence remains. Otherwise, without the presence of chloramphenicol, HP will not be able to align with the primer, the DNA polymerase will not act and the SG will not fluoresce since the small amount absorbed in the HP will be quenched when absorbed in the Cu-TCPP that is involved in the process. It is important to avoid errors due to background fluorescence. The detection limit (0.3 pg/ mL), as well as the repeatability, is excellent.

The use of systems that combine DNA with MOF through weak interactions is an application of the concept of MOF as a quencher agent. It is important to note that MOFs have properties like organic 2D nanostructures (graphene), so DNA can interact in a similar way and be absorbed on the surface of the nanostructure, but in this case the extinction of fluorescence occurs through a PET rather than FRET process (Cui et al., 2020). In any case, MOF-DNA based sensors have advantages such as: a) a greater capacity for interaction of the MOF with the analyte, thanks to greater pi interactions; b) greater effectiveness as a quencher agent, when metallic ions such as Zn^{2+} or Cu^{2+} are exposed in the nanostructure; and c) not only heavy metals, but ions such as S^{2-}, Cu^{2+} and other thiols of biological interest can be detected (Wu et al., 2020). Despite these possibilities and the advances made, efforts should be made towards the synthesis of MOFs with greater stability and biocompatibility, as well as the use of less complex detection techniques.

Other systems use the phenomenon of quenching but with more sophisticated developments. The use of molecularly printed polymers (MIP) has been increasing due to the simplicity of their synthesis and the high specificity for the analyte (Wackerlig and Schirhagl, 2016). These compounds are prepared from a functional monomer, a crosslinking agent, a catalyst, and the analyte molecule as a template, as shown in Figure 3-19.

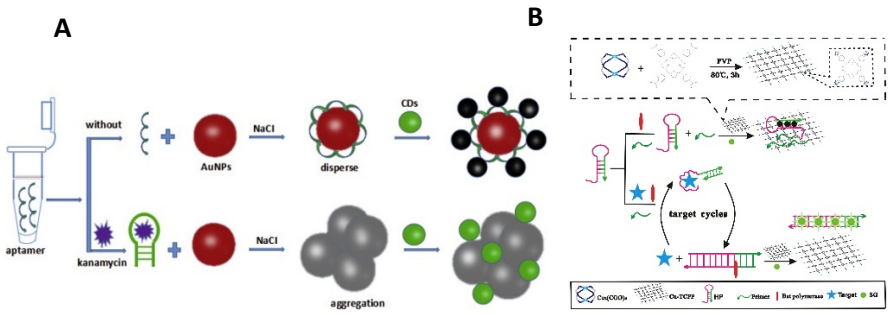

Figure 3-18. Application of alternative nanomaterials to GO as quencher agents. A) detection of kanamycin with aptamers and AuNPs. Reprinted from ref (Jinlong Wang et al., 2020), Copyright 2020, with permission from Elsevier. B) chloramphenicol detection by aptamers and MOF . Reprinted from ref (Yang et al., 2018), Copyright 2018, with permission from Elsevier.

MIPs are materials with high stability, which means that they can be used in extreme conditions, such as extreme pH, high temperature, and inorganic solvents. For example, the detection of ciprofloxacin is reported using two nanomaterials: CdTe-QDs; and carbon nanotubes functionalized with carboxylic acids (COOH @ MWCNT) (Yuphintharakun et al., 2018). The detection system is based on the use of a MIP, prepared from APTES, TEOS, ciprofloxacin, and NH3 as a catalyst. COOH-functionalized MWCNTs are highly soluble and contain key functional groups for the MIP synthesis process and the subsequent recognition of ciprofloxacin. Additionally, the QDs are incorporated to generate a fluorescent system that can be quenched in the presence of the template analyte, a response that is proportional to the presence of the analyte (Figure 48). The quenching mechanism is not typical FRET since the spectra of MWCNT or ciprofloxacin do not overlap with QDs. Rather, it is attributed to an electron transfer mechanism between QDs and ciprofloxacin. The amino group of APTES plays a fundamental role in the interaction of ciprofloxacin with the system, which allows a detection limit of 0.066 ng/mL.

Finally, Peng et al (Peng et al., 2020) recently developed a system for the simultaneous detection of three antibiotics: sulfadimethoxine (SDM), enrofloxacin (ENR), and thiamphenicol (TAP). For this, SiO_2 nanoparticles were synthesized, which served to stabilize the MnO_2 nanoflowers, generating a SiO_2 @ MnO_2 nanocomposite. This composite has a brown color which changes noticeably in the presence of analytes. A chromatographic sensor, based on capillarity, was developed. The nanocomposite, that is conjugated to the respective antibodies only by weak interactions, is deposited on the test lines. At the beginning of the test, the strong brown lines appear, but when the sample is placed in the presence of the analyte, the lines disappear. This behavior allows two detection limits: one with the naked eye and the another much lower limit using image processing

software. Additionally, serum glutathione concentration (GSH) is evaluated as an indicator of antibiotic exposure.

Gold nanoclusters were synthesized with arginine (Arg) and 6-aza-2-thiothymine (ATT) ATT / Arg / AuNCs. Arginine was used to increase fluorescence by the way it interacts with ATT. However, when the ARG is in the presence of Mn (II) it disengages from the nanocluster, resulting in a decrease in its intensity. By combining the SiO_2 @ MnO_2-based antibiotic detection system, the authors found that GSH can reduce MnO2 to Mn (II), with subsequent interaction with Arg and corresponding quenching. Thus, the immunochromatographic biosensor shows the disappearance of the colored lines in the presence of GSH (because of the disintegration of the nanocomposite) and additionally, when subjected to UV light, quenching can be correlated with the presence of the analyte. The system may seem complex but the possibility of simultaneous detection of several substances of interest in a real matrix is quite interesting. The naked eye detection limits were 0.25 µg/L (SDM), 1.25 µg/L (ENR), and 1.25 µg/L (TAP); the limit for GSH was 1.23 nM.

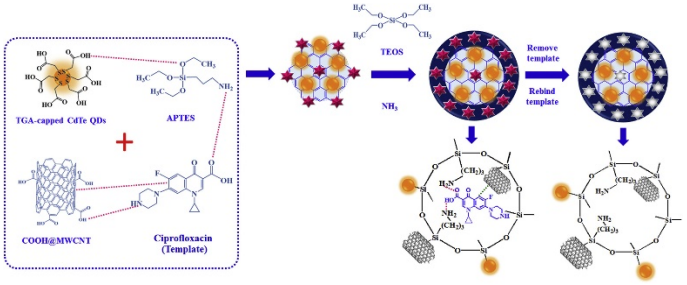

Figure 3-19. Sophisticated systems for the detection of antibiotics. A) use of MIP for the detection of ciprofloxacin. Reprinted from ref (Yuphintharakun et al., 2018), Copyright 2018, with permission from Elsevier.

The atomic thickness configuration in MnOx nano blades makes the Mn paramagnetic centers more available to attack by protons in aqueous solutions, and provides different anchor points for functionalization with other molecules (Qian et al., 2020). MnOx nano blades have been able to be loaded with large amounts of therapeutic agents, working very well as drug delivery vehicles (Qian et al., 2020). These nanostructures have a large surface area and can have catalytic activity, for example in the presence of glutathione (GSH) when they are in an acidic environment (Xu et al., 2016). This catalytic property with GSH enables their use in activatable systems for sensors. Like TMDCs, these materials have been used as fluorescence quenching agents (He et al., 2015)

3.4. Conclusions and outlooks

The development and diversification of nanomaterials have fueled the advancement of optical biosensors for the detection of various pollutants. Nanomaterials have highly desirable and adjustable optoelectronic properties depending on their size and chemical structure. In this review we presented the use of these nanomaterials in fluorescent systems to generate much more sensitive and specific signals. Some of them, such as quantum dots and carbon dots, have high fluorescence emission intensity and can be used as donors in quenching-based processes. Meanwhile, nanomaterials such as graphene, graphene oxide, metallic nanoparticles, and other

inorganic 2 D materials such as transition metal dialcogens and organo-metallic frameworks, are often used as process acceptors in fluorescence quenching, with excellent results. The selection of the most suitable nanomaterial will depend on the characteristics of the analyte to be detected, considering factors such as its concentration and chemical nature. Usually, the detection of low molecular weight molecules, such as some ions or pesticides, presents better LODs with turn-on type biosensors, which decrease the nonspecific background signals. To improve the sensitivity and specificity of biosensors, various biomediators have been explored, finding that the aptamer-nanomaterial combination generates the best results. It should be borne in mind that in the same detection system it is possible to combine two or more nanomaterials, using these simultaneously as donor-acceptors in quenching processes or as supports for the bioconjugation of other molecules. It is also possible to combine various techniques, such as quenching and catalytic detection (DNAzymes). In this sense, the bioconjugation technique also plays a fundamental role since the performance of fluorescent nanomaterials can be diminished by using certain chemical strategies to link them with the appropriate biomediators.

Table 3-1, presents some of the most common fluorescent nanomaterials used in detection systems for pollutants of environmental concern, a standout feature being the excellent LODs. It is possible to infer that although carbon dots (CD) have advantages such as low toxicity, high solubility, and potential for green synthesis, they still need to be optimized against the LODs that QDs present. Nanomaterials such as organo-metallic frameworks (MOF) show excellent performance as extinguishing agents and are presumed to be the most widely applied, replacing G and GO in some applications.

To further drive the development of nanomaterial-based fluorescent biosensors, efforts must be made to obtain more sustainable, economical, and stable nanomaterials. The use of nanomaterials should also be developed in complementary techniques, such as the extraction and concentration of the analyte to be detected. Some authors have also explored the use of enzymes to amplify signals in detection, reusing the emitting nanostructure or the organic fluorophore several times in the same reading.

Finally, properties such as the toxicity of these systems in the environment must be evaluated, to ensure that their use for the detection of contaminants in water sources does not generate additional pollution problems, and to achieve the massification of portable detection systems, especially in developing countries.

Table 3-1. Nanomaterials used in fluorescent biosensor for the detection of pollutants, with outstanding LOD

Nanomaterial	Pollutant	Quenching technique	Real sample	LOD	Reference
CD	Total Chromium	IFE	Water	0.708 ppb	(D. et al., 2019)
CD	Hg (II)	Non fluorescente ground complex	Lake water	0.014 µM	(G. Liu et al., 2019)
CD	Bisphenol S	FRET	Milk	2 nM	(Chen et al., 2018)

CD	Nonylphenol	DET, Non fluorescente ground complex	-	0.1 µM	(Singh et al., 2020)
CD- NP	Kanamycin residue	FRET	Milk	18 nM	(Jinlong Wang et al., 2020)
QD	Malathion	IFE, Electrostatic interactions	Tap and lake water	4 pM	(Bala et al., 2018b)
QD- MWCNT	Acetamiprid	FRET	River water and cabbage leaves	0.7 nM	(Lin et al., 2016)
QD- NP	Chlorpyrifos Diazinon Malathion	FRET	Spinach	0.73 ng/mL 6.7 ng/ mL 0.74 ng/mL	(Cheng et al., 2018b)
QD- GO	Diazinon	FRET	Surface water, cucumber and apple	0,13 nM	(Arvand and Mirroshandel, 2019)
QD	Paraoxon Parathion Dichlorvos Deltamethrin	DET	Apple	1.2 pM 0.94 pM 11.7 pM 0.38 pM	(Hu et al., 2019)
QD	Hg (II)	RET, Excimers	Tap water	3.33 nM	(Guo et al., 2019)
QD	Hg (II)	DET	Fresh and sea water	1 nM	(T. Liu et al., 2019)
QD- MWCNT	Ciprofloxacin	FRET	Chicken muscle and milk	0.066 ng/mL	(Yuphintharakun et al., 2018)
Si-QD	Hg (II) Cu (II)	FRET Non fluorescente ground complex	Water	10 nM	(Jia et al., 2018)
Au nanoclusters	Hg (II)	FRET	Tap and lake water	10 nM	(Wang et al., 2016)
Cu nanoclusters	Hg (II) S 2-	DET, Non fluorescente ground complex	Pond and river water	1.7 nM 1.02 nM	(Maruthupandi et al., 2020)
Ag nanoclusters	Hg (II)	RET, Non fluorescente ground complex	Tap and lake water	4.5 nM	(Li and Wei, 2017)
SiO2@MnO2 Nanocomposites	Sulfadimethoxine Enrofloxacin Thiamphenicol Gluthation	Non fluorescente ground complex	Human serum and milk	0.25 µg/l 1.25 µg/l 1.25 µg/L 1.23 nM	(Peng et al., 2020)
TMDC (WS2) Nanosheets (as quencher)	Hg (II)	FRET	Tap and lake water	0.1 nM	(Ge et al., 2017)
TMDC (MoS2) Nanosheets (as quencher)	As (III)	FRET	Tap and lake water	18 nM	(Ravikumar et al., 2018)
MOF (as quencher)	Hg (II)	FRET	Water	8 nM	(Marieeswaran and Panneerselvam, 2020)
MOF (as quencher)	Chloramphenicol	FRET	Milk	0.3 pg/mL	(Yang et al., 2018)

3.5. References

Abdul, S., Nor, R., Zobir, M., 2019. Synthesis, Technology and Applications of Carbon Nanomaterials. Elsevier, Oxford.

Agency, E. environment, 2015. Decision (EU) 2015/495.
Amini, A., Kazemi, S., Safarifard, V., 2020. Metal-organic framework-based nanocomposites for sensing applications – A review. Polyhedron 177, 114260. https://doi.org/10.1016/j.poly.2019.114260
Arvand, M., Mirroshandel, A.A., 2019. An efficient fluorescence resonance energy transfer system from quantum dots to graphene oxide nano sheets: Application in a photoluminescence aptasensing probe for the sensitive detection of diazinon. Food Chem 280, 115–122. https://doi.org/10.1016/j.foodchem.2018.12.069
Arvand, M., Mirroshandel, A.A., 2017. Highly-sensitive aptasensor based on fluorescence resonance energy transfer between L-cysteine capped ZnS quantum dots and graphene oxide sheets for the determination of edifenphos fungicide. Biosens Bioelectron 96, 324–331. https://doi.org/10.1016/j.bios.2017.05.028
Azadmanjiri, J., Srivastava, V.K., Kumar, P., Sofer, Z., Min, J., Gong, J., 2020. Graphene-Supported 2D transition metal dichalcogenide van der waals heterostructures. Applied Materials Today 19. https://doi.org/10.1016/j.apmt.2020.100600
Bagheri, E., Ansari, L., Abnous, K., Taghdisi, S.M., Ramezani, P., Ramezani, M., Alibolandi, M., 2020. Silica – Quantum Dot Nanomaterials as a Versatile Sensing Platform. Critical Reviews in Analytical Chemistry 0, 1–22. https://doi.org/10.1080/10408347.2020.1768358
Bai, Y., Xu, T., Zhang, X., 2020. Graphene-based biosensors for detection of biomarkers. Micromachines (Basel) 11. https://doi.org/10.3390/mi11010060
Bala, R., Mittal, S., Sharma, R.K., Wangoo, N., 2018a. A supersensitive silver nanoprobe based aptasensor for low cost detection of malathion residues in water and food samples. Spectrochimica Acta - Part A: Molecular and Biomolecular Spectroscopy 196, 268–273. https://doi.org/10.1016/j.saa.2018.02.007
Bala, R., Swami, A., Tabujew, I., Peneva, K., Wangoo, N., Sharma, R.K., 2018b. Ultra-sensitive detection of malathion using quantum dots-polymer based fluorescence aptasensor. Biosensors and Bioelectronics 104, 45–49. https://doi.org/10.1016/j.bios.2017.12.034
Barua, S., Dutta, H.S., Gogoi, S., Devi, R., Khan, R., 2018. Nanostructured MoS2-Based Advanced Biosensors: A Review. ACS Applied Nano Materials 1, 2–25. https://doi.org/10.1021/acsanm.7b00157
Berezin, M.Y., Achilefu, S., 2010. Fluorescence lifetime measurements and biological imaging. Chemical Reviews 110, 2641–2684. https://doi.org/10.1021/cr900343z
Bilal, M., Adeel, M., Rasheed, T., Zhao, Y., Iqbal, H.M.N., 2019. Emerging contaminants of high concern and their enzyme-assisted biodegradation – A review. Environment International. https://doi.org/10.1016/j.envint.2019.01.011
Blagoi, G., 2004. Fluorescence Resonance Energy Transfer (FRET) Based Sensors for Bioanalysis. University of New Orleans Theses and Dissertations.
Bleeker, E.A.J., de Jong, W.H., Geertsma, R.E., Groenewold, M., Heugens, E.H.W., Koers-Jacquemijns, M., van de Meent, D., Popma, J.R., Rietveld, A.G., Wijnhoven, S.W.P., Cassee, F.R., Oomen, A.G., 2013. Considerations on the EU definition of a nanomaterial: Science to support policy making. Regulatory Toxicology and Pharmacology 65, 119–125. https://doi.org/10.1016/j.yrtph.2012.11.007
Bo, L., Shengen, Z., Chang, C.-C., Zhanfeng, D., Hongxiang, L., 2015. Emerging Pollutants - Part II: Treatment. Water Environment Research 87, 1873–1900. https://doi.org/10.2175/106143015X14338845156461
Brouwer, M., Huss, A., van der Mark, M., Nijssen, P.C.G., Mulleners, W.M., Sas, A.M.G., van Laar, T., de Snoo, G.R., Kromhout, H., Vermeulen, R.C.H., 2017. Environmental exposure to pesticides and the risk of Parkinson's disease in the Netherlands. Environment International 107, 100–110. https://doi.org/10.1016/j.envint.2017.07.001
Buonasera, K., Pezzotti, G., Pezzotti, I., Cano, J.B., Giardi, M.T., 2015. Biosensors: new frontiers for the environmental analysis. Revista Politécnica 7, 93–100.
Campuzano, S., Yáñez-Sedeño, P., Pingarrón, J.M., 2019. Carbon dots and graphene quantum dots in electrochemical biosensing. Nanomaterials 9, 1–18. https://doi.org/10.3390/nano9040634

Cardoso Dos Santos, M., Algar, W.R., Medintz, I.L., Hildebrandt, N., 2020. Quantum dots for Förster Resonance Energy Transfer (FRET). TrAC - Trends in Analytical Chemistry 125, 115819. https://doi.org/10.1016/j.trac.2020.115819

Cayuela, A., Soriano, M.L., Carrillo-Carrión, C., Valcárcel, M., 2016. Semiconductor and carbon-based fluorescent nanodots: The need for consistency. Chemical Communications 52, 1311–1326. https://doi.org/10.1039/c5cc07754k

Chaparro-Narváez, P., Castañeda-Orjuela, C., 2015. Mortalidad debida a intoxicación por plaguicidas en Colombia entre 1998 y 2011. Biomédica 35, 90–102. https://doi.org/10.7705/biomedica.v35i0.2472

Chen, K., Zhang, W., Zhang, Yuhuan, Huang, L., Wang, R., Yue, X., Zhu, W., Zhang, D., Zhang, X., Zhang, Ying, Wang, J., 2018. Label-free fluorescence aptasensor for sensitive determination of bisphenol S by the salt-adjusted FRET between CQDs and MoS2. Sensors and Actuators, B: Chemical 259, 717–724. https://doi.org/10.1016/j.snb.2017.12.116

Chen, N., He, Y., Su, Y., Li, X., Huang, Q., Wang, H., Zhang, X., Tai, R., Fan, C., 2012. Biomaterials The cytotoxicity of cadmium-based quantum dots q. Biomaterials 33, 1238–1244. https://doi.org/10.1016/j.biomaterials.2011.10.070

Cheng, N., Song, Y., Fu, Q., Du, D., Luo, Y., Wang, Y., Xu, W., Lin, Y., 2018a. Aptasensor based on fluorophore-quencher nano-pair and smartphone spectrum reader for on-site quantification of multi-pesticides. Biosensors and Bioelectronics 117, 75–83. https://doi.org/10.1016/j.bios.2018.06.002

Cheng, N., Song, Y., Fu, Q., Du, D., Luo, Y., Wang, Y., Xu, W., Lin, Y., 2018b. Aptasensor based on fluorophore-quencher nano-pair and smartphone spectrum reader for on-site quantification of multi-pesticides. Biosensors and Bioelectronics 117, 75–83. https://doi.org/10.1016/j.bios.2018.06.002

Chuang, C.S., Su, H.L., Lin, C.L., Kao, C.H., 2017. Risk of Parkinson disease after organophosphate or carbamate poisoning. Acta Neurol Scand 136, 129–137. https://doi.org/10.1111/ane.12707

Chun, G.N., Li, Y. Le, Jiang, X., Zheng, X.F., Ya, Y.W., Shuang, Y.Huan., 2016. Fluorescence resonance energy transfer-based biosensor composed of nitrogen-doped carbon dots and gold nanoparticles for the highly sensitive detection of organophosphorus pesticides. Analytical Sciences 32, 951–956. https://doi.org/10.2116/analsci.32.951

Cui, C., Wang, Q., Xin, C., Liu, Q., Deng, X., Liu, T., Xu, X., Zhang, X., 2020. Covalent organic framework with bidentate ligand sites as reliable fluorescent sensor for Cu2+. Microporous and Mesoporous Materials 299, 110122. https://doi.org/10.1016/j.micromeso.2020.110122

Cui, S., Xu, S., Song, H., Xu, W., Chen, X., Zhou, D., Yin, Z., Han, W., 2015. Highly sensitive and selective detection of mercury ions based on up-conversion FRET from NaYF4:Yb3+/Er3+ nanophosphors to CdTe quantum dots. RSC Advances 5, 99099–99106. https://doi.org/10.1039/c5ra16200a

D., P., Singh, L., Thakur, A., Kumar, P., 2019. Green synthesis of glowing carbon dots from Carica papaya waste pulp and their application as a label-freechemo probe for chromium detection in water. Sensors and Actuators, B: Chemical 283, 363–372. https://doi.org/10.1016/j.snb.2018.12.027

Ding, H., Yu, S.B., Wei, J.S., Xiong, H.M., 2016. Full-color light-emitting carbon dots with a surface-state-controlled luminescence mechanism. ACS Nano 10, 484–491. https://doi.org/10.1021/acsnano.5b05406

Dolan, T., Howsam, P., Parsons, D.J., Whelan, M.J., 2013. Is the EU Drinking Water Directive Standard for Pesticides in Drinking Water Consistent with the Precautionary Principle ?

Dolati, S., Ramezani, M., Nabavinia, M.S., Soheili, V., Abnous, K., Taghdisi, S.M., 2018. Selection of specific aptamer against enrofloxacin and fabrication of graphene oxide based label-free fluorescent assay. Analytical Biochemistry 549, 124–129. https://doi.org/10.1016/j.ab.2018.03.021

Doose, S., Neuweiler, H., Sauer, M., 2009. Fluorescence Quenching by Photoinduced Electron Transfer: A Reporter for Conformational Dynamics of Macromolecules. ChemPhysChem 10, 1389–1398. https://doi.org/10.1002/cphc.200900238

Dou, X., Chu, X., Kong, W., Luo, J., Yang, M., 2015. A gold-based nanobeacon probe for fluorescence sensing of organophosphorus pesticides. Analytica Chimica Acta 891, 291–297. https://doi.org/10.1016/j.aca.2015.08.012

Dulkeith, E., Ringler, M., Klar, T.A., Feldmann, J., Javier, A.M., Parak, W.J., 2005. Gold nanoparticles quench fluorescence by phase induced radiative rate suppression. Nano Letters 5, 585–589. https://doi.org/10.1021/nl0480969

Dzudzevic Cancar, H., Soylemez, S., Akpinar, Y., Kesik, M., Göker, S., Gunbas, G., Volkan, M., Toppare, L., 2016. A Novel Acetylcholinesterase Biosensor: Core-Shell Magnetic Nanoparticles Incorporating a Conjugated Polymer for the Detection of Organophosphorus Pesticides. ACS Appl Mater Interfaces 8, 8058–8067. https://doi.org/10.1021/acsami.5b12383

Ejeian, F., Etedali, P., Mansouri-Tehrani, H.A., Soozanipour, A., Low, Z.X., Asadnia, M., Taheri-Kafrani, A., Razmjou, A., 2018. Biosensors for wastewater monitoring: A review. Biosens Bioelectron 118, 66–79. https://doi.org/10.1016/j.bios.2018.07.019

Ellen MacArthur Foundation., 2015. Economía circular [WWW Document]. URL https://www.ibm.com/developerworks/ssa/local/im/que-es-big-data/

European environment agency, 2013. Directive 2013/39/EU of the European parliament and of the council. EU.

European environment agency, 2006. EC 1881/2006.

FAO, 2018. Pesticides indicators [WWW Document]. FAOSTAT. URL http://www.fao.org/faostat/en/#data/EP/visualize (accessed 3.17.21).

Gaponik, N., Talapin, D. V., Rogach, A.L., Hoppe, K., Shevchenko, E. V., Kornowski, A., Eychmüller, A., Weller, H., 2002. Thiol-capping of CDTe nanocrystals: An alternative to organometallic synthetic routes. Journal of Physical Chemistry B 106, 7177–7185. https://doi.org/10.1021/jp025541k

Garcia-Rodríguez, A., Matamoros, V., Fontàs, C., Salvadó, V., 2014. The ability of biologically based wastewater treatment systems to remove emerging organic contaminants--a review. Environmental science and pollution research international 21, 11708–11728. https://doi.org/10.1007/s11356-013-2448-5

Gaudin, V., 2017. Advances in biosensor development for the screening of antibiotic residues in food products of animal origin – A comprehensive review. Biosensors and Bioelectronics 90, 363–377. https://doi.org/10.1016/j.bios.2016.12.005

Ge, J., Xin-Geng, Du, Y.H., Chen, J.J., Zhang, L., Bai, D.M., Ji, D.Y., Hu, Y.L., Li, Z.H., 2017. Highly sensitive fluorescence detection of mercury (II) ions based on WS2 nanosheets and T7 exonuclease assisted cyclic enzymatic amplification. Sensors and Actuators, B: Chemical 249, 189–194. https://doi.org/10.1016/j.snb.2017.04.094

Ge, L., Li, S.P., Lisak, G., 2020. Advanced sensing technologies of phenolic compounds for pharmaceutical and biomedical analysis. Journal of Pharmaceutical and Biomedical Analysis 179, 112913. https://doi.org/10.1016/j.jpba.2019.112913

Geldert, A., Kenry, Lim, C.T., 2017. Paper-based MoS2 nanosheet-mediated FRET aptasensor for rapid malaria diagnosis. Scientific Reports 7, 1–8. https://doi.org/10.1038/s41598-017-17616-3

Guo, H., Li, J., Li, Y., Wu, D., Ma, H., Wei, Q., Du, B., 2019. Exciton energy transfer-based fluorescent sensor for the detection of Hg 2+ through aptamer-programmed self-assembly of QDs. Analytica Chimica Acta 1048, 161–167. https://doi.org/10.1016/j.aca.2018.10.021

Hamza, R.A., Iorhemen, O.T., Tay, J.H., 2016. Occurrence, impacts and removal of emerging substances of concern from wastewater. Environ Technol Innov. https://doi.org/10.1016/j.eti.2016.02.003

Hassani, S., Momtaz, S., Vakhshiteh, F., Maghsoudi, A.S., Ganjali, M.R., Norouzi, P., Abdollahi, M., 2017. Biosensors and their applications in detection of organophosphorus pesticides in the environment. Archives of Toxicology 91, 109–130. https://doi.org/10.1007/s00204-016-1875-8

Hassanzadeh, J., Al Lawati, H.A.J., Al Lawati, I., 2019. Metal-organic framework loaded by rhodamine b as a novel chemiluminescence system for the paper-based analytical devices and its application for total phenolic content determination in food samples. Analytical Chemistry 91, 10631–10639. https://doi.org/10.1021/acs.analchem.9b01862

He, D., Yang, Xiaoxiao, He, Xiaoxiao, Wang, K., Yang, Xue, He, Xing, Zou, Z., 2015. A sensitive turn-on fluorescent probe for intracellular imaging of glutathione using single-layer MnO2 nanosheet-quenched fluorescent carbon quantum dots. Chemical Communications 51, 14764–14767. https://doi.org/10.1039/c5cc05416h

He, Z.J., Kang, T.F., Lu, L.P., Cheng, S.Y., 2020. An electrochemiluminescence sensor based on CdSe@CdS-functionalized MoS2 and a GOD-labeled DNA probe for the sensitive detection of Hg(ii). Analytical Methods 12, 491–498. https://doi.org/10.1039/c9ay02524c

Henna, T.K., Pramod, K., 2020. Graphene quantum dots redefine nanobiomedicine. Materials Science and Engineering C 110. https://doi.org/10.1016/j.msec.2020.110651

Hermanson, G., 2008. Bioconjugate techniques, third. ed, Pierce biotechnology. New york.

Hu, T., Xu, J., Ye, Y., Han, Y., Li, X., Wang, Z., Sun, D., Zhou, Y., Ni, Z., 2019. Visual detection of mixed organophosphorous pesticide using QD-AChE aerogel based microfluidic arrays sensor. Biosens Bioelectron 136, 112–117. https://doi.org/10.1016/j.bios.2019.04.036

Huang, H., Li, J., Zhu, J.J., 2011. Electrochemiluminescence based on quantum dots and their analytical application. Analytical Methods 3, 33–42. https://doi.org/10.1039/c0ay00608d

Huang, J., Su, X., Li, Z., 2017. Metal ion detection using functional nucleic acids and nanomaterials. Biosensors and Bioelectronics 96, 127–139. https://doi.org/10.1016/j.bios.2017.04.032

Ibáñez, M., Gracia-Lor, E., Bijlsma, L., Morales, E., Pastor, L., Hernández, F., 2013. Removal of emerging contaminants in sewage water subjected to advanced oxidation with ozone. Journal of Hazardous Materials 260, 389–398. https://doi.org/10.1016/j.jhazmat.2013.05.023

Jia, X., Li, L., Yu, J., Gao, X., Yang, X., Lu, Z., Zhang, X., Liu, H., 2018. Facile synthesis of BCNO quantum dots with applications for ion detection, chemosensor and fingerprint identification. Spectrochimica Acta Part A: Molecular and Biomolecular Spectroscopy 203, 214–221. https://doi.org/10.1016/j.saa.2018.05.099

Kalantar-zadeh, K., Ou, J.Z., Daeneke, T., Strano, M.S., Pumera, M., Gras, S.L., 2015. Two-Dimensional Transition Metal Dichalcogenides in Biosystems. Advanced Functional Materials 25, 5086–5099. https://doi.org/10.1002/adfm.201500891

Kanellis, V.G., 2018. Sensitivity limits of biosensors used for the detection of metals in drinking water. Biophysical Reviews 10, 1415–1426. https://doi.org/10.1007/s12551-018-0457-9

Kaur, N., Prabhakar, N., 2017. Current scenario in organophosphates detection using electrochemical biosensors. TrAC - Trends in Analytical Chemistry 92, 62–85. https://doi.org/10.1016/j.trac.2017.04.012

Kaushal, S., Nanda, S.S., Samal, S., Yi, D.K., 2020. Strategies for the Development of Metallic-Nanoparticle-Based Label-Free Biosensors and Their Biomedical Applications. ChemBioChem 21, 576–600. https://doi.org/10.1002/cbic.201900566

Kenry, Geldert, A., Zhang, X., Zhang, H., Lim, C.T., 2016. Highly Sensitive and Selective Aptamer-Based Fluorescence Detection of a Malarial Biomarker Using Single-Layer MoS2 Nanosheets. ACS Sensors 1, 1315–1321. https://doi.org/10.1021/acssensors.6b00449

Khansili, N., Rattu, G., Krishna, P.M., 2018. Label-free optical biosensors for food and biological sensor applications. Sensors and Actuators, B: Chemical 265, 35–49. https://doi.org/10.1016/j.snb.2018.03.004

Ko, J., Jeong, B.G., Chang, J.H., Joung, J.F., Yoon, S.Y., Lee, D.C., Park, S., Huh, J., Yang, H., Bae, W.K., Jang, S.G., Bang, J., 2020. Chemically resistant and thermally stable quantum dots prepared by shell encapsulation with cross-linkable block copolymer ligands. NPG Asia Materials 12. https://doi.org/10.1038/s41427-020-0200-4

Kołątaj, K., Krajczewski, J., Kudelski, A., 2020. Plasmonic nanoparticles for environmental analysis. Environmental Chemistry Letters 18, 529–542. https://doi.org/10.1007/s10311-019-00962-1

Kumari, Y., Kaur, G., Kumar, Rajesh, Singh, S.K., Gulati, M., Khursheed, R., Clarisse, A., Gowthamarajan, K., Karri, V.V.S.N.R., Mahalingam, R., Ghosh, D., Awasthi, A., Kumar, Rajan, Yadav, A.K., Kapoor, B., Singh, P.K., Dua, K., Porwal, O., 2019. Gold nanoparticles: New routes across old boundaries. Advances in Colloid and Interface Science 274, 102037. https://doi.org/10.1016/j.cis.2019.102037

Lakowicz, J.R., 2006. Principles of Fluorescence Spectroscopy, Third. ed, Geofisica pura e applicata. Springer. https://doi.org/10.1007/BF02629943

Lee, E.H., Lim, H.J., Lee, S.D., Son, A., 2017. Highly Sensitive Detection of Bisphenol A by NanoAptamer Assay with Truncated Aptamer. ACS Applied Materials and Interfaces 9, 14889–14898. https://doi.org/10.1021/acsami.7b02377

Lee, E.S., Kim, G.B., Ryu, S.H., Kim, H., Yoo, H.H., Yoon, M.Y., Lee, J.W., Gye, M.C., Kim, Y.P., 2018. Fluorescing aptamer-gold nanosensors for enhanced sensitivity to bisphenol A. Sensors and Actuators, B: Chemical 260, 371–379. https://doi.org/10.1016/j.snb.2018.01.018

Lee, S., Park, K., Kim, K., Choi, K., Kwon, I.C., 2008. Activatable imaging probes with amplified fluorescent signals. Chemical Communications 4250–4260. https://doi.org/10.1039/b806854m

Li, C., Wei, C., 2017. DNA-templated silver nanocluster as a label-free fluorescent probe for the highly sensitive and selective detection of mercury ions. Sensors and Actuators, B: Chemical 242, 563–568. https://doi.org/10.1016/j.snb.2016.11.091

Li, D., Yuan, X., Li, C., Luo, Y., Jiang, Z., 2020. A novel fluorescence aptamer biosensor for trace Pb(II) based on gold-doped carbon dots and DNAzyme synergetic catalytic amplification. Journal of Luminescence 221, 117056. https://doi.org/10.1016/j.jlumin.2020.117056

Li, H., Yan, X., Lu, G., Su, X., 2018. Carbon dot-based bioplatform for dual colorimetric and fluorometric sensing of organophosphate pesticides. Sens Actuators B Chem 260, 563–570. https://doi.org/10.1016/j.snb.2017.12.170

Li, X., Tang, X., Chen, X., Qu, B., Lu, L., 2018. Label-free and enzyme-free fluorescent isocarbophos aptasensor based on MWCNTs and G-quadruplex. Talanta 188, 232–237. https://doi.org/10.1016/j.talanta.2018.05.092

Li, X., Yun, W., Guo, W., Zhang, W., Yang, L., 2019. Simple, one step and sensitive fluorescent nanoprobe for simultaneous detection of Pb2+ and Cu2+ based on pincer enzyme strand and signal amplification strategy. Sensors and Actuators, B: Chemical 301, 127170. https://doi.org/10.1016/j.snb.2019.127170

Li, Y., Yuan, M., Khan, A.J., Wang, L., Zhang, F., 2019. Peptide-gold nanocluster synthesis and intracellular Hg2+ sensing. Colloids and Surfaces A: Physicochemical and Engineering Aspects 579, 123666. https://doi.org/10.1016/j.colsurfa.2019.123666

Lin, B., Yu, Y., Li, R., Cao, Y., Guo, M., 2016. Turn-on sensor for quantification and imaging of acetamiprid residues based on quantum dots functionalized with aptamer. Sensors and Actuators, B: Chemical 229, 100–109. https://doi.org/10.1016/j.snb.2016.01.114

Liu, G., Jia, H., Li, N., Li, X., Yu, Z., Wang, J., Song, Y., 2019. High-fluorescent carbon dots (CDs) originated from China grass carp scales (CGCS) for effective detection of Hg(II) ions. Microchemical Journal 145, 718–728. https://doi.org/10.1016/j.microc.2018.11.044

Liu, M., Khan, A., Wang, Z., Liu, Y., Yang, G., Deng, Y., He, N., 2019. Aptasensors for pesticide detection. Biosens Bioelectron 130, 174–184. https://doi.org/10.1016/j.bios.2019.01.006

Liu, M., Liu, T., Li, Y., Xu, H., Zheng, B., Wang, D., Du, J., Xiao, D., 2015. A FRET chemsensor based on graphene quantum dots for detecting and intracellular imaging of Hg2+. Talanta 143, 442–449. https://doi.org/10.1016/j.talanta.2015.05.023

Liu, M.L., Chen, B. Bin, Li, C.M., Huang, C.Z., 2019. Carbon dots: Synthesis, formation mechanism, fluorescence origin and sensing applications. Green Chemistry 21, 449–471. https://doi.org/10.1039/c8gc02736f

Liu, N., Tang, M., 2020. Toxicity of different types of quantum dots to mammalian cells in vitro : An update review. Journal of Hazardous Materials 399, 122606. https://doi.org/10.1016/j.jhazmat.2020.122606

Liu, T., Wang, W., Jian, D., Li, J., Ding, H., Yi, D., Liu, F., Wang, S., 2019. Quantitative remote and on-site Hg2+ detection using the handheld smartphone based optical fiber fluorescence sensor (SOFFS). Sensors and Actuators, B: Chemical 301, 127168. https://doi.org/10.1016/j.snb.2019.127168

Londoño Franco, L.F., Londoño Muñoz, P.T., Muñoz Garcia, F.G., 2016. Los Riesgos De Los Metales Pesados En La Salud Humana Y Animal. Biotecnoloía en el Sector Agropecuario y Agroindustrial 14, 145. https://doi.org/10.18684/BSAA(14)145-153

Luo, D., Zhou, T., Tao, Y., Feng, Y., Shen, X., Mei, S., 2016. Exposure to organochlorine pesticides and non-Hodgkin lymphoma: A meta-analysis of observational studies. Sci Rep 6, 1–11. https://doi.org/10.1038/srep25768

Machado, S.C., Martins, I., 2018. Risk assessment of occupational pesticide exposure: Use of endpoints and surrogates. Regulatory Toxicology and Pharmacology 98, 276–283. https://doi.org/10.1016/j.yrtph.2018.08.008

Majdinasab, M., Mitsubayashi, K., Marty, J.L., 2019. Optical and Electrochemical Sensors and Biosensors for the Detection of Quinolones. Trends in Biotechnology 37, 898–915. https://doi.org/10.1016/j.tibtech.2019.01.004

Manetsch, R., Krasinski, A., Radic, Z., Raushel, J., Taylor, P., Sharpless, K.B., Kolb, H.C., 2004. In situ click chemistry: enzyme inhibitors made to their own specifications. J. Am. Chem. Soc. 126, 12809–12818.

Marcoux, M.A., Matias, M., Olivier, F., Keck, G., 2013. Review and prospect of emerging contaminants in waste - Key issues and challenges linked to their presence in waste treatment schemes: General aspects and focus on nanoparticles. Waste Management 33, 2147–2156. https://doi.org/10.1016/j.wasman.2013.06.022

Marican, A., Durán-Lara, E.F., 2018. A review on pesticide removal through different processes. Environmental Science and Pollution Research 25, 2051–2064. https://doi.org/10.1007/s11356-017-0796-2

Marieeswaran, M., Panneerselvam, P., 2020. A magnetic nanoscale metal-organic framework (mnmof) as a viable fluorescence quencher material for ssdna and for the detection of mercury ions: Via a novel quenching-quenching mechanism. RSC Advances 10, 3705–3714. https://doi.org/10.1039/c9ra08274c

Maruthupandi, M., Thiruppathi, D., Vasimalai, N., 2020. One minute synthesis of green fluorescent copper nanocluster: The preparation of smartphone aided paper-based kit for on-site monitoring of nanomolar level mercury and sulfide ions in environmental samples. Journal of Hazardous Materials 392, 122294. https://doi.org/10.1016/j.jhazmat.2020.122294

Mazur, C.S., Marchitti, S.A., Zastre, J., 2015. P-glycoprotein inhibition by the agricultural pesticide propiconazole and its hydroxylated metabolites: Implications for pesticide-drug interactions. Toxicology Letters 232, 37–45. https://doi.org/10.1016/j.toxlet.2014.09.020

McGhee, C.E., Loh, K.Y., Lu, Y., 2017. DNAzyme sensors for detection of metal ions in the environment and imaging them in living cells. Current Opinion in Biotechnology 45, 191–201. https://doi.org/10.1016/j.copbio.2017.03.002

Mei, J., Liao, T., Kou, L., Sun, Z., 2017. Two-Dimensional Metal Oxide Nanomaterials for Next-Generation Rechargeable Batteries. Advanced Materials 29, 1–25. https://doi.org/10.1002/adma.201700176

Mirzaei, A., Chen, Z., Haghighat, F., Yerushalmi, L., 2016. Removal of pharmaceuticals and endocrine disrupting compounds from water by zinc oxide-based photocatalytic degradation: A review. Sustainable Cities and Society 27, 407–418. https://doi.org/10.1016/j.scs.2016.08.004

Molaei, M.J., 2020. Principles, mechanisms, and application of carbon quantum dots in sensors: a review. Analytical Methods 12, 1266–1287. https://doi.org/10.1039/c9ay02696g

Neema, P.M., Tomy, A.M., Cyriac, J., 2020. Chemical sensor platforms based on fluorescence resonance energy transfer (FRET) and 2D materials. TrAC - Trends in Analytical Chemistry 124, 115797. https://doi.org/10.1016/j.trac.2019.115797

Nsibande, S.A., Forbes, P.B.C., 2016. Fluorescence detection of pesticides using quantum dot materials – A review. Analytica Chimica Acta 945, 9–22. https://doi.org/10.1016/j.aca.2016.10.002

Odeh, F., Nsairat, H., Alshaer, W., Ismail, M.A., Esawi, E., Qaqish, B., Bawab, A. Al, Ismail, S.I., 2020. Aptamers chemistry: Chemical modifications and conjugation strategies. Molecules 25. https://doi.org/10.3390/molecules25010003

Oh, S.M., Patil, S.B., Jin, X., Hwang, S.J., 2018. Recent Applications of 2D Inorganic Nanosheets for Emerging Energy Storage System. Chemistry - A European Journal 24, 4757–4773. https://doi.org/10.1002/chem.201704284

Ong, T.T.X., Blanch, E.W., Jones, O.A.H., 2020. Surface Enhanced Raman Spectroscopy in environmental analysis, monitoring and assessment. Science of the Total Environment 720, 137601. https://doi.org/10.1016/j.scitotenv.2020.137601

Pandey, S., Bodas, D., 2020. High-quality quantum dots for multiplexed bioimaging: A critical review. Advances in Colloid and Interface Science 278, 102137. https://doi.org/10.1016/j.cis.2020.102137

Patel, N., Khan, Z.A., Shahane, S., Rai, D., Chauhan, D., Kant, C., Chaudhary, V.K., 2020. Emerging pollutants in aquatic environment: Source, effect, and challenges in biomonitoring and bioremediation- A review. Pollution 6, 99–113. https://doi.org/10.22059/POLL.2019.285116.646

Paul, K.C., Chuang, Y.H., Cockburn, M., Bronstein, J.M., Horvath, S., Ritz, B., 2018. Organophosphate pesticide exposure and differential genome-wide DNA methylation. Science of the Total Environment 645, 1135–1143. https://doi.org/10.1016/j.scitotenv.2018.07.143

Pehlivan, Z.S., Torabfam, M., Kurt, H., Ow-Yang, C., Hildebrandt, N., Yüce, M., 2019. Aptamer and nanomaterial based FRET biosensors: a review on recent advances (2014–2019). Microchimica Acta 186. https://doi.org/10.1007/s00604-019-3659-3

Pelle, F. Della, Compagnone, D., 2018. Nanomaterial-based sensing and biosensing of phenolic compounds and related antioxidant capacity in food. Sensors (Switzerland) 18. https://doi.org/10.3390/s18020462

Peng, T., Dai, X., Zhang, Y., Zheng, P., Wang, J., Wang, S., Wang, Z., Zeng, Y., Li, J., Jiang, H., 2020. Facile synthesis of SiO2@MnO2 nanocomposites and their applications on platforms for sensitively sensing antibiotics and glutathione. Sensors and Actuators, B: Chemical 304, 127314. https://doi.org/10.1016/j.snb.2019.127314

Plácido, J., Bustamante-López, S., Meissner, K.E., Kelly, D.E., Kelly, S.L., 2019a. Comparative study of the characteristics and fluorescent properties of three different biochar derived carbonaceous nanomaterials for bioimaging and heavy metal ions sensing. Fuel Processing Technology 196, 106163. https://doi.org/10.1016/j.fuproc.2019.106163

Plácido, J., Bustamante-López, S., Meissner, K.E., Kelly, D.E., Kelly, S.L., 2019b. Microalgae biochar-derived carbon dots and their application in heavy metal sensing in aqueous systems. Science of the Total Environment 656, 531–539. https://doi.org/10.1016/j.scitotenv.2018.11.393

Prakash, O., Talat, M., Hasan, S.H., Pandey, R.K., 2008. Enzymatic detection of mercuric ions in ground-water from vegetable wastes by immobilizing pumpkin (Cucumis melo) urease in calcium alginate beads. Bioresource Technology 99, 4524–4528. https://doi.org/10.1016/j.biortech.2007.08.073

Pundir, C.S., Chauhan, N., 2012. Acetylcholinesterase inhibition-based biosensors for pesticide determination: A review. Analytical Biochemistry 429, 19–31. https://doi.org/10.1016/j.ab.2012.06.025

Qian, X., Han, X., Yu, L., Xu, T., Chen, Y., 2020. Manganese-Based Functional Nanoplatforms: Nanosynthetic Construction, Physiochemical Property, and Theranostic Applicability. Advanced Functional Materials 30, 1–40. https://doi.org/10.1002/adfm.201907066

Rajabnejad, S.H., Badibostan, H., Verdian, A., Karimi, G.R., Fooladi, E., Feizy, J., 2020. Aptasensors as promising new tools in bisphenol A detection - An invisible pollution in food and environment. Microchemical Journal 155, 104722. https://doi.org/10.1016/j.microc.2020.104722

Rani, M., Shanker, U., 2018. Degradation of traditional and new emerging pesticides in water by nanomaterials: recent trends and future recommendations. International Journal of Environmental Science and Technology 15, 1347–1380. https://doi.org/10.1007/s13762-017-1512-y

Ravikumar, A., Panneerselvam, P., Radhakrishnan, K., Christus, A.A.B., Sivanesan, S., 2018. MoS 2 nanosheets as an effective fluorescent quencher for successive detection of arsenic ions in aqueous system. Applied Surface Science 449, 31–38. https://doi.org/10.1016/j.apsusc.2017.12.098

Rodenas, T., 2019. Introduction, in: Metal-Organic Frameworks (MOFs) for Environmental Applications. pp. 1–4. https://doi.org/https://doi.org/10.1007/978-3-642-40872-4_375-1

Rodenas, T., Luz, I., Prieto, G., Seoane, B., Miro, H., Corma, A., Kapteijn, F., Llabrés I Xamena, F.X., Gascon, J., 2015. Metal-organic framework nanosheets in polymer composite materials for gas separation. Nature Materials 14, 48–55. https://doi.org/10.1038/nmat4113

Rodriguez, D.C., Carvajal, S., Peñuela, G., 2013. Effect of chlorpyrifos on the inhibitio of the enzyme acetylcholinesterase by cross-linking in water suppky samples and milk from dairy cattle. Talanta 1–7.

Safarpour, M., Arefi-Oskoui, S., Khataee, A., 2020. A review on two-dimensional metal oxide and metal hydroxide nanosheets for modification of polymeric membranes. Journal of Industrial and Engineering Chemistry 82, 31–41. https://doi.org/10.1016/j.jiec.2019.11.002

Sharma, S., Umar, A., Sood, S., Mehta, S.K., Kansal, S.K., 2018. Photoluminescent C-dots: An overview on the recent development in the synthesis, physiochemical properties and potential applications. Journal of Alloys and Compounds 748, 818–853. https://doi.org/10.1016/j.jallcom.2018.03.001

Shtenberg, G., Massad-Ivanir, N., Segal, E., 2015. Detection of trace heavy metal ions in water by nanostructured porous Si biosensors. Analyst 140, 4507–4514. https://doi.org/10.1039/c5an00248f

Singh, S., Nigam, P., Pednekar, A., Mukherjee, S., Mishra, A., 2020. Carbon quantum dots functionalized agarose gel matrix for in solution detection of nonylphenol. Environmental Technology (United Kingdom) 41, 322–328. https://doi.org/10.1080/09593330.2018.1498133

Singh, V., Joung, D., Zhai, L., Das, S., Khondaker, S.I., Seal, S., 2011. Graphene based materials: Past, present and future. Progress in Materials Science 56, 1178–1271. https://doi.org/10.1016/j.pmatsci.2011.03.003

Sousa, J.C.G., Ribeiro, A.R., Barbosa, M.O., Pereira, M.F.R., Silva, A.M.T., 2018. A review on environmental monitoring of water organic pollutants identified by EU guidelines. Journal of Hazardous Materials 344, 146–162. https://doi.org/10.1016/j.jhazmat.2017.09.058

Stahel, W.R., 2016. The circular economy. Nature. https://doi.org/10.1038/531435a

Stock, N., Biswas, S., 2012. Synthesis of metal-organic frameworks (MOFs): Routes to various MOF topologies, morphologies, and composites. Chemical Reviews. https://doi.org/10.1021/cr200304e

Sultan, I.A., 2014. Detection of enrofloxacin residue in livers of livestock animals obtained from a slaughterhouse in Mosul city. Journal of Veterinary Science and Technology 5, 2–4. https://doi.org/10.4172/2157-7579.1000168

Swierczewska, M., Lee, S., Chen, X., 2011. The design and application of fluorophore-gold nanoparticle activatable probes. Physical Chemistry Chemical Physics 13, 9929–9941. https://doi.org/10.1039/c0cp02967j

Tao, H., Fan, Q., Ma, T., Liu, S., Gysling, H., Texter, J., Guo, F., Sun, Z., 2020. Two-dimensional materials for energy conversion and storage. Progress in Materials Science 111, 100637. https://doi.org/10.1016/j.pmatsci.2020.100637

Tian, H., Xu, X., Qu, J., Li, H., Hu, Y., Huang, L., 2020. Biodegradation of phenolic compounds in high saline wastewater by biofilms adhering on aerated membranes. Journal of Hazardous Materials 392, 122463. https://doi.org/10.1016/j.jhazmat.2020.122463

UN, n.d. Objetivos de desarrollo sostenible [WWW Document]. URL https://www.undp.org/content/undp/es/home/sustainable-development-goals.html (accessed 4.23.20).
United States environmental protection agency, 2016. Toxic Substances Control Act. USA.
Vasimalai, N., Fernández-Argüelles, M.T., Espiña, B., 2018. Detection of Sulfide Using Mercapto Tetrazine-Protected Fluorescent Gold Nanodots: Preparation of Paper-Based Testing Kit for On-Site Monitoring. ACS Applied Materials and Interfaces 10, 1634–1645. https://doi.org/10.1021/acsami.7b11769
Wackerlig, J., Schirhagl, R., 2016. Applications of Molecularly Imprinted Polymer Nanoparticles and Their Advances toward Industrial Use: A Review. Analytical Chemistry 88, 250–261. https://doi.org/10.1021/acs.analchem.5b03804
Wang, Jinlong, Lu, T., Hu, Y., Wang, X., Wu, Y., 2020. A label-free and carbon dots based fluorescent aptasensor for the detection of kanamycin in milk. Spectrochimica Acta - Part A: Molecular and Biomolecular Spectroscopy 226, 117651. https://doi.org/10.1016/j.saa.2019.117651
Wang, J., Qiu, F., Wu, H., Li, X., Zhang, T., Niu, X., Yang, D., Pan, J., Xu, J., 2017. Fabrication of fl uorescent carbon dots-linked isophorone diisocyanate and β -cyclodextrin for detection of chromium ions. Spectrochimica Acta Part A: Molecular and Biomolecular Spectroscopy 179, 163–170. https://doi.org/10.1016/j.saa.2017.02.031
Wang, Jiaqi, Sui, Q., Lyu, S., Huang, Y., Huang, S., Wang, B., Xu, D., Zhao, W., Kong, M., Zhang, Y., Hou, S., Yu, G., 2020. Science of the Total Environment Source apportionment of phenolic compounds based on a simultaneous monitoring of surface water and emission sources : A case study in a typical region adjacent to Taihu Lake watershed. Science of the Total Environment 722, 137946. https://doi.org/10.1016/j.scitotenv.2020.137946
Wang, J., Wu, Y., Zhou, P., Yang, W., Tao, H., Qiu, S., Feng, C., 2018. A novel fluorescent aptasensor for ultrasensitive and selective detection of acetamiprid pesticide based on the inner filter effect between gold nanoparticles and carbon dots. The Analyst. https://doi.org/10.1039/C8AN01166D
Wang, P., Zhao, L., Shou, H., Wang, J., Zheng, P., Jia, K., Liu, X., 2016. Dual-emitting fluorescent chemosensor based on resonance energy transfer from poly(arylene ether nitrile) to gold nanoclusters for mercury detection. Sensors and Actuators, B: Chemical 230, 337–344. https://doi.org/10.1016/j.snb.2016.02.041
Wang, Q.H., Kalantar-Zadeh, K., Kis, A., Coleman, J.N., Strano, M.S., 2012. Electronics and optoelectronics of two-dimensional transition metal dichalcogenides. Nature Nanotechnology 7, 699–712. https://doi.org/10.1038/nnano.2012.193
Wu, F., Ye, J., Cao, Y., Wang, Z., Miao, T., Shi, Q., 2020. Recent advances in fluorescence sensors based on DNA–MOF hybrids. Luminescence 43–47. https://doi.org/10.1002/bio.3790
Wu, M., Hou, P., Dong, L., Cai, L., Chen, Z., Zhao, M., Li, J., 2019. Manganese dioxide nanosheets: From preparation to biomedical applications. International Journal of Nanomedicine 14, 4781–4800. https://doi.org/10.2147/IJN.S207666
Wu, X., Wang, P., Hou, S., Wu, P., Xue, J., 2019. Fluorescence sensor for facile and visual detection of organophosphorus pesticides using AIE fluorogens-SiO2-MnO2 sandwich nanocomposites. Talanta 198, 8–14. https://doi.org/10.1016/j.talanta.2019.01.082
Xu, M., Obodo, D., Yadavalli, V.K., 2018. The design, fabrication, and applications of flexible biosensing devices – a review. Biosensors and Bioelectronics 124–125, 96–114. https://doi.org/10.1016/j.bios.2018.10.019
Xu, X., Ray, R., Gu, Y., Ploehn, H.J., Gearheart, L., Raker, K., Scrivens, W.A., 2004. Electrophoretic analysis and purification of fluorescent single-walled carbon nanotube fragments. Journal of the American Chemical Society 126, 12736–12737. https://doi.org/10.1021/ja040082h
Xu, X.Y., Yan, B., Lian, X., 2018. Wearable glove sensor for non-invasive organophosphorus pesticide detection based on a double-signal fluorescence strategy. Nanoscale 10, 13722–13729. https://doi.org/10.1039/c8nr03352h

Xu, Y., Chen, X., Chai, R., Xing, C., Li, H., Yin, X.B., 2016. A magnetic/fluorometric bimodal sensor based on a carbon dots-MnO2 platform for glutathione detection. Nanoscale 8, 13414–13421. https://doi.org/10.1039/c6nr03129c

Yan, X., Li, H., Su, X., 2018. Review of optical sensors for pesticides. TrAC Trends in Analytical Chemistry 103, 1–20. https://doi.org/10.1016/J.TRAC.2018.03.004

Yang, Q., Zhou, L., Wu, Y.X., Zhang, K., Cao, Y., Zhou, Y., Wu, D., Hu, F., Gan, N., 2018. A two dimensional metal–organic framework nanosheets-based fluorescence resonance energy transfer aptasensor with circular strand-replacement DNA polymerization target-triggered amplification strategy for homogenous detection of antibiotics. Analytica Chimica Acta 1020, 1–8. https://doi.org/10.1016/j.aca.2018.02.058

Youn, H., Lee, K., Her, J., Jeon, J., Mok, J., So, J. in, Shin, S., Ban, C., 2019. Aptasensor for multiplex detection of antibiotics based on FRET strategy combined with aptamer/graphene oxide complex. Scientific Reports 9, 1–9. https://doi.org/10.1038/s41598-019-44051-3

Yun, W., Wu, H., Liu, X., Fu, M., Jiang, J., Du, Y., Yang, L., Huang, Y., 2017. Simultaneous fluorescent detection of multiple metal ions based on the DNAzymes and graphene oxide. Analytica Chimica Acta 986, 115–121. https://doi.org/10.1016/j.aca.2017.07.015

Yuphintharakun, N., Nurerk, P., Chullasat, K., Kanatharana, P., Davis, F., Sooksawat, D., Bunkoed, O., 2018. A nanocomposite optosensor containing carboxylic functionalized multiwall carbon nanotubes and quantum dots incorporated into a molecularly imprinted polymer for highly selective and sensitive detection of ciprofloxacin. Spectrochimica Acta - Part A: Molecular and Biomolecular Spectroscopy 201, 382–391. https://doi.org/10.1016/j.saa.2018.05.034

Zhan, Y., Yang, J., Guo, L., Luo, F., Qiu, B., Hong, G., Lin, Z., 2019. Targets regulated formation of boron nitride quantum dots – Gold nanoparticles nanocomposites for ultrasensitive detection of acetylcholinesterase activity and its inhibitors. Sensors and Actuators, B: Chemical 279, 61–68. https://doi.org/10.1016/j.snb.2018.09.097

Zhang, W., Asiri, A.M., Liu, D., Du, D., Lin, Y., 2014. Nanomaterial-based biosensors for environmental and biological monitoring of organophosphorus pesticides and nerve agents. TrAC - Trends in Analytical Chemistry 54, 1–10. https://doi.org/10.1016/j.trac.2013.10.007

Zhang, X.-B., Kong, R.-M., Lu, Y., 2011. Metal Ion Sensors Based on DNAzymes and Related DNA Molecules. Annu Rev Anal Chem 4, 1–7. https://doi.org/10.1038/jid.2014.371

Zhang, Y., Zheng, B., Zhu, C., Zhang, X., Tan, C., Li, H., Chen, B., Yang, J., Chen, J., Huang, Y., Wang, L., Zhang, H., 2015. Single-layer transition metal dichalcogenide nanosheet-based nanosensors for rapid, sensitive, and multiplexed detection of DNA. Advanced Materials 27, 935–939. https://doi.org/10.1002/adma.201404568

Zhao, F., Wu, J., Ying, Y., She, Y., Wang, J., Ping, J., 2018. Carbon nanomaterial-enabled pesticide biosensors: Design strategy, biosensing mechanism, and practical application. https://doi.org/10.1016/j.trac.2018.06.017

4. Highly sensitive fluorescent biosensor based on Acetylcholinesterase and carbon dots-graphene oxide quenching test for analytical and commercial organophosphate pesticide detection.

Abstract

Chlorpyrifos formulations are the most used in Colombia and other countries for crop protection, and their presence has been proven in many water sources. The application of nanomaterials, including carbon quantum dots (CD), can significantly improve the performance of optical biosensors for quick and accurate detection of these pesticides. In this work, naturally fluorescent and non-toxic CD were conjugated with acetylcholinesterase (AChE) as a bioreceptor, to produce a fluorescent biosensor. This system was modulated with graphene oxide (GO), showing a fluorescence recovery in the presence of the pesticide. The biosensor was evaluated for the detection of pure chlorpyrifos (CPF), profenofos (PF), and a commercial formulation called Lorsban®. A limit of detection (LOD) as low as 0.14 ppb and 2.05 ppb for chlorpyrifos and Lorsban® respectively was obtained. Profenofos did not show any recovery with this system at the evaluated concentrations. The system also showed a good selectivity in the presence of proteins (BSA) and other organic substances (Glucose) usually present in drinking water. The specificity was also evaluated against cypermethrin and methomyl commercial formulations showing minimal interference. To the best of our knowledge, this is one of the few works reporting the detection of commercial pesticide formulations with promising results.

Keywords: Carbon dots, nanomaterial, fluorescent biosensor, pesticide, chlorpyrifos, enzyme.

Published in:
Frontiers in Environmental Science. Elsevier
Date: March 14, 2022
Cite as:
Gaviria, M. I., Barrientos, K., Arango, J. P., Cano, J. B., & Peñuela, G. A. (2022). Highly sensitive fluorescent biosensor based on Acetylcholinesterase and carbon dots-graphene oxide quenching test for analytical and commercial organophosphate pesticide detection. *Frontiers in Environmental Science*, *10*, 1–13. https://doi.org/10.3389/FENVS.2022.825112

4.1. Introduction

The intense use of pesticides has been a common practice for almost 60 years in the agricultural value chain (Vinotha Alex & Mukherjee, 2021). In this way, it is possible to find pesticides with a target in rodents, insects, plants, or microorganisms that can compromise food, wood, or other raw material production. According to the Food and Agriculture Organization (FAO) in 2018, the world consumption of pesticides reached 4 million tons, with Asia at first place followed by the USA and Latin America (FAO, 2018). Humans can get exposed to pesticides in different ways. For instance, farmers in developing countries, like Colombia, are one of the main groups exposed, but also workers of the production and transportation of the pesticide. Furthermore, the public in general is exposed through the consumption of food (fruits and vegetables) but usually in lower amounts. Pesticides could be on water sources too, thanks to runoff processes. This exposure to pesticides is related to serious diseases, like non-Hodgkin lymphoma (Luo et al., 2016), Parkinson´s disease (Mostafalou & Abdollahi, 2018) as well as respiratory and reproductive disorders (Ramírez & Lacasaña, 2001). Moreover, some pesticides can cause oxidative stress in the cell, leading to cytotoxic and genotoxic effects (Ubaid ur Rahman et al., 2021).

Organophosphate pesticides (OP) are the most used insecticides worldwide, especially after organochlorine pesticides were prohibited in the '70s due to their high environmental persistence and toxicity (Sidhu et al., 2019). OP exhibits neurotoxicity because they can block the acetylcholinesterase enzyme (AChE) irreversibly (Vinotha Alex & Mukherjee, 2021). That blockage causes the accumulation of acetylcholine (ACh), a key neuro-transmissor for the synaptic process in the neuro-muscular interface (Sidhu et al., 2019). Specifically, the effects of ACh accumulation are the hyperstimulation of muscarinic and nicotinic receptors (Jokanović, 2018), with intoxication symptoms such as sweating, miosis, and diarrhea. OP acute exposure can cause death while chronic exposure causes nervous, reproductive, and respiratory affections even more than 30 years after exposure (King & Aaron, 2015). Among OP, Chlorpyrifos (CPF) is the main active principle used in a wide range of crops, and it has a relatively low persistence and low toxicity. However, CPF and CPF-oxon as common bioactive products, block AChE (Ubaid ur Rahman et al., 2021). EPA recently banned CPF (august 2021) so is still being used in developing countries under the commercial names of Lorsban, Dursban, Equity, Suscon, Empire20, and Whitmire PT270. On the other hand, Profenofos (PF) is an OP widely used in agriculture. The presence of PF in the biological system has gained importance due to bioaccumulation in the food chain (Mishra et al., 2015).

For OP detection, robust techniques are used such as chromatography (HPLC, HPTLC, LC/MS, GC/μECD, GC/MS), spectrophotometry, and FT-Raman spectroscopy (Talari et al., 2021). Those methods require pretreatment of samples from natural sources such as rivers, which means that analysis times are not very short and an increase its cost [13]. In this context, biosensors have become promising tools for rapid and effective OP detection. The interest in biosensors for OP detection is a growing research area because of their ease of handling, the low-cost potential of their components, and the possibility of real-time quantification (Gaviria-Arroyave et al., 2020). Biosensors can act as alarms when the water enters the water treatment plants for human

consumption with a pesticide. Once the alarm is made, the presence of the pesticide can be confirmed with chromatographic techniques.

In recent years, optical biosensors based on nanomaterials have been developed with lower detection limits and greater stability. The application of nanomaterials, including Carbon Dots (CD), can significantly improve the performance of the systems. CD are zero-dimension quasi-spherical nanoparticles, composed primarily of carbon and oxygen, usually with sizes below 10 nm (Abdul et al., 2019; Campuzano et al., 2019). CDs have gained a lot of attention because they have optoelectronic properties like quantum dots, especially when it comes to fluorescence. CD, unlike quantum dots, have excellent biocompatibility (Liu et al., 2019).

To promote the real application of biosensors, their sensitivity and specificity must be improved, as well as their performance tested in conditions close to fieldwork. In this work, we investigate how CD can significantly improve the performance of optical biosensors. We developed a biosensor to detect chlorpyrifos and profenofos in water. The system is based on AChE as a biomediator, CD acting as a fluorescent transductor, and graphene oxide (GO) as a quenching agent. The CD were synthesized by our laboratory in previous works (Barrientos, Gaviria, Arango, Londoño, et al., 2021) from African-oil palm biochar. The biosensor was evaluated under different concentrations of pure pesticides (chlorpyrifos and profenofos) and commercial pesticides (Lorsban®), obtaining a limit of detection (LOD) as low as 0.14 ppb and 2.05 ppb for chlorpyrifos and Lorsban® respectively. Profenofos did not show any recovery with this system at the evaluated concentrations. The system also shows a good selectivity against proteins (BSA) and other organic substances (glucose) usually present in drinking water, even in tests with tap water. The specificity was also evaluated against two types of pesticides: cypermethrin (pyrethroid type) and methomyl (carbamate type), showing expected behavior with a slight system response with cypermethrin and a marked response with methomyl. To the best of our knowledge, it is one of the few works where the performance of the system is tested against residues of the commercial formulation and not only using pure pesticides. The positive results allow progress in the integration of nanomaterials in the development of biosensors, as well as advance in the commercial projection of these systems to protect the health of rural communities.

4.2. Experimental section

Chemical used

All chemicals were analytical grade. Acetone and acetonitrile were bought from PanReac AppliChem® and used as received. Commercial solutions of chlorpyrifos (Lorsban®), methomyl (Lannate® 40), and cypermethrin (Invetrina® 200 EC) were bought from a local distributor, and dilutions were made using double deionized water. For conjugation steps, EDC (1-ethyl-3-[3-dimethylaminopropyl]carbodiimide), NHS (N-hydroxysuccinimide), and 2-mercaptoethanol (ME) were bought from Thermo Fisher. Single-layered graphene oxide (GO) was purchased from ACS material. Analytical standards of Chlorpyrifos (CPF) and profenofos (PF), as well as acetylcholinesterase (AChE) from Electrophorus electricus, Acetylthiocholine (ACTh), and DTNB

(5,5'-dithio-bis-(2-nitrobenzoic acid)), were bought from Merck. All tests were carried out in triplicates. Carbon dots (CD) were synthesized from African-oil palm biochar (Elaeis guineensis) according to our previous work (Barrientos, Gaviria, Arango, Londoño, et al., 2021). Double deionized water was used through all the experiments (Milli-Q ultrapure water system with a 0.22 µm filter, Merck Millipore).

Conjugation procedure

The covalent conjugation technique was used, through carbodiimide chemistry following the protocol described by (Thermo scientific, n.d.). EDC was used in the presence of NHS, to obtain an amide bond between carboxylic acids from the CD and primary amines present in the AChE. Briefly, 500 ppm of CD water solution were put in contact with 0.05 M of EDC and 0.1 M of NHS and let them react for 15 minutes. Then, ME (0.5 M final concentration) was added to stop the activation of the carboxylic groups, followed by 2 h dialysis (3.5 kDa, 4 water changes). Before the addition of the AChE, the pH was adjusted to 7.45 with sodium bicarbonate. An appropriate amount of AChE (final concentration of 5 U mL^{-1}) was added and left for the reaction for 2 h. Finally, the remaining carboxylic active sites of the CD must be blocked to prevent non-specific detection. For that, Ethanolamine (20 mM final concentration) in Phosphate buffer pH 7.45 was added, followed by 30 minutes of dialysis (3.5 kDa, 2 water changes). The AChE-CD conjugates were stored under 4°C until detection assays and remained active for at least 1 week.

Enzymatic activity

The enzymatic activity of the free and conjugated enzyme was evaluated following the protocol described by Ellman (Ellman et al., 1961). In typical free AChE activity evaluation, 25 µL of DTNB (0.01 M), 25 µL of ACTh (2 mM) and 10 µL of AChE with different activity were mixed with 40 µL of phosphate buffer (0.1 M, pH 8). For the conjugated AChE the same reaction mixture was used but added 50 uL of the sample instead of pure AChE and the phosphate buffer. The solutions were mixed completely and the formation of 2-nitro-5-thiobenzoic acid (TNB) as reaction product (416 nm) was monitored at 37 °C for 20 minutes to determine the enzymatic activity. For preliminary Lorsban® evaluation, 25 µL of the pesticide at different concentrations was mixed with 25 µL of AChE (100 U mL^{-1}) and subsequently incubated at 37°C for 30 minutes. Then, 50 µL of ACTh (5 mM) and 50 µL of phosphate buffer (0.1 M, pH 8) were added and the mixture was incubated again at 37°C for 25 minutes. Finally, 150 µL of DTNB and 200 µL of Mili Q water were added and vigorously mixed for 5 minutes. Absorbance spectra were taken between (300-800 nm) and the peak for TNB formation (416 nm) was monitored.

Characterization techniques

UV-Vis and fluorescence measurements (spectrum and punctual) were done in a Varioskan Lux (Thermo scientific, SkanIt Software 4.1) on a 200 µL working volume microplates (Falcon™ non-treated black 96-well) at 25°C with 1 nm optical step. The stability of the AChE-CD conjugates were investigated through Z potential techniques on a Nanoplus-3. The measurement was performed

using 0.2 µm filtered solutions in a DTS1070 cell, with water as a dispersant (Refractive Index: 1.330). The shape and size of the AChE-CD conjugates were taken using High-Resolution Transmission Electronical Microscopy (HR-TEM) on an FEI-Tecnai F20 Super Twin TMP.

Pesticide detection

Chlorpyrifos and Lorsban® were evaluated in a range between 0 and 0.1 ppm, while profenofos was evaluated between 0 and 10 ppm. For this purpose, different dilutions were made in Milli-Q water. For the detection assay, 890 µL of the conjugate and 10 µL of graphene oxide (100 ppm GO final concentration) were vigorously mixed in different vials. After 15 minutes, 100 µL of the appropriate dilution of the pesticide were added to reach a desired final concentration. The solution was vigorously mixed and let sit for another 15 minutes until fluorescence recovery analysis. The amount of the pesticide dilution was replaced by Milli-Q water for the control.

The relativity fluorescence recovery of CD at emission and excitation wavelength of 420 nm and 320 nm (respectively), against increasing concentration of the evaluated pesticides were plotted. Higher concentrations of chlorpyrifos, profenofos, and Lorsban® cause higher fluorescence recovery. The limits of detection (LOD) and quantification (LOQ) of the system were calculated based on the parameters of the analytical curve in the linear range (from the semilog plot), using the following equations adapted from (Khoris et al., 2021):

$$LOD \leq e^{\frac{F_0+3.3\sigma-c}{s}} \qquad \text{Equation 1}$$

$$LOQ \leq e^{\frac{F_0+10\sigma-c}{s}} \qquad \text{Equation 2}$$

With F0 σ, c and s are the fluorescence signal of the blank, the standard deviations of the blank, the y-intercept, and the slope of the calibration curve, respectively.

All experiments were treated and analyzed in triplicate. For LOD calculations, a one-way ANOVA was performed using R-studio software and $p \leq 0.05$ was considered as statistically significant.

4.3. Results and discussion

Conjugate characterization

CD were synthesized from African-oil palm (*Elais guinensis*) and characterized in our previous work (Barrientos, Gaviria, Arango, Londoño, et al., 2021). The CD have plenty of carboxylic groups and they had a maximum emission peak at λ= 420 nm under excitation of λ=320 nm. The CD showed a brownish-yellow color under daylight and blue emission under ultraviolet light (insert in Figure

4-3A). They were stable in an aqueous solution for several weeks without losing their optical properties. Figure 4-1 shows the kinetic curves for the activity of the conjugate of CD and AChE, at two enzymatic concentrations (1 and 5 U mL^{-1}) and a fixed concentration of the substrate ACTh of 0.5 mM. Based on literature review and previous works done by our research group (Betancur et al., 2018; Rodriguez et al., 2013), preliminary assays with free AChE between 1 and 5 U mL^{-1} and ACTh between 0.25 and 0.75 mM were done to optimize enzymatic and substrate expenditure. AChE concentration was the only significant factor (p-value < 0.001, n= 4). We found that even though for the free enzyme the maximum activity is obtained for the concentration of 1 U mL^{-1} (data not showed), in the case of the conjugate the best performance is obtained at 5 U mL^{-1} with a Vmax of 35.88 $\mu molmL^{-1}min^{-1}$, versus 15.14 $\mu molmL^{-1}min^{-1}$. Additionally, the conjugate at 5 U mL^{-1} retains 87% of the activity compared to the free enzyme. This phenomenon can be explained by the enzyme-substrate affinity constant evaluated for the free enzyme since when the CD are conjugated with AChE it is possible that the active site is affected, or its environment is modified reducing the affinity of acetylcholine at lower amounts of enzyme. Furthermore, some authors report the inhibition of AChE activity by some CD, especially those with antioxidant properties (Suner et al., 2021). The insert in Figure 2B shows the decreasing of the absorbance intensity at 416 nm, indicating a lineal inhibition of the free AChE at 5 U mL^{-1} in the presence of Lorsban® for a range between 0 and 500 ppb. This range of concentrations suggests a good approach for the evaluation of the biosensor. For further assays, a fixed enzyme and substrate concentration of 5 U mL^{-1} and 0.5 mM were used, respectively.

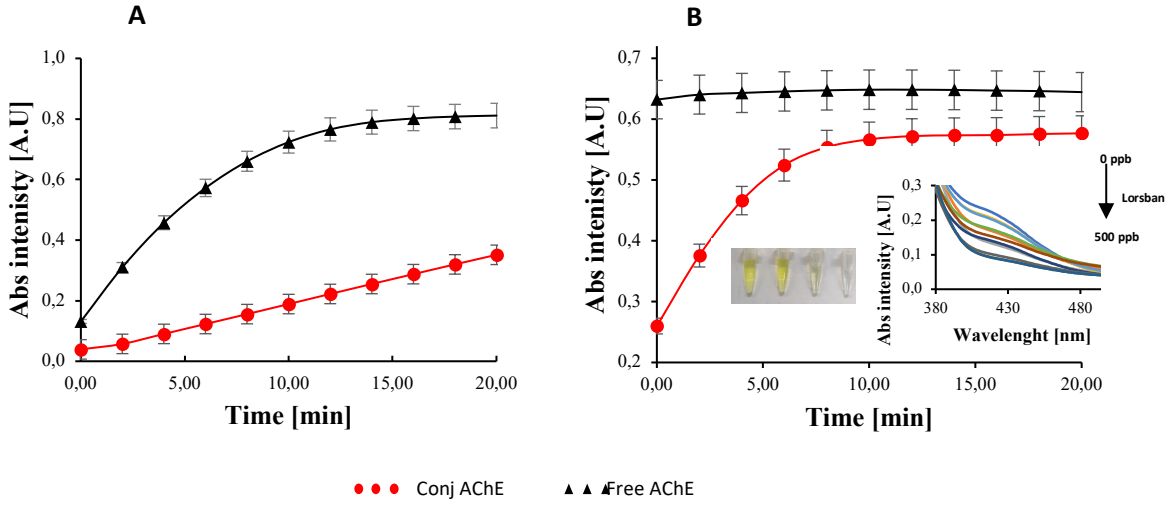

Figure 4-1. Kinetic curves of the free and conjugated enzyme at different concentrations. A) AChE at 1 U mL-1 and B) AChE at 5 U mL-1. The insert in B shows the linear inhibition of the free AChE at 5 U mL-1 with increasing concentrations of Lorsban (0, 50, 100, 150, 200, 250, 300, 350, 400, 450 y 500 ppb). n= 4 independent experiments.

To verify the conjugation between CD and AChE (amide bond formation), the UV-Vis and fluorescence emission spectrum for the free CD, mixed CD and AChE, and conjugated CD with AChE are shown in Figure 4-2. The CD have an absorption peak at 280 nm possibly attributable to n-π* transition of C=O bonds (Zheng et al., 2015), as does the unconjugated mixture of CD and AChE. In

the same graph, we can see the conjugated mixture CD and AChE presents a higher peak at the same wavelength, due to the absorption of the amide bond whose presence has increased due to conjugation (Song & Zhang, 2019). The formation of an apparent new peak at 260 nm associated with the conjugation process is also observed, although the signal is noisy (Sharma et al., 2019). Regarding the fluorescence spectrum, for all the samples, a maximum emission peak was obtained at 420 nm with 320 nm as excitation value. We can see in the fluorescence spectrum (Figure 4-2), how the conjugated mixture decreases the original fluorescence of the CD, this is due to the modification of the surface chemical groups in the CD; this mechanism is directly responsible for the fluorescence (Liu et al., 2019).

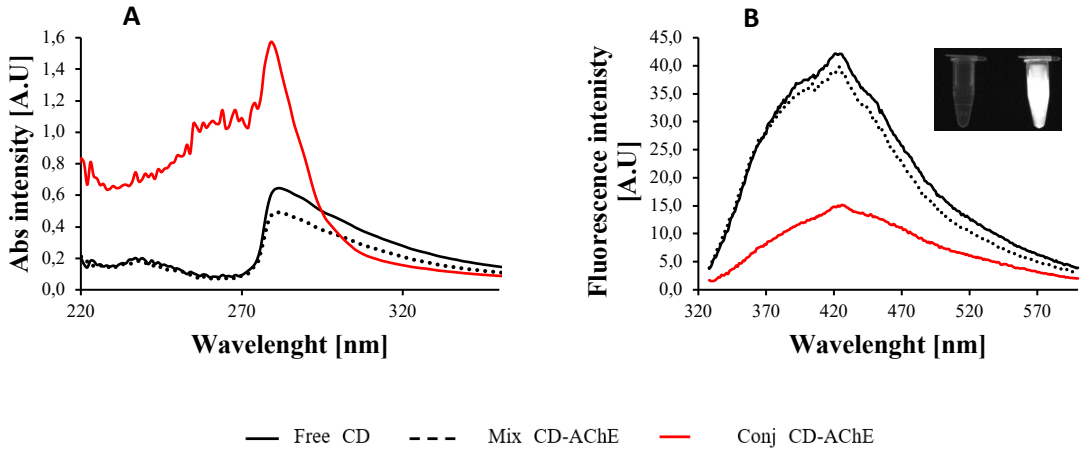

Figure 4-2. A) UV-Vis spectrum showing the increase of the peak at 280 nm for the conjugated CD and AChE at 5 U mL-1, due to the amide bond formation. B) fluorescence emission spectrum (Excitation at 320 nm)showing the decreasing of the fluorescence of the CD for the conjugation of CD and AChE at 5 U mL-1. The insert in B shows the CD under UV light and the mili Q water control

The stability and morphology of the conjugate were verified with HR-TEM and Z potential. Figure 4-3B represents a TEM image of AChE conjugated carbon dots at a concentration of 5 U/mL and 500 ppm, respectively. In a previous work (Barrientos, Gaviria, Arango, Londoño, et al., 2021), the HR-TEM was utilized to investigate the morphology and average size of the carbon dots derived from *Elaeis guineensis*, in that study, we obtained nanoparticles mono-dispersed with an average-sized of 2.5 ± 0.7 nm, which are close to the average-size obtained, in this work, of 3.7 ± 0.5 nm as seen in the histogram of particle diameter distribution of carbon dots (Figure 4-3D). Besides, Figure 4-3B revealed particles with a nearly spherical shape and an average diameter of 16.95 ± 3.93, which is comparable with the dimensions reported for the acetylcholinesterase tetramer from *Electrophorus electricus* (Bourne et al., 1999; Raves et al., 1998), and TEM images obtained from the enzyme to study its location in the cell (Blotnick-Rubin & Anglister, 2018; Dobbertin et al., 2009). The AChE particles are surrounded by carbon dots, which could be given by the union of the carboxylic acids present on the surface of the carbon dots (Barrientos, Gaviria, Arango, Placido, et al., 2021) with the amines of the lysine (272) and arginine (1560) residues available on the surface of the enzyme (Figure 4-3E). Because of similarities in size, shape, and availability of amines, the TEM images

suggest that conjugation of carbon dots with the AChE enzyme has been given because of our conjugation protocol.

Furthermore, the HR-TEM images in Figure 4-3B and Figure 4-3C reveal the change in the aggregation morphology of the CD for the conjugate with AChE and the conjugate in the presence of GO. We found that quite particles of AChE are surrounded by a lot of CD, forming aggregates. This aggregation could explain the decrease in the fluorescence intensity for the conjugate compared to the bare CD, as shown in the insert. For the conjugate in the presence of GO, the aggregation is stronger in the TEM images and even at the naked eye. As we can expect, the decreasing of the fluorescence intensity of the conjugate is almost complete in the presence of GO (100 ppm) and the mechanism of quenching is discussed in the next section.

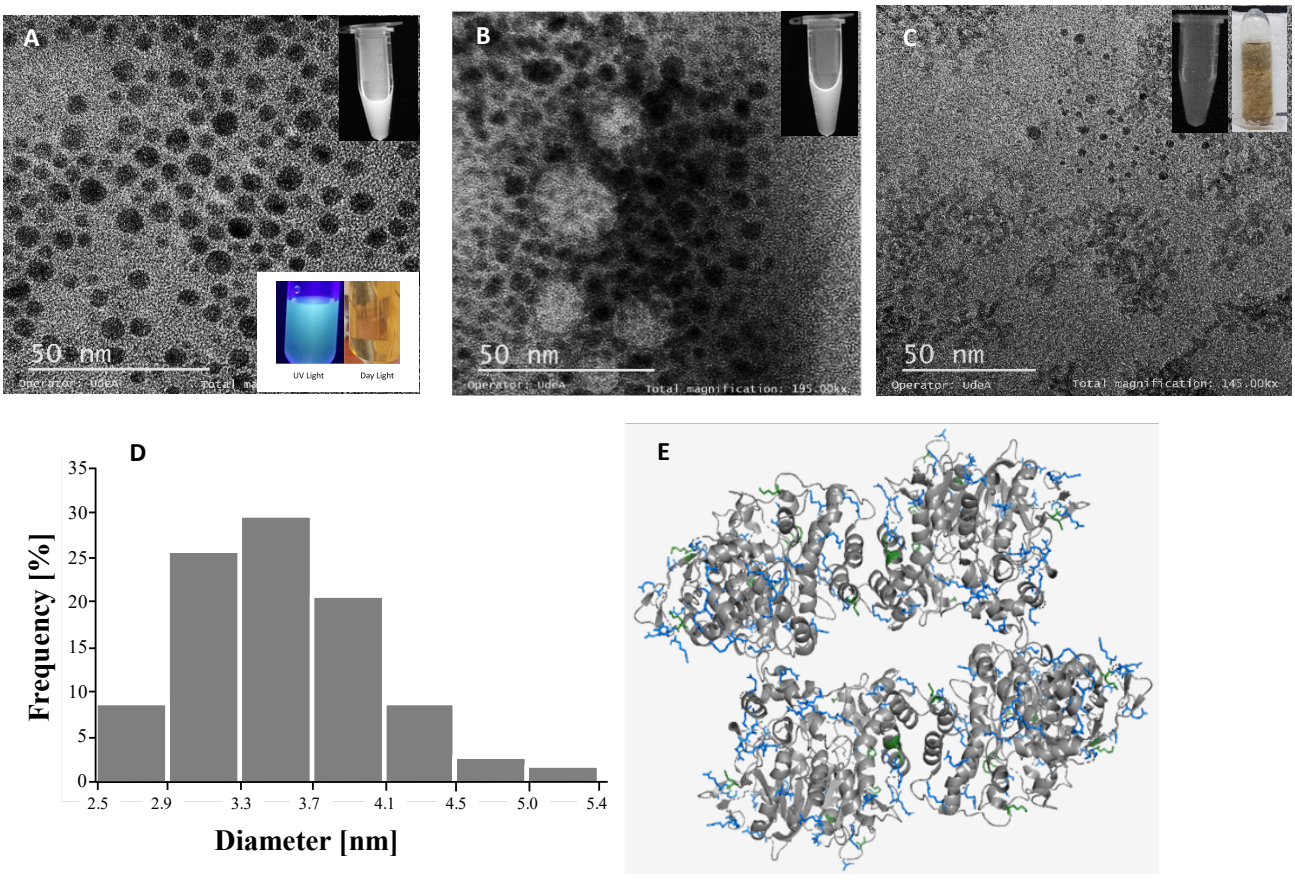

Figure 4-3. HR-TEM imagesfor A) CD, B) CD conjugated with AChE at 5 U mL-1 and C) CD-AChE conjugate and GO at 100 ppm. D) CD histogram and E) Ribbon model of the AChE enzyme structure (PDB ID 1C2O) and representation of amino acids Lysine (green) and Arginine (blue). The inserts in A, B, and C show the changes in the fluorescence intensity under UV light. The insert in C also shows the aggregation of the conjugate in the presence of GO at 100 ppm as the main mechanism for CD fluorescence quenching

The Z potential is an indicator of conjugate stability since it is a measure of the charge repulsion or attraction between the particles from their surface to the boundary of the diffuse layer (Nanoparticles, 2019). The measurements affording a value of -51.27 mV, indicating that besides

the big size and broad distribution of populations, the conjugate particles have great stability. This finding also supports that the aggregation of the conjugate in the presence of GO is not related to the stability of the conjugate itself but the interactions of the chemical groups in both molecules.

Finally, the storage stability of the CD-AChE conjugate was verified (Figure 4-4). Freshly conjugate was stored at 4°C for 30 days and the fluorescence signal was monitored. The fluorescence intensity of the conjugate at 16 days shows an increase, probably due to the disintegration of the amide bond between the CD and the AChE or the decay of weak interactions between particles, so that the CD regains some of their initial fluorescence. However, at 24 days, the fluorescence of the CD decay almost at the initial value, reaching a minimum value of 43% at 30 days. This effect could be explained since the CD alone in solution have shown great stability, but the interactions with the residuals of the enzyme and the by-products of the synthesis and conjugation processes are unknown. The CD after 30 days could be aggregated, losing their fluorescence. Furthermore, the poor stability of enzymes at physiological pH and under temperature changes is reported (Ramnani et al., 2016). Some authors advise improving the stability through immobilization, reaching up to 70% of initial activity within 30 days for electrochemical systems (Zhang et al., 2021).

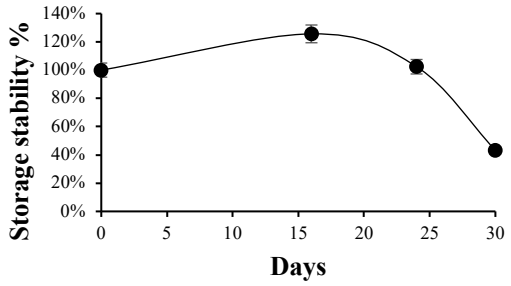

Figure 4-4. Percentage of storage stability at 4°C for the CD-AChE conjugate showing the retention of 43% of initial activity within 30 days.

Pesticide detection mechanism

The detection mechanism of the proposed sensor is shown in Figure 4-5. CD are covalently bonded to AChE causing a decrease in the fluorescence intensity as we previously described in HR-TEM images (Figure 4-3). Then we added an optimized GO concentration of 100 ppm, reducing to 57 % the initial fluorescence and indicating the quenching phenomena in a turned-off system. GO is a flat sheet of carbon atoms one atom thick, which are linked by sp2 hybridization (Gaviria-Arroyave et al., 2020). Since CD are biochar-derived through a carbonization method, is possible that they present the same hexatomic ring of atoms as GO, causing π–π spontaneous interactions promoting fluorescence quenching (Zheng et al., 2015).

Aromatic residues in the AChE and cyclic groups in the CD, interact with sp2 hybridization groups in the GO, bringing the former closer to the CD so that the quenching is probably generated through the FRET principle. When the pesticides molecules are present, the molecules interact with the enzyme due to their affinity and the ability of the organophosphorus pesticides to irreversible inhibit

the AChE (Berger & Schaumburg, 2005; S. Chen & Cashman, 2013; Ratner & Jabre, 2016). Consequently, the enzyme will undergo conformational changes (Cacciotti et al., 2020; Colovic et al., 2013; Pang et al., 2009; Sánchez-Santed et al., 2016) leading to a CD/AChE/Pesticide complex. Therefore, the π–π interactions between the complex and the GO are weakened because the groups involved are shielded, a behavior seen in the interaction between CD complex with GO (Chang et al., 2010; He et al., 2010; M. Li et al., 2013). As a result, the CD are detached from the GO, leading to emission of fluorescence by the conjugate complex in presence of the pesticide. GO, as well as other carbonaceous nanomaterials, have a high surface-to-volume ratio, highly distance-dependent fluorescence quenching ability (Bai et al., 2020), and high energy/electron transfer capability which make it a universal quenching agent for the development of FRET-based biosensors (Lee et al., 2020). However, to the best of our knowledge, few studies report the use of GO and AChE in optical systems for pesticide detection. Most of the works reported GO and AChE in electrochemical sensors, thanks to the stabilization and insulation properties of GO in such systems (Bao et al., 2019; da Silva et al., 2018; Dong et al., n.d.; Shamagsumova et al., 2021). Other works reported the use of CD alone for direct pesticide detection in turning-off systems (Alvandi et al., 2021) and based on the FRET mechanism with the analyte (Tafreshi et al., 2020). Recently, there are some works reporting biosensors based on CD-AChE conjugates for pesticide detection (Inner filter effect-IFE and FRET mechanisms), using different quenching agents like Cu^{2+} ions (Reshma et al., 2019; Xu et al., 2019), 2,3-diaminophenazine (DAP) (Huang et al., 2019), dopamine (H. Li et al., 2020), Gold Nanoclusters (Suo et al., 2020).

CD applications in fluorescence biosensing could be through different mechanisms such as static quenching, dynamic quenching, photo-induced electron transfer, FRET, and IFE. For the FRET mechanism to occur, characteristics such as the overlapping of the emission spectra of the energy donor (CD) with the absorption of the quencher (GO), and the distance between both species within 10 nm must be met (Pirsaheb et al., 2019). Other important aspects are the stability of the donor's fluorescence emission and the high absorptivity of the quencher. As we can see in Figure 6A, the absorption spectrum of GO covers a broad range of wavelengths (approximately 240–700 nm), partially overlapping the fluorescence spectrum of CD and making possible the quenching phenomena through the FRET principle, which has been widely reported in the literature (Arvand & Mirroshandel, 2019; Pirsaheb et al., 2019; Zhou et al., 2020). Additionally, biomolecules like enzymes and single-stranded nucleic acids can interact with the GO through π–π stacking or hydrogen bonding, decreasing the distance and facilitating FRET (Lee et al., 2020). Furthermore, it has been sufficiently reported in the literature that optical biosensors based on CD conjugated with other biomolecules, and GO acting as a quencher for the detection of different analytes, used FRET as the mechanism of detection (Cheng et al., 2018; Ding et al., 2015; Zhou et al., 2020). GO is rich in functional groups such as carboxyl, hydroxyl, epoxy, etc. Those groups are present both on the basal plane and edges leading to a heterogeneous electronic structure with the best probability of interaction with the analyte and thus, giving more sensible systems (Neema et al., 2020).

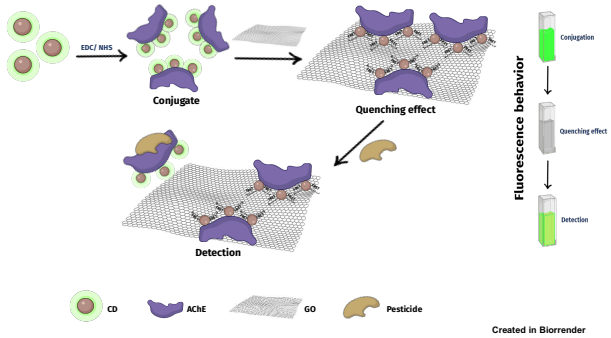

Figure 4-5. The detection mechanism of the proposed biosensor, showing the quenching of the fluorescence for the CD conjugated with AChE in the presence of GO, and the recovery of the fluorescence signal in the presence of the pesticide.

Chlorpyrifos and profenofos detection

To verify the ability and sensibility of the system to detect pesticides, different concentrations of CPF (0 to 0.1 ppm) and PF (0 to 1ppm) were analyzed. For CPF detection, Figure 4-6B shows the rising in the fluorescence response with the increasing concentration of the pesticide. Also, Figure 6D displays the good exponential correspondence between fluorescence intensity and CPF concentration. This is consistent with the detection mechanism previously explained, that is, the more CPF is in the system, the more CD-AChE complex detached from GO sheets increasing the distance and making FRET impossible, causing the fluorescence recovery of the CD. Furthermore, the fluorescence intensity shows a good linear correlation with the natural logarithm of CPF concentration in the range of 2.5 ppb to 0.1 ppm (7.1 nM to 285.2 nM). The linear regression equation for this range (R^2 = 0.9866, ***p < 0.001) was F= 31.842 + 1.5059 ln C, where F and C are the fluorescence intensity and CPF concentration, respectively. The LOD was determined as low as 0.14 ppb (0.41 nM) with a LOQ of 1.4 ppb (3.99 nM).

Despite the good results for CPF detection, the system seems to be less sensitive to PF, since the recovery of the fluorescence was obtained just for the higher concentration evaluated (1 ppm) as is shown in Figure 4-6C. Concentrations below 1 ppm did not cause fluorescence recovery and in fact, decreased the signal. Those results could be explained because CPF is known to be a more potent inhibitor of AChE than other OP like monocrotos, acephate, and profenofos (Das et al., 2006). Furthermore, PF is a less recalcitrant pollutant since its DT50 (semi degradation rate) is just 8 days compared with 30 days for CPF (Ismail & Ngan, 2005). No linear range, LOD, or LOQ were found for PF.

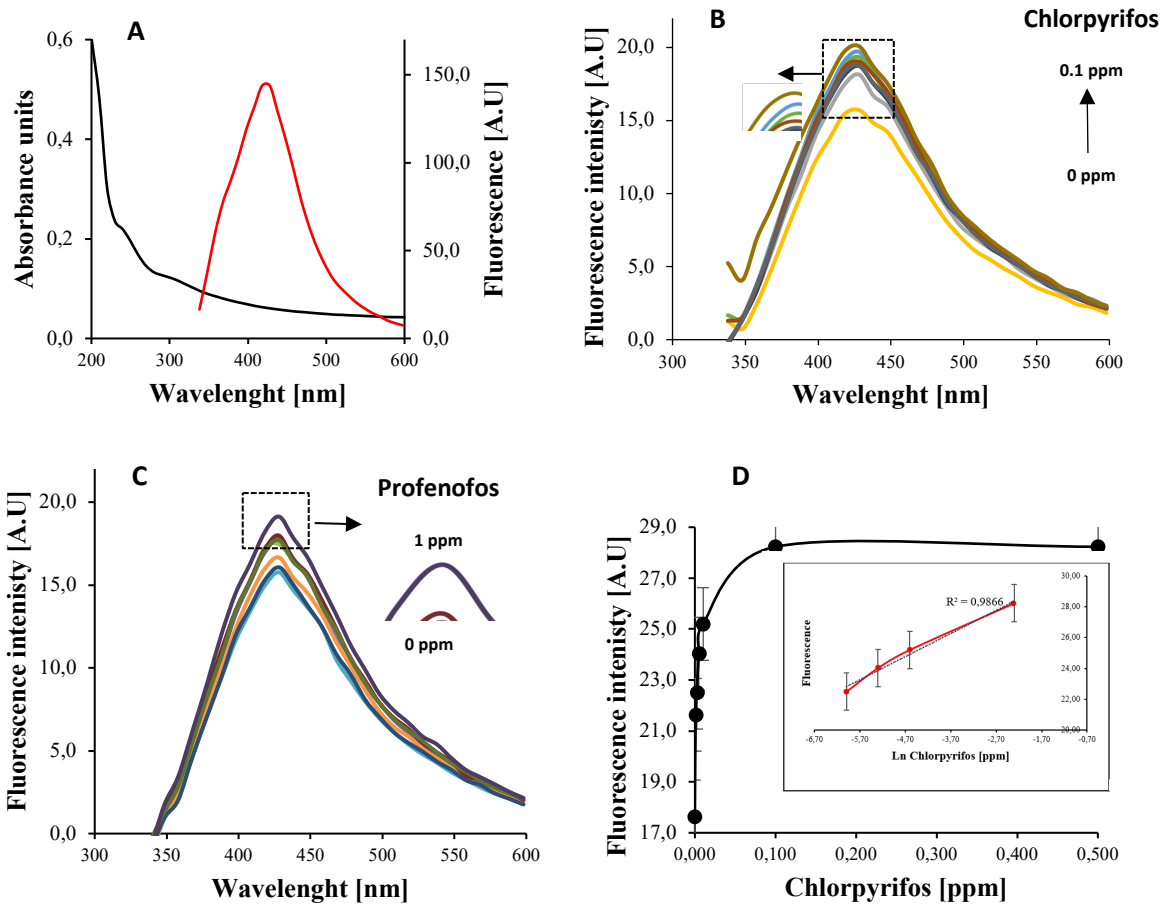

Figure 4-6. A) UV-vis absorbance spectrum of the GO showing a partial overlapping with CD emission spectra at 320 nm (excitation wavelength). Emission spectra for B) Chlorpyrifos between 0 and 0.1 ppm and C) Profenofos between 0 and 1 ppm.D) Exponential relationship between the Fluorescence intensity (λem = 420 nm) and the concentration of chlorpyrifos. Inset: Linear relationship between the Fluorescence intensity (λem = 420 nm) and the natural logarithmic value of chlorpyrifos concentration. Profenofos only shows detection at 1 ppm and does not show linear behavior in any range.

Performance comparison of different highly sensitive electrochemical and fluorescence methods based on AChE and nanomaterials for OP detection are shown in Table 4-1. The LOD of this work is lower than other methods based on simple strategies and nanomaterials. This work uses a non-doped CD and a simple well-established quencher (GO), obtaining a sensitive LOD with a simple and reproducible methodology. Furthermore, the wider linear range shows the viability of the system for real-world applications. Other reported methods with ultra-low LOD and wider linear ranges are based on more sophisticated strategies like using metal-organic frameworks (MOF), dopped CD, or a combination of multiple nanomaterials; in those methods, the sensibility is improved but practical applications could be difficult.

Table 4-1. Comparison of the present method with other reported highly-sensitive electrochemical and fluorescence methods based on AChE and nanomaterials for OP detection

Detection method	Nanomaterial	Electrode	Analyte	LOD	Linear range	Ref

Electrochemical	Titanium oxide nanorods (TiO2-NRs) and reduced graphene oxide (rGO)	GCE	Dichlorvos	2.23 $\times10^{-9}$ M	2.26 $\times10^{-9}$ M to 5.65$\times10^{-8}$ M	(Zhang et al., 2021)
Electrochemical	Semiconducting single-walled carbon nanotubes (s-SWCNTs)	GCE	Methyl parathion	3.75 $\times10^{-11}$ M	1$\times10^{-10}$M to 5$\times10^{-6}$ M	(Kumar & Sundramoorthy, 2019)
Photo-Electrochemical	Magnetic nanocrystal clusters	mGCE	Chlorpyrifos	3.75 $\times10^{-10}$ M	2.85 $\times10^{-9}$ M to 2.85 $\times10^{-6}$ M	(Mao et al., 2017)
Electrochemical	Zinc based Metal-Organic Framework (MOF)	Gold microelectrodes	Chlorpyrifos	1.7 $\times10^{-11}$ M	2.85 $\times10^{-11}$ M to 2.85 $\times10^{-10}$ M	(Nagabooshanam et al., 2019)
Detection method	**Fluorescent material**	**Quencher**	**Analyte**	**LOD**	**Linear range**	**Ref**
Fluorescence	Quantum dots (QD)	H_2O_2 production	Malaoxon, paraoxon, dibrom, and dichlorvos.	5 $\times10^{-8}$ M	5 $\times10^{-9}$ M to 1 $\times10^{-9}$ M	(Wei et al., 2017)
Fluorescence	Aggregation-induced emission fluorogens (BSPOTPE)	SiO_2–MnO_2	Paraoxon	3.6 $\times10^{-9}$ M	3.6 $\times10^{-9}$ M to 3.6 $\times10^{-7}$ M	(Wu et al., 2019)
Fluorescence	CD	Au nano clusters	Diazinon	2.7 $\times10^{-9}$ M	-	(Suo et al., 2020)
Fluorescence	CD	$Cu2^{+}$	Paraoxon Chlorpyrifos	7.6 $\times10^{-9}$ M 1.3 $\times10^{-12}$ M	-	(Reshma et al., 2019)
Fluorescence	N-doped CD	Au NPs	Carbaryl	2.9 $\times10^{-10}$ M	9.9 $\times10^{-10}$ M to 7.4 $\times10^{-7}$M	(Y. Chen et al., 2020)
Fluorescence	CD	GO	Chlorpyrifos Lorsban*	4.1 × 10^{-10} M 5.8 × 10^{-9} M	7.1 × 10^{-9} to 2.85× 10^{-7} M 2.8 × 10^{-9} M to 7.1 × 10^{-8} M	This work

*LOD and linear range are expressed in molarity concerning the molecular weight of Chlorpyrifos.

Detection of commercial Chlorpyrifos (Lorsban®)

The response of the system in the presence of different concentrations (0 to 0.1 ppm) of Lorsban as a commercial OP model was evaluated. Lorsban is a milky white color, an emulsion in water formulation that contains 40.2% of Chlorpyrifos as a main active principle and other non-declared ingredients like coadjutants. Those ingredients could be solvents, humectants, thickeners, surfactants among others. The coadjutants are needed to allow practical application of the active compound (water dilution) and increase its performance (better penetration and stability). However, those ingredients could interfere in the detection of chlorpyrifos as an active compound in real-world applications and the verification of the analytical parameters between pure compound and commercial formulation should be done. Figure 4-7A shows the increase in the fluorescence signal with increasing concentration of Lorsban. Figure 4-7B evidence the exponential relationship between fluorescence intensity and Lorsban concentration. As was expected, the performance of the system for Lorsban seems to be less sensitive than pure chlorpyrifos detection, with a LOD of 2.05 ppb (5.84 nM) and a narrow linear range between 1 ppb and 25 ppb (2.8 nM to 71 nM). The linear regression equation for this range (R2 = 0.9872, **p < 0.01) was F= 26.1470 + 1.2401 ln C, where F and C are the fluorescence intensity and Lorsban concentration, respectively. Those results confirm that other substances present in the formulation reduce the sensibility of the sensor. The mechanism could be explained through the shielding effect of some ions over the conjugate and the steric effect of the substances, neither reducing the possibility of the conjugate CD-AChE to interact with the active principle or the ability of the conjugate to detach from the GO in the presence of less amount of compound. Furthermore, the loss of enzymatic activity under pH variations is well known (Işık, 2020) and the pH value for Lorsban solutions in the evaluated range of concentrations increase above the optimal reported value for AChE activity (7.5) reaching 8 and suggesting a potential step of pH sample adjust for field implementation. However, the system is still sensible enough for the detection of Lorsban residues, and the good LOD combined with the simplicity of the system, suggests its implementation potential reducing the steps of field sample processing before evaluation. As far as we know, works on biosensors reporting commercial OP detection are very scarce, so the present results contribute to the state of the art.

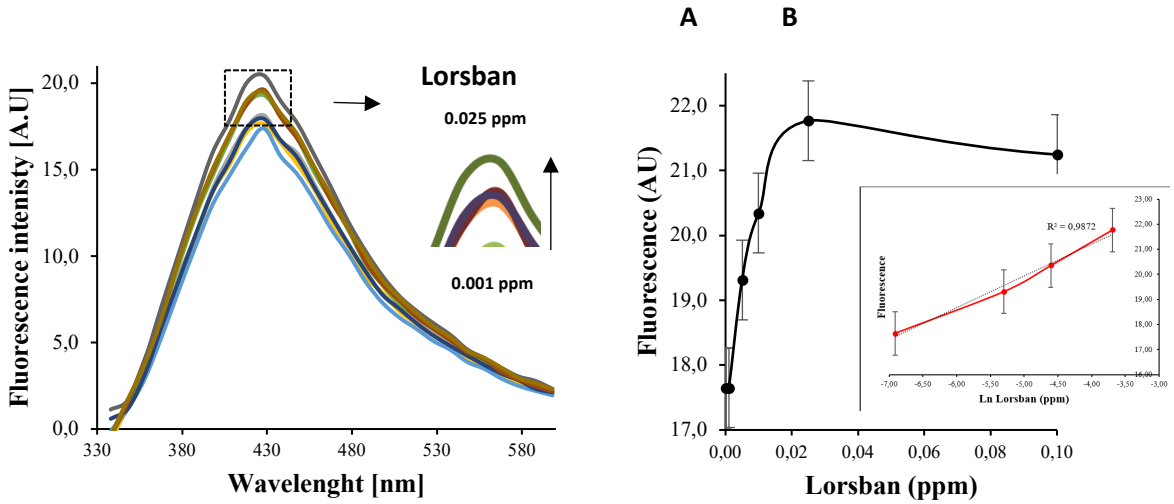

Figure 4-7. A) Lorsban between 0 and 0.1 ppm. B) Exponential relationship between the Fluorescence intensity (λem = 420 nm) and the concentration of Lorsban. Insert Linear relationship between the Fluorescence intensity (λem = 420 nm) and the natural logarithmic value of Lorsban concentration.

Selectivity and matrix effect of the system

To evaluate the selectivity of the system, different substances commonly found in water sources and two non- organophosphate commercial pesticides were selected. Briefly, 0.1 ppm of glucose, bovine serum albumin (BSA), Lannate® (methomyl, carbamate type), and Invetrina® (Cipermetrin, pyrethroid type) were tested individually with the system using tap water and compared with 0.01 ppm of CPF. As shown in Figure 4-8A, the system did not respond to the presence of glucose, BSA, or Lannate® as the model carbamate pesticide. This behavior is interesting since is known that AChE is inhibited by carbamate pesticides (Kaur & Prabhakar, 2017), but in this work, the combination of nanomaterials like CD and GO could have a protective effect increasing the specificity of the system (Vinotha Alex & Mukherjee, 2021). Additionally, OP covalently phosphorylates AChE's serine residues, causing a non-reversible strong inhibition effect. Whereas carbamates like methomyl form a less stable complex that can easily split from AChE through spontaneous hydrolysis (decarbamylation) (Colovic et al., 2013). On the other hand, Invetrina shows a signal comparable with CPF detection. Pyrethroid substances are esters, with an alcohol and acid moiety. The acid moiety usually contains a dimethylcyclopropane ring with a variable radical and within the alcohol moiety, most of the synthetic pyrethroids contain aromatic rings and sometimes a cyano group (Sogorb & Vilanova, 2002). Even though pyrethroids are not known as AChE inhibitory compounds, aromatic and other chemical groups may cause interference in the measure leading to a false positive. This could be inferred also from the matrix effect assay (Figure 4-8B) when the CPF detection in the presence of Invetrina and lanate did not show interference because the affinity of the AChE for CPF is more specifical and stronger than the random chemical groups interact with the Cipermetrin.

Regarding the matrix effect, groups of the same substances used for the selectivity test were evaluated at 0.025 ppm in the presence of 0.01 ppm of CPF and Lorsban® (L) in tap water. Figure 8B shows that detection of CPF is affected by common organic molecules like glucose (Glu) and BSA, but not by the presence of non-organophosphate pesticides. Instead, detection of Lorsban® is not affected by glucose or BSA and is slightly affected by the other pesticides. As expected, the coadjutants in the commercial formulation of Lorsban protect the active principle against other molecules that could degrade it or make a shielding effect. In the case of CPF, the active principle is bare and exposed to the environmental effect of other molecules. Both in selectivity and matrix effect, the different ions present in tap water seem to not influence the performance of the system, fostering its field application.

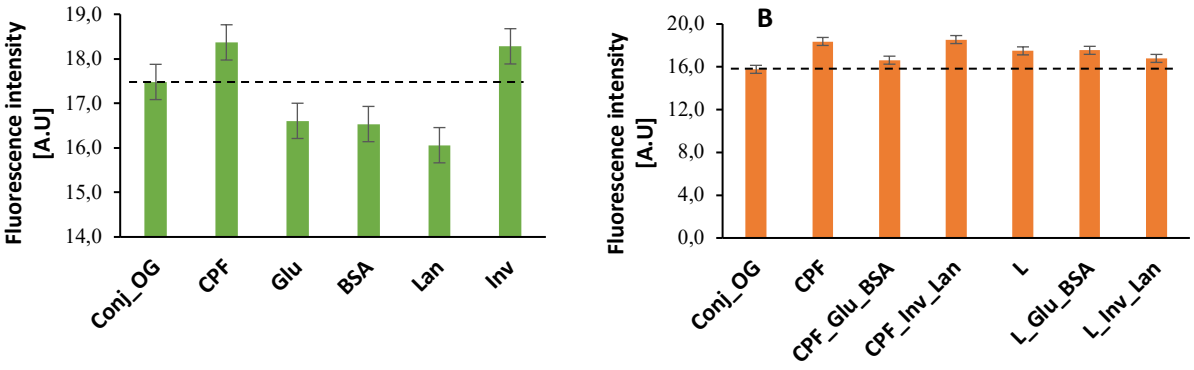

Figure 4-8. Fluorescence response of the system in the presence of 0.1 ppm of different analytes in tap water. A) selectivity of the system for individual tests and B) matrix effect of some mixes. The dotted line indicates the baseline (CD-AChE conjugate with GO).

4.4. Conclusions

In summary, a sensitive biosensor based on acetylcholinesterase and carbon dots- graphene oxide quenching test was developed for the detection of analytical grade chlorpyrifos. Furthermore, the system shows good results for the detection of a commercial formula called Lorsban®, based on chlorpyrifos. This should be highlighted because, in the fumigation of crops, commercial formulations such as Lorsban® are used instead of pure chlorpyrifos. To the best of our knowledge, few works report commercial pesticide detection. The conjugation between acetylcholinesterase enzyme and carbon dots was deeply characterized and powerful insights about the chemical group's interactions as well as size and stability were obtained. The results suggested that the biosensor works through a FRET principle, using graphene oxide (GO) as a universal quenching agent. In this way, the system exhibited a good exponential relationship of the fluorescence recovery and the pesticide concentration, obtaining an ultra-low LOD of 0.14 ppb and 2.05 ppb for chlorpyrifos and Lorsban® respectively. Those results agree with the state of the art reporting the high sensibility of the fluorescence systems, especially with the incorporation of nanomaterials in turning-on mode. The biosensor showed good results in tap water and the presence of possible coexisting substances, indicating the potential of field implementation. However, the specificity, sensibility, and repeatability of the biosensor, in general, is still a major limiting for their implementation into point-of-care systems. In the present work, the repeatability of the data must be improved, considering the inherent challenges of the enzymatic-based systems, and detecting commercial pesticide formulations in field samples. In this sense, strategies like the use of single-stranded nucleic acids (aptamers) instead of enzymes and the immobilization of the biomolecules could be applied for future works. Nevertheless, and given its simplicity, this work paves the way for the implementation of portable systems based on nanotechnology for the detection of environmental pollutants.

4.5. References

Abdul, S., Nor, R., & Zobir, M. (2019). Synthesis, Technology and Applications of Carbon Nanomaterials. Elsevier.

Alvandi, N., Assariha, S., Esfandiari, N., & Jafari, R. (2021). Off–on sensor based on concentration-dependent multicolor fluorescent carbon dots for detecting pesticides. Nano-Structures and Nano-Objects, 26, 100706. https://doi.org/10.1016/j.nanoso.2021.100706

Arvand, M., & Mirroshandel, A. A. (2019). An efficient fluorescence resonance energy transfer system from quantum dots to graphene oxide nano sheets: Application in a photoluminescence aptasensing probe for the sensitive detection of diazinon. Food Chemistry, 280(November 2018), 115–122. https://doi.org/10.1016/j.foodchem.2018.12.069

Bai, Y., Xu, T., & Zhang, X. (2020). Graphene-based biosensors for detection of biomarkers. Micromachines, 11(1). https://doi.org/10.3390/mi11010060

Bao, J., Huang, T., Wang, Z., Yang, H., Geng, X., Xu, G., Samalo, M., Sakinati, M., Huo, D., & Hou, C. (2019). 3D graphene/copper oxide nano-flowers based acetylcholinesterase biosensor for sensitive detection of organophosphate pesticides. Sensors and Actuators, B: Chemical, 279(May 2018), 95–101. https://doi.org/10.1016/j.snb.2018.09.118

Barrientos, K., Gaviria, M. I., Arango, J. P., Londoño, M. E., & Jaramillo, M. (2021). Synthesis, Characterization and Ecotoxicity Evaluation of Biochar-Derived Carbon Dots from Spruce Tree, Purple Moor-Grass and African Oil Palm. Processes, 9(1095), 16.

Barrientos, K., Gaviria, M. I., Arango, J. P., Placido, J., Bustamante, S., Londoño, M. E., & Jaramillo, M. (2021). Synthesis, Characterization and Ecotoxicity Evaluation of Biochar-Derived Carbon Dots from Spruce Tree, Purple Moor-Grass and African Oil Palm. Processes, 9(1095).

Berger, A. R., & Schaumburg, H. H. (2005). Human Toxic Neuropathy Caused by Industrial Agents. Peripheral Neuropathy, 2, 2505–2525. https://doi.org/10.1016/B978-0-7216-9491-7.50115-0

Betancur, J., Morales, D. F., Peñuela, G. A., & Cano, J. B. (2018). Detección de Clorpirifos en Leche usando un Biosensor Enzimático Amperométrico basado en Acetilcolinesterasa. Información Tecnológica, 29(6), 113–122. https://doi.org/10.4067/s0718-07642018000600113

Blotnick-Rubin, E., & Anglister, L. (2018). Fine Localization of Acetylcholinesterase in the Synaptic Cleft of the Vertebrate Neuromuscular Junction. Frontiers in Molecular Neuroscience, 0, 123. https://doi.org/10.3389/FNMOL.2018.00123

Bourne, Y., Grassi, J., Bougis, P. E., & Marchot, P. (1999). Conformational Flexibility of the Acetylcholinesterase Tetramer Suggested by X-ray Crystallography. Journal of Biological Chemistry, 274(43), 30370–30376. https://doi.org/10.1074/JBC.274.43.30370

Cacciotti, I., Pallotto, F., Scognamiglio, V., Moscone, D., & Arduini, F. (2020). Reusable optical multi-plate sensing system for pesticide detection by using electrospun membranes as smart support for acetylcholinesterase immobilisation. Materials Science and Engineering: C, 111, 110744. https://doi.org/10.1016/J.MSEC.2020.110744

Campuzano, S., Yáñez-Sedeño, P., & Pingarrón, J. M. (2019). Carbon dots and graphene quantum dots in electrochemical biosensing. Nanomaterials, 9(4), 1–18. https://doi.org/10.3390/nano9040634

Chang, H., Tang, L., Wang, Y., Jiang, J., & Li, J. (2010). Graphene fluorescence resonance energy transfer aptasensor for the thrombin detection. Analytical Chemistry, 82(6), 2341–2346. https://doi.org/10.1021/ac9025384

Chen, S., & Cashman, J. R. (2013). Organophosphate Exposure: Detection and Remediation. In Advances in Molecular Toxicology (1st ed., Vol. 7). Elsevier B.V. https://doi.org/10.1016/B978-0-444-62645-5.00006-7

Chen, Y., Qin, X., Yuan, C., Shi, R., & Wang, Y. (2020). Double responsive analysis of carbaryl pesticide based on carbon quantum dots and Au nanoparticles. Dyes and Pigments, 181(April), 108529. https://doi.org/10.1016/j.dyepig.2020.108529

Cheng, X., Cen, Y., Xu, G., Wei, F., Shi, M., Xu, X., Sohail, M., & Hu, Q. (2018). Aptamer based fluorometric determination of ATP by exploiting the FRET between carbon dots and graphene oxide. Microchimica Acta, 185(2), 1–8. https://doi.org/10.1007/s00604-018-2683-z

Colovic, M. B., Krstic, D. Z., Lazarevic-Pasti, T. D., Bondzic, A. M., & Vasic, V. M. (2013). Acetylcholinesterase Inhibitors: Pharmacology and Toxicology. Current Neuropharmacology, 11(3), 315–335. https://doi.org/10.2174/1570159x11311030006

da Silva, M. K. L., Vanzela, H. C., Defavari, L. M., & Cesarino, I. (2018). Determination of carbamate pesticide in food using a biosensor based on reduced graphene oxide and acetylcholinesterase enzyme. Sensors and Actuators, B: Chemical, 277(August), 555–561. https://doi.org/10.1016/j.snb.2018.09.051

Das, G. P., Jamil, K., & Rahman, M. F. (2006). Effect of four organophosphorus compounds on human blood acetylcholinesterase: In vitro studies. Toxicology Mechanisms and Methods, 16(8), 455–459. https://doi.org/10.1080/15376520600719281

Ding, Y., Ling, J., Wang, H., Zou, J., Wang, K., Xiao, X., & Yang, M. (2015). Fluorescent detection of Mucin 1 protein based on aptamer functionalized biocompatible carbon dots and graphene oxide. Analytical Methods, 7(18), 7792–7798. https://doi.org/10.1039/c5ay01680k

Dobbertin, A., Hrabovska, A., Dembele, K., Camp, S., Taylor, P., Krejci, E., & Bernard, V. (2009). Targeting of Acetylcholinesterase in Neurons In Vivo: A Dual Processing Function for the Proline-Rich Membrane Anchor Subunit and the Attachment Domain on the Catalytic Subunit. Journal of Neuroscience, 29(14), 4519–4530. https://doi.org/10.1523/JNEUROSCI.3863-08.2009

Dong, J., Zhao, H., Qiao, F., Liu, P., Wang, X., & Ai, S. (n.d.). Quantum dot immobilized acetylcholinesterase for the determination of organophosphate pesticides using graphene-chitosan nanocomposite modified electrode †. https://doi.org/10.1039/c3ay26599d

Ellman, G. L., Curtney, K. D., Andres, V., & Feather-Stone, R. M. (1961). A new and rapid colorimetric determination of acetylcholinesterase activity. Biochemical Pharmacology, 7, 88–95.

FAO. (2018). Pesticides indicators. FAOSTAT. http://www.fao.org/faostat/en/#data/EP/visualize

Gaviria-Arroyave, M. I., Cano, J. B., & Peñuela, G. A. (2020). Nanomaterial-based fluorescent biosensors for monitoring environmental pollutants: A critical review. Talanta Open, 2(June), 100006. https://doi.org/10.1016/j.talo.2020.100006

He, S., Song, B., Li, D., Zhu, C., Qi, W., Wen, Y., Wang, L., Song, S., Fang, H., & Fan, C. (2010). A graphene nanoprobe for rapid, sensitive, and multicolor fluorescent DNA analysis. Advanced Functional Materials, 20(3), 453–459. https://doi.org/10.1002/adfm.200901639

Huang, S., Yao, J., Chu, X., Liu, Y., Xiao, Q., & Zhang, Y. (2019). One-Step Facile Synthesis of Nitrogen-Doped Carbon Dots: A Ratiometric Fluorescent Probe for Evaluation of Acetylcholinesterase Activity and Detection of Organophosphorus Pesticides in Tap Water and Food [Research-article]. Journal of Agricultural and Food Chemistry, 67(40), 11244–11255. https://doi.org/10.1021/acs.jafc.9b03624

Işık, M. (2020). High Stability of Immobilized Acetylcholinesterase on Chitosan Beads. ChemistrySelect, 5(15), 4623–4627. https://doi.org/10.1002/slct.202000559

Ismail, B. S., & Ngan, C. K. (2005). Dissipation of chlorothalonil, chlorpyrifos, and profenofos in a Malaysian agricultural soil: A comparison between the field experiment and simulation by the PERSIST model. Journal of Environmental Science and Health - Part B Pesticides, Food Contaminants, and Agricultural Wastes, 40(2), 341–353. https://doi.org/10.1081/PFC-200045560

Jokanović, M. (2018). Neurotoxic effects of organophosphorus pesticides and possible association with neurodegenerative diseases in man: A review. Toxicology, 410(September), 125–131. https://doi.org/10.1016/j.tox.2018.09.009

Kaur, N., & Prabhakar, N. (2017). Current scenario in organophosphates detection using electrochemical biosensors. TrAC - Trends in Analytical Chemistry, 92, 62–85. https://doi.org/10.1016/j.trac.2017.04.012

Khoris, I. M., Ganganboina, A. B., Suzuki, T., & Park, E. Y. (2021). Self-assembled chromogen-loaded polymeric cocoon for respiratory virus detection. Nanoscale, 13(1), 388–396. https://doi.org/10.1039/d0nr06893d

King, A. M., & Aaron, C. K. (2015). Organophosphate and Carbamate Poisoning. Emergency Medicine Clinics of North America, 33(1), 133–151. https://doi.org/10.1016/j.emc.2014.09.010

Kumar, T. H. V., & Sundramoorthy, A. K. (2019). Electrochemical biosensor for methyl parathion based on single-walled carbon nanotube/glutaraldehyde crosslinked acetylcholinesterase-wrapped bovine serum albumin nanocomposites. Analytica Chimica Acta, 1074, 131–141. https://doi.org/10.1016/j.aca.2019.05.011

Lee, J., Kim, J., Kim, S., & Min, D. (2020). Biosensors based on graphene oxide and its biomedical application. January.

Li, H., Su, D., Gao, H., Yan, X., Kong, D., Jin, R., Liu, X., Wang, C., & Lu, G. (2020). Design of Red Emissive Carbon Dots: Robust Performance for Analytical Applications in Pesticide Monitoring. Analytical Chemistry, 92(4), 3198–3205. https://doi.org/10.1021/ACS.ANALCHEM.9B04917

Li, M., Zhou, X., Guo, S., & Wu, N. (2013). Detection of lead (II) with a "turn-on" fluorescent biosensor based on energy transfer from CdSe/ZnS quantum dots to graphene oxide. Biosensors and Bioelectronics, 43(1), 69–74. https://doi.org/10.1016/j.bios.2012.11.039

Liu, M. L., Chen, B. Bin, Li, C. M., & Huang, C. Z. (2019). Carbon dots: Synthesis, formation mechanism, fluorescence origin and sensing applications. Green Chemistry, 21(3), 449–471. https://doi.org/10.1039/c8gc02736f

Luo, D., Zhou, T., Tao, Y., Feng, Y., Shen, X., & Mei, S. (2016). Exposure to organochlorine pesticides and non-Hodgkin lymphoma: A meta-analysis of observational studies. Scientific Reports, 6(1), 1–11. https://doi.org/10.1038/srep25768

Mao, H., Yan, Y., Hao, N., Liu, Q., Qian, J., Chen, S., & Wang, K. (2017). Dual signal amplification coupling dual inhibition effect for fabricating photoelectrochemical chlorpyrifos biosensor. Sensors and Actuators, B: Chemical, 238, 239–248. https://doi.org/10.1016/j.snb.2016.07.072

Mishra, I. P., Sabat, G., & Mohanty, B. K. (2015). Phytotoxicity of Profenofos 50% EC (curacron 50 EC) to Vigna radiata,L. seedlings: II. Studies on Biochemical Parameters. International Journal of Applied Sciences and Biotechnology, 3(1), 101–105. https://doi.org/10.3126/ijasbt.v3i1.12063

Mostafalou, S., & Abdollahi, M. (2018). The link of organophosphorus pesticides with neurodegenerative and neurodevelopmental diseases based on evidence and mechanisms. Toxicology, 409(July), 44–52. https://doi.org/10.1016/j.tox.2018.07.014

Nagabooshanam, S., Roy, S., Mathur, A., Mukherjee, I., Krishnamurthy, S., & Bharadwaj, L. M. (2019). Electrochemical micro analytical device interfaced with portable potentiostat for rapid detection of chlorpyrifos using acetylcholinesterase conjugated metal organic framework using Internet of things. Scientific Reports, 9(1), 1–9. https://doi.org/10.1038/s41598-019-56510-y

Nanoparticles, G. M. (2019). Green Synthesis, Characterization and Applications of Nanoparticles. In Green Synthesis, Characterization and Applications of Nanoparticles. https://doi.org/10.1016/c2017-0-02526-0

Neema, P. M., Tomy, A. M., & Cyriac, J. (2020). Chemical sensor platforms based on fluorescence resonance energy transfer (FRET) and 2D materials. TrAC - Trends in Analytical Chemistry, 124, 115797. https://doi.org/10.1016/j.trac.2019.115797

Pang, Y. P., Singh, S. K., Gao, Y., Lassiter, T. L., Mishra, R. K., Zhu, K. Y., & Brimijoin, S. (2009). Selective and Irreversible Inhibitors of Aphid Acetylcholinesterases: Steps Toward Human-Safe Insecticides. PLOS ONE, 4(2), e4349. https://doi.org/10.1371/JOURNAL.PONE.0004349

Pirsaheb, M., Mohammadi, S., & Salimi, A. (2019). Current advances of carbon dots based biosensors for tumor marker detection, cancer cells analysis and bioimaging. TrAC - Trends in Analytical Chemistry, 115, 83–99. https://doi.org/10.1016/j.trac.2019.04.003

Ramírez, J. A., & Lacasaña, M. (2001). Pesticides: Classification, Uses, Toxicological Aspects and Exposure Assesment. Arch Prev Riesgos Labo, 4(2), 67–75.

Ramnani, P., Saucedo, N. M., & Mulchandani, A. (2016). Carbon nanomaterial-based electrochemical biosensors for label-free sensing of environmental pollutants. Chemosphere, 143, 85–98. https://doi.org/10.1016/j.chemosphere.2015.04.063

Ratner, M. H., & Jabre, J. F. (2016). Neurobehavioral toxicology. The Curated Reference Collection in Neuroscience and Biobehavioral Psychology, 423–439. https://doi.org/10.1016/B978-0-12-809324-5.03117-5

Raves, M. L., Giles, K., Schrag, J. D., Schmid, M. F., Phillips, G. N., Chiu, W., Howard, A. J., Silman, I., & Sussman, J. L. (1998). Quaternary Structure of Tetrameric Acetylcholinesterase. Structure and Function of Cholinesterases and Related Proteins, 351–356. https://doi.org/10.1007/978-1-4899-1540-5_97

Reshma, Gupta, B., Sharma, R., & Ghosh, K. K. (2019). Facile and visual detection of acetylcholinesterase inhibitors by carbon quantum dots. New Journal of Chemistry, 43(25), 9924–9933. https://doi.org/10.1039/c9nj02347j

Rodriguez, D. C., Carvajal, S., & Peñuela, G. (2013). Effect of chlorpyrifos on the inhibitio of the enzyme acetylcholinesterase by cross-linking in water suppky samples and milk from dairy cattle. Talanta, 1–7.

Sánchez-Santed, F., Colomina, M. T., & Herrero Hernández, E. (2016). Organophosphate pesticide exposure and neurodegeneration. Cortex, 74, 417–426. https://doi.org/10.1016/J.CORTEX.2015.10.003

Shamagsumova, R., Rogov, A., Shurpik, D., Stoikov, I., & Evtugyn, G. (2021). Acetylcholinesterase Biosensor Based on Reduced Graphene Oxide – Carbon Black Composite for Determination of Reversible Inhibitors. Electroanalysis, 33, 1–11. https://doi.org/10.1002/elan.202100385

Sharma, S. K., Micic, M., Li, S., Hoar, B., Paudyal, S., Zahran, E. M., & Leblanc, R. M. (2019). Conjugation of Carbon Dots with β-Galactosidase Enzyme: Surface Chemistry and Use in Biosensing. Molecules, 24(18), 3275. https://doi.org/10.3390/molecules24183275

Sidhu, G. K., Singh, S., Kumar, V., Dhanjal, D. S., Datta, S., & Singh, J. (2019). Toxicity, monitoring and biodegradation of organophosphate pesticides: A review. Critical Reviews in Environmental Science and Technology, 49(13), 1135–1187. https://doi.org/10.1080/10643389.2019.1565554

Sogorb, M. A., & Vilanova, E. (2002). Enzymes involved in the detoxification of organophosphorus, carbamate and pyrethroid insecticides through hydrolysis. Toxicology Letters, 128(1–3), 215–228. https://doi.org/10.1016/S0378-4274(01)00543-4

Song, J., & Zhang, J. (2019). Self-illumination of Carbon Dots by Bioluminescence Resonance Energy Transfer. June, 1–7. https://doi.org/10.1038/s41598-019-50242-9

Suner, S. S., Sahiner, M., Ayyala, R. S., Bhethanabotla, V. R., & Sahiner, N. (2021). Versatile Fluorescent Carbon Dots from Citric Acid and Cysteine with Antimicrobial, Anti-biofilm, Antioxidant, and AChE Enzyme Inhibition Capabilities. Journal of Fluorescence, 31(6), 1705–1717. https://doi.org/10.1007/s10895-021-02798-x

Suo, Z., Liu, X., Hou, X., Liu, Y., Lu, J., Xing, F., Chen, Y., & Feng, L. (2020). Ratiometric Assays for Acetylcholinesterase Activity and Organo-Phosphorous Pesticide Based on Superior Carbon Quantum Dots and BLGF-Protected Gold Nanoclusters FRET Process. ChemistrySelect, 5(29), 9254–9260. https://doi.org/10.1002/slct.202002042

Tafreshi, F. A., Fatahi, Z., Ghasemi, S. F., Taherian, A., & Esfandiari, N. (2020). Ultrasensitive fluorescent detection of pesticides in real sample by using green carbon dots. PLoS ONE, 15(3), 1–17. https://doi.org/10.1371/journal.pone.0230646

Talari, F. F., Bozorg, A., Faridbod, F., & Vossoughi, M. (2021). A novel sensitive aptamer-based nanosensor using rGQDs and MWCNTs for rapid detection of diazinon pesticide. Journal of Environmental Chemical Engineering, 9(1), 104878. https://doi.org/10.1016/j.jece.2020.104878

Thermo scientific. (n.d.). Instructions NHS and Sulfo-NHS. Thermofisher. Retrieved October 17, 2019, from https://www.thermofisher.com/order/catalog/product/24500?SID=srch-srp-24500

Ubaid ur Rahman, H., Asghar, W., Nazir, W., Sandhu, M. A., Ahmed, A., & Khalid, N. (2021). A comprehensive review on chlorpyrifos toxicity with special reference to endocrine disruption: Evidence of mechanisms, exposures and mitigation strategies. Science of the Total Environment, 755. https://doi.org/10.1016/j.scitotenv.2020.142649

Vinotha Alex, A., & Mukherjee, A. (2021). Review of recent developments (2018–2020) on acetylcholinesterase inhibition based biosensors for organophosphorus pesticides detection. Microchemical Journal, 161(November 2020). https://doi.org/10.1016/j.microc.2020.105779

Wei, J., Cao, J., Hu, H., Yang, Q., Yang, F., Wan, J., Su, H., He, C., Li, P., & Wang, Y. (2017). Sensitive and selective detection of oxo-form organophosphorus pesticides based on CdSe/ZnS quantum dots. Molecules, 22(9), 1–11. https://doi.org/10.3390/molecules22091421

Wu, X., Wang, P., Hou, S., Wu, P., & Xue, J. (2019). Fluorescence sensor for facile and visual detection of organophosphorus pesticides using AIE fluorogens-SiO2-MnO2 sandwich nanocomposites. Talanta, 198(January), 8–14. https://doi.org/10.1016/j.talanta.2019.01.082

Xu, X., Cen, Y., Xu, G., Wei, F., Shi, M., & Hu, Q. (2019). A ratiometric fluorescence probe based on carbon dots for discriminative and highly sensitive detection of acetylcholinesterase and butyrylcholinesterase in human whole blood. Biosensors and Bioelectronics, 131(February), 232–236. https://doi.org/10.1016/j.bios.2019.02.031

Zhang, J., Hu, H., & Yang, L. (2021). Ultra-highly sensitive and stable acetylcholinesterase biosensor based on TiO2-NRs and rGO. Microchemical Journal, 168(March), 106435. https://doi.org/10.1016/j.microc.2021.106435

Zheng, X. T., Ananthanarayanan, A., Luo, K. Q., & Chen, P. (2015). Glowing graphene quantum dots and carbon dots: Properties, syntheses, and biological applications. Small, 11(14), 1620–1636. https://doi.org/10.1002/smll.201402648

Zhou, J., Ai, R., Weng, J., Li, L., Zhou, C., Ma, A., Fu, L., & Wang, Y. (2020). A “on-off-on” fluorescence aptasensor using carbon quantum dots and graphene oxide for ultrasensitive detection of the major shellfish allergen Arginine kinase. Microchemical Journal, 158, 105171. https://doi.org/10.1016/j.microc.2020.105171.

5. Fluorescent Nanostructured Carbon Dot-Aptasensor for Chlorpyrifos detection: elucidating the interaction mechanism.

Abstract

Chlorpyrifos (CPF) is a commonly used insecticide found in many water sources that is related to several negative health effects. Biosensors based on aptamers (single-stranded nucleic acid oligonucleotides) are promising alternatives to achieve the detection of CPF and other pesticides in natural waters. However, several challenges need to be addressed to promote the real application of functional aptasensing devices. In this work, an ssDNA aptamer (S1) is combined with carbon quantum dots (CD) and graphene oxide (GO) to produce a stable fluorescent aptasensor. For a deeper understanding of the system, the molecular interaction mechanism was studied through docking modeling, showing that the stem-loops and the higher guanine (G) content are crucial for better interaction. The model also suggests the possibility of a truncated aptamer generation to improve the binding affinity. The biosensor was evaluated for CPF detection, showing a low LOD of 0.01 µg L^{-1} and good selectivity even compared to other organophosphates pesticides (OPs) like profenofos. Finally, the proposed aptasensor was evaluated in some natural water samples showing a good recovery above 2.85 nM and evidencing the need of protecting ssDNA aptamers from an erratic interaction with the aromatic groups of dissolved organic matter (humic substances). This work paves the way for a better aptasensors design and the on-site implementation of novel devices for environmental monitoring.

Keywords: Aptamers, chlorpyrifos, fluorescent biosensor, carbon dots, graphene oxide.

Highlights

- A biosensor was developed based on ssDNA aptamer and Carbon Dots for CPF detection.
- The docking mechanism of interaction for the aptamer and CPF was proposed.
- The biosensor shows low LOD for CPF and good selectivity.
- The biosensor showed good detection of CPF in superficial waters.

Prepared for submission to:
Analytica Chimica Acta. Elsevier

5.1. Introduction

The agricultural value chain has been heavily reliant on pesticides for almost 60 years. According to the Food and Agriculture Organization (FAO) in 2018, the world consumption of pesticides reached 4 million tons and by 2020, the top 5 countries with the highest annual consumption (data in thousands of tons) were the United States (407), Brazil (377), China (262), Argentina (245), and the Russian Federation (90) (FAO, 2022). Pesticides can be absorbed by people in a variety of ways. For instance, one of the most vulnerable groups of agriculture workers is in developing nations like Colombia. Runoff processes may have introduced pesticides into water sources as well. Pesticide exposure has been linked to major illnesses like non-Hodgkin lymphoma. (Luo et al., 2016), Parkinson´s disease (Mostafalou & Abdollahi, 2018) as well as respiratory and reproductive disorders (Ramírez & Lacasaña, 2001). According to estimates, more than 300,000 people died because of pesticide poisoning (M. Liu et al., 2019).

The most widely used insecticides worldwide are organophosphate pesticides (OPs). Because they can irreversibly inhibit the acetylcholinesterase enzyme (AChE), OPs can cause neurotoxicity (Vinotha Alex & Mukherjee, 2021). Chlorpyrifos (CPF), one of the OPs, is the primary active ingredient used in many crops and has a relatively low persistence and toxicity. However, typical bioactive compounds like CPF and CPF-oxon block AChE. Despite its ban in 2021 by EPA, CPF is still being used in developing nations under the brand names Lorsban, Dursban, Equity, Suscon, Empire 20, and Whitmire PT27 (Gaviria et al., 2022).

For the detection of pesticides including OPs, some high-precision analytical technologies have been used, including gas chromatography (GC), high-performance liquid chromatography (HPLC), and mass spectrometry (MS) (Talari et al., 2021). However, due to their drawbacks, such as complicated operation, high cost, and lengthy-time consumption, there is an urgent need for the development of a simple, quick, stable detection technology for OPs. Especially for on-site monitoring.

In this scenario, biosensors have emerged as viable instruments for quick and accurate OPs detection. More stable optical biosensors based on nanomaterials have been created recently, achieving lower detection limits (Gaviria et al., 2022) (X. Zhu et al., 2022) (Raveendran & Kizhakayil, 2021). The application of nanomaterials, including Carbon Quantum Dots (CD), can significantly improve the performance of the systems (Abdul et al., 2019; Campuzano et al., 2019). CD are carbonaceous nanomaterials with sizes less than 10 nm. CDs are non-toxic and they benefit from all of the Quantum dots' advantages, including spectral tunability of the emission spectrum and resistance to photo-bleaching (Pehlivan et al., 2019). Due to their natural fluorescence, CDs have attracted a lot of attention (M. L. Liu et al., 2019). Even though CD increase sensitivity, the use of biomolecules with higher specificity must be considered to promote the commercial application of biosensors.

Aptamers are short single-stranded oligonucleotides (RNA or DNA) developed through the Systematic Evolution of Ligands by the Exponential Enrichment (SELEX) method, which can selectively bind to their targets with high affinity (M. Liu et al., 2019). Aptamers have recently drawn

a lot of interest as recognition components for a variety of targets, including small compounds, proteins, and pesticides (M. Liu et al., 2019). Over enzymes and antibodies commonly used for OPs detection, aptamers have several benefits, including higher thermostability, protease resistance, cost-effectiveness, in vitro production, minimum batch-batch variation, small size, simplicity of modification and handling, and target flexibility (Phopin & Tantimongcolwat, 2020). Aptameric technology is still in an early stage of development, and only since 2004 have there been existing reports in SCOPUS. The main technical problem in developing aptamers for OPs recognition is the small molecular structure of the targets, limiting the interactions between their functional groups and aptamer sequences and making the SELEX process quite complex. Only roughly 20 established pesticide targets have aptamers after 30 years of development; CPF is among those pesticides (Phopin & Tantimongcolwat, 2020).

The mechanism for OPs and other small molecule detection using biosensors based on fluorescent nanomaterials and aptamers is related to the so-called Förster resonance energy transfer (FRET); also referred to as fluorescence resonance energy transfer (Pehlivan et al., 2019). FRET is a non-radiative energy transfer process that typically takes place between two fluorophores (or a fluorophore and a quencher) at about 10 nm (Förster distance), where an emitter is close to an acceptor and transfers energy from an excited state through dipole-dipole interactions (Gaviria-Arroyave et al., 2020). The possibility of that interaction is reflected in an overlap of absorbance-emission spectra. Graphene oxide (GO) is an excellent quenching agent because of its high efficiency and reproducibility. GO is an innovative nanomaterial made of a two-dimensional graphitic carbon structure that is only one atom thick. Additionally, it has many functional groups with oxygen on the surface, including carboxyl, hydroxyl, and epoxy groups. Because of the carbonaceous skeleton of GO, single-stranded oligonucleotides can be absorbed through hydrophobic and π stacking interactions, making the fluorescence of the CD to be quenched by FRET (Cheng et al., 2018).

In this work, we integrate the fluorescent properties of CD with a DNA aptamer, and the quenching properties of GO, to develop a biosensor for CPF detection in water samples. To get deeper into the detection mechanism, we use bioinformatic tools for modeling the CPF-aptamer interaction. It is essential to understand the tertiary structure of aptamers and their interactions with the target molecule. For this purpose, in silico methods have been used including aptamer-target docking models and computational tools to predict aptamer structures and thermodynamic properties. Thus, they might enable the modification of a specific set of nucleotides to enhance aptamer performance, saving experimental time compared to the traditional trial-and-error method (Oliveira et al., 2022). This methodology could be applied for future aptasensor simulations under key conditions like [Na+], pH, or temperature, thus leading to an optimizing system.

Finally, we evaluated the biosensor for the detection of CPF in superficial water samples taken from different sites in Antioquia, Colombia. The results showed that the developed aptasensor is a promising alternative for the detection of CPF. However, further research must be carried out to improve the selectivity and reduce the interference of the system. This work paves the way for optimization steps in the aptamer's design and application as fluorescent probes.

5.2. Materials and methods

Chemicals and reagents

Aptamer S1 (Jiao et al., 2017)(ZhaoJing et al., 2012) was synthesized by Eurogentec® with the characteristics presented in Table 5-1. S1 was prepared at 32.24 uM using double-filtered (0.2 um) PBS (1 X) and keep it at -20°C until use. The 5' Amino modifier C6 was included to use the carbodiimide conjugation technique. All chemicals were analytical grade. An analytical standard of Chlorpyrifos (CPF) and PBS tablets were bought from Merck. Carbon dots (CD) were synthesized pyrolytically from African oil palm biochar (*Elaeis guineensis*) according to our previous work (Barrientos et al., 2021). For conjugation steps, EDC (1-ethyl-3-[3-dimethylaminopropyl] carbodiimide), NHS (N-hydroxysuccinimide), and 2-mercaptoethanol (ME) were bought from Thermo Fisher. Single-layered graphene oxide (GO) was purchased from ACS material. All tests were carried out in triplicates. Double deionized water was used throughout all the experiments (Milli-Q ultrapure water system with a 0.22 µm filter, Merck Millipore).

Table 5-1. ssDNA aptamer characteristics

Sequence	**5-CCTGCCACGCTCCGCAAGCTTAGGGTTACGCCTGCAGCGATTCTTGATCGCGCTGCTGGTAATCCTTCTTTAAGCTTGGCACCCGCATCGT- 3**
Length	91 pb
Modifications	5' Amino Modifier C6
Purification	PAGE
Scale	10 µmol
Melting point	75.9 °C
Molecular weight	28025.2 g/mol

Conjugation procedure

The covalent conjugation technique was used through carbodiimide chemistry following the protocol described in our previous work (Gaviria et al., 2022) with some modifications. Briefly, 500 mg L-1 of CD water solution was put in contact with 0.05 M of EDC and 0.1 M of NHS and let them react for 15 minutes followed by 2 h dialysis (3.5 kDa, 4 water changes). Before the addition of S1, the pH was adjusted to 7.45 with sodium bicarbonate and an optimized NaCl concentration of 0.137 M was adjusted by using PBS tablets. An appropriate amount of S1 (final concentration of 1 µM) was added and left reacting for 4 h at 25°C and 50 rpm. The S1 conjugate was left overnight at 4°C followed by 30 minutes of dialysis (3.5 kDa, 2 water changes). The S1 conjugates were stored under 4°C until detection assays and remained active for at least 1 week.

Instrumentation

UV-Vis and fluorescence measurements (spectrum and punctual) were done in a Varioskan Lux (Thermo scientific, SkanIt Software 4.1) on a 200 µL working volume microplates (Falcon™ non-treated black 96-well) at 25°C with 1 nm optical step. To verify the conjugation between aptamer

and CD, agarose gel electrophoresis was used in 6.0% agarose gel with 0.5 × TBE buffer at 100 V for 1 h. For the verification of the recovery in spiked samples, UPLC MS-MS chromatography was used as standard gold (Water manufacturer; Xevo TqD, UPLC-HClass; serial MS QCA032; pump F11QSM343A; Injector F11SDI5616).

Molecular simulation

For a better understanding of the interaction mechanism between S1 and CPF, some steps from a software workflow were applied as described in Figure 5-1, based on the proposal by Oliveira and collaborators (Oliveira et al., 2022). Briefly, using the S1 sequence, the 5 most probable secondary structures were generated with the Mfold web server, considering the minimization of the free energy (Zuker, 2003). Each secondary structure was refined with PyMOL software by adding the hydrogens that are usually omitted in the Mfold prediction since those hydrogens play a major role in aptamer's interaction with targets (Stasiewicz et al., 2019). Before the docking simulation, the CPF tertiary structure (CID 2730) was obtained from the PubChem database (National Center for Biotechnology Information, 2022) in SDF format followed by a cleaning step and hydrogen addition with PyMOL. Both S1 and CPF tertiary structures were saved in PDB format. Finally, the docking models were evaluated by each combination of S1 - CPF tertiary structures using the free HDOCK web server (Tuszynska et al., 2015). The model with the lowest docking score (more possible binding model) was selected.

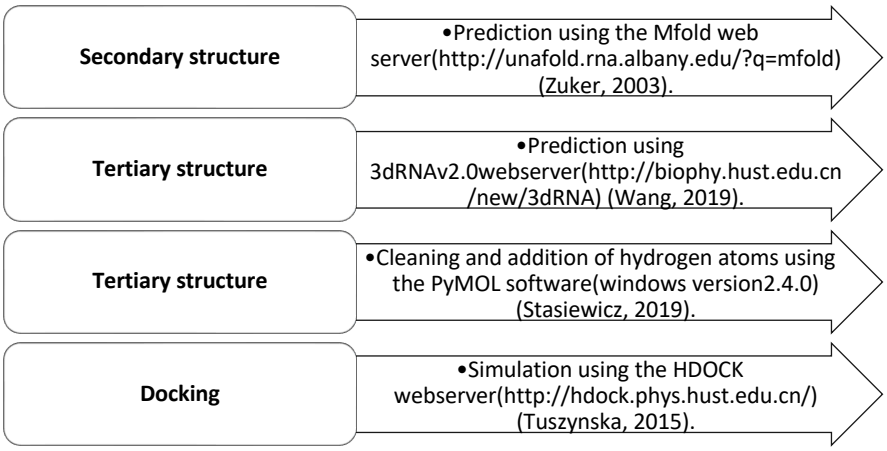

Figure 5-1. Workflow for the in-silico simulation of the S1-CPF interaction. Modified from (Oliveira et al., 2022)

Pesticide detection

CPF was evaluated in a range between 0 and 0.1 mg L-1. For this purpose, different dilutions were made in Milli-Q water from a stock solution of 100 mg L-1 preserved in methanol. For the detection assay, 440 µL of the conjugate and 10 µL of GO (100 mg L-1 GO final optimized concentration) were vigorously mixed in different vials. After 30 minutes at 50 rpm, 50 µL of the appropriate dilution of the pesticide were added to reach the desired final concentration. The solution was vigorously

mixed and incubated for 1 h hour (optimized time) until fluorescence recovery analysis. The amount of the pesticide dilution was replaced by Milli-Q water for control. The fluorescence intensity (recovery) at emission and excitation wavelengths of 420 and 320 nm (respectively) was recorded and plotted against the CPF concentrations (higher recovery means higher CPF concentration). For the estimation of the limits of detection (LOD) and quantification (LOQ), a semilog plot in the linear range was generated and the parameters of the curve were used to estimate LOD as the concentration corresponding to the mean blank value plus 3 times the standard deviation (SD) of the blank (Takahashi et al., 2021). The LOQ was defined in the same way, considering a 10 times parameter. All experiments were treated and analyzed in triplicate. For LOD calculations, a one-way ANOVA was performed using R-studio software, and $p \leq 0.05$ was considered statistically significant.

Pesticide detection in superficial water

Superficial water samples were taken from 3 different locations in the department of Antioquia, Colombia. Some physicochemical parameters of the samples were evaluated (pH, COD, electric conductivity, and true color), as they can be influential variables in the detection assay. Even though the water samples were taken from some rural locations with previous reports of pesticide pollution by run-off water, the UPLC/MS evaluation showed no CPF detection. Considering this, the samples were used as an actual matrix for the experimental procedure of spiked samples. For each sample, 3 CPF concentrations were used (0.1, 1 y 10 µg L-1) and the recovery of the aptasensor was compared to UPHLC/MS as standard gold. All experiments were treated and analyzed in triplicate and the %RSD parameter was estimated.

5.3. Results and discusión

Conjugate characterization

CD were synthesized pyrolytically from African oil palm (*Elaeis guineensis*) and characterized in our previous work (Barrientos et al., 2021). The CD have plenty of carboxylic groups and they had a maximum emission peak at λ= 420 nm under excitation of λ=320 nm. CD have a brownish-yellow color under daylight and blue emission under ultraviolet light (insert in Figure 2A). To demonstrate superficial modification of the CD by a covalent conjugation with S1 (amide bond formation), UV-Vis and fluorescence spectra were evaluated, as well as agarose gel electrophoresis. The UV-Vis spectrum in Figure 5-2A showed the CD with an absorption peak of 260 nm, in agreement with our previous work reported the peak for the CD of *Elaeis guineensis* between 260 y 280 nm possibly attributable to n-π* transition of C=O bonds (Barrientos et al., 2021). In the same figure, the spectra for the simple mix of CD and S1 (without conjugation) and the conjugate CD-S1 are shown, evidencing a remarkable peak at 260 nm for the conjugate. Since both, the simple mix and the conjugate have the same amount of CD and S1, the increase of the peak at 260 nm in the conjugate could be attributable to amide-bond formation between the amino C6 modifier at the 5' termini of the aptamer and the free carboxylic acids in the CD. In fluorescent probes based on nanomaterials and aptamers, usually, peaks between 260 and 280 nm are found (Yüce & Kurt, 2017). Also, is known

that DNA aptamers like S1 have an absorption peak at 260 nm (Ren et al., 2019). Regarding the fluorescence spectrum shown in Figure 5-2B, for all the samples, a maximum emission peak was obtained at 420 nm with 320 nm as the excitation value. We can see in the fluorescence spectrum, how the conjugated mixture decreases the original fluorescence of the CD, this is due to the modification of the surface chemical groups in the CD; this mechanism is directly responsible for the fluorescence (M. L. Liu et al., 2019). Although the fluorescence peak remains around 428 nm for all the samples, the conjugate showed a slight red shift from 418 nm to 428 nm. Different authors have reported this behavior as evidence of conjugation (Cheng et al., 2018) (Tang et al., 2016)(Ren et al., 2019).

Figure 5-2C shows that the conjugate CD-S1 moves slower than the bare S1 (lines 2 and 3 respectively) due to the increase in the mass-to-charge ratio in the conjugate (Cheng et al., 2018). Lines 4 and 5 correspond to another aptamer-CD combination not used in this work. Finally, a following in the stability of the conjugate stored at 4°C was done. Figure 5-2D shows the characteristic fluorescence emission peak at 428 nm for the fresh conjugate. After 8 days, the fluorescence of the conjugate decreased by 24 % probably due to aggregate formation, and a blue shift to 418 nm appeared. The same behavior could be observed after 15 days. However, after 21 days, the fluorescence intensity grew, and the blue shift was encouraged. This increase in the fluorescence intensity has been observed in our previous work (Gaviria et al., 2022), and together with the blue shift, is evidence of the loss of the covalent amide bond, thus showing a trend to a recovery of the bare CD fluorescence intensity. Those results evidence the successful conjugation of the CD-S1 and suggest the priority use of the fresh conjugate for the detection experiments.

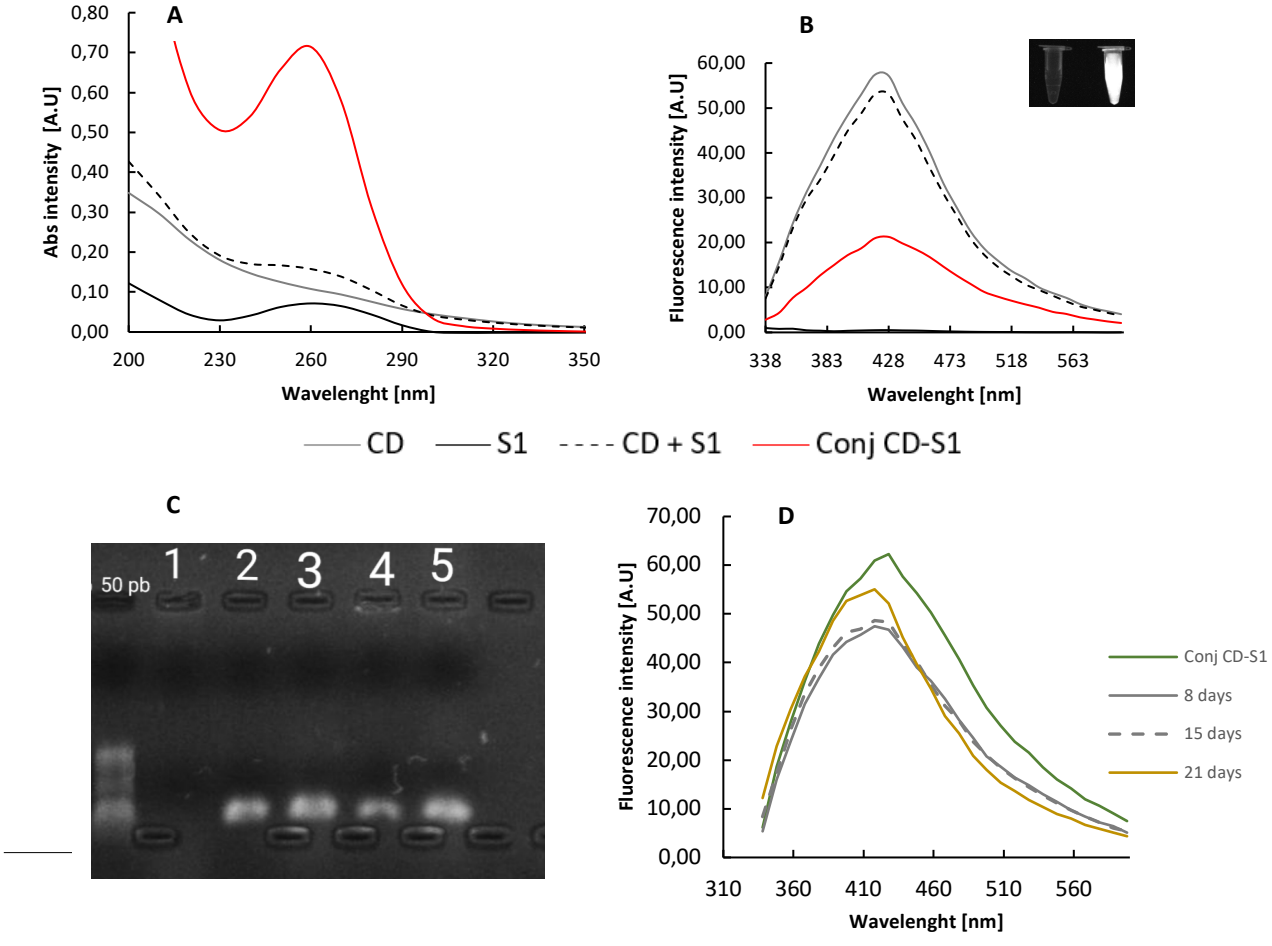

Figure 5-2. A) UV-Vis spectrum showing the increase of the peak at 260 nm for the conjugated CD and S1 at 1 µM, due to the amide bond formation. B) fluorescence emission spectrum (Excitation at 320 nm)showing the decreasing of the fluorescence of the CD for the conjugation of CD and S1 at 1 µM. The inserts show the CD under UV light and the mili Q water control. C) showing conjugate CD-S1 (line 2) moving slower than bare S1 (line 3). D) showing the stability follow-up of the conjugate and suggesting the use of fresh conjugate for the detection assays.

Molecular interaction and docking model

The detection mechanism of the proposed sensor is shown in Figure 5-3. CD are covalently bonded to S1 causing a decrease in the fluorescence intensity. Then we added an optimized GO concentration of 100 mg L-1, reducing to 63 % the initial fluorescence and indicating the quenching phenomena (FRET) in a turned-off system. GO is reported as a highly efficient quencher, especially when it's used with aptamers since mRNA and ssDNA are absorbed in GO through π interactions using their organic nitrogenous bases (Pehlivan et al., 2019). When the pesticide molecules are present, the molecules interact with the aptamers and the desorption happened due to structural changes in the aptamers since there are highly selective to their targets. This mechanism (turn-on mode) has been reported by several authors (Cheng et al., 2018)(Singh et al., 2023) (Dadmehr et al., 2023).

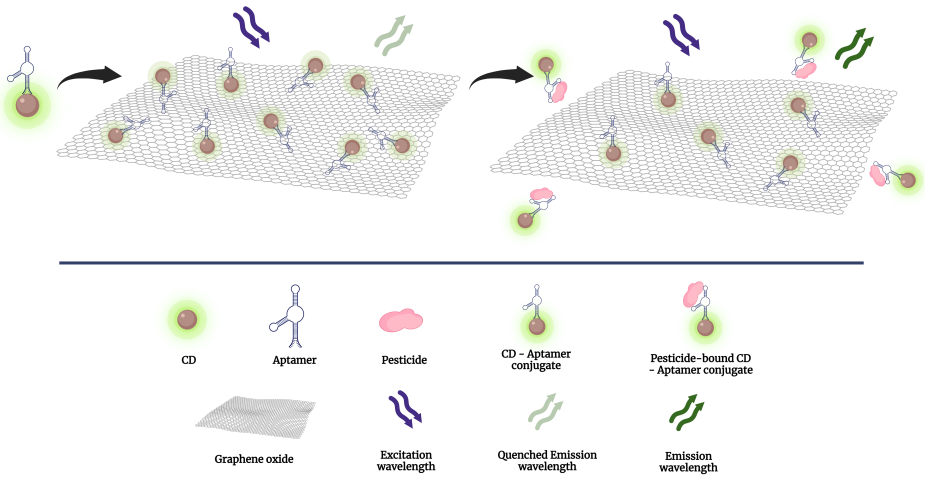

Figure 5-3. The detection mechanism of the proposed sensor

For the docking model, the secondary structure of the aptamer sequence in the lowest energy state was predicted with a Gibbs free energy (G) of -15.47 kcal mol-1 at 37°C to explore the binding of S1 aptamer to CPF (Figure 5-4A). A greater negative ΔG value results in a more stable aptamer-target complex and it depends on the relationship between the enthalpy, and entropy changes (ΔH, and ΔS respectively) at a given temperature (ΔG =ΔH−T·ΔS) (Onaş et al., 2022). For the secondary structure of S1, we found -182.3 kcal mol-1 and -0.537.9 kcal (K mol)-1 for ΔH and ΔS respectively. The negative enthalpy value implies an increased number of interactions between the aptamer and the target, but this parameter also considers the solvent interactions. The entropy value could be related to the loss of the rotation and translation degrees of freedom of the aptamer-target complex compared to the free molecules. The results suggest that S1-CPF interactions are driven by enthalpy-

entropy compensation since both parameters have favorable contributions (Onaş et al., 2022). The secondary structure (Figure 5-4A) also has a higher content of G (24%) compared to the other generated structures. A more stable nucleic acid sequence is made possible by this structural feature and the G content is also known by generating G quadruplets, crucial areas, and binding sites (Zeng et al., 2022). The S1 secondary structure exhibits stem-loops and internal loops that could undergo conformational changes by stacking forces and electrostatic interactions leading to specific recognition areas for CPF.

With the secondary structure, five probable tertiary structures were generated. For each tertiary structure, the binding model to CPF was conducted using the molecular docking technique in the HDOCK webserver. The model with the lowest docking score (more probable binding site) is represented in Figure 5-4B and suggests that the CPF molecule is embedded in the S1 pocket. The main binding sites (distances below 5 Å) are T33, G34, T48, G50, C51, G87, C86, A87, and T88. Those residues are pointed out in the secondary structure and evidence of the importance of G content and the loops. The CPF molecules connect to the stem-loop region of S1 through conjugation interactions, and these interactions are crucial for the stable binding of both CPF molecules and the aptamer (Zeng et al., 2022). The most common interaction forces in the detection of OPs through aptamers have been described as, the C–H bond, π-π interactions, and H-bond interactions (Kadam et al., 2022). For the S1-CPF model, the results show that the interactions are primary π-π, thus some modifications could be proposed to obtain stronger forces like H-bonds. This is important considering that S1-GO interactions are also π-π stacking, but a better detection implies a stronger attraction force between S1 and CPF than the S1 and GO. For instance, it seems like the pocket is not blocked by the CD conjugation, since the model shows a good distance between the conjugation site (5') and the pocket. Future works should use advanced bioinformatic tools like the PLIP web server (Salentin et al., 2015) for the identification of specific chemical groups related to the interactions with small molecules.

To improve the interaction between S1 and CPF, the size of the stem-loop can be changed, and mutations can be made to better fit the desired range of analyte concentration. Given the high amount of guanine in S1, it is important to carefully examine the mechanism of G-quadruplexes. Regarding the results of the 3D model, it could be inferred that a smaller or truncated aptamer could be generated to obtain a better docking score and more stable interactions. Moreover, there are a few reports about the molecular interaction between aptamers and OPs targets, so these findings represent an important contribution to the current state of the art.

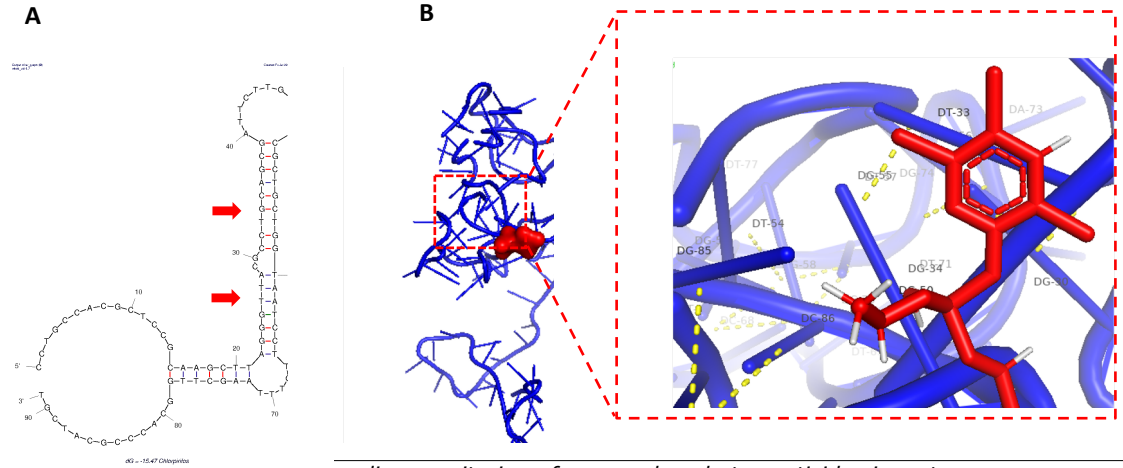

Figure 5-4. Molecular interaction of chlorpyrifos with S1 aptamer. A) secondary structure indicating the most probable interaction sites. C) 3D structure showing the interaction site with the lower docking score. Insert: zoom of the interaction site in C showing the corresponding residues and the π- π interactions like yellow dotted lines.

Quantification of CPF

Different CPF concentrations (0 to 0.1 mg L-1) were examined. Figure 5-5A shows the rise in fluorescence response for CPF detection as a function of pesticide concentration. Despite the differences in the fluorescence signal at the concentration range being low, a good exponential correlation between fluorescence intensity and CPF concentration is shown in Figure 5-5B. Moreover, Figure 5-5C shows a good linear relationship of fluorescence with the natural logarithm of CPF concentration between 0 and 7.5 µg L-1 (0 to 21.6 nM). The linear regression equation for this range (R2= 0.9907, ***p < 0.001, n=3) was F = 25.45 + 0.3122 Ln C, where F and C are the fluorescence intensity and CPF concentration, respectively. The LOD and LOQ were calculated as low as 0.01 µg L-1 (0.028 nM) and 0.1 µg L-1 (0.28 nM) respectively. This is consistent with the detection mechanism previously described, according to which the more CPF present in the system, the more CD-S1 conjugates detached from GO sheets, resulting in an increase in distance and the inability to perform FRET, which results in the fluorescence recovery of the CD. However, some strategies mentioned in the previous section Molecular interaction and docking model should be applied in future works to improve the overall performance of the proposed aptasensor.

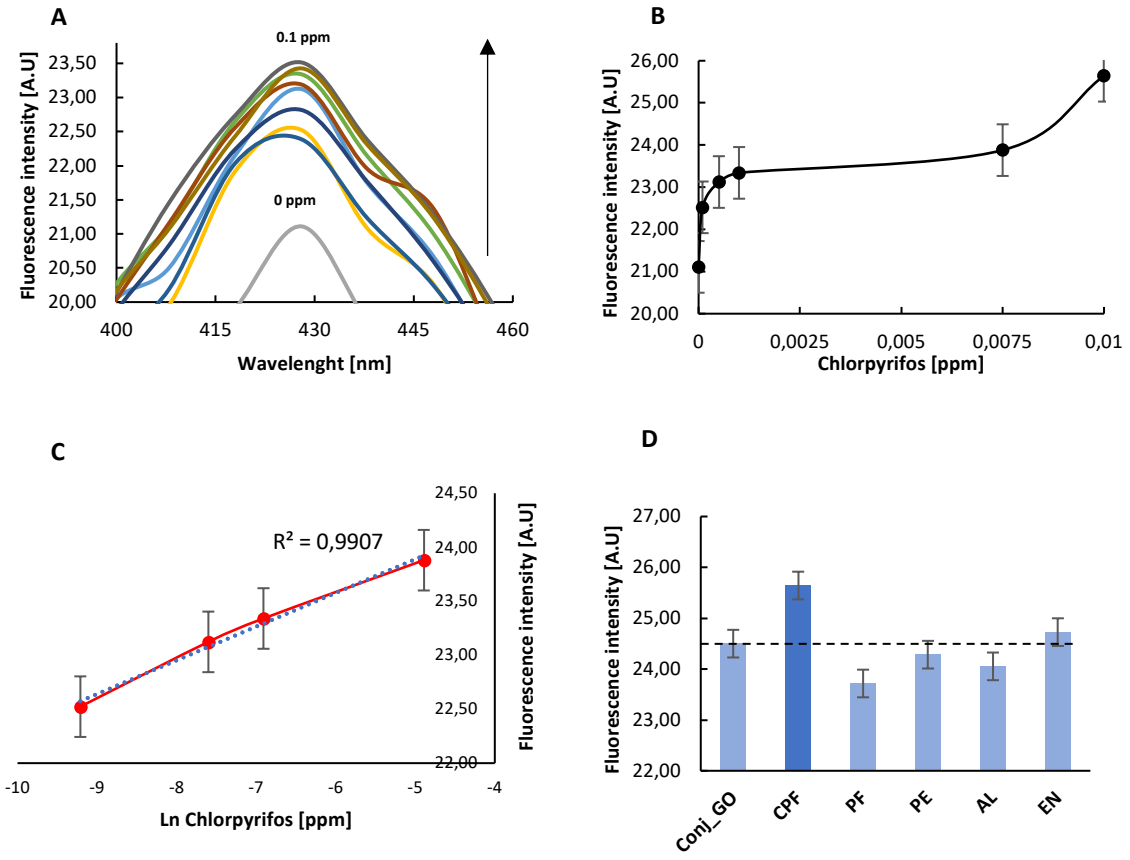

Figure 5-5. A)Emission spectra for Chlorpyrifos between 0 and 0.1 µg L^{-1} show the recovery of the fluorescence. B) Exponential relationship between the Fluorescence intensity (λem = 420 nm) and the concentration of chlorpyrifos. C) Linear relationship between the Fluorescence intensity (λem = 420 nm) and the natural logarithmic value of chlorpyrifos concentration. D) Selectivity of the system for individual tests of chlorpyrifos(CPF), profenofos (PF), permethrin (PE), aldicarb (AL) and endosulfan (EN). Interference factors at 0.025 µg L^{-1} and CPF at 0.01 µg L^{-1}. The dotted line indicates the baseline (CD-S1 conjugate with GO). n= 3 independent experiments

The LOD of the proposed fluorescent probe based on CD-S1 and GO was compared with other aptasensors for OPs detection as illustrated in Table 5-2. Comparison of the present method with other reported highly-sensitive aptasensors for OP detection The LOD of this work is like or even lower than other sophisticated methods but uses simple strategies and nanomaterials. This work uses a non-doped CD and a simple well-established quencher (GO), obtaining a sensitive LOD with a simple and reproducible methodology. However, the narrow linear range of the system should be improved for field application.

Regarding selectivity, different pesticides were evaluated at 0.025 µg L-1 in the presence of 0.01 µg L-1 of CPF. Analogs of CPF or jointly applied insecticides were the types of interfering chemicals selected for the study. The results (Figure 5-5D) show that the system is selective since the response to CPF is remarkable compared to the other class of pesticides (other organophosphates, pyrethroid, carbamate, organochlorine). The fact that the system did not detect profenofos or permethrin matters since most of the enzymatic systems based on acetylcholinesterase commonly used for OPs detection cannot differentiate between CPF and PF structures and those systems are also interfered with by pyrethroid compounds like permethrin (Gaviria et al., 2022). The small signal to endosulfan (organochlorine) has been reported previously in other aptameric systems for OPs (Arvand and Mirroshandel, 2017). These findings demonstrated that the CD-S1/GO ensemble assay had good selectivity toward CPF, which may be attributable to the aptamer's high specificity toward CPF via the development of the FRET system. However, some pretreatment steps could be considered to increase specificity and amplify the output signal.

Table 5-2. Comparison of the present method with other reported highly-sensitive aptasensors for OP detection

Detection method	Nanomaterial	Aptamer type	Pesticide	LOD (µg L^{-1})	Ref
Fluorescence	None	Tetramethylrhodamine (TAMRA)-labeled ap-tamer and cDNA.	Phorate Profenofos Isocarbophos Omethoate	0.333 0.167 0.267 0.333	(Li et al., 2022)
Fluorescence	Gold nanoparticle. MOF	ssDNA	Chlorpyrifos	1.33	(Q. Liu et al., 2019)
Fluorescence	l-cysteine capped ZnS quantum dot and GO	ssDNA	Edifenphos	0.1	(Arvand and Mirroshandel, 2017)
Fluorescence	GO	ssDNA	Acephate	4	(Singh et al., 2023)
Microcantilever - optical	None	ssDNA	Profenofos	1.3	(C. Li et al., 2018)
Ratiometric-electrochemical	carbon nanohorns/Au nanoparticles	Hairpin DNA	Malathion Omethoate	0.013 0.028	(Zhu et al., 2023)

Electrochemical	Complexes of GO and polyaniline (GO@PANI). Gold nanoparticles	ssDNA	Profenofos	0.105	(Wang et al., 2022)
Colorimetric	MOF. Fe-Co magnetic nanoparticles. Fe-N-C nanozymes	Carboxyl functionalized aptamer and cDNA	Phorate Profenofos Isocarbophos Omethoate	0.16 0.16 0.03 1.6	(Shen et al., 2022)
Fluorescence	Carbon dots and GO	ssDNA	Chlorpyrifos	0.01	This work

CPF recovery in real water samples

All the samples related in Table 5-3 showed "not detected" results of CPF by UHPLC/MS, then they were used as a matrix for spiked-recovery assay using three different CPF concentrations. The results shown in Table 5-4 are closely correlated with some physicochemical parameters of the samples (Table 5-3). For the samples of Santa Elena and San Cristóbal localities spiked with 1 or 10 µg L-1, the recovery rates were found between 84.3% and 125.13% with a maximum %RSD value of 6.75%. Those values agree with the UHPLC recoveries and confirm the potential of the method. However, the samples of the same localities with the lowest amount of CPF (0.5 µg L-1) did not show any signal, suggesting a stronger interference effect for the lowest amount of pesticide and confirming the need for optimization of the aptamer structure.

The spiked samples of the Rio Grande reservoir did not show any recovery signal with the proposed method, suggesting that some parameters like low electric conductivity, higher COD, and Color have a strong influence on the performance of the aptasensor. Ionic strength is well known as a critical factor in the design of biosensors based on aptamers and some works reported the influence of certain salts (KCl, NaCl, $MgCl_2$, Na_2CO_3) when in a concentration above 100 mM (Park et al., 2022).

Rio grande sample had a greenish color and presence of the superficial vegetation. The true color parameter of the water is due to the presence of dissolved organic matter (humic substances) or certain metals such as iron, manganese, or copper. The organic matter is confirmed with a higher value of COD. Some organic components like dissolved humic acid had fluorescence excitation/emission wavelengths that could interfere with the FRET sensing mechanisms (Park et al., 2022). Also, humic substances have been studied because their aromatic groups could interact with ssDNA leading to a partial or total shielding effect. In this sense, a recent work (Peng et al., 2022) reported that the carboxyl group and aromaticity of the natural organic matter, the presence of cations (i.e., valency and concentration), and the relative amounts of ssDNA and organic matter in the system all had an impact on the interactions. The shielding effect of the organic matter in ssDNA is determined by interactions between the aromatic portions in the organic matter and the exposed nucleobases of ssDNA. Aldrich humic acid showed a higher interference. Regarding the cation bridging effect, Ca2+ showed the highest interference (above $Mg2^{+}$), since when Ca^{2+} is present even a small amount of Aldrich humic acid could completely inhibit the detection by ssDNA aptamers like S1 (Peng et al., 2022).

The findings imply that the fluorescence-based aptasensor can accurately assess >2.85 nM of CPF in superficial waters. However, the use of pretreatments or the implementation of protective techniques for the ssDNA before the actual use of the proposed aptasensor in field samples will be a must.

Table 5-3. Detailed locations and some physicochemical parameters of the superficial water samples

Sample	Coordinates	Description	pH	Electric conductivity (µS/cm)	COD (mg O_2/L)	Color (UC)
Santa Elena locality	6.2187712N 75.50241516W	Santa Elena creek high part	6.18	1368	<25.0	14.8
San Cristóbal Locality	6.3036804215 75.65491622W	San Cristobal creek "La Iguaná"	6.84	81.3	<25.0	10
Rio Grande reservoir	6.50564438N 75.53597286W	Rio Grande rersevoir	6.5	52.8	39.6	36.4

Table 5-4. Recovery of CPF from real samples. n=3

Sample	Spiked (µg L^{-1})	Measured by this method (µg L^{-1})	% Recovery (this method)	% RSD	Measured by UHPLC (µg L^{-1})	% Recovery (UHPLC)
Santa Elena locality	0.5	0.06	11.81	4.22	0.36	72
	1	0.84	84.30	3.74	0.7	70
	10	8.83	88.29	2.43	10.05	100.5
San Cristóbal Locality	0,5	0.10	19.72	1.17	0.41	82
	1	1.25	125.13	6.75	0.81	81
	10	10.25	102.53	3.97	8.32	83.2
Rio grande reservoir	0.5	-	-	-	0.37	74.00
	1	-	-	-	0.74	74.00
	10	-	-	-	8.07	80.70

5.4. Conclusions

A novel fluorescence nanostructured biosensor based on ssDNA aptamer and carbon dots-graphene oxide was developed for the detection of CPF in water. The molecular mechanism of interaction between the aptamer and the target was proposed using bioinformatic tools and a docking energy model, elucidating the specific pocket for the detection in S1 and the most probable residues involved. This modeling gives important insights for system optimization. The system works through a FRET mechanism and shows good results for the detection of the pesticide with an exponential relationship of the fluorescence recovery and the pesticide concentration, obtaining a low LOD of 0.01 µg L-1. As it was expected, the specificity of the system is good since other pesticides which are usually detected with enzymatic systems did not show any signal. Moreover, the aptasensor was evaluated for the recovery of CPF in superficial natural water samples, showing a good performance in the detection of CPF amounts above 2.85 nM in the water samples with higher conductivity and low amounts of dissolved organic matter (humic substances). This field evaluation and the explanation about the performance is scarce in aptasensors works, so this development is highly valuable for the current state of the art. Strategies like the optimization of the aptamer structure,

pretreatment steps, or the protection of the aptamer are crucial for the use of the systems in field assays. However, the proposed system integrates two types of nanomaterials with a novel aptamer technique in a simple way, reaching a lower LOD compared to other high-complex systems. This work paves the way for the implementation of novel systems based on nanotechnology and aptamers for the detection of environmental pollutants.

5.5. References

Abdul, S., Nor, R., & Zobir, M. (2019). Synthesis, Technology and Applications of Carbon Nanomaterials. Elsevier.

Arvand, M., & Mirroshandel, A. A. (2017). Highly-sensitive aptasensor based on fluorescence resonance energy transfer between L-cysteine capped ZnS quantum dots and graphene oxide sheets for the determination of edifenphos fungicide. Biosensors and Bioelectronics, 96, 324–331. https://doi.org/10.1016/j.bios.2017.05.028

Barrientos, K., Gaviria, M. I., Arango, J. P., Londoño, M. E., & Jaramillo, M. (2021). Synthesis, Characterization and Ecotoxicity Evaluation of Biochar-Derived Carbon Dots from Spruce Tree, Purple Moor-Grass and African Oil Palm. Processes, 9(1095), 16.

Campuzano, S., Yáñez-Sedeño, P., & Pingarrón, J. M. (2019). Carbon dots and graphene quantum dots in electrochemical biosensing. Nanomaterials, 9(4), 1–18. https://doi.org/10.3390/nano9040634

Cheng, X., Cen, Y., Xu, G., Wei, F., Shi, M., Xu, X., Sohail, M., & Hu, Q. (2018). Aptamer based fluorometric determination of ATP by exploiting the FRET between carbon dots and graphene oxide. Microchimica Acta, 185(2), 1–8. https://doi.org/10.1007/s00604-018-2683-z

Dadmehr, M., Shahi, S. C., Malekkiani, M., Korouzhdehi, B., & Tavassoli, A. (2023). A stem-loop like aptasensor for sensitive detection of aflatoxin based on graphene oxide/AuNPs nanocomposite platform. Food Chemistry, 402. https://doi.org/10.1016/j.foodchem.2022.134212

FAO. (2022, October 15). Pesticides Use. FAOSTAT.

Gaviria, M. I., Barrientos, K., Arango, J. P., Cano, J. B., & Peñuela, G. A. (2022). Highly sensitive fluorescent biosensor based on Acetylcholinesterase and carbon dots-graphene oxide quenching test for analytical and commercial organophosphate pesticide detection. Frontiers in Environmental Science, 10, 1–13. https://doi.org/10.3389/FENVS.2022.825112

Gaviria-Arroyave, M. I., Cano, J. B., & Peñuela, G. A. (2020). Nanomaterial-based fluorescent biosensors for monitoring environmental pollutants: A critical review. Talanta Open, 2(June), 100006. https://doi.org/10.1016/j.talo.2020.100006

Jiao, Y., Hou, W., Fu, J., Guo, Y., Sun, X., Wang, X., & Zhao, J. (2017). A nanostructured electrochemical aptasensor for highly sensitive detection of chlorpyrifos. Sensors and Actuators, B: Chemical, 243, 1164–1170. https://doi.org/10.1016/j.snb.2016.12.106

Kadam, U. S., Trinh, K. H., Kumar, V., Lee, K. W., Cho, Y., Can, M. H. T., Lee, H., Kim, Y., Kim, S., Kang, J., Kim, J. Y., Chung, W. S., & Hong, J. C. (2022). Identification and structural analysis of novel malathion-specific DNA aptameric sensors designed for food testing. Biomaterials, 287. https://doi.org/10.1016/j.biomaterials.2022.121617

Li, C., Zhang, G., Wu, S., & Zhang, Q. (2018). Aptamer-based microcantilever-array biosensor for profenofos detection. Analytica Chimica Acta, 1020, 116–122. https://doi.org/10.1016/j.aca.2018.02.072

Li, H., Huang, X., Huang, J., Bai, M., Hu, M., Guo, Y., & Sun, X. (2022). Fluorescence Assay for Detecting Four Organophosphorus Pesticides Using Fluorescently Labeled Aptamer. Sensors (Basel, Switzerland), 22(15). https://doi.org/10.3390/s22155712

Liu, M., Khan, A., Wang, Z., Liu, Y., Yang, G., Deng, Y., & He, N. (2019). Aptasensors for pesticide detection. Biosensors and Bioelectronics, 130(January), 174–184. https://doi.org/10.1016/j.bios.2019.01.006

Liu, M. L., Chen, B. Bin, Li, C. M., & Huang, C. Z. (2019). Carbon dots: Synthesis, formation mechanism, fluorescence origin and sensing applications. Green Chemistry, 21(3), 449–471. https://doi.org/10.1039/c8gc02736f

Liu, Q., Wang, H., Han, P., & Feng, X. (2019). Fluorescent aptasensing of chlorpyrifos based on the assembly of cationic conjugated polymer-aggregated gold nanoparticles and luminescent metal–organic frameworks. The Analyst, 144(20), 6025–6032. https://doi.org/10.1039/c9an00943d

Luo, D., Zhou, T., Tao, Y., Feng, Y., Shen, X., & Mei, S. (2016). Exposure to organochlorine pesticides and non-Hodgkin lymphoma: A meta-analysis of observational studies. Scientific Reports, 6(1), 1–11. https://doi.org/10.1038/srep25768

Mostafalou, S., & Abdollahi, M. (2018). The link of organophosphorus pesticides with neurodegenerative and neurodevelopmental diseases based on evidence and mechanisms. Toxicology, 409(July), 44–52. https://doi.org/10.1016/j.tox.2018.07.014

National Center for Biotechnology Information. (2022, November 6). PubChem Compound Summary for CID 2730, Chlorpyrifos. .

Oliveira, R., Pinho, E., Sousa, A. L., Dias, Ó., Azevedo, N. F., & Almeida, C. (2022). Modelling aptamers with nucleic acid mimics (NAM): From sequence to three-dimensional docking. PLoS ONE, 17(3 March). https://doi.org/10.1371/journal.pone.0264701

Onaş, A. M., Dascălu, C., Raicopol, M. D., & Pilan, L. (2022). Critical Design Factors for Electrochemical Aptasensors Based on Target-Induced Conformational Changes: The Case of Small-Molecule Targets. In Biosensors (Vol. 12, Issue 10). MDPI. https://doi.org/10.3390/bios12100816

Park, J., Yang, K. A., Choi, Y., & Choe, J. K. (2022). Novel ssDNA aptamer-based fluorescence sensor for perfluorooctanoic acid detection in water. Environment International, 158. https://doi.org/10.1016/j.envint.2021.107000

Pehlivan, Z. S., Torabfam, M., Kurt, H., Ow-Yang, C., Hildebrandt, N., & Yüce, M. (2019). Aptamer and nanomaterial based FRET biosensors: a review on recent advances (2014–2019). In Microchimica Acta (Vol. 186, Issue 8). Springer-Verlag Wien. https://doi.org/10.1007/s00604-019-3659-3

Peng, B., Liao, P., & Jiang, Y. (2022). Preferential interactions of surface-bound engineered single stranded DNA with highly aromatic natural organic matter: Mechanistic insights and implications for optimizing practical aquatic applications. Water Research, 223. https://doi.org/10.1016/j.watres.2022.119015

Phopin, K., & Tantimongcolwat, T. (2020). Pesticide aptasensors—state of the art and perspectives. In Sensors (Switzerland) (Vol. 20, Issue 23, pp. 1–40). MDPI AG. https://doi.org/10.3390/s20236809

Ramírez, J. A., & Lacasaña, M. (2001). Pesticides: Classification, Uses, Toxicological Aspects and Exposure Assesment. Arch Prev Riesgos Labo, 4(2), 67–75.

Raveendran, V., & Kizhakayil, R. N. (2021). Fluorescent Carbon Dots as Biosensor, Green Reductant, and Biomarker. ACS Omega, 6(36), 23475. https://doi.org/10.1021/ACSOMEGA.1C03481

Ren, J., Liang, G., Man, Y., Li, A., Jin, X., Liu, Q., & Pan, L. (2019). Aptamer-based fluorometric determination of Salmonella Typhimurium using Fe3O4 magnetic separation and CdTe quantum dots. PLoS ONE, 14(6). https://doi.org/10.1371/journal.pone.0218325

Salentin, S., Schreiber, S., Haupt, V. J., Adasme, M. F., & Schroeder, M. (2015). PLIP: Fully automated protein-ligand interaction profiler. Nucleic Acids Research, 43(W1), W443–W447. https://doi.org/10.1093/nar/gkv315

Shen, Z., Xu, D., Wang, G., Geng, L., Xu, R., Wang, G., Guo, Y., & Sun, X. (2022). Novel colorimetric aptasensor based on MOF-derived materials and its applications for organophosphorus pesticides determination. Journal of Hazardous Materials, 440. https://doi.org/10.1016/j.jhazmat.2022.129707

Singh, P., Kumar, S., & Verma, S. K. (2023). Development of fluorescent aptasensor for detection of acephate by utilizing graphene oxide platform. Talanta, 252. https://doi.org/10.1016/j.talanta.2022.123843

Stasiewicz, J., Mukherjee, S., Nithin, C., & Bujnicki, J. M. (2019). QRNAS: Software tool for refinement of nucleic acid structures. BMC Structural Biology, 19(1). https://doi.org/10.1186/s12900-019-0103-1

Takahashi, R., Yasuda, T., Ohmuro-Matsuyama, Y., & Ueda, H. (2021). BRET Q-Body: A Ratiometric Quench-based Bioluminescent Immunosensor Made of Luciferase-Dye-Antibody Fusion with Enhanced Response. Analytical Chemistry, 93(21), 7571–7578. https://doi.org/10.1021/acs.analchem.0c05217

Talari, F. F., Bozorg, A., Faridbod, F., & Vossoughi, M. (2021). A novel sensitive aptamer-based nanosensor using rGQDs and MWCNTs for rapid detection of diazinon pesticide. Journal of Environmental Chemical Engineering, 9(1), 104878. https://doi.org/10.1016/j.jece.2020.104878

Tang, T., Deng, J., Zhang, M., Shi, G., & Zhou, T. (2016). Quantum dot-DNA aptamer conjugates coupled with capillary electrophoresis: A universal strategy for ratiometric detection of organophosphorus pesticides. Talanta, 146, 55–61. https://doi.org/10.1016/j.talanta.2015.08.023

Tuszynska, I., Magnus, M., Jonak, K., Dawson, W., & Bujnicki, J. M. (2015). NPDock: A web server for protein-nucleic acid docking. Nucleic Acids Research, 43(W1), W425–W430. https://doi.org/10.1093/nar/gkv493

Vinotha Alex, A., & Mukherjee, A. (2021). Review of recent developments (2018–2020) on acetylcholinesterase inhibition based biosensors for organophosphorus pesticides detection. Microchemical Journal, 161(November 2020). https://doi.org/10.1016/j.microc.2020.105779

Wang, G., Dong, H., Han, J., Zhang, M., Huang, J., Sun, J., Guan, F., Shen, Z., Xu, D., Sun, X., Guo, Y., & Zhao, S. (2022). Interference-resistant aptasensor with tetrahedral DNA nanostructure for profenofos detection based on the composites of graphene oxide and polyaniline. Bioelectrochemistry, 148. https://doi.org/10.1016/j.bioelechem.2022.108227

Yüce, M., & Kurt, H. (2017). How to make nanobiosensors: Surface modification and characterisation of nanomaterials for biosensing applications. In RSC Advances (Vol. 7, Issue 78, pp. 49386–49403). Royal Society of Chemistry. https://doi.org/10.1039/c7ra10479k

Zeng, H., Yang, H., Tang, Y., Niu, X., & Wu, Y. (2022). Aptamer-enhanced the Ag(I) ion-3,3’,5,5’-tetramethylbenzdine catalytic system as a novel colorimetric biosensor for ultrasensitive and selective detection of paraquat. Spectrochimica Acta - Part A: Molecular and Biomolecular Spectroscopy, 280. https://doi.org/10.1016/j.saa.2022.121571

ZhaoJing, L., Zhang, C., Yuan, L., Li, W., QiuHui, H., & XianJin, L. (2012). Selection of chlorpyrifos-binding ssDNA aptamer by SELEX. Jiangsu Journal of Agricultural Sciences , 28(1), 198–203.

Zhu, C., Liu, X., Li, Y., Yu, D., Gao, Q., & Chen, L. (2023). Dual-ratiometric electrochemical aptasensor based on carbon nanohorns/anthraquinone-2-carboxylic acid/Au nanoparticles for simultaneous detection of malathion and omethoate. Talanta, 253, 123966. https://doi.org/10.1016/j.talanta.2022.123966

Zhu, X., Han, L., Liu, H., & Sun, B. (2022). A smartphone-based ratiometric fluorescent sensing system for on-site detection of pyrethroids by using blue-green dual-emission carbon dots. Food Chemistry, 379(January), 132154. https://doi.org/10.1016/j.foodchem.2022.132154

Zuker, M. (2003). Mfold web server for nucleic acid folding and hybridization prediction..2003. Nucleic Acids Res, 31, 3406–3415.

6. Portable fluorescent biosensor for in situ monitoring of pesticides using nanostructured probes: evaluation for chlorpyrifos recovery in drinking water sources in rural areas of Antioquia, Colombia.

Abstract

In the last decade, biosensors and nanometric strategies have shown promising results in meeting the growing demand for environmental monitoring, offering fast, selective, and easy-to-use portable platforms for the detection of pollutants in water. However, few commercial biosensors are available for environmental monitoring applications. In this work, a portable fluorescent biosensor device was designed, constructed, and evaluated for Chlorpyrifos (CPF) analysis in superficial water samples of Antioquia, Colombia. Enzymatic and aptameric nanostructured fluorescent probes based on Carbon quantum dots (CD), which were developed in our previous work, were tested. The optimization of the biosensor parameters showed that the specific combination of a LED (325 nm), filter (425 nm), and photodiode, improves the LOD of the enzymatic probe giving a low value of 0.082 µg L^{-1} and wider linear range. The evaluation of 9 superficial samples from the localities of Santa Elena, San Cristóbal, and Rio Grande reservoir in Antioquia, Colombia exhibited the potential quantification of CPF in natural samples from 1 µg L^{-1} and great optimization potential. Electric conductivity along with dissolved organic matter were identified as the main parameters influencing the detection in real samples. This work contributes to the potential implementation of the optical biosensor in a growing environmental monitoring market.

Keywords: fluorescent device, prototype, pesticides, carbon dots, acetylcholinesterase enzyme.

Highlights

- A portable fluorescent biosensor was designed, constructed, and evaluated in real samples for chlorpyrifos detection.
- An enzymatic-nanostructured fluorescent probe based on carbon dots was selected for the prototype evaluation.
- The device shows low LOD for chlorpyrifos and a good performance in superficial samples.
- The influence of some physicochemical parameters in chlorpyrifos detection was discussed.

Under review for submission

6.1. Introduction

Recently, several authors have reported an increased interest in using advanced biosensors for lab-on-a-chip systems to enhance point-of-care (POC) diagnostics (Mukherjee et al., 2022). In those systems, fluorescence transduction exhibit many advantages, like the low consumption of reagents, short response times, and higher sensibility (Gaviria-Arroyave et al., 2020). The POC potential application in different fields like health, environmental analysis, and forensics, among others, has been extensively reviewed (Liu et al., 2020; Myers and Lee, 2015).

However, there is still a lack of commercial fluorescent-based biosensors due mainly to challenges in the stability of the probes, difficult low-cost developments, lack of repeatability, poor portability, and low usability (Myers and Lee, 2015). Moreover, biosensor systems expect to allow multiplexed detection to increase the amount of information obtained in a single assay (Liao et al., 2018).

The development of fluorescent biosensors with nanomaterials improves the miniaturization of various instrument elements. The sensor's compact size makes it possible to combine various processes into a single device to create real-time monitoring of multiple materials, which is highly helpful in natural water characterization. Additionally, the introduction of nanomaterials enhances their physical and chemical characteristics, increases sensitivity, shortens analysis times, boosts measurement accuracy, and demonstrates high-throughput multiplex detection (Ejeian et al., 2018). The effectiveness of nanobiosensors depends on the hypersensitivity of nanostructures to pollutants and the specific interaction of small biomolecules as biorecognition elements.

In this context, fluorescent biosensors are promising alternatives for the detection of environmental pollutants. Such sensors offer a significant advantage in detecting the smallest amount of pollutants in complicated matrices. Powerful nanomaterial-based fluorescent biosensors that exhibit extraordinary properties for detecting chemical reagents and biological processes have been the focus of a rapidly expanding field of research (Gaviria-Arroyave et al., 2020). Different authors have examined the effect of biosensors on the assessment of the quality of groundwater and river water (Ejeian et al., 2018)(Park et al., 2022), and an increase in initiative actions based on real-time biosensing of water sources was also noted.

One of the main pollutants in natural water sources are pesticides. Pesticide compounds are widely used for the prevention and control of pests, primarily in agriculture and forestry. The effects on the environment caused by the excess of pesticides in the soils include acidification, fertility and microbial biodiversity decrease, damage to fauna, and water pollution (Gaviria et al., 2023). Regarding human exposure, pesticides are related to nervous diseases like Alzheimer's and Parkinson's. The largest reported pesticide usage across all classes was herbicides, at 44%, followed by insecticides (29%), fungicides (26%), and fumigants (1%) (Kalyani et al., 2020). Many biosensors have been created for quick and easy insecticides assessment, however, there are still some drawbacks to the real detection of residues in the environment (Song et al., 2022). POC testing is useful for cutting down on the time and expenses associated with sample preparation and result creation. It also offers ease of use with little training and higher sensitivity. Additionally, in-field

pesticide detection will aid in controlling usage and ensuring correct disposal, thereby reducing its hazardous impact on the environment (Kalyani et al., 2020). The World Health Organization created the acronym "ASSURED" to abbreviate the main characteristics expected from POC solutions: affordable, sensitive, specific, user-friendly, rapid and robust, equipment-free, and deliverable to end-users (Kalyani et al., 2020).

In this work, we developed a portable device to detect an insecticide in natural water sources. We selected chlorpyrifos (CPF) as a model compound since it is one of the main active principles used in Colombia, in a wide range of crops. CPF and CPF-oxon, as common bioactive products, block AChE and damage the nervous system (Gaviria et al., 2022b). Our device was designed specially to integrate fluorescent probes previously developed (Gaviria et al., 2022b), based on Carbon quantum dots (CD), Graphene oxide (GO), and enzyme/aptamers like recognition biomolecules. The instrument meets the requirements for POC technologies since it used a low amount of reagents, and it's portable and easy to integrate. Moreover, the device consists of basic electronic circuits and a simple user interface. Our technology is one of the few developments based on optical transduction allowing single pesticide detection (Mukherjee et al., 2022). Finally, we evaluated the device for the detection of spiked CPF concentrations in superficial water samples taken from different sites in Antioquia, Colombia. The results showed that our Instrument is a promising alternative for the sensible detection of CPF in close-to-real environments.

6.2. Materials and methods

Portable device

The portable prototype was made for fluorescence transduction. The operation is based on the modulation of the fluorescence suffered by the CD nanomaterial as a fluorescent transducer, when in the presence of the pesticide (or interest pollutant). This nanomaterial is pyrolytically synthesized from the residual African oil palm biochar and has also been characterized and standardized in our previous work (Barrientos et al., 2021). Detection is carried out by acetylcholinesterase enzyme (AChE) (Gaviria et al., 2022b) or aptamers (Gaviria et al., 2022a) into the CD. The pesticide concentration will be proportional to a fluorescence recovery (turn-on mode). The prototype is designed for the measurement of fluorescence in a cuvette (liquid medium, portable, 150 µL per sample) and is made up of the following elements:

- A measurement cell that allows the integration of light sources and detectors, as well as their isolation from ambient light. The excitation light is generated by an LED (Light emitting diode) type source at 325+5 nm (DUV325-FW5 (Roithner LaserTechnik). The detection of the emitted fluorescence is carried out using a photodiode (BPW34 (Vishay Semiconductors), coupled to a "High-pass" type optical filter with a cut-off wavelength of 400nm+/-8nm, pass lengths of 425nm - 1600nm and rejection lengths of 200nm - 375nm (15-210 Edmund Optics).

- A circuit in charge of the conditioning and acquisition of the fluorescence signals, as well as the control of the prototype and its communication with other systems. The circuit consists of a microcontroller as the central element (PIC32MX250F128B (Microchip Technology Inc), a high-resolution analog-to-digital converter (AD7495 Analog Devices), amplifiers for signal conditioning (LMC6081 de Texas Instruments, and a current-controlled driver for driving the LED. In addition, it has USB and UART communications interfaces for integration with other systems.
- A user interface developed with Python programming and the PyQt5 graphical library. With USB communication and serial communication through a virtual port. The prototype is equipped with a user interface using a touch screen and local data storage. The interface allows the user to adjust different parameters: dark time adaptation, light time, cycles, LED intensity, and Gain. The last two parameters were found the most relevant for the prototype operation in preliminary assays (not shown).

Characterization techniques and instrumentation

To compare the results obtained with the prototype, fluorescence measurements (spectrum and punctual) were done in a Varioskan Lux (Thermo scientific, SkanIt Software 4.1) on a 200 µL working volume microplates (Falcon™ non-treated black 96-well) at 25°C with 1 nm optical step. Also, for the verification of the recovery in spiked samples, UPLC MS-MS chromatography was used as standard gold (Water manufacturer; Xevo TqD, UPLC-HClass; serial MS QCA032; pump F11QSM343A; Injector F11SDI5616). Starna 225 µL quartz cells (AF002, path length 3mm, work range 170 nm to 2700 nm, 5.5 mm x 5.5 mm x 30 mm) were used for the fluorescence measurement in the portable prototype.

Evaluation of the prototype for CPF detection

Detailed information about reagents, the development of the conjugates, and the protocol for the detection of CPF for the enzymatic (Gaviria et al., 2022b) and aptameric (Gaviria et al., 2022a) probes can be consulted in our previous works. For the prototype evaluation, 150 µL of the detection solutions were added to the special cell used for the fluorescence intensity measurements. The parameters for the aptameric system were 101 and 63, for gain and LED intensity respectively. For the enzymatic system, low recovery was seen for the above parameters, so 1001 and 63 for gain and LED respectively, were explored. In both systems, the dark period was zero and the light period was 10 s. The recovery at emission and excitation wavelengths of 420 and 320 nm (respectively) was recorded through 5 cycles and plotted against the CPF concentrations. The first cycle was obviated since represents the “warm-up” of the system. For the estimation of the limits of detection (LOD) and quantification (LOQ), a semi log plot in the linear range was generated and the parameters of the curve were used to estimated LOD as the concentration corresponding to the mean blank value plus 3 times the standard deviation (SD) of the blank (Takahashi et al., 2021). The LOQ was defined in the same way, considering a 10 times parameter. All experiments were treated and analyzed in

triplicate. For LOD calculations, a one-way ANOVA was performed using R-studio software and $p \leq 0.05$ was considered statistically significant.

Evaluation of the prototype for CPF recovery in real samples

Before the evaluation of the real samples, three samples and one CPF concentration was selected for an optimization assay. This analysis was made to find the influence of two factors of the prototype (Gain and intensity of the LED) in the fluorescence recovery (percentage) for the enzymatic system. The data was used to optimize the combination of those factors and applied to the superficial water samples evaluation. A two-way ANOVA was performed using R-studio software and $p \leq 0.05$ was considered statistically significant.

Superficial water samples were taken from 9 different locations in the department of Antioquia, Colombia. Physicochemical parameters of superficial water samples were determined with different instrumentation, following the standard methods for pH (SM 4500 H+ B; Ed 23 2017), temperature (SM 2250B; Ed. 2017), electric conductivity (SM 2510 B; Ed. 23, 2017), true color (SM 2120 C; Ed 23 2017), and COD (SM 5220 D; Ed. 23, 2017). The results were correlated with the detection assay.

Since the UPLC/MS evaluation showed no CPF detection, the samples were used as an actual matrix for the experimental procedure of spiked samples. For each sample, 4 CPF concentrations were used (0.1, 1, 10 y 100 µg L^{-1}). The recoveries using the enzymatic system both, in the Varioskan Lux and the portable prototype, were compared with UPHLC/MS as standard gold. All experiments were treated and analyzed in triplicate and the %RSD parameter was estimated. R-studio and Microsoft Power BI were used for the graphical exploration of the data.

6.3. Results and discussion

Design principles of the portable prototype

In the fluorescence of biosensors, a light source (of the appropriate wavelength) is necessary to achieve the excitation of the biological material. In addition, an optical detector is necessary to allow an electrical signal to be obtained from the light emitted by the biological material, and an optical filter that avoids (or reduces) the erroneous quantification of excitation light as emitted light (Tjandra et al., 2019). In this application, the chosen light source is an LED. Its low power and ease-of-use features make it ideal for today's low-cost, portable applications. In addition, LED technology allows devices with low spectral bandwidth to be obtained, facilitating the filtering and detection stage. The developed system shown in Figure 6-1, allows the integration of different types of LEDs. However, to ensure compatibility with the excitation spectrum of the biomediators used in this project (CD) a led of 325 ± 5 nm with a bandwidth of 11 nm was implemented. Figure 1B highlighted

the 90° disposition between the LED and the photodiode since preliminary tests showed that alineation like the best for increasing the fluorescence signal.

The LED drive consists of a controlled current source, which can be digitally driven via SPI (Serial Port Interface) communication. This circuit was implemented using the TLC5917 integrated circuit from Texas Instruments. The TLC5917 allows handling 63 different current levels for the excitation LED (where 0 corresponds to 0 mA and 63 to 20 mA), allowing its brightness to be varied. The mentioned allows the adaptation of the equipment to the most favorable measurement conditions for different biomediators. In the current application, the maximum current level for driving the LED was set to 20 mA.

Regarding analogic data processing, this stage allows conditioning of the output signal of the photodiode (current in the order of microamperes) to allow its subsequent digitization. It consists of two amplification stages: A trans-resistance amplifier and a programmable gain amplifier. Optionally, there is the possibility of reverse biasing the photodiode to increase its speed (not used in the current application). Both amplification stages were implemented using precision operational amplifiers, reference LMC6081 from Texas Instruments. The first stage (trans resistance amplifier) performs the conversion of the photodiode current to an output voltage, with a gain of 10MV/A. The second stage further amplifies said voltage, with a gain that can be selected between the following values: 1, 11, 101, and 1001.

To transform the analogic data into a digital one, the amplified signal is taken to a conversion process. For this, the integrated circuit AD7495 from Analog Devices is used. This ADC (Analog to digital converter) has an SPI communication interface, and provides a conversion speed of up to one million samples per second. For the conversion, a resolution of 12 bits is available, which allows arbitrary units for fluorescence detection in the range of 0 to 4095. The voltage reference (needed for the conversion process) is built into the AD7495, allowing for less circuit complexity and cost.

For the communication of the system, two different methods were implemented: USB communication and serial communication. Both methods provide the same functionalities, but both are implemented to allow greater flexibility when interfacing with different systems (personal computers, embedded computers for sensor networks, etc). USB communication was implemented on a virtual serial port model, so that for both cases, from the point of view of the user system, it is serial communication. The implemented communication protocol is based on a serial terminal-type system, with a series of defined commands that allow the system to initiate measurements or even carry out verification operations (operation tests). Briefly, the implemented commands are shown in Table 6-1.

Finally, for proper operation, the fluorescence system requires a 5 VDC power supply. The respective voltage regulators have been implemented internally to obtain a 3.3 VDC power supply required for the digital logic systems. A voltage reference for reverse biasing of the photodiode has also been implemented (for future applications).

Table 6-1. Implemented measurement commands in the portable prototype

Command and parameters	Value Range
Slow: I start the fluorescence measurement process, using a slow sampling frequency (5 samples per second).	-
DarkMins: Number of minutes of darkness (for adaptation of the biological material).	0-100 min
Lightsecs: Duration of light stimulation (in seconds).	0-100 s
Cycles: Number of cyclic repetitions of the measurement process.	0-100 cycles
Gain: Gain for the programmable gain amplifier.	0= Gain 1 1= Gain 11 2= Gain 101 3= Gain 1001
LedLevel: control the current for the excitation of the LED.	0-63 (20 mA)

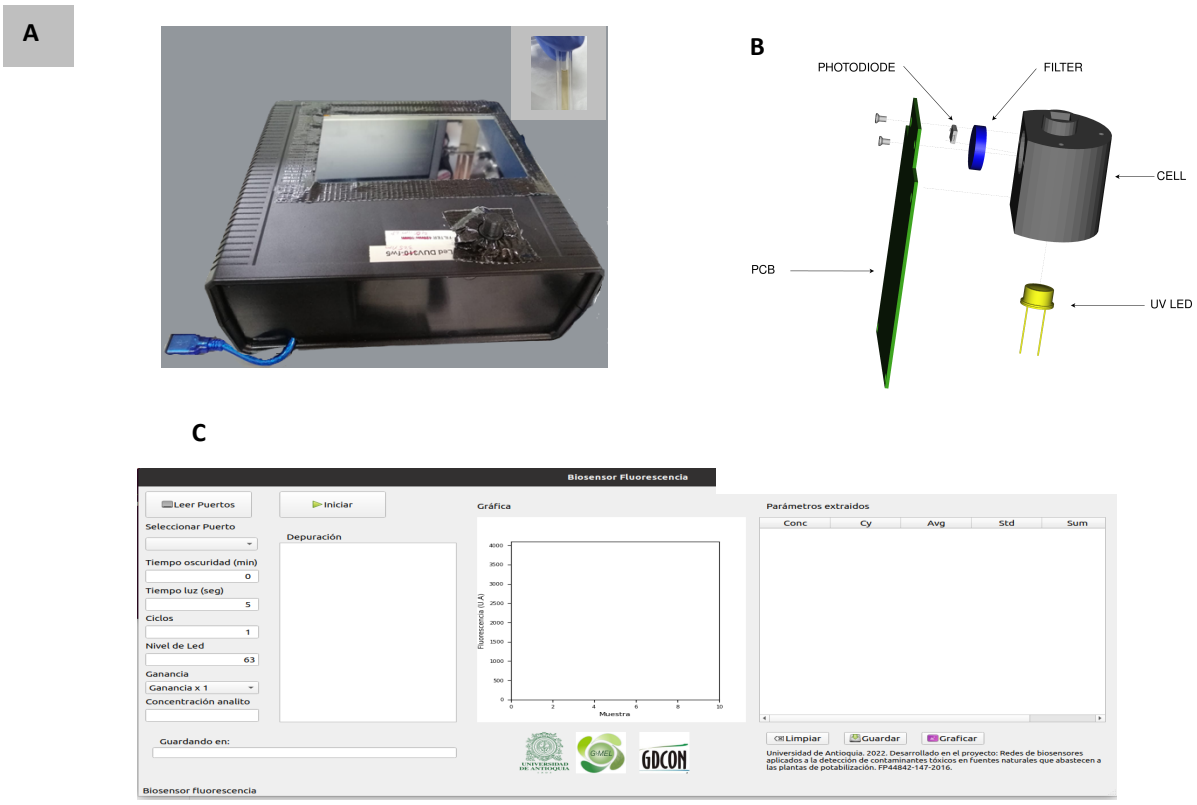

Figure 6-1. A) General schematic illustration of the portable device for pesticide detection. The insert shows the measuring cell. B) 3D representation of the disposition of the optical components, highlighting the 90° position between de LED and the photodiode. C) Detailed of the electronic interface.

CPF quantification in the prototype using two fluorescent probes

For the aptameric system, Figure 6-2A shows a good linear relationship of fluorescence with the natural logarithm of CPF concentration between 0 and 7.5 µg L^{-1} (0 to 21.6 nM). The linear regression equation for this range (R2= 0.91, ***p < 0.001, n=3) was F = 49.92 + 5.2175 Ln C, where F and C are the fluorescence intensity and CPF concentration, respectively. The LOD and LOQ were calculated as low as 0.079 µg L^{-1} (0.196 nM) and 0.79 µg L-1 (1.96 nM) respectively. Even though the linear range is conserved, the LOD is higher than our previous work with the same aptameric system but using a Varioskan Lux (Thermo scientific, SkanIt Software 4.1) for the signal acquisition (Gaviria et al., 2022a). This behavior is expected, since portable instruments could have higher standard deviation values, affecting the LOD establishment. However, the current LOD is still low enough to consider this system highly sensible. Additionally, the system is still useful for CPF detection below de limits established by Colombian law (Ministerio de la protección social, 2007).

Regarding the enzymatic system, Figure 6-2B shows a good linear relationship of fluorescence with the natural logarithm of CPF concentration between 0 and 0.1 mg L^{-1} (0 to 285.2 nM). The linear regression equation for this range (R2= 0.92, ***p < 0.001, n=3) was F = 433.42 + 30.914 Ln C. The LOD and LOQ were calculated as low as 0.082 µg L^{-1} (0.23 nM) and 0.82 µg L^{-1} (2.34 nM) respectively. In this case, the LOD is lower compared to our previous work (Gaviria et al., 2022b). Moreover, the wide linear range is better for the implementation in field samples. For this reason, only the enzymatic system will be used for the assays of CPF recovery from superficial water samples in the next section.

The fluorescence recovery behavior with the portable prototype was compared to data obtained from the commercial Varioskan Lux both, for the aptameric and enzymatic systems. For the aptameric system, the results shown in Figure 6-2C suggest a good agreement between the two methods. However, with the prototype is possible to appreciate differences among different concentrations. This is especially true for the higher values of CPF. Regarding the enzymatic system in Figure 6-2D, the results in the prototype allow identifying the increase in the fluorescence signal (directly associated with CPF detection) masked in the Varioskan at higher concentration values. Moreover, the standard error for the prototype is lower in this case, explaining the improvement in the LOD value. The increase in the resolution for the two biological probes is evidence of the better performance that nanomaterials like CD offer to optical biosensors (Hu et al., 2021). The combination of the CD, with the biomolecules and the modulation with GO, is potentialized by the development of a prototype with an optical system designed and constructed specifically for biological phenomena.

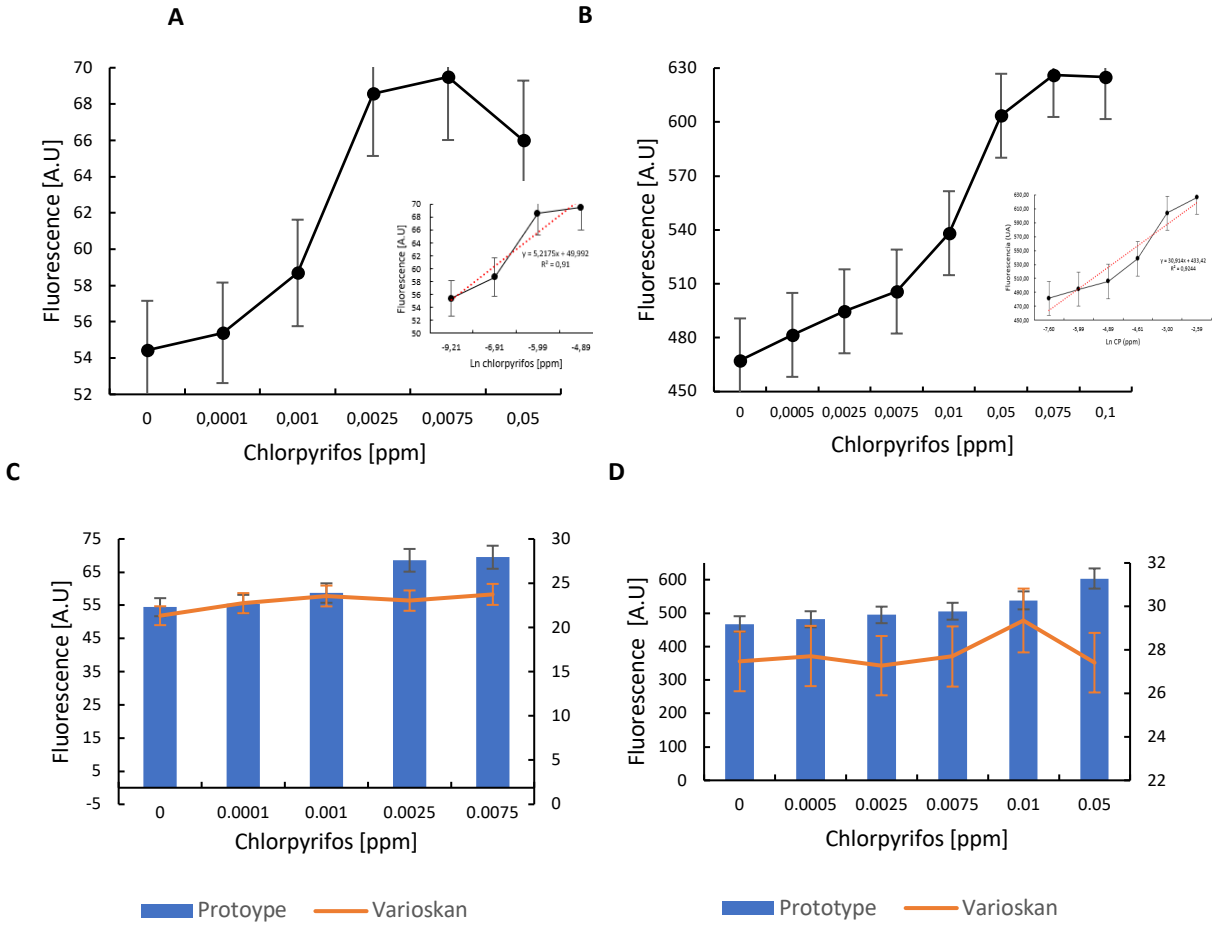

Figure 6-2. . Prototype evaluation showing the exponential relationship between the Fluorescence intensity (λem = 420 nm) and the concentration of chlorpyrifos for A) the aptameric system and B) the enzymatic system. Comparison of the fluorescence intensity depending on the chlorpyrifos concentration using the portable prototype and the varioskan for C) aptameric system and D) enzymatic system. n= 3 independent experiments.

Prototype performance for CPF recovery in real samples

Using the enzymatic system, an optimization assay was performed using the data of three superficial water samples, and a spiked CPF concentration of 1 µg L^{-1} (central point). The results showed that only the Led intensity has a direct influence on the fluorescence recovery percentage (***$p < 0.001$, n=4). Neither gain nor the interaction between the factors is relevant in the prototype operation. This is important because working at higher gain values has been shown to increase the error in the measurements, so for the evaluation of the 9 samples and the comparison with the gold standard, the data acquired at Led 63 and Gain 101 will be used. Although the interaction is insignificant, a response surface graph was made, showing a tendency for higher fluorescence recovery for the highest values of both factors (Figure 6-3).

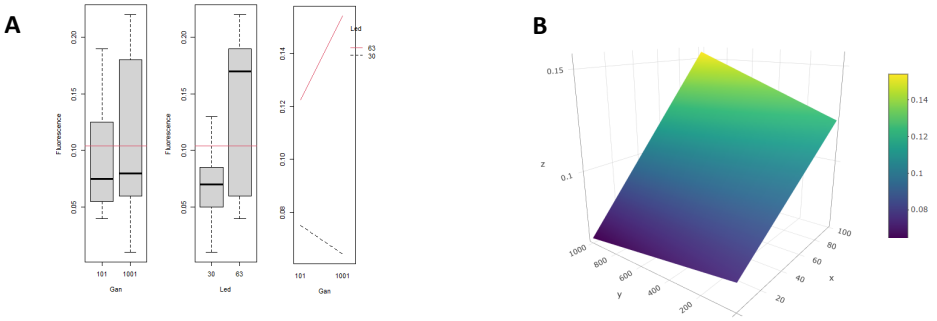

Figure 6-3. A) Mean plots and interaction graphs for the gain and the led intensity as relevant factors. B) Response Surface of the model (x= Led, y= Gain, z= fluorescence recovery percentage).

The 9 samples were taken from three different sites in the department of Antioquia, Colombia. The description of main sites and some physicochemical parameters are described in Table 6-2.

Table 6-2. Physicochemical parameters of the superficial water samples

Site	Sample number	Description	pH	Electric conductivity (µS/cm)	Color (UC)	COD (mg /L)
Santa Elena locality	1	Santa Elena creek high part	6.18	1368	14.8	<25.0
	2	"Chorro clarín" creek	5.95	1407	13.0	<25
	3	Santa Barbara creek	6.92	1410	<10	<25
San Cristóbal Locality	4	San Cristobal creek "La Iguaná"	6.84	81	<10	<25
	5	"Los azules" creek	7.10	67	<10	<25
	6	"La iguaná" upstream	6.83	37	<10	<25
	7	"Hato" creek	6.33	19	28.0	<25
	8	"La Aurora" creek	7.22	107	<10	<25
Rio Grande reservoir	9	Rio Grande reservoir	6.50	53	39.6	36.4

The nine samples were spiked with different CPF concentrations (0.5, 1, 10,100 µg L^{-1}) and the percentage of the recovery in the prototype was compared with UHPLC-MS as standard gold. The complete results are listed in Table 6-3. A general analysis could be made based on the exploratory graphics presented in Figure 6-4. Power BI software was used to compare the average recovery of the prototype with the UHPLC in the three main sites (Figure 6-4A), we can see that the prototype presents more variations than the standard, as was expected. Also, the recovery is higher in the Santa Elena locality (samples 1 to 3), which is also the site with the highest electric conductivity. The recovery of the prototype seems to be influenced by the electric conductivity since this response decreases directly with the ionic concentration in the samples. This behavior was reported

previously for other biomolecules (Park et al., 2022). The average recoveries were 65.88 % and 80.77% for the prototype and UHPLC respectively.

For the prototype, the recovery rates were found between 24.05% and 186.52%, with an average RSD of 5.05% (a maximum atypical value of 15.98% was found for sample number 3). The high variation in the recovery range suggests that it is still a lot to optimize for both, the fluorescent probe, and the processing signal of the prototype. However, considering the novelty of the developed fluorescent probe and the integration with nanomaterials, this is a promising solution for the on-site detection of CPF.

Getting deeper into the influence of the different physicochemical parameters in the recovery for the prototype, Figure 6-4C shows the mean graphs of the recovery values as a function of those parameters. We can see that perhaps the electric conductivity seems to be relevant, and the figure shows a certain patron, but this is not significant. The same conclusion could be made for the other parameters evaluated (pH, color, and COD). In this case, the behavior is almost completely random, and the parameters were not significant to the recovery. Figure 6-4B shows that the accuracy (recoveries closer to 100%), seems to be different among the two systems. That means, for the UHPLC more CPF concentration leads to higher recoveries. Contrary, for the prototype, the lowest values (0.5 µg L-1) are closer to 100% and sometimes are overestimated; but high concentration values lead to an underestimation probably for a saturation phenomenon.

Regarding specific site analysis, we can see that the different samples from the Santa Elena locality are relatively similar in the physicochemical parameters like the prototype results. For these samples, a higher overestimation for 0.5 µg L^{-1} was seen. San Cristobal samples had a higher variability for the electric conductivity parameter, impacting the recovery in the prototype. Finally, Rio grande was the most atypical sample, since the COD and color were high. Two of the fourth spiked CPF concentrations were not detected at all. Those kinds of results were analyzed in our previous work (Gaviria et al., 2022a) where this sample was not detected at any concentration. The role of humic substances and other compounds related to dissolved organic matter should be further investigated.

As a general conclusion of this section, the portable prototype when in use with an enzymatic probe can accurately assess >2.85 nM (1 µg L^{-1}) of CPF in superficial waters using only 150 µL of the sample. However, the need for some kind of pretreatments and advanced research about the more detailed influence of physicochemical parameters on recovery is urgent before the possibility of commercial implementation.

Table 6-3. Recovery of CPF from real samples using the prototype. n=4

Sample	Spiked (µg L^{-1})	Measured by prototype (µg L^{-1})	% Recovery (Prototype)	% RSD	Measured by UHPLC (µg L^{-1})	% Recovery (UHPLC)
1	0.5	0.52	103.18	1.44	0.36	72
	1	0.24	23.82	2.07	0.7	70
	10	7.21	72.14	1.33	10.05	100.5
	100	24.05	24.05	1.51	79.60	79.60
2	0.5	0.93	186.52	1.71	0.43	86.00

	1	0.59	58.67	1.82	0.76	76.00
	10	2.87	28.74	0.96	10.05	100.50
	100	55.76	55.76	2.69	87.45	87.45
3	0.5	0.82	164.48	15.98	0,39	78,00
	1	0.36	35.89	1.02	0,77	77,00
	10	6.62	66.22	10.94	8,67	86,70
	100	29.12	29.12	4.06	98,77	98,77
4	0.5	0.23	46.13	5.90	0.41	82
	1	0.69	68.83	10.28	0.81	81
	10	2.80	27.97	3.82	8.32	83.2
	100	79.01	79.01	10.57	101.15	101.15
5	0.5	0.62	124.64	2.83	0.33	66.00
	1	1.12	112.28	5.63	0.81	81.00
	10	5.62	56.17	12.59	7.36	73.60
	100	33.44	33.44	11.86	82.37	82.37
6	0.5	0.27	54.05	2.71	0.38	76.00
	1	0.77	77.30	2.74	0.65	65.00
	10	15.75	157.49	7.66	8.40	84.00
	100	52.64	52.64	4.52	99.46	99.46
7	0.5	0.70	139.91	7.53	0.37	74.00
	1	0.33	32.94	9.21	0.72	72.00
	10	7.91	79.08	6.94	8.05	80.50
	100	22.62	22.62	1.25	85.51	85.51
8	0.5	0.41	81.23	8.21	0.36	72,00
	1	0.57	56.91	10.97	0.72	72,00
	10	3.49	34.85	6.37	8.07	80,70
	100	29.61	29.61	3.64	85.33	85,33
9	0.5	-	-	-	0.37	74.00
	1	1.38	137.84	0.85	0.74	74.00
	10	-	-	-	8.07	80.70
	100	18.14	18.14	0.29	84.33	84.33

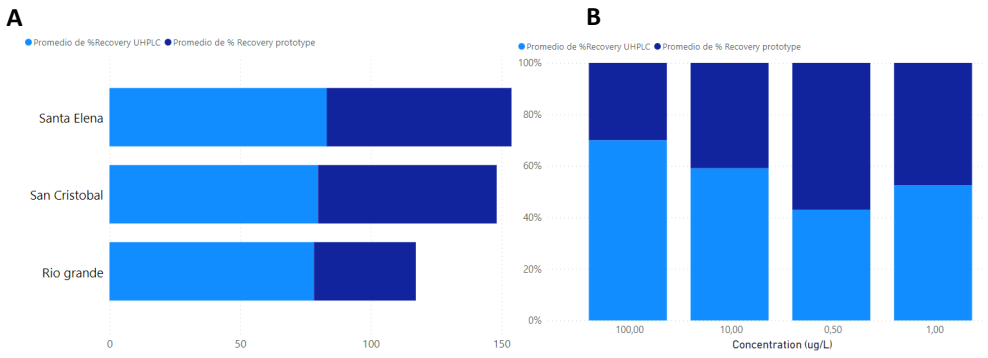

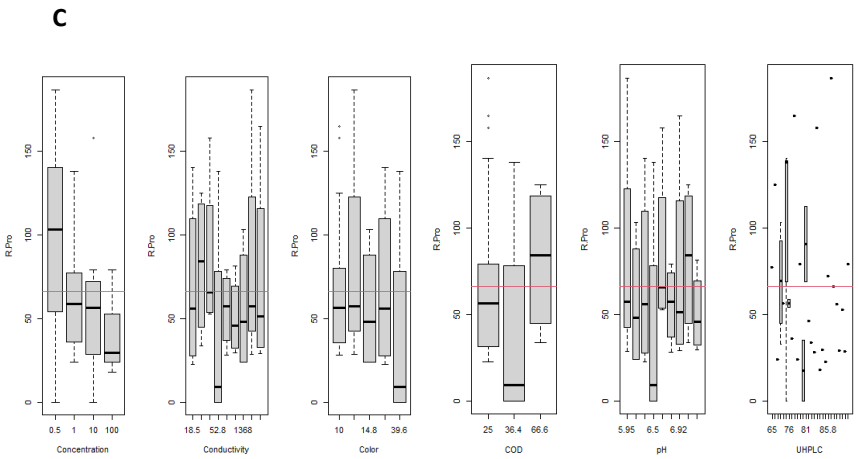

Figure 6-4. A) Average % of the recovery for the prototype (dark blue) and UHPLC (light blue) in three main sampling sites B) Average % of the recovery for the prototype and UHPLC as a function of the CPF concentration. C) Mean plots showing the % of the recovery in the prototype as a function of (left to right): CPF concentration, electric conductivity, color, COD; and the correlation with the % of the recovery in UHPLC.

Potential market for optical biosensors market in environmental monitoring

In the last decade, biosensors and nanometric strategies have shown promise in meeting the growing demand for environmental monitoring, offering fast, selective, and easy-to-use portable platforms for the detection of pollutants in water. The world market for biosensors is estimated at USD 24.9 billion by the year 2021 and is expected to grow at an annual rate of 8.0% by the year 2030 (Grand view research, 2021), with optical-type biosensors having a great role due to their versatility, which will make its growth rate higher than the average market rate (8.9%) (Grand view research, 2021). The on-site testing or "Point of care" (PoC) segment has been dominating the biosensor market and accounted for the largest share of revenue at about 49.6% in 2020 (Grand view research, 2021). Technological advances and novel product development such as ultra-sensitive printable biosensors for on-site testing applications for toxin and pesticide detection are among the main drivers of segment growth during the forecast period. However, the medical segment dominated the biosensor market and accounted for the largest share of revenue at 66.6%.

Few commercial biosensors are available for environmental monitoring applications, in contrast to medical biosensors. Among environmental applications, portable sensors for water physical parameters have been largely available, but for specific pollutants, sensor portability has been less well addressed. Before they can be used in natural water monitoring, most of the currently available biosensors must be greatly enhanced in terms of sensitivity, selectivity, functionality, etc.

Biosensors have been developed for both organic substances and heavy metals. Among commercial optical biosensors, is worth highlighting the Surface plasmon resonance (SPR) sold by SENSIA in

Spain for the detection of carbaryl; also the low-cost and portable SPR sensor commercialized by Texas Instruments Inc for tracking various biomolecule contaminants in soil or water (Ejeian et al., 2018).

More than 3.000 results are found in the World intellectual property organization database (Patentscope) for optical biosensors and pesticides detection in water (World intellectual property organization, 2022). The main country of registration is the USA, and the top 5 applicant institutions are: 1) Genentech inc, 2) Pivot Bio inc, 3) Clinical micro sensor inc, 4) the University of California and 5) the University of Michigan. In the last 10 years, the period with the highest amount of applications was 2020, but the growing trend is still. The unbalanced between patents and current commercial products could be explained by growing technology advances but restrictive regulation for real implementation.

6.4. Conclusions

A portable prototype for on-site detection of CPF was designed, constructed, and evaluated. The optimization steps of the system suggest that contrary to the aptameric systems, enzymatic fluorescent probes are good enough for future use in real-sample detection. The enzymatic probe is made of CD as a fluorescent transductor, Acetylcholinestare enzyme, and modulation with GO as we reported in our previous works. The LOD of the enzymatic probe in the portable transductor improves compared with the commercial lab equipment Varioskan Lux. This result suggests the effectiveness of the specific LED, filter, and photodiode combination for the performance of the assays, as well as the advanced signal processing. The evaluation of the system in nine superficial water samples showed that without any type of pretreatments and using only 150 µL of the sample, the system could detect CPF accurately from 1 µg L^{-1} (2.85 nM), with great improvement potential and tolerable %RSD. The market for optical biosensors applied to environmental monitoring is still in an early stage, so this type of development paves the way for field implementation. Different routes for system improvement could be addressed. Since the specificity and sensibility of the current system have been improved with the incorporation of nanomaterials, the hot topics to keep working on are i) increasing the repeatability, ii) improving the accuracy related to the standard gold, iii) working on the portability and usability of the systems with cloud-based interfaces and iv) developed simple instructions for the users.

6.5. References

Barrientos, K., Gaviria, M.I., Arango, J.P., Londoño, M.E., Jaramillo, M., 2021. Synthesis, Characterization and Ecotoxicity Evaluation of Biochar-Derived Carbon Dots from Spruce Tree, Purple Moor-Grass and African Oil Palm. Processes 9, 16.

Ejeian, F., Etedali, P., Mansouri-Tehrani, H.A., Soozanipour, A., Low, Z.X., Asadnia, M., Taheri-Kafrani, A., Razmjou, A., 2018. Biosensors for wastewater monitoring: A review. Biosens Bioelectron 118, 66–79. https://doi.org/10.1016/j.bios.2018.07.019

Gaviria, M.I., Arango, J.P., Barrientos, K., Cano, J.B., Peñuela, G., 2022a. Ultra-sensible nanostructured carbon dot- aptasensor for chlorpyrifos detection: a molecular analysis of the interaction mechanism.

Gaviria, M.I., Arango, J.P., Barrientos, K., Jaramillo, M., 2023. Optical Biosensors for Environmental Analysis, in: Encyclopedia of Sensors and Biosensors. Elsevier, pp. 528–548. https://doi.org/10.1016/b978-0-12-822548-6.00156-4

Gaviria, M.I., Barrientos, K., Arango, J.P., Cano, J.B., Peñuela, G.A., 2022b. Highly sensitive fluorescent biosensor based on Acetylcholinesterase and carbon dots-graphene oxide quenching test for analytical and commercial organophosphate pesticide detection. Front Environ Sci 10, 1–13. https://doi.org/10.3389/FENVS.2022.825112

Gaviria-Arroyave, M.I., Cano, J.B., Peñuela, G.A., 2020. Nanomaterial-based fluorescent biosensors for monitoring environmental pollutants: A critical review. Talanta Open 2, 100006. https://doi.org/10.1016/j.talo.2020.100006

Grand view research, 2021. Biosensors Market Size, Share & Trends Analysis Report By Application (Medical, Agriculture, Environment) By Technology (Thermal, Electrochemical, Optical), By End-use, By Region, And Segment Forecasts, 2021 - 2028 [WWW Document]. Market analysis report. URL https://www.grandviewresearch.com/industry-analysis/biosensors-market (accessed 4.24.21).

Hu, J., Sun, Y., Aryee, A.A., Qu, L., Zhang, K., Li, Z., 2021. Mechanisms for carbon dots-based chemosensing, biosensing, and bioimaging: A review. Anal Chim Acta 338885. https://doi.org/10.1016/j.aca.2021.338885

Kalyani, N., Goel, S., Jaiswa, S., 2020. Point-of-Care Sensors for On-Site Detection of Pesticides, in: Nanosensors for Environmental Applications. Springer, pp. 197–224.

Liao, Z., Wang, J., Zhang, P., Zhang, Y., Miao, Y., Gao, S., 2018. Biosensors and Bioelectronics Recent advances in micro fl uidic chip integrated electronic biosensors for multiplexed detection. Biosensors and Bioelectronic 121, 272–280. https://doi.org/10.1016/j.bios.2018.08.061

Liu, D., Wang, J., Wu, L., Huang, Y., Zhang, Y., Zhu, M., Wang, Y., Zhu, Z., Yang, C., 2020. Trends in Analytical Chemistry Trends in miniaturized biosensors for point-of-care testing. Trends in Analytical Chemistry 122, 115701. https://doi.org/10.1016/j.trac.2019.115701

Ministerio de la protección social, 2007. Resolución 2115/2007. Gaceta Oficial 23. https://doi.org/10.1017/CBO9781107415324.004

Mukherjee, S., Ghosh, K., Bhattacharyya, S., Behera, B.K., Singh, O.K., Pal, S., 2022. A Review on Recent Trends in Advancement of Bio-Sensory Techniques Toward Pesticide Detection. Food Anal Methods. https://doi.org/10.1007/s12161-022-02382-4

Myers, F.B., Lee, L.P., 2015. Innovations in optical microfluidic technologies for point-of-care diagnostics † 2015–2031. https://doi.org/10.1039/b812343h

Park, J., Yang, K.A., Choi, Y., Choe, J.K., 2022. Novel ssDNA aptamer-based fluorescence sensor for perfluorooctanoic acid detection in water. Environ Int 158. https://doi.org/10.1016/j.envint.2021.107000

Song, D., Liu, J., Xu, W., Han, X., Wang, H., Zhuo, Y., Li, C., Long, F., 2022. On-site rapid and simultaneous detection of acetamiprid and fipronil using a dual-fluorescence lab-on-fiber biosensor. Microchimica Acta 189. https://doi.org/10.1007/s00604-022-05327-0

Takahashi, R., Yasuda, T., Ohmuro-Matsuyama, Y., Ueda, H., 2021. BRET Q-Body: A Ratiometric Quench-based Bioluminescent Immunosensor Made of Luciferase-Dye-Antibody Fusion with Enhanced Response. Anal Chem 93, 7571–7578. https://doi.org/10.1021/acs.analchem.0c05217

Tjandra, A.D., Chang, J.Y.H., Ladame, S., Chandrawati, R., 2019. Optical sensors, in: Bioengineering Innovative Solutions for Cancer. Elsevier Ltd., pp. 23–45. https://doi.org/10.1016/B978-0-12-813886-1.00003-6

World intellectual property organization, 2022. PATENTSCOPE database [WWW Document]. Optical biosensor for pesticide and water.

7. Thesis conclusions and future outlook

Carbonaceous nanomaterials, specifically Carbon quantum dots (CD) Significantly improved the sensibility and selectivity of the fluorescence biosensors when in combination with enzymes and aptamers. The use of CD allowed the quantification of chlorpyrifos as a model organophosphate pesticide (OP) with an ultra-low limit of detection (LOD), even in a complex matrix like superficial water.

Optical biosensors based on the Foster energy transfer (FRET) phenomenon between a fluorescent donor (CD) and a quencher (Graphene oxide-GO) were constructed using two different biomolecules: cholinesterase-type enzymes and aptamers. Using FRET, the developed biosensors operate in a "turning-on" mode, showing a fluorescence recovery signal proportional to the concentration of the pesticide.

Enzymatic systems based on acetylcholinesterase enzyme (AChE) have been extensively used for OP determination and showed good sensibility and stability, but poor selectivity. In this work, the use of CD and GO along with AChE, allowed us to efficiently detect chlorpyrifos with good LODs and selectivity compared with other works. The system was optimized to use lower amounts of reagents and follow a short protocol. However, the stability of the systems should be improved beyond 8 days to allow real-field applications.

Aptameric systems have been reported as highly sensible and selective, and those features were proven in this work using the same platform based on CD and GO. The optimization of aptameric systems implies a deep knowledge of the molecular mechanisms behind the interaction with targets, especially with small molecules like chlorpyrifos. In this work, the application of easy-to-use bioinformatic tools allowed us to identify the sites and types of interactions, projecting the possible construction of a small or "truncated" aptamer with improved stability against interference conditions.

Even if commercial nanostructured biosensors have increased in the last years for medical use, environmental monitoring applications remain overdue. In this work, a portable device based on the fluorescent transduction of CD for chlorpyrifos detection was developed. The evaluation of the device in lab samples showed an improved LOD for the enzymatic system, attributable to the lower noise and the tailored design. The evaluation of the portable device in superficial water samples obtained from rural areas of Antioquia showed, in some cases, acceptable recovery levels compared to chromatographic techniques. However, the influence of physicochemical parameters like electric conductivity (due to the presence of some ions) seems to have a potential interference effect on the prototype performance.

Finally, we can conclude that fluorescent biosensors are promising alternatives for on-site detection of environmental concern pollutants like pesticides. The integration of nanomaterials and tailored-

made devices is key to fostering the commercial implementation of those systems. To reach the mentioned, some hot topics should be addressed in the next research steps:

- Optimize the chemical characteristics of the synthesized CD and work for more environmental-friendly options in the synthesis process.
- Explore the use of lateral flow assays for improving the stability of the developed fluorescence probes (aptameric and enzymatic systems).
- When working in a liquid medium, apply some processes for the protection of the DNA aptamer against interference mechanisms.
- Develop low-cost and simple sample pretreatment steps to avoid the ionic influence on pesticide detection.
- Improve the design of the portable device to allow more portability and cloud data storage.

8. Appendix I: Synthesis, Characterization and Ecotoxicity Evaluation of Biochar-Derived Carbon Dots from Spruce Tree, Purple Moor-Grass and African Oil Palm.

Abstract

Biochar-derived C-Dots from *Picea, Molinia caerulea* and *Elaeis guineensis* were synthesized through a hydrothermal process, and their physicochemical and optical characteristics and environmental effects were compared. These C-Dots were characterized by techniques such as Attenuated Total Reflection–Fourier Transform Infrared (ATR-FTIR), UV-Vis spectrophotometry, fluorescence spectroscopy, dynamic light scattering (DLS), Z potential, and High-Resolution Transmission Electronical Microscopy (HR-TEM). The ecotoxicity tests were performed using the Microtox™ test, making this study one of the few that use this method. The C-Dots from *Molinia caerulea* showed the best quantum yield (QY) of 8.39% and moderate ecotoxicity, while *Elaeis guineensis* has the lowest QY (2.31%) but with zero toxicity. Furthermore, the C-Dots from *Picea* presents good optical properties but showed high toxicity and limits its use. Finally, all C-Dots showed functional groups that could be biofunctionalized with biomolecules, especially C-Dots from *Molinia caerulea* and *Elaeis guineensis* show potential for use in the development of optical biosensors.

Keywords: biochar; carbon dots; nanoparticle; fluorescence; ecotoxicity

Published in:
Procesess. MDPI
Date: June 24, 2021
Cite as:
Barrientos, K., Gaviria, M. I., Arango, J. P., Londoño, M. E., & Jaramillo, M. (2021). Synthesis, Characterization and Ecotoxicity Evaluation of Biochar-Derived Carbon Dots from Spruce Tree, Purple Moor-Grass and African Oil Palm. *Processes*, *9*(1095), 16.
https://doi.org/10.3390/pr9071095

8.1. Introduction

Non-pollutant energy access is one of the sustainable development goals defined by the United Nations (UN) to achieve sustainability by 2030 [1], so much research efforts have been focused mainly on the use of plant biomass for energy and biofuels production from high-temperature deconstructive methods such as pyrolysis, gasification, and thermal liquefaction [2–5]. Pyrolysis is a method with complete absence of oxygen and process temperatures around 300–700◦C. The three main products from pyrolysis are synthesis gas (syngas), bio-oils, and biochar [6]. Syngas and bio-oils are widely used for electricity, heat, and biofuel production while biochar is used in bioremediation and amendments processes in soils [6–8]. However, the use of biochar is limited due to the variability of the physicochemical properties that depend on the original biomass and the thermal process conditions. Therefore, alternatives for the use of biochar are necessary for the integral sustainability of the pyrolysis process and to close biological cycles following circular economy principles [9,10]. Biochar from the pyrolysis process usually exhibits a porous and semi-crystalline structure with a large surface area. This kind of structure maintains the surface chemical groups (aromatics and negative charge groups), the mineral compounds and gives it biological resistance [11,12]. Those characteristics make the biochar a good precursor for more add-value carbonaceous materials, like C-Dots [12–14]. Recently, the interest on synthesis strategies for nanomaterials is growing, using waste biomass and biochar [15–18]. Carbon dots (C-Dots) are quasi-spherical nanoparticles that are made mainly from carbon and oxygen, usually with sizes below 10 nm [19–22]. These nanomaterials have gained attention because of their excellent photoluminescence yields and high photostability, which make them comparable to traditional quantum dots, but less toxic for biological systems [19,23,24]. C-Dots are attractive for their application as fluorescent probes for bioimaging [25,26], drug delivery [27–29], and optical biosensors development for environmental [30,31], agroindustry [32,33], and public health [34–37], with detection limits on nM order [38–40]. The obtention of different types of C-Dots depends on the original feedstock, the physicochemical characteristics of the feedstock, synthesis conditions [23], and the doping with heteroatoms and surface modifications [41]. Therefore, the characterization of the feedstock and the synthesized C-Dots is necessary. Currently, C-Dots synthesis includes methods like laser ablation, arc discharge, solvothermal oxidation, hydrothermal treatment, and microwave irradiation. Combining some of these methods like hydrothermal treatment with natural sources or waste materials, like biochar, becomes an excellent strategy for cost reduction, continuous precursor supply, and the obtention of low toxicity nanomaterials [16]. Biochar has been employed as a precursor for C-dots production by different authors and different feedstocks such as sugar cane bagasse [42], microalgae biomass [21], flower waste, ornamentals plants and fruits [15,43]. Besides, the toxicity studies of nanomaterials like C-Dots are significant areas of research since there is a wide debate about the possible risks associated with the widespread use of nanomaterials [44,45]. These risks are correlated with their size, shape, and chemical characteristics that can interact with biological systems causing a blockage of some signaling routes [46]. Although the study of the toxicology effect of C-dots related to human health

is more widespread, the effects of these particles in the environment, especially in aquatic environments are less evaluated and are fundamental to determine the impact of these nanoparticles on water quality, and their effect on the biodiversity of aquatic ecosystems [47–50]. The aim of this article was to compare the physicochemical and optical characteristics and the environmental effects of biochar-derived C-Dots from three different feed-stocks: *spruce tree* (Picea), purple moor-grass (*Molinia caerulea*), and African oil palm(*Elaeis guineensis*). The biochar from *Picea* and *Molinia caerulea* was donated by two welsh companies that produced biochar from two highly produced biomasses in Wales. However, the feedstock of *Elaeis guineensis* was selected because it was intended to use materials available in Colombia to be part of the bioeconomy process. Colombia is the fourth producer of palm oil in the world and the first in America, which makes it generate annually about 400,000 tons of waste (approximately 2% of world production), to which must be added value to contribute to the closing of cycles. The C-Dots were obtained through a hydrothermal method and their chemical structure, toxicity, and stability were characterized through different techniques like FTIR, UV-Vis, Fluorescence spectrophotometry, Z potential, DLS, TEM, and ecotoxicity.

8.2. Materials and Methods

Reagents

Three types of biochar were evaluated in this research, purple moor grass-biochar(*Molinia caerulea*), spruce tree-biochar (*Picea*), and African oil palm-biochar (*Elaeis guineensis*).Purple moor grass-biochar was kindly donated by Henfron Farm (Elan Valley, LD6 5HE,UK) and it was prepared with an Exeter Biocharcoal Retort (Carbon Compost Ltd.; Exeter,UK) in pyrolysis mode and temperatures between 300◦C and 375◦C for 4 h. Spruce tree-biochar was kindly provided by Common Visions LTD (Swansea, Wales, UK). African oil palm-biochar was kindly donated by the "Grupo de Investigación de Energías Alternativas– Centro de Desarrollo Tecnológico del Carbón" research group (GEAB-CIDTEC) from the Universidad Popular del Cesar, UPC Colombia. African oil palm-biochar was prepared at the "Centro Corporación de Investigación de la Palma de Aceite– Cenipalma" and the process involves the pyrolysis of oil palm trunk using FAO (Food and Agriculture Organization of the United Nations) technology and temperatures between 200◦C and400◦C [51]. All biochar were conserved at room conditions until use. Ultrapure water system (Barnstead Smart2Pure, Thermo Scientific, Pittsburg, CA, USA) was used through all the experimental setting. Acetone and potassium permanganate (KMnO4) were bought from Merck Millipore (Burlington, VT, USA). All chemicals were analytical grade.2.2.

Biochar Characterization

African oil palm-biochar and purple moor grass-biochar were characterized by "Grupo interdisciplinario de estudios moleculares" research group (GIEM) from Universidad de Antioquia. The characterization process followed the guide given in the standards NTC5167 for pH and ashes measurement, NTC 370 for total organic Nitrogen measurement and AOAC 98002 for sulfur

measurement. Other characteristics of the oil pam-biochar and purple moor grass-biochar could be consulted in Supplementary Material. The identification of biochar functional groups was performed through Attenuated Total Reflection–FourierTransform Infrared (ATR-FTIR) in a Perkin Elmer (Waltham, MA, USA) instrument between3000 $cm^{-1}$and 650 cm^{-1} frequency range and 32 running scans at a resolution of 4 cm−1.2.3.

Synthesis of Biochar-Derived C-Dots

Biochar-derived C-Dots were synthesized using previously reported methods by Placido et al. [13,21] employing a hydrothermal method in presence of a strong oxidation reagent ($KMnO_4$). First, the biochar was shattered into small pieces using a mortar and then passed through a 425µm sieve (Woven Wire, Endecotts), the sieved biochar was used for the C-dots production. The depolymerization reaction was performed with 10 g of biochar mixed with a solution of $KMnO_4$ 10% (w/v) in a 500 mL Erlenmeyer flask. The depolymerization reaction was carried on an autoclave (SA-300H, Sturdy, Wilmington, DE,USA) at 121◦C and 15 psi for 60 min. After the reaction, the biochar solutions were centrifuged (SL 8, Thermo Scientific) for 5 min at 1000 rpm to separate the liquid (supernatant) and solid phases (remaining biochar). The supernatant was filtered with a 0.22µm syringe filter (Merck Millipore, Burlington, VT, USA). The filtered liquid was mixed with Acetone and centrifugated (SL 8, Thermo Scientific) again (1000 rpm, 5 min) until the production of two liquid phases. The upper liquid phase was withdrawn, and later roto evaporated (BM500,Yamato, Santa Clara, CA, USA) at 85◦C and 750 HPa. The Carbon-dots were purified by using overnight dialysis (3.5 KDa MWCO, Standard RC Dry Dialysis, Labs Spectra/PorTM3) and freeze-dried (18LC-16WW-TS, Thermo Scientific) for 32 h. The newly synthesized C-Dots were kept in a solid state at $4^{\circ C}$ until use.

Characterization of Biochar-Derived C-Dots

C-Dots were characterized by various spectroscopic and morphological techniques. The fluorescence emission and excitation spectra and the UV-Vis spectra were performed at C-Dots concentration of 500 ppm in a Varioskan Lux (Thermo scientific, SkanIt Software4.1) on a 200µL working volume microplates (Falcon™non-treated black 96-well) and20◦C with 1 nm optical step. The identification of C-Dots functional groups was performed through Attenuated Total Reflection–Fourier Transform Infrared (ATR-FTIR) in a PerkinElmer instrument between 4000 $cm^{-1}$and 650 cm^{-1} frequency range and 32 running scans at a resolution of 4 cm^{-1}. The stability of the synthesized C-Dots at a concentration of1000 ppm was examined through Dynamic light scattering (DLS) and Z potential techniques on a Nanoplus-3. The measurement was performed using 0.2µm filtered solutions in aB0631009 cell, with water as a dispersant (Refractive Index: 1.3328). The shape and size of the C-Dots were taken using High-Resolution Transmission Electronical Microscopy (HR-TEM) on a FEI-Tecnai F20 Super Twin TMP.

Quantum Yield Measurement

The quantum yield (QY) of the synthesized C-Dots was calculated through comparative method, using quinine sulfate in 0.5 M H_2SO_4 and based on previous reports [15,16]. The QY was calculated according to the following equation:

$$Y = QY_{ref}\left(I_{sam}/I_{ref}\right) * \left(A_{ref}/A_{sam}\right) * \left(n^2_{sam}/n^2_{ref}\right) \quad (1)$$

where suffix "ref" and "sam" refers to the standard reference and sample, respectively. "I" is the integrated fluorescent emission intensity, "n" is the refractive index of the solvent and "A" is the intensity of absorbance. All the measurements were done at maximum intensity.

Ecotoxicity Assay

The C-Dots aquatic toxicity was evaluated via an ecotoxicity assay performed on a Microtox™ Model 500 Analyzer. The Microtox™ test is based on the measurement of *Vibrio fischeri* bioluminescence changes which correspond to cell viability, specifically, the toxicity is related to fluorescence inhibition of the bacteria [52]. An 81.9% Basic Test with 9 double dilutions was applied, starting from the concentration of 1000 ppm for all the C-Dots samples. The results were calculated, considering the Gamma function after 5 and 15 min, and were reported as EC50, that is, the concentration that causes the 50% inhibition of the fluorescence of the microorganism [53]. Gamma [54] as:

$$Gamma = \left(I_c/I_t\right) - 1 \quad (2)$$

where I_c is the average light reading of filtrates of the control solutions and I_t is the light reading of a filtrate of a particular concentration of the test material.

8.3. Results and Discussion

Biochar Characterization

The characteristics of the three types of biochar are shown in Table 8-1. All materials have alkaline pH, a characteristic attributed to the thermal decomposition of hydroxyl bonds and other weak bonds within the biochar structure produced under medium to high temperatures of synthesis [55]. The biochars exhibited variable nitrogen (N) and sulfur (S) content, which is related to the initial content of the source and the temperature of the synthesis process. It has been reported that with increasing temperatures, more N and S were lost in the material [56,57]. The loss of N in the biochars was attributed to the removal of N via volatilization at relatively low temperatures (~200 °C) [57]. Some works suggest that the pyrolysis temperature is an important factor that influences the speciation of sulfur in the biochar, since there is a much higher fraction of sulfur in organosulfur

form for biochar produced at high temperatures, while the biochars at lower temperatures have sulfate, organosulfur, and sulfide [56,58].

Table 8-1. Physicochemical characteristics of biochar.

Parameter	*Picea*	*Molinia Caerulea*	*Elaeis Guineensis*
pH	8.9	9.58	8.26
% N (total organic)	0.29	3.42	0.2
% S (total)	0.43	1.46	1.5
% Ash	-	6.80	11.1
Source	[59]	This work	This work

Among the analyzed materials, Molinia's biochar has the highest organic nitrogen content, while the biochar of *Molinia caerulea* and *Elaeis guineensis* have the highest sulfur content. Nitrogen values for biochar from *Picea* and *Elaeis guineensis* are comparable with those reported for biochar obtained from dairy manure [60], hardwood [61], eucalypt [62], willow [63–65], and bagasse from 14 agriculture waste [66]. The three materials reported in this study stand out for having a higher amount of sulfur than some of those reported in the literature [67].

The N and S content is important because these heteroatoms are associated with aromatic rings forming various functional groups on the biochar surfaces [55,68], which influences the properties of the material and its different applications [67,69]. Specifically, in the production of C-Dots from biochar, the N and S heteroatoms can be manipulated to act as electron donors or acceptors, and this process affects the characteristics and optical properties of the C-Dots that are obtained [70].

For the determination of the presence of functional groups on the biochar surface and the C-Dots, the Fourier transform infrared spectroscopy (FTIR) was used. The biochars FTIR spectrum of biochar derived from *Picea*, *Molinia caerulea*, and *Elaeis guineensis* (Figure 8-1) doesn't show peaks with high intensities, which is supported by several authors [71–74], and it's due to the pyrolysis process, which is performed in biomass to produce biochar, because it promotes the rupture of several functional groups and the progressive carbonization of the material. However, all the spectra showed similar peaks at 744, 813, 877, 1574, and 1700 cm^{-1}.

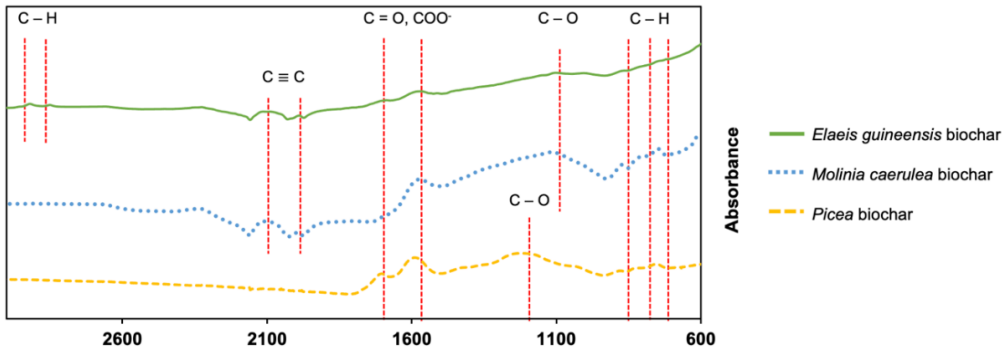

Figure 8-1. Picea, Molinia caerulea, and Elaeis guineensis biochar FTIR spectra

The peaks at 744, 813, and 877 cm^{-1} are associated with the carbon linkages, more specifically C–H bending, and the peaks at 1574 and 1700 cm^{-1} are associated with carboxyl groups. Besides, the *Molinia caerulea* and *Elaeis guineensis* biochar shows a C-O group (1111 cm^{-1}) that corresponds to a secondary alcohol, while the *Picea* biochar shows the C-O group (1196 cm^{-1}) associated with a tertiary alcohol. These groups are mostly found in biochar that is obtained from sources that tend to be polar, hydrophilic, and relatively reactive, such as lignocellulosic feedstocks. Furthermore, the oxygen-containing functional groups have variable charge, at a higher pH, the carboxylic acids give up protons and become negatively charged (-COO-) [71,75,76].

The spectra of *Molinia* cerulea and *Elaeis guineensis* show peaks at 2000 and 2100 cm^{-1}, corresponding to triple bond of alkynes that are part of the lignocellulose [77–79]. Finally, only the biochar of *Elaeis guineensis* shows the presence of asymmetric (2910 cm^{-1}) and symmetric (2850 cm^{-1}) C–H stretching bands associated with aliphatic functional groups, which decrease in intensity due to structural changes that happened during pyrolysis that produce a decrease in aliphatic compounds [80,81]. The spectra obtained from the biochar of *Picea*, *Molinia caerulea*, and *Elaeis guineensis*, don't show high intensities due to the carbonization processes to which the biomass is subjected. In addition, the functional groups are related to lignocellulosic feedstocks such as those used in this work. Finally, it is suggested that the differences found in the spectra may be due to the conditions of the thermal conversion process of biochar, since many authors [21,82] report that variables such as reactor type, heating rate, temperature, residence time, oxygen concentration, etc. are significant variables that can affect the characteristics of biochar produced.

Carbon Dots Characterization

Chemical Characterization

The FTIR spectra of the three biochar-derived C-Dots are depicted in Figure 8-2. These spectra, unlike those obtained for biochar, show an increase in the intensity of the bands and a change in their position, which suggests an increase in the amount (per unit volume) of some functional groups, and a change in the state of hybridization or electronic distribution of molecular bonds. Furthermore, the absence of the bands between 1700 and 2100 cm^{-1} suggests the formation of other functional groups due to the hydrothermal process with $KMnO_4$.

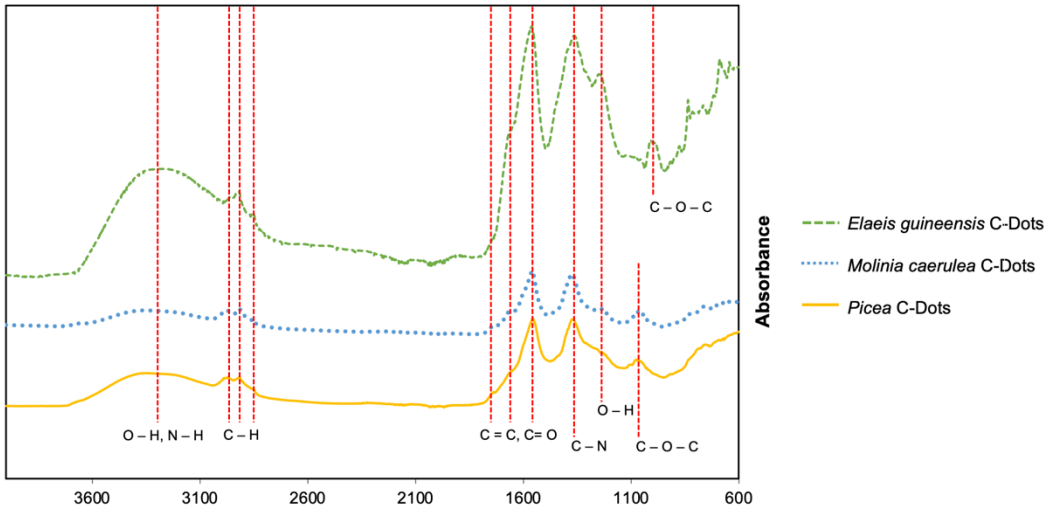

Figure 8-2. Picea, Molinia caerulea, and Elaeis guineensis C-Dots FTIR spectra.

The bands between 700 and 900 cm^{-1} shown in the spectra are associated with con C –H bending, as are the spectra of biochar. The existence of C–O–C bonds leads to the ab-sorption peak at 990 cm^{-1} for *Elaeis guineensis* C-Dots and 1045 cm−1 for *Picea* and *Molinia caerulea* C-Dots [83,84], and the peak at 1236 cm^{-1} is associated with C–O stretching [85,86]. One of the most intense peaks of all the spectra occurs at 1370 cm^{-1} which corresponds to C–N [87–89]; the bands located around 1550–1750 cm^{-1} are assigned, for some authors to C=N [89,90], while other authors associated these bands with the stretching vibration of C=C and carbonyl bonds (C=O) [83–85,91]. Moreover, the band around 1700 cm^{-1} could indicate the vibration of the carbonyl bond of a carboxylic acid, however, because it's weak, it could represent the deprotonation of the group and the apparition of the carboxylate group (COO-) [20]. The presence of carbonyl groups could allow, in future works, the functionalization of these carbonaceous materials with molecules that have amine groups available through the carbodiimide technique.

Finally, the peaks displayed between 2850 cm^{-1} and 2950 cm^{-1} are from C–H stretching vibration [91–93], and the broad absorption band within 3100–3600 cm^{-1} derives from the stretching vibration of hydroxyl bonds (O–H) and N–H [83,84]. This data suggest that the C-Dots obtained from *Picea*, *Molinia caerulea* and *Elaeis guineensis* present large hydrophilic groups indicating the formation of water-soluble materials, and the presence of carbonyl moieties suggest that the C-Dots could be slightly negatively charged.

Morphology and Stability

The HR-TEM and the DLS were utilized to investigate the morphology and average size of the biochar-derived C-Dots. The size distribution obtained by measuring the hydrodynamic diameter of C-Dots (1000 ppm) derived from *Picea, Molinia caerulea*, and *Elaeis guineensis*; by DLS indicates that these nanoparticles have a total hydrodynamic diameter of 113 ± 13.4, 122.7 ± 2, and 105.4 ± 7.1 nm and the polydispersity index are 0.19 ± 0.01, 0.18 ± 0.04, and 0.2 ± 0.03, respectively. Besides,

the DLS graphs show that the three types of C-Dots are bimodal and have a second population of particles with hydrodynamic diameter less than 5 nm. However, HR-TEM images (Figure 3) reveal that the three types of the extracted biochar nanoparticles (*Picea, Molinia caerulea*, and *Elaeis guineensis*) are mono-dispersed, and they have a nearly spherical shape with an average size of 4.2 ± 1.2, 6.2 ± 1.9 and 2.5 ± 0.7 nm, respectively (Figure 8-3) (the size distribution was determined with 100 particles, which are founded in various TEM images related to different zones in the sample). Besides, the HR-TEM images show some aggregation between the particles, which explains the total hydrodynamic diameter measured with DLS. It is comparable to other reported works [94–96]. C-Dots derived from *Elaeis guineensis* biochar are smaller than the other particles and the C-Dots derived from *Molinia caerulea* biochar have the greatest variability in size. However, since all the particles are in the range less than 10 nm, they are considered C-Dots.

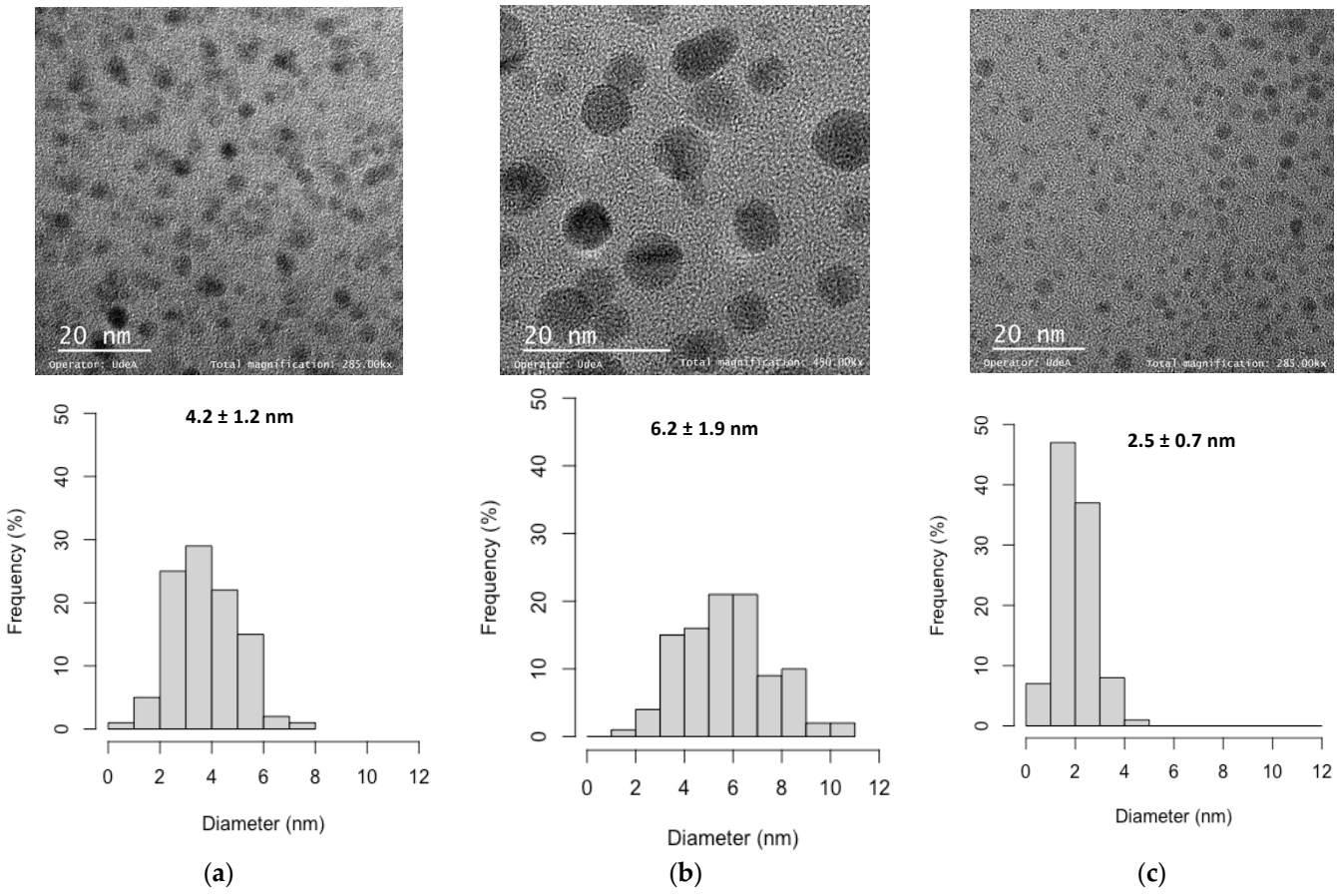

Figure 8-3. TEM images of (a) Picea, (b) Molinia caerulea and (c) Elaeis guineensis. Histogram of particle diameter distribution of C-Dots (inset).

The Z potential is an indicator of nanoparticles stability since it is a measure of the charge repulsion or attraction between the particles from its surface to the boundary of the diffuse layer. The

measurements affording a value of –58.85 ± 7.7, −48.7 ± 1.2, and −56.2 ± 6.2 for C-Dots synthesized from *Picea, Molinia caerulea*, and *Elaeis guineensis*, respectively. These values indicate that the nanoparticles have great stability.

Optical Properties

The fluorescence spectra (Figure 8-4) show the maximum emission wavelength (λem) at similar value: 430, 420, and 420 nm for *Picea, Molinia caerulea*, and *Elaeis guineensis*, respectively. The maximum excitation wavelength is also similar, ranging from 300 nm to 320 nm. The optimal excitation and emission wavelength combination are shown as an insert of Figure 4. All the obtained C-Dots show a brownish yellow color under daylight and blue emission under UV light.

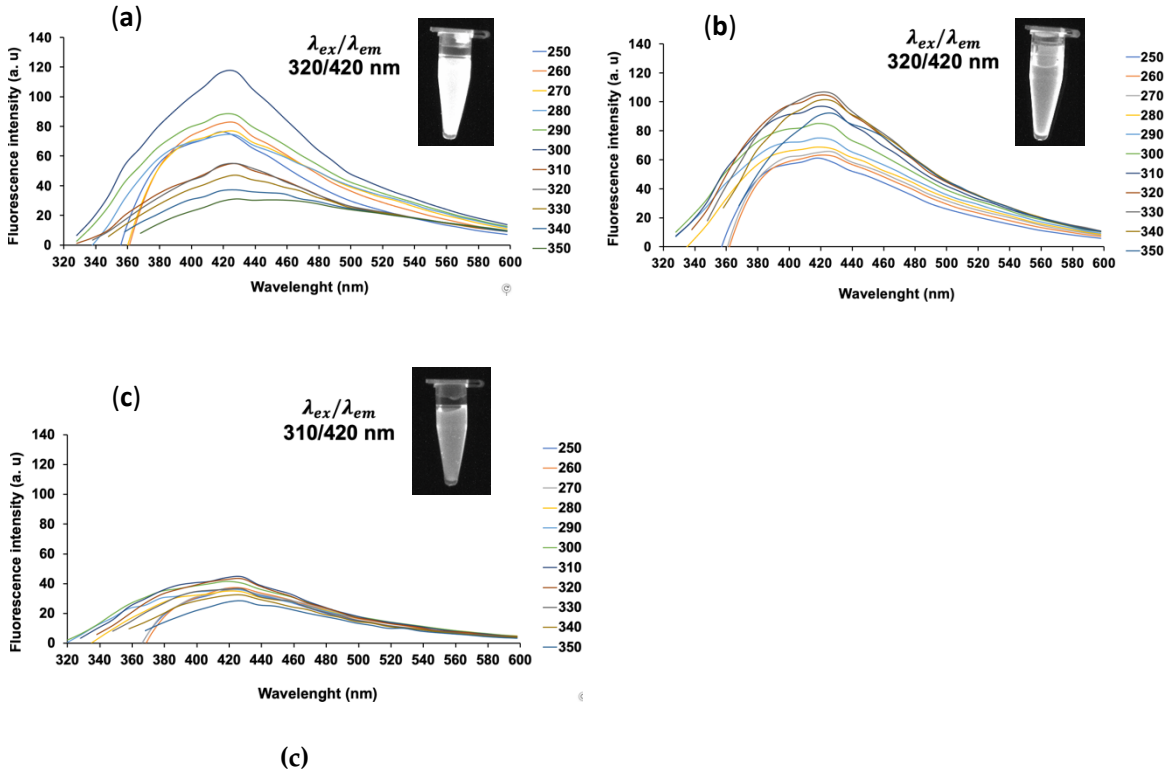

Figure 8-4. Emission spectra of C-Dots under different excitation wavelengths. (a) Picea. (b) Molinia caerulea. (c) Elaeis guineensis.

Usually, C-Dots exhibit an excitation-dependent photoluminescence that are related to state defects [17]. This behavior is particular for *Elaeis guineensis* whose intensity de-crease between 360 nm and 400 nm. In this range is also a red shift photoluminescence that could be explained by the surface oxidation degree as a theory for the fluorescence origin [23]. Some authors found these defects can trap excitons, and the radiation from the recombination of trapped excitons causes the red-shift emission [97–99]. The band gap between the lowest unoccupied molecular orbital and the highest occupied molecular orbital reduces with the increase of oxygen content on the C-dots surface, that

is, red-shifted emission is derived from increasing surface oxidation degree [23,100]. For *Picea* and *Molinia caerulea*, there is no visible red shift phenomenon, and the emission peak is pre-served for the different excitation wavelengths, just changing its intensity. This behavior could be explained by the surface functional groups as an alternative theory for the fluorescence origin [23]. According to that, surface states are correlated to surface functional groups, such as C = O and C = N. Those groups are present in all the C-dots (Figure 8-2) and were proved to be closely related to the fluorescence [101,102]. The functional groups can introduce new energy levels and further produce new electron transitions [23].

The UV-Vis spectra (Figure 8-5) were investigated at a concentration of 500 ppm. *Picea* and *Molinia caerulea* show the same behavior, a characteristic slight absorption signal at 244 nm, while *Elaeis guineensis* shows a slight absorption signal at 244 nm and a more visible signal at 280 nm. Absorption signals between 240 nm and 290 nm are attributed to the π–π* or n–π* transitions and suggest the presence of C = O, C = C, and C = N surface functional groups [103]. On the other hand, the signal at 244 nm could be attributed precisely to n–π* transitions and could explain the slightly blue shift in the fluorescence spectra of *Picea* and *Molinia caerulea* when they are exciting with longer wavelengths [16,104].

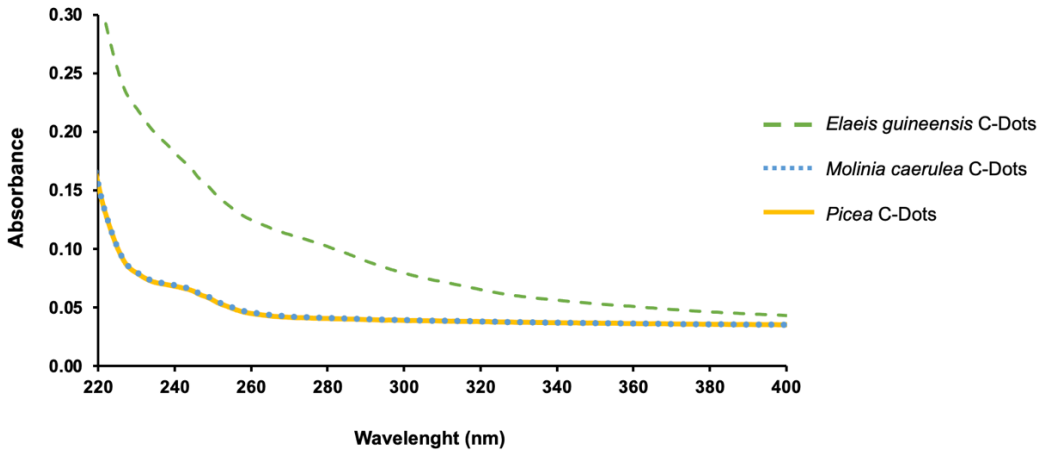

Figure 8-5. UV-Vis spectra of Picea, Molinia caerulea, and Elaeis guineensis C-Dots

The Quantum Yields (QY) of the *Picea, Molinia caerulea* and *Elaeis guineensis* C-Dots were 5.44, 8.39, 2.31% respectively, using quinine sulfate (QY of 0.54 in 0.5 M H_2SO_4 [105]) as the reference. Table 8-2 shows the comparison of several biomass-derived C-Dots QYs and excitation wavelengths with the results obtained in this work. Moreover, for C-Dots derived from biomass using the hydrothermal method, the QYs can range from 2.3% to 21.7% depending mostly on its size, carbon precursor, and processing parameters [106–108]. It is suggested that the low quantum yield obtained for the C-Dots synthesized from *Elaeis guineensis*, is because the biochar from this source is one with the lowest nitrogen and sulfur content (Table 8-1), compared to *Picea* and *Molinia*

caerulea, which influence the production of C-Dots with heteroatoms and are related to the increase in fluorescence intensity and its quantum yield [109–111]. For instance, Zhu et al. [99], obtained C-Dots doped with nitrogen and synthesized from citric acid and ethylenediamine with a QY of 80%. Likewise, several authors have shown an increase in the QY of C-Dots through doping with nitrogen or sulfur heteroatoms [112–117].

Table 8-2. Comparison of several hydrothermally produced C-Dots with different biomass pre-cursors.

Carbon Precursor	$\lambda_{exc}(nm)$	QY%	Reference
Willow Bark	360	6	[118]
Pomelo peel	360	6.9	[119]
Citrus pectin	360	1.1	[120]
Sugarcane juice	390	5.67	[95]
Winter melon	360	7.51	[121]
Coffee beans	365	3.80	[122]
Picea	310	5.44	This work
Molinia caerulea	320	8.39	This work
Elaeis guineensis	310	2.31	This work

Ecotoxicity

In the present work, the aquatic toxicity analysis was carried out because environmental applications of C-Dots are projected (detection of heavy metals, pesticides, and endocrine disruptors) but also to determine the toxic potential that this nanomaterial may have at the end of its life cycle, by encountering water sources and aquatic biota. The Microtox™ test results for the different C-Dots samples are shown in Figure 8-6. The gamma value equal to unity represents the EC50 in percentage value, which can be seen to be met and exceeded for very low values of *Picea* (2.35% with slightly erratic values) and higher values of *Molinia caerulea* (41.92%). In the case of *Elaeis guineensis* C-Dots, the unit value is not reached, and the projected slope implies that extremely high values would be necessary to cause any toxic effect (858.6%).

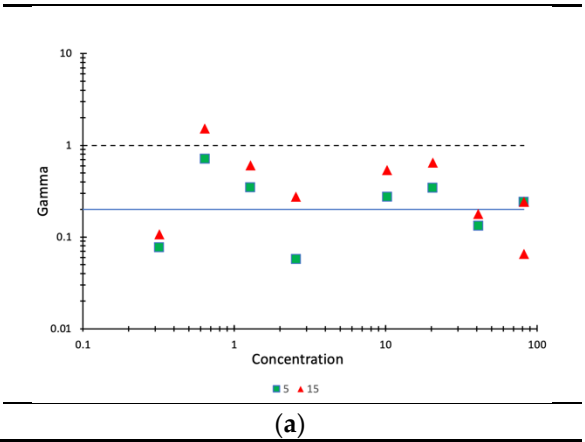

(a)

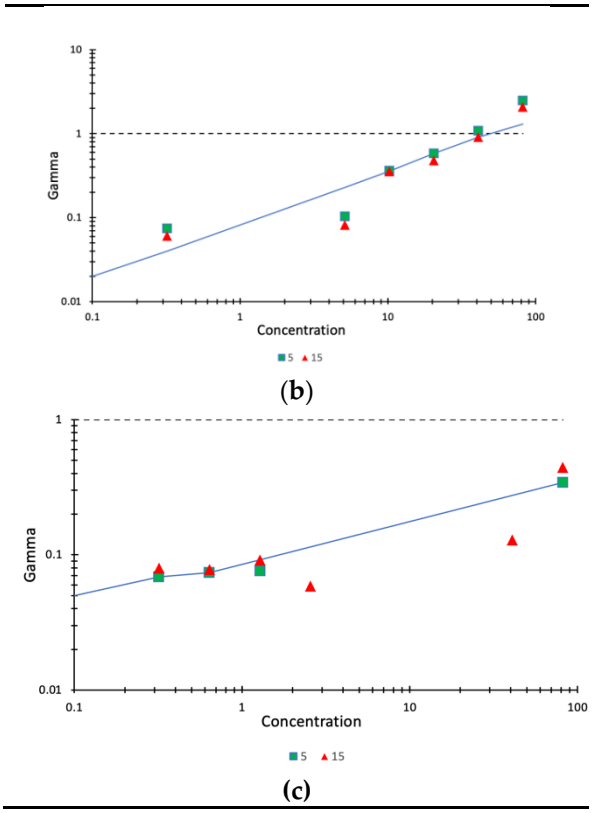

Figure 8-6. Aquatic toxicity test results for Picea (a), Molinia caerulea (b), and Elaeis guineensis (c). Gamma = 1 corresponds to the EC50. Horizontal axis corresponds to the percentage of the concentration, where 100% equals 1000 ppm.

The different samples present EC50 values in concentration units, taken at 15 min of the test of 23.5 mg/L, 419.2 mg/L and 8586 mg/L for *Picea, Molinia caerulea* and *Elaeis guineensis* C-Dots respectively. According to these results, we can classify them as highly toxic (*Picea* C-Dots), moderately toxic (*Molinia caerulea* C-Dots) and non-toxic (*Elaeis guineensis* C-Dots) [123].

The toxicity of nanomaterials, in general, is a growing field of study, which includes initiatives like US NanoEPA [124] and EU NanoSafety cluster [125]. Toxicity depends on starting material, dose, size, surface chemistry, and durability; additionally, various routes of exposure are considered with different effects on organisms [126]. *Picea* C-Dots present a marked toxicity, which can be explained by the characteristic mentioned previously and their smaller size (Figure 8-3). Most studies focused on the safety of nanomaterials agree that size is the main factor of toxicity of nanomaterials with respect to the material on a macroscopic scale, mainly due to their effects through biological barriers, in the surface area and the density of absorption; This triggers endocytosis/exocytosis, oxidative stress, reactive oxygen species (ROS), cell damage and apoptosis [127].

C-Dots have a lower toxicity than quantum dots, traditionally synthesized from heavy metals [127]. However, ecotoxicological evaluations of C-Dots are scarce, despite being a priority test in terms of safety. Few studies have been carried out in bioindicator organisms such as microcrustaceans (*Daphnia magna*) and zebra fish (*Danio rerio*), showing that concentrations up to 200 mg/L can be

cleared without acute toxic effects [128]. However, in the present work, it was found that *Picea* C-Dots are toxic for *Vibrio fischeri* at lower values. This shows that the Microtox™ assays are more sensitive [123] and that more data is needed at the ecotoxicological level to follow the in vivo testing process. The damage routes of C-Dots in these organisms are related to oxidative stress [128]. However, several authors agree that carbonaceous nanomaterials have little or no bioaccumulation capacity, so there would be no chronic toxicity [127]. Future work is required to further clarify these findings.

8.4. Conclusions

This work shows that *Picea* C-Dots have excellent optical properties. However, they exhibit high ecotoxicity, which limits their applications. *Molinia caerulea* and *Elaeis guineensis* C-Dots have low or no toxicity, but *Elaeis guineensis* C-Dots has the lowest fluorescence intensity with respect to the others. All the C-Dots have high values of negative Z potential, which indicate colloidal stability. Besides, they have excellent chemical groups on the surface that would allow for easy functionalization to other molecules, so they have the potential, especially *Molinia caerulea and Elaeis guineensis* C-Dots, for use in the development of optical biosensors with applications in the detection of environmental contaminants and pathogens. However, the optical properties (quantum yield) could be optimized to improve their performance. These results allow for the encouragement of the valorization of agro-industrial waste for its transformation into biochar and its use beyond soil amendment. Finally, future works could include more studies focused on the optimization of the optical properties of C-Dots, as well as the study of their ecotoxicology that allows a safe application of these nanomaterials in different fields of knowledge.

8.5. References

1. United Nations. The Sustainable Development Goals Report, New York 2020, ISSN:2521-6899
2. Benedetti, V.; Patuzzi, F.; Baratieri, M. Characterization of char from biomass gasification and its similarities with activated carbon in adsorption applications. Appl. Energy 2018, 227, 92–99, doi:10.1016/j.apenergy.2017.08.076.
3. Yao, Z.; You, S.; Ge, T.; Wang, C.-H. Biomass gasification for syngas and biochar co-production: Energy application and economic evaluation. Appl. Energy 2018, 209, 43–55, doi:10.1016/j.apenergy.2017.10.077.
4. Vamvuka, D.; Sfakiotakis, S.; Pantelaki, O. Evaluation of gaseous and solid products from the pyrolysis of waste biomass blends for energetic and environmental applications. Fuel 2019, 236, 574–582, doi:10.1016/j.fuel.2018.08.145.
5. Kong, X.; Zhu, Y.; Lei, H.; Wang, C.; Zhao, Y.; Huo, E.; Lin, X.; Zhang, Q.; Qian, M.; Mateo, W.; et al. Synthesis of graphene-like carbon from biomass pyrolysis and its applications. Chem. Eng. J. 2020, 399, 125808, doi:10.1016/j.cej.2020.125808.
6. Li, J.; Dai, J.; Liu, G.; Zhang, H.; Gao, Z.; Fu, J.; He, Y.; Huang, Y. Biochar from microwave pyrolysis of biomass: A review. Biomass Bioenergy 2016, 94, 228–244, doi:10.1016/j.biombioe.2016.09.010.

7. Chen, T.; Liu, R.; Scott, N.R. Characterization of energy carriers obtained from the pyrolysis of white ash, switchgrass and corn stover—Biochar, syngas and bio-oil. Fuel Process. Technol. 2016, 142, 124–134, doi:10.1016/j.fuproc.2015.09.034.
8. Muegue, L.C.D.; González, J.C.A.; Mesa, G.P. Characterization and Potential Use of Biochar for the Remediation of Coal Mine Waste Containing Efflorescent Salts. Sustainability 2017, 9, 2100, doi:10.3390/su9112100.
9. Giri, B.S.; Goswami, M.; Singh, R. Review on Application of Agro-Waste Biomass Biochar for Adsorption and Bioremediation Dye. Biomed. J. Sci. Tech. Res. 2017, 1, 1928–1930.
10. Aresta, M.; Dibenedetto, A.; Angelini, A. Catalysis for the Valorization of Exhaust Carbon: From CO2 to Chemicals, Materials, and Fuels. Technological Use of CO2. Chem. Rev. 2014, 114, 1709–1742, doi:10.1021/cr4002758.
11. Shalini, S.S.; Palanivelu, K.; Ramachandran, A.; Raghavan, V. Biochar from biomass waste as a renewable carbon material for climate change mitigation in reducing greenhouse gas emissions—A review. Biomass Convers. Biorefin. 2020, 1–21, doi:10.1007/s13399-020-00604-5.
12. Tan, X.; Liu, S.-B.; Liu, Y.-G.; Gu, Y.-L.; Zeng, G.-M.; Hu, X.-J.; Wang, X.; Jiang, L.-H. Biochar as potential sustainable precursors for activated carbon production: Multiple applications in environmental protection and energy storage. Bioresour. Technol. 2017, 227, 359–372, doi:10.1016/j.biortech.2016.12.083.
13. Plácido, J.; Bustamante-López, S.; Meissner, K.; Kelly, D.; Kelly, S. NanoRefinery of carbonaceous nanomaterials: Comple-menting dairy manure gasification and their applications in cellular imaging and heavy metal sensing. Sci. Total Environ. 2019, 689, 10–20, doi:10.1016/j.scitotenv.2019.06.390.
14. Plácido, J.; López, S.B.; Meissner, K.; Kelly, D.; Kelly, S. Multivariate analysis of biochar-derived carbonaceous nanomaterials for detection of heavy metal ions in aqueous systems. Sci. Total Environ. 2019, 688, 751–761, doi:10.1016/j.scitotenv.2019.06.342.
15. Pourreza, N.; Ghomi, M. Green synthesized carbon quantum dots from Prosopis juliflora leaves as a dual off-on fluorescence probe for sensing mercury (II) and chemet drug. Mater. Sci. Eng. C 2019, 98, 887–896, doi:10.1016/j.msec.2018.12.141.
16. Atchudan, R.; Edison, T.N.J.I.; Perumal, S.; Selvam, N.C.S.; Lee, Y.R. Green synthesized multiple fluorescent nitrogen-doped carbon quantum dots as an efficient label-free optical nanoprobe for in vivo live-cell imaging. J. Photochem. Photobiol. A Chem. 2019, 372, 99–107, doi:10.1016/j.jphotochem.2018.12.011.
17. Vasimalai, N.; Vilas-Boas, V.; Gallo, J.; Cerqueira, M.D.F.; Menéndez-Miranda, M.; Costa-Fernández, J.M.; Diéguez, L.; Espiña, B.; Fernández-Argüelles, M.T. Green synthesis of fluorescent carbon dots from spices for in vitro imaging and tumour cell growth inhibition. Beilstein J. Nanotechnol. 2018, 9, 530–544, doi:10.3762/bjnano.9.51.
18. Kang, C.; Huang, Y.; Yang, H.; Yan, X.F.; Chen, Z.P. A Review of Carbon Dots Produced from Biomass Wastes. Nanomaterials 2020, 10, 2316, doi:10.3390/nano10112316.
19. Campuzano, S.; Yáñez-Sedeño, P.; Pingarrón, J.M. Carbon Dots and Graphene Quantum Dots in Electrochemical Biosensing. Nanomaterials 2019, 9, 634, doi:10.3390/nano9040634.
20. Plácido, J.; Bustamante-López, S.; Meissner, K.; Kelly, D.; Kelly, S. Comparative study of the characteristics and fluorescent properties of three different biochar derived carbonaceous nanomaterials for bioimaging and heavy metal ions sensing. Fuel Process. Technol. 2019, 196, 106163, doi:10.1016/j.fuproc.2019.106163.
21. Plácido, J.; Bustamante-López, S.; Meissner, K.; Kelly, D.; Kelly, S. Microalgae biochar-derived carbon dots and their appli-cation in heavy metal sensing in aqueous systems. Sci. Total Environ. 2019, 656, 531–539, doi:10.1016/j.scitotenv.2018.11.393.
22. Abdul, S.; Nor, R.; Zobir, M. Synthesis, Technology and Applications of Carbon Nanomaterials; Elsevier: Oxford, UK, 2019.
23. Liu, M.L.; Bin Chen, B.; Li, C.M.; Huang, C.Z. Carbon dots: Synthesis, formation mechanism, fluorescence origin and sensing applications. Green Chem. 2019, 21, 449–471, doi:10.1039/c8gc02736f.
24. Wang, R.; Lu, K.-Q.; Tang, Z.-R.; Xu, Y.-J. Recent progress in carbon quantum dots: Synthesis, properties and applications in photocatalysis. J. Mater. Chem. A 2017, 5, 3717–3734, doi:10.1039/C6TA08660H.
25. Liu, W.; Li, C.; Ren, Y.; Sun, X.; Pan, W.; Li, Y.; Wang, J.; Wang, W. Carbon dots: Surface engineering and applications. J. Mater. Chem. B 2016, 4, 5772–5788, doi:10.1039/c6tb00976j.

26. Zheng, M.; Liu, S.; Li, J.; Qu, D.; Zhao, H.; Guan, X.; Hu, X.; Xie, Z.; Jing, X.; Sun, Z. Integrating Oxaliplatin with Highly Lu-minescent Carbon Dots: An Unprecedented Theranostic Agent for Personalized Medicine. Adv. Mater. 2014, 26, 3554–3560, doi:10.1002/adma.201306192.
27. Yuan, Y.; Guo, B.; Hao, L.; Liu, N.; Lin, Y.; Guo, W.; Li, X. Doxorubicin-loaded environmentally friendly carbon dots as a novel drug delivery system for nucleus targeted cancer therapy. Colloids Surfaces B Biointerfaces 2017, 159, 349–359, doi:10.1016/j.colsurfb.2017.07.030.
28. D'Souza, S.L.; Deshmukh, B.; Bhamore, J.R.; Rawat, K.A.; Lenka, N.; Kailasa, S.K. Synthesis of fluorescent nitrogen-doped carbon dots from dried shrimps for cell imaging and boldine drug delivery system. RSC Adv. 2016, 6, 12169–12179, doi:10.1039/c5ra24621k.
29. Mehta, V.N.; Chettiar, S.S.; Bhamore, J.R.; Kailasa, S.K.; Patel, R.M. Green Synthetic Approach for Synthesis of Fluorescent Carbon Dots for Lisinopril Drug Delivery System and their Confirmations in the Cells. J. Fluoresc. 2017, 27, 111–124, doi:10.1007/s10895-016-1939-4.
30. Wang, C.; Pan, C.; Wei, X.; Yang, F.; Wu, W.; Mao, L. Emissive carbon dots derived from natural liquid fuels and its biological sensing for copper ions. Talanta 2020, 208, 120375, doi:10.1016/j.talanta.2019.120375.
31. Radhakrishnan, K.; Sivanesan, S.; Panneerselvam, P. Turn-On fluorescence sensor based detection of heavy metal ion using carbon dots@graphitic-carbon nitride nanocomposite probe. J. Photochem. Photobiol. A Chem. 2020, 389, 112204, doi:10.1016/j.jphotochem.2019.112204.
32. Brachi, P. Synthesis of fluorescent carbon quantum dots (CQDs) through the mild thermal treatment of agro-industrial res-idues assisted by γ-alumina. Biomass Convers. Biorefinery 2020, 10, 1301–1312, doi:10.1007/s13399-019-00503-4.
33. Luo, X.; Han, Y.; Chen, X.; Tang, W.; Yue, T.; Li, Z. Carbon dots derived fluorescent nanosensors as versatile tools for food quality and safety assessment: A review. Trends Food Sci. Technol. 2020, 95, 149–161, doi:10.1016/j.tifs.2019.11.017.
34. Bui, T.T.; Park, S.-Y. A carbon dot–hemoglobin complex-based biosensor for cholesterol detection. Green Chem. 2016, 18, 4245–4253, doi:10.1039/c6gc00507a.
35. Pirsaheb, M.; Mohammadi, S.; Salimi, A. Current advances of carbon dots based biosensors for tumor marker detection, cancer cells analysis and bioimaging. TrAC Trends Anal. Chem. 2019, 115, 83–99, doi:10.1016/j.trac.2019.04.003.
36. Chen, Z.-H.; Han, X.-Y.; Deng, L.-X.; Lin, Z.-Y.; Mu, F.-Y.; Zhang, S.; Shi, G.; Zhang, M. A self-calibrating logic system and oxidase-based biosensor using Tb3+-doped carbon dots/DNA conjugates. Talanta 2019, 191, 235–240, doi:10.1016/j.talanta.2018.08.035.
37. Bhattacharyya, D.; Sarswat, P.K.; Free, M.L. Quantum dots and carbon dots based fluorescent sensors for TB biomarkers detection. Vacuum 2017, 146, 606–613, doi:10.1016/j.vacuum.2017.02.003.
38. He, L.; Yang, Y.; Kim, J.; Yao, L.; Dong, X.; Li, T.; Piao, Y. Multi-layered enzyme coating on highly conductive magnetic biochar nanoparticles for bisphenol A sensing in water. Chem. Eng. J. 2020, 384, 123276, doi:10.1016/j.cej.2019.123276.
39. Liu, M.L.; Bin Chen, B.; He, J.H.; Li, C.M.; Li, Y.F.; Huang, C.Z. Anthrax biomarker: An ultrasensitive fluorescent ratiometry of dipicolinic acid by using terbium(III)-modified carbon dots. Talanta 2019, 191, 443–448, doi:10.1016/j.talanta.2018.08.071.
40. Spanu, D.; Binda, G.; Dossi, C.; Monticelli, D. Biochar as an alternative sustainable platform for sensing applications: A review. Microchem. J. 2020, 159, 105506, doi:10.1016/j.microc.2020.105506.
41. Liu, H.; Ding, J.; Zhang, K.; Ding, L. Construction of biomass carbon dots based fluorescence sensors and their applications in chemical and biological analysis. TrAC Trends Anal. Chem. 2019, 118, 315–337, doi:10.1016/j.trac.2019.05.051.
42. Brachi, P. Synthesis of carbon dots (CDs) through the fluidized bed thermal treatment of residual biomass assisted by γ-alumina. Appl. Catal. B Environ. 2020, 263, 118361, doi:10.1016/j.apcatb.2019.118361.
43. Pooja, D.; Singh, L.; Thakur, A.; Kumar, P. Green synthesis of glowing carbon dots from Carica papaya waste pulp and their application as a label-freechemo probe for chromium detection in water. Sens. Actuators B Chem. 2019, 283, 363–372, doi:10.1016/j.snb.2018.12.027.
44. Hardman, R. A Toxicologic Review of Quantum Dots: Toxicity Depends on Physicochemical and Environmental Factors. Environ. Health Perspect. 2006, 114, 165–172, doi:10.1289/EHP.8284.
45. Oberdörster, G.; Oberdörster, E.; Oberdörster, J. Nanotoxicology: An Emerging Discipline Evolving from Studies of Ultrafine Particles. Environ. Health Perspect. 2005, 113, 823–839, doi:10.1289/ehp.7339.

46. Chunying, C.; Haifang, W. Biomedical Applications and Toxicology of Carbon Nanomaterials; John Wiley & Sons: Hoboken, NJ, USA, 2016.
47. Wang, F.; Chen, P.; Feng, Y.; Xie, Z.; Liu, Y.; Su, Y.; Zhang, Q.; Wang, Y.; Yao, K.; Lv, W.; et al. Facile synthesis of N-doped carbon dots/g-C3N4 photocatalyst with enhanced visible-light photocatalytic activity for the degradation of indomethacin. Appl. Catal. B Environ. 2017, 207, 103–113, doi:10.1016/j.apcatb.2017.02.024.
48. Farre, M.; Gajda-Schrantz, K.; Kantiani, L.; Barceló, D. Ecotoxicity and analysis of nanomaterials in the aquatic environment. Anal. Bioanal. Chem. 2008, 393, 81–95, doi:10.1007/s00216-008-2458-1.
49. Jahan, S.; Bin Yusoff, I.; Alias, Y.B.; Bin Abu Bakar, A.F. Reviews of the toxicity behavior of five potential engineered nano-materials (ENMs) into the aquatic ecosystem. Toxicol. Rep. 2017, 4, 211–220, doi:10.1016/j.toxrep.2017.04.001.
50. Rana, S.; Kalaichelvan, P.T. Ecotoxicity of Nanoparticles. ISRN Toxicol. 2013, 2013, 574648, doi:10.1155/2013/574648.
51. Díaz, L.C.; Pino, N.; Peñuela, G. Biochar from oil palm waste as an amendment for the remediation of soil disturbed by open-cast coal mining. Glob. Adv. Res. J. Eng. Technol. Innov. 2016, 5, 17–22.
52. Erzinger, G.S.; Schmoeller, F.; Pinto, L.H.; Américo, L.; Hemmersbach, R.; Hauslage, J.; Häder, D.-P. Bioluminescence systems in environmental biosensors. In Bioassays; Elsevier: Amsterdam, The Netherlands, 2017; pp. 242–262, doi:10.1016/B978-0-12-811861-0.00012-7.
53. Environmental Technology Centre. Biological Test Method: Reference Method for Determining the Toxicity of Sediment using Luminescent Bacteria in a Solid-Phase Test. Report EPS 1/RM/42, Ottawa 2002. ISBN 0-660-18911-9.
54. ASTM (American Society for Testing and Materials). Standard Guide for Conducting Sediment Toxicity Tests with Luminescent Bacteria; Draft No. 8. ASTM. Philadelphia, PA, USA, 1995.
55. Panahi, H.K.S.; Dehhaghi, M.; Ok, Y.S.; Nizami, A.-S.; Khoshnevisan, B.; Mussatto, S.I.; Aghbashlo, M.; Tabatabaei, M.; Lam, S.S. A comprehensive review of engineered biochar: Production, characteristics, and environmental applications. J. Clean. Prod. 2020, 270, 122462, doi:10.1016/j.jclepro.2020.122462.
56. Zhao, B.; Xu, H.; Zhang, T.; Nan, X.; Ma, F. Effect of pyrolysis temperature on sulfur content, extractable fraction and release of sulfate in corn straw biochar. RSC Adv. 2018, 8, 35611–35617, doi:10.1039/C8RA06382F.
57. Zheng, H.; Wang, Z.; Deng, X.; Zhao, J.; Luo, Y.; Novak, J.; Herbert, S.; Xing, B. Characteristics and nutrient values of biochars produced from giant reed at different temperatures. Bioresour. Technol. 2013, 130, 463–471, doi:10.1016/j.biortech.2012.12.044.
58. Cheah, S.; Malone, S.C.; Feik, C.J. Speciation of Sulfur in Biochar Produced from Pyrolysis and Gasification of Oak and Corn Stover. Environ. Sci. Technol. 2014, 48, 8474–8480, doi:10.1021/es500073r.
59. Palviainen, M.; Berninger, F.; Bruckman, V.J.; Köster, K.; de Assumpção, C.R.M.; Aaltonen, H.; Makita, N.; Mishra, A.; Kulmala, L.; Adamczyk, B.; et al. Effects of biochar on carbon and nitrogen fluxes in boreal forest soil. Plant Soil 2018, 425, 71–85, doi:10.1007/s11104-018-3568-y.
60. Cantrell, K.B.; Hunt, P.G.; Uchimiya, M.; Novak, J.M.; Ro, K. Impact of pyrolysis temperature and manure source on physi-cochemical characteristics of biochar. Bioresour. Technol. 2012, 107, 419–428, doi:10.1016/j.biortech.2011.11.084.
61. Nguyen, T.T.N.; Wallace, H.; Xu, C.-Y.; van Zwieten, L.; Weng, Z.H.; Xu, Z.; Che, R.; Tahmasbian, I.; Hu, H.-W.; Bai, S.H. The effects of short term, long term and reapplication of biochar on soil bacteria. Sci. Total Environ. 2018, 636, 142–151, doi:10.1016/j.scitotenv.2018.04.278.
62. Abujabhah, I.S.; Doyle, R.; Bound, S.A.; Bowman, J. The effect of biochar loading rates on soil fertility, soil biomass, potential nitrification, and soil community metabolic profiles in three different soils. J. Soils Sediments 2016, 16, 2211–2222, doi:10.1007/s11368-016-1411-8.
63. Agegnehu, G.; Nelson, P.; Bird, M.I. Crop yield, plant nutrient uptake and soil physicochemical properties under organic soil amendments and nitrogen fertilization on Nitisols. Soil Tillage Res. 2016, 160, doi:10.1016/j.still.2016.02.003.
64. Agegnehu, G.; Nelson, P.; Bird, M.I. The effects of biochar, compost and their mixture and nitrogen fertilizer on yield and nitrogen use efficiency of barley grown on a Nitisol in the highlands of Ethiopia. Sci. Total Environ. 2016, 569, 869–879, doi:10.1016/j.scitotenv.2016.05.033.

65. Agegnehu, G.; Bass, A.M.; Nelson, P.; Bird, M.I. Benefits of biochar, compost and biochar–compost for soil quality, maize yield and greenhouse gas emissions in a tropical agricultural soil. Sci. Total Environ. 2016, 543, 295–306, doi:10.1016/j.scitotenv.2015.11.054.
66. Prakongkep, N.; Gilkes, R.J.; Wiriyakitnateekul, W. Forms and solubility of plant nutrient elements in tropical plant waste biochars. J. Plant Nutr. Soil Sci. 2015, 178, 732–740, doi:10.1002/jpln.201500001.
67. Hossain, Z.; Bahar, M.; Sarkar, B.; Donne, S.W.; Ok, Y.S.; Palansooriya, K.N.; Kirkham, M.B.; Chowdhury, S.; Bolan, N. Biochar and its importance on nutrient dynamics in soil and plant. Biochar 2020, 2, 379–420, doi:10.1007/s42773-020-00065-z.
68. Brennan, J.K.; Bandosz, T.J.; Thomson, K.T.; Gubbins, K.E. Water in porous carbons. Colloids Surfaces A Physicochem. Eng. Asp. 2001, 187, 539–568, doi:10.1016/S0927-7757(01)00644-6.
69. Liu, G.; Li, S.; Cheng, M.; Zhao, L.; Zhang, B.; Gao, Y.; Xu, Y.; Liu, F.; Lu, G. Facile synthesis of nitrogen and sulfur co-doped carbon dots for multiple sensing capacities: Alkaline fluorescence enhancement effect, temperature sensing, and selective detection of Fe3+ ions. New J. Chem. 2018, 42, 13147–13156, doi:10.1039/c8nj02086h.
70. Xu, Q.; Kuang, T.; Liu, Y.; Cai, L.; Peng, X.; Sreeprasad, T.S.; Zhao, P.; Yu, Z.; Li, N. Heteroatom-doped carbon dots: Synthesis, characterization, properties, photoluminescence mechanism and biological applications. J. Mater. Chem. B 2016, 4, 7204–7219, doi:10.1039/C6TB02131J.
71. Suárez-Hernández, L.; Barrera-Zapata, R. Morphological and physicochemical characterization of biochar produced by gasi-fication of selected forestry species. Rev. Fac. Ing. 2017, 26, 123–130, doi:10.19053/01211129.v26.n46.2017.7324.
72. Shaaban, A.; Se, S.M.; Dimin, M.F.; Juoi, J.M.; Husin, M.H.M.; Mitan, N.M.M. Influence of heating temperature and holding time on biochars derived from rubber wood sawdust via slow pyrolysis. J. Anal. Appl. Pyrolysis. 2014, 107, 31–39, doi:10.1016/j.jaap.2014.01.021.
73. Zhao, S.X.; Ta, N.; Wang, X.D. Effect of temperature on the structural and physicochemical properties of biochar with apple tree branches as feedstock material. Energies 2017, 10, 1293, doi:10.3390/en10091293.
74. Gámiz, B.; Hall, K.; Spokas, K.A.; Cox, L. Understanding activation effects on low-temperature biochar for optimization of herbicide sorption. Agronomy 2019, 9, 588, doi:10.3390/agronomy9100588.
75. Brewer, C.E. Biochar Characterization and Engineering. Ph.D. Thesis, Digital Repository, Iowa State University, Ames, IA, USA, 2012, doi:10.31274/etd-180810-2233.
76. Liu, Q.; Wang, S.; Zheng, Y.; Luo, Z.; Cen, K. Mechanism study of wood lignin pyrolysis by using TG-FTIR analysis. J. Anal. Appl. Pyrolysis. 2008, 82, 170–177, doi:10.1016/j.jaap.2008.03.007.
77. Yang, T.; Lua, A.C. Characteristics of activated carbons prepared from pistachio-nut shells by physical activation. J. Colloid Interface Sci. 2003, 267, 408–417, doi:10.1016/S0021-9797(03)00689-1.
78. Chemerys, V.; Baltrėnaitė, E. Influence of Intrinsic Properties of Lignocellulosic Feedstock on Adsorptive Properties of Biochar. J. Environ. Eng. 2018, 144, doi:10.1061/(asce)ee.1943-7870.0001420.
79. Kołodyńska, D.; Bąk, J.; Kozioł, M.; Pylypchuk, L.V. Investigations of Heavy Metal Ion Sorption Using Nanocomposites of Iron-Modified Biochar. Nanoscale Res. Lett. 2017, 12, doi:10.1186/s11671-017-2201-y.
80. Jouiad, M.; Al-Nofeli, N.; Khalifa, N.; Benyettou, F.; Yousef, L.F. Characteristics of slow pyrolysis biochars produced from rhodes grass and fronds of edible date palm. J. Anal. Appl. Pyrolysis. 2015, 111, 183–190, doi:10.1016/j.jaap.2014.10.024.
81. Tang, Y.; Alam, M.S.; Konhauser, K.O.; Alessi, D.S.; Xu, S.; Tian, W.J.; Liu, Y. Influence of pyrolysis temperature on production of digested sludge biochar and its application for ammonium removal from municipal wastewater. J. Clean. Prod. 2019, 209, 927–936, doi:10.1016/j.jclepro.2018.10.268.
82. Zuo, P.; Lu, X.; Sun, Z.; Guo, Y.; He, H. A review on syntheses, properties, characterization and bioanalytical applications of fluorescent carbon dots. Microchim. Acta 2016, 183, 519–542, doi:10.1007/s00604-015-1705-3.
83. Mei, S.; Wei, X.; Hu, Z.; Wei, C.; Su, D.; Yang, D.; Zhang, G.; Zhang, W.; Guo, R. Amphipathic carbon dots with sol-vent-dependent optical properties and sensing application. Opt. Mater. 2019, 89, 224–230, doi:10.1016/j.optmat.2019.01.021.
84. Wei, X.; Mei, S.; Yang, D.; Zhang, G.; Xie, F.; Zhang, W.; Guo, R. Surface States Induced Photoluminescence Enhancement of Nitrogen-Doped Carbon Dots Via Post-Treatments. Nanoscale Res. Lett. 2019, 14, 172, doi:10.1186/s11671-019-3008-9.

85. Chao, D.; Lyu, W.; Liu, Y.; Zhou, L.; Zhang, Q.; Deng, R.; Zhang, H. Solvent-dependent carbon dots and their applications in the detection of water in organic solvents. J. Mater. Chem. C 2018, 6, 7527–7532, doi:10.1039/c8tc02184h.
86. Zhang, L.; Liu, W.; Zhuang, H.; Zhang, J.; Chen, C.; Wang, Y.; Shan, S. Environmentally friendly synthesis of photoluminescent biochar dots from waste soy residues for rapid monitoring of potentially toxic elements. RSC Adv. 2019, 9, 21653–21659, doi:10.1039/c9ra03001h.
87. Prekodravac, J.; Vasiljević, B.; Marković, Z.; Jovanović, D.; Kleut, D.; Špitalský, Z.; Mičušik, M.; Danko, M.; Bajuk-Bogdanović, D.; Todorović-Marković, B. Green and facile microwave assisted synthesis of (metal-free) N-doped carbon quantum dots for catalytic applications. Ceram. Int. 2019, 45, 17006–17013, doi:10.1016/j.ceramint.2019.05.250.
88. Ju, J.; Zhang, R.; He, S.; Chen, W. Nitrogen-doped graphene quantum dots-based fluorescent probe for the sensitive turn-on detection of glutathione and its cellular imaging. RSC Adv. 2014, 4, 52583–52589, doi:10.1039/c4ra10601f.
89. Villanueva, F.Y.; Manioudakis, J.; Naccache, R.; Majewski, M.B. Carbon Dot-Sensitized Photoanodes for Visible Light-Driven Organic Transformations. ACS Appl. Nano Mater. 2020, 3, 2756–2765, doi:10.1021/acsanm.0c00094.
90. Dastidar, D.G.; Mukherjee, P.; Ghosh, D.; Banerjee, D. Carbon quantum dots prepared from onion extract as fluorescence turn-on probes for selective estimation of Zn2+ in blood plasma. Colloids Surfaces A Physicochem. Eng. Asp. 2021, 611, 125781, doi:10.1016/j.colsurfa.2020.125781.
91. Dager, A.; Uchida, T.; Maekawa, T.; Tachibana, M. Synthesis and characterization of Mono-disperse Carbon Quantum Dots from Fennel Seeds: Photoluminescence analysis using Machine Learning. Sci. Rep. 2019, 9, doi:10.1038/s41598-019-50397-5.
92. Ţucureanu, V.; Matei, A.; Avram, A.M. FTIR Spectroscopy for Carbon Family Study. Crit. Rev. Anal. Chem. 2016, 46, 502–520, doi:10.1080/10408347.2016.1157013.
93. Kuo, T.R.; Sung, S.Y.; Hsu, C.W.; Chang, C.J.; Chiu, T.C.; Hu, C.C. One-pot green hydrothermal synthesis of fluorescent nitrogen-doped carbon nanodots for in vivo bioimaging. Anal. Bioanal. Chem. 2016, 408, 77–82, doi:10.1007/s00216-015-9138-8.
94. Pham-Truong, T.N.; Ranjan, C.; Randriamahazaka, H.; Ghilane, J. Nitrogen doped carbon dots embedded in poly(ionic liquid) as high efficient metal-free electrocatalyst for oxygen reduction reaction. Catal. Today 2019, 335, 381–387, doi:10.1016/j.cattod.2018.12.046.
95. Mehta, V.N.; Jha, S.; Kumar, S. One-pot green synthesis of carbon dots by using Saccharum of fi cinarum juice for fl uorescent imaging of bacteria (Escherichia coli) and yeast (Saccharomyces cerevisiae) cells. Mater. Sci. Eng. C 2014, 38, 20–27, doi:10.1016/j.msec.2014.01.038.
96. Thambiraj, S.; Shankaran, D.R. Green synthesis of highly fluorescent carbon quantum dots from sugarcane bagasse pulp. Appl. Surf. Sci. 2016, 390, 435–443, doi:10.1016/j.apsusc.2016.08.106.
97. Liu, H.; He, Z.; Jiang, L.P.; Zhu, J.J. Microwave-assisted synthesis of wavelength-tunable photoluminescent carbon nanodots and their potential applications. ACS Appl. Mater. Interfaces 2015, 7, 4913–4920, doi:10.1021/am508994w.
98. Liu, M.L.; Yang, L.; Li, R.S.; Chen, B.B.; Liu, H.; Huang, C.Z. Large-scale simultaneous synthesis of highly photoluminescent green amorphous carbon nanodots and yellow crystalline graphene quantum dots at room temperature. Green Chem. 2017, 19, 3611–3617, doi:10.1039/c7gc01236e.
99. Zhu, S.; Meng, Q.; Wang, L.; Zhang, J.; Song, Y.; Jin, H.; Zhang, K.; Sun, H.; Wang, H.; Yang, B. Highly photoluminescent carbon dots for multicolor patterning, sensors, and bioimaging. Angew. Chem. Int. Ed. 2013, 52, 3953–3957, doi:10.1002/anie.201300519.
100. Shen, D.; Long, Y.; Wang, J.; Yu, Y.; Pi, J.; Yang, L.; Zheng, H. Tuning the fluorescence performance of carbon dots with a reduction pathway. Nanoscale 2019, 11, 5998–6003, doi:10.1039/C8NR09587F.
101. Zhang, Y.; Yuan, R.; He, M.; Hu, G.; Jiang, J.; Xu, T.; Zhou, L.; Chen, W.; Xiang, W.; Liang, X. Multicolour nitrogen-doped carbon dots: Tunable photoluminescence and sandwich fluorescent glass-based light-emitting diodes. Nanoscale 2017, 9, 17849–17858, doi:10.1039/C7NR05363K.
102. Wang, L.; Zhu, S.J.; Wang, H.Y.; Qu, S.N.; Zhang, Y.L.; Zhang, J.H.; Chen, Q.D.; Xu, H.L.; Han, W.; Yang, B.; et al. Common origin of green luminescence in carbon nanodots and graphene quantum dots. ACS Nano 2014, 8, 2541–2547, doi:10.1021/nn500368m.

103. Moradi, S.; Sadrjavadi, K.; Farhadian, N.; Hosseinzadeh, L.; Shahlaei, M. Easy synthesis, characterization and cell cytotoxicity of green nano carbon dots using hydrothermal carbonization of Gum Tragacanth and chitosan bio-polymers for bioimaging. J. Mol. Liq. 2018, 259, 284–290, doi:10.1016/j.molliq.2018.03.054.
104. Zhang, Q.; Xie, S.; Yang, Y.; Wu, Y.; Wang, X.; Wu, J.; Zhang, L.; Chen, J.; Wang, Y. A facile synthesis of highly nitrogen-doped carbon dots for imaging and detection in biological samples. J. Anal. Methods Chem. 2018, 2018, doi:10.1155/2018/7890937.
105. Zhang, J.; Yang, L.; Yuan, Y.; Jiang, J.; Yu, S.H. One-Pot Gram-Scale Synthesis of Nitrogen and Sulfur Embedded Organic Dots with Distinctive Fluorescence Behaviors in Free and Aggregated States. Chem. Mater. 2016, 28, 4367–4374, doi:10.1021/acs.chemmater.6b01360.
106. Chen, W.; Li, D.; Tian, L.; Xiang, W.; Wang, T.; Hu, W.; Hu, Y.; Chen, S.; Chen, J.; Dai, Z. Synthesis of graphene quantum dots from natural polymer starch for cell imaging. Green Chem. 2018, 20, 4438–4442, doi:10.1039/c8gc02106f.
107. Ramanan, V.; Thiyagarajan, S.K.; Raji, K.; Suresh, R.; Sekar, R.; Ramamurthy, P. Outright green synthesis of fluorescent carbon dots from eutrophic algal blooms for in vitro imaging. ACS Sustain. Chem. Eng. 2016, 4, 4724–4731, doi:10.1021/acssuschemeng.6b00935.
108. Zhang, J.; Liu, X.; Zhou, J.; Huang, X.; Xie, D.; Ni, J.; Ni, C. Carbon dots derived from algae as H2O2 sensors: The importance of nutrients in biomass. Nanoscale Adv. 2019, 1, 2151–2156, doi:10.1039/c9na00049f.
109. Liu, H.; Li, Z.; Sun, Y.; Geng, X.; Hu, Y.; Meng, H.; Ge, J.; Qu, L. Synthesis of Luminescent Carbon Dots with Ultrahigh Quantum Yield and Inherent Folate Receptor-Positive Cancer Cell Targetability. Sci. Rep. 2018, 8, doi:10.1038/s41598-018-19373-3.
110. Shen, L.; Zhang, L.; Chen, M.; Chen, X.; Wang, J. The production of pH-sensitive photoluminescent carbon nanoparticles by the carbonization of polyethylenimine and their use for bioimaging. Carbon 2013, 55, 343–349, doi:10.1016/j.carbon.2012.12.074.
111. Wang, S.; Niu, H.; He, S.; Cai, Y. One-step fabrication of high quantum yield sulfur- and nitrogen-doped carbon dots for sensitive and selective detection of Cr(vi). RSC Adv. 2016, 6, 107717–107722, doi:10.1039/C6RA21059G.
112. Huang, Q.; Li, Q.; Chen, Y.; Tong, L.; Lin, X.; Zhu, J.; Tong, Q. High quantum yield nitrogen-doped carbon dots: Green synthesis and application as “off-on” fluorescent sensors for the determination of Fe3+ and adenosine triphosphate in biological samples. Sensors Actuators B Chem. 2018, 276, 82–88, doi:10.1016/j.snb.2018.08.089.
113. Li, M.; Yu, C.; Hu, C.; Yang, W.; Zhao, C.; Wang, S.; Zhang, M.; Zhao, J.; Wang, X.; Qiu, J. Solvothermal conversion of coal into nitrogen-doped carbon dots with singlet oxygen generation and high quantum yield. Chem. Eng. J. 2017, 320, 570–575, doi:10.1016/j.cej.2017.03.090.
114. Wang, Y.; Xia, Y. Optical, electrochemical and catalytic methods for in-vitro diagnosis using carbonaceous nanoparticles: A review. Microchim. Acta 2019, 186, 50, doi:10.1007/s00604-018-3110-1.
115. Xu, Q.; Li, B.; Ye, Y.; Cai, W.; Li, W.; Yang, C.; Chen, Y.; Xu, M.; Li, N.; Zheng, X.; et al. Synthesis, mechanical investigation, and application of nitrogen and phosphorus co-doped carbon dots with a high photoluminescent quantum yield. Nano Res. 2018, 11, 3691–3701, doi:10.1007/s12274-017-1937-0.
116. Dong, Y.; Pang, H.; Bin Yang, H.; Guo, C.; Shao, J.; Chi, Y.; Li, C.M.; Yu, T. Carbon-Based Dots Co-doped with Nitrogen and Sulfur for High Quantum Yield and Excitation-Independent Emission. Angew. Chem. Int. Ed. 2013, 52, 7800–7804, doi:10.1002/anie.201301114.
117. Ding, H.; Wei, J.-S.; Xiong, H.-M. Nitrogen and sulfur co-doped carbon dots with strong blue luminescence. Nanoscale 2014, 6, 13817–13823, doi:10.1039/c4nr04267k.
118. Qin, X.; Lu, W.; Asiri, A.M.; Al-Youbi, A.O.; Sun, X. Green, low-cost synthesis of photoluminescent carbon dots by hydro-thermal treatment of willow bark and their application as an effective photocatalyst for fabricating Au nanoparticles–reduced graphene oxide nanocomposites for glucose detection. Catal. Sci. Technol. 2013, 3, 1027.
119. Lu, W.; Qin, X.; Liu, S.; Chang, G.; Zhang, Y.; Luo, Y.; Asiri, A.M.; Al-Youbi, A.O.; Sun, X. Economical, Green Synthesis of Fluorescent Carbon Nanoparticles and Their Use as Probes for Sensitive and Selective Detection of Mercury(II) Ions. Anal. Chem. 2012, 84, 5351–5357, doi:10.1021/ac3007939.

120. Zhao, X.J.; Zhang, W.L.; Zhou, Z.Q. Sodium hydroxide-mediated hydrogel of citrus pectin for preparation of fluorescent carbon dots for bioimaging. Colloids Surfaces B Biointerfaces 2014, 123, 493–497, doi:10.1016/j.colsurfb.2014.09.048.
121. Feng, X.; Jiang, Y.; Zhao, J.; Miao, M.; Cao, S.; Fang, J.; Shi, L. Easy synthesis of photoluminescent N-doped carbon dots from winter melon for bio-imaging. RSC Adv. 2015, 5, 31250–31254, doi:10.1039/c5ra02271a.
122. Hsu, P.-C.; Shih, Z.-Y.; Lee, C.-H.; Chang, H.-T. Synthesis and analytical applications of photoluminescent carbon nanodots. Green Chem. 2012, 14, 917–920, doi:10.1039/c2gc16451e.
123. Niemirycz, E.; Nichthauser, J.; Staniszewska, M.; Nałęcz-Jawecki, G.; Bolałek, J. The Microtox® biological test: Application in toxicity evaluation of surface waters and sediments in Poland. Oceanol. Hydrobiol. Stud. 2007, 36, 151–163, doi:10.2478/v10009-007-0030-5.
124. EPA's Science Policy Council. Nanotechnology White Paper, EPA 100/B-07/001, Washington. 2007. www.epa.gov/osa (accessed Jun 11, 2021)
125. Savolainen, K.; Backman, U.; Brouwer, D.; Fadeel, B.; Fernandes, T.; Kuhlbusch, T.; Landsiedel, R.; Lynch, I.; Pylkkanen, L. Nanosafety in Europe 2015–2025: Towards Safe and Sustainable Nanomaterials and Nanotechnology Innovations; Finnish Institute of Occupational Health: Helsinki, Finland, 2013.
126. Saleh, T.A. Nanomaterials: Classification, properties, and environmental toxicities. Environ. Technol. Innov. 2020, 20, 101067, doi:10.1016/j.eti.2020.101067.
127. Alas, M.O.; Alkas, F.B.; Sukuroglu, A.A.; Alturk, R.G.; Battal, D. Fluorescent carbon dots are the new quantum dots: An overview of their potential in emerging technologies and nanosafety. J. Mater. Sci. 2020, 55, 15074–15105, doi:10.1007/s10853-020-05054-y.
128. Yao, K.; Lv, X.; Zheng, G.; Chen, Z.; Jiang, Y.; Zhu, X.; Wang, Z.; Cai, Z. Effects of Carbon Quantum Dots on Aquatic Envi-ronments: Comparison of Toxicity to Organisms at Different Trophic Levels. Environ. Sci. Technol. 2018, 52, 14445–14451, doi:10.1021/acs.est.8b04235.

9. Appendix II: additional results of the doctoral thesis

During the doctoral project other research projects and publications related with environmental topics, were carried out as follows:

Conference and conference papers

- Gaviria, M. I., Cano, J. B., Barrientos, K., Arango, J. P., & Peñuela, G. (2020). Desarrollo de un biosensor óptico para el monitoreo en línea de pesticidas organofosforados en aguas: resultados preliminares. In ACOFI (Ed.), II Encuentro nacional de estudiantes de doctorado en ingeniería (pp. 63–70). www.acofi.edu.co.
- Desarrollo de un biosensor óptico para el monitoreo en línea de pesticidas organofosforados en agua. Concurso de carteles. Foro para la apropiación social de tecnologías para la gestión sostenible del agua. 28 al 30 de octubre de 2020. Red temática gestión de la calidad y disponibilidad del agua. CONACYT.
- Carbon quantum dots and Acetylcholinesterase- based fluorescent biosensor for pesticide detection in waters. Presentaciones orales. Congreso internacional Expoingeniería. 27 al 29 de octubre de 2022. Universidad de Antioquia.

Grade's Project (Advisor)

- Ramirez, V. (2021). *Evaluación del uso de aptámeros para el desarrollo de un biosensor basado en carbon dots para la detección de pesticidas organofosforados en agua*. Universidad EIA.
- Henao, J. P. (2021). *Estandarización del cultivo de Entonaema liquescens para la obtención de un bioformulado con potencial en la degradación de aceite lubricante usado.* Universidad EIA.
- Godin. Ana Rosa, & Vega, D. (2022). *Sistema para la detección de plaguicidas organofosforados basado en Carbon Dots y acetilcolinesterasa*. Universidad EIA.
- Alvarez, M. P. (2022). *Evaluación toxicológica de carbon dots producidos a partir de molinia caerulea y elaeis guineensis*. Universidad EIA.

Grade's Project (Jury)

- Rios, C. D. (2021). *Síntesis y caracterización de Carbon-Dots a partir de una fuente renovable*. Universidad EIA.

Master's Project (Jury)

- Roldán, B. (2021). *Configuración de la estrategia de producto como servicio en el sector mobiliario de instituciones de educación superior*. Universidad de Antioquia.
- Galarcio, J. (2021). *Diseño de un modelo de apoyo a la toma de decisiones en el marco del sistema de reembolso de depósito como herramienta de responsabilidad extendida en empaques y envases*. Universidad de Antioquia.